

TOPICS IN THE BEHAVIOUR OF ATMOSPHERIC
TRACE GASES

Mohammad Aslam Khan Khalil
Ph.D., University of Texas at Austin

A dissertation submitted to the faculty
of the Oregon Graduate Center
in partial fulfillment of the
requirements for the degree
Doctor of Philosophy
in
Environmental Science
November 1979

This dissertation has been examined and approved by the following
Examination Committee:

Reinhold A. Rasmussen, Dissertation Advisor
Professor

Douglas F. Barofsky
Professor

John A. Cooper
Professor

Fred N. Alyea
Principal Research Scientist
Georgia Institute of Technology

PREFACE

My studies in Environmental Science began a little over two years ago. In this dissertation I have collected my initial attempts at understanding some aspects of the effects of human activities on the global environment. I have written this dissertation with a very broad group of readers in mind. Any one reader is likely to find many parts which can be skipped without losing sight of the reasoning leading to the conclusions. It is a common belief that a dissertation is not widely read. I have also kept this in mind, and so, to a certain extent, I have written this work for myself. It collects together the framework and calculations in such a way as to allow me to reconstruct my thinking at a later time. Then, the points of view taken can be re-evaluated, reiterated, discarded, or improved upon as the need arises. It is possible for any other reader to do the same. The work is simple and expressed in detail, but I have not been able to arrive at any firm conclusions about who would benefit most from reading it. In this regard I quote Melville: "worth the consideration of those to whom it may prove worth considering."

I want to take this opportunity to thank those who were a part of this work.

Professor R. A. Rasmussen introduced me to this field and guided the research. He provided the financial support to carry out the work and gave me numerous opportunities to travel to meetings and courses in

various parts of the U. S. and Canada. Dr. Rasmussen provided the required measurements on which this work is based. He provided constant encouragement, taught me, advised me and allowed me to collaborate with him through almost daily research meetings. It is not possible to list all that Dr. Rasmussen has done on my behalf, but I am extremely grateful for all his efforts.

Without the encouragement and support from my wife, Giti, this work could not have been completed. I am most grateful to her.

I thank David Pierotti, whose critique of this work has led to many improvements. I also thank John Rau, whose keen questioning has helped to improve the work. Furthermore, David Pierotti and John Rau have provided encouragement and friendship during the past two years which have been an invaluable aid in completing this work.

Dr. Douglas Barofsky was instrumental in getting me to OGC and making it possible for me to start in this field. During the past two years I have benefitted from numerous discussions with him. He has been the chairman of my scholastic committee and his advice and planning in this capacity made it possible for me to complete this intensive program within the planned time. Dr. Barofsky also served on the dissertation committee. I thank him for all his efforts on my behalf. I thank Dr. John Cooper and Dr. James Huntzicker. I have learned from them and benefitted from numerous discussions with them, as well as their support of my work. I also thank Dr. Fred N. Alyea (Georgia Institute of Technology) for reading the dissertation, providing a cri-

tique and several discussions.

I have benefitted from discussions with many other colleagues and friends -- most notably Dr. John G. Watson, Jitendra Shah, Lorne Isabelle, Ken Norton, George Nelson, Dr. Edward Kushner and Dr. Michael Gold. I thank all of them.

I thank Ms. Edie Taylor who typed this long dissertation with intelligence, speed, accuracy and style which made the production of the dissertation seem so easy.

I thank Ms. Maureen Seaman and Ms. Chris Lightcap of the OGC Library for obtaining many papers and books which were needed to conduct the research for this dissertation. Finally, I thank Ms. Barbara Ryall for drawing most of the figures.

This work was supported by the National Science Foundation Grants DPP 77-23468 and ATM 78-09711 and by the National Aeronautics and Space Administration grant NSG 7457. I thank Dr. Fred Dehn of PP&G Industries for financial support which was used to initiate the studies of methylchloroform.

M.A.K.Khalil

30th November 1979
Department of Environmental Science
Oregon Graduate Center
Beaverton, Oregon 97006

TABLE OF CONTENTS

	Page
PREFACE	iii
ABSTRACT	xi
1. INTRODUCTION	1
PART I.	
A STUDY OF METHYL CHLOROFORM AND ITS IMPLICATIONS	8
2. LIFETIME CALCULATIONS: GLOBAL BUDGETS	9
(a) Introduction	9
(b) The Method of Global Averaging: Application to CH ₃ CCl ₃ , CFCl ₃ (F-11) and CCl ₂ F ₂ (F-12)	11
(c) The Method of Hemispherical Averages	17
(d) Conclusions	25
3. LIFETIME CALCULATIONS: CHEMISTRY	30
(a) Introduction	30
(b) Hydroxyl Radical Sink of Trace Gases	31
(c) Lifetimes of Selected Trace Gases	43
(d) Estimates of Mean HO Radical Concentrations in the Troposphere	50
(e) Conclusions	63
(f) Effects of New (October 1979) Rate Constants for HO + CH ₃ CCl ₃ → H ₂ O + CH ₂ CCl ₃ .	65

Table of Contents (Continued)

4. AN ANALYSIS OF CYCLIC FLUCTUATIONS IN THE GLOBAL SOURCE STRENGTHS OF TRACE GASES	75
(a) Introduction	75
(b) Theoretically Predicted Concentrations of a Trace Gas with a Fluctuating Source	78
(c) Effects of Source Fluctuations on Lifetime Calculations	81
(d) An Analysis of the CH_3CCl_3 Source Function	85
(e) A Look at $\Delta_2(t)$ in the CH_3CCl_3 Source Function	88
(f) Comparison of Theory and Observations	91
(g) Analysis of CH_3CCl_3 Observed Time Series Using Non-Parametric Statistics	94
(h) Summary and Conclusions	101
5. SOURCES AND INTERHEMISPHERIC GRADIENTS: APPLICATIONS TO CH_3CCl_3 AND OTHER TRACE GASES	112
(a) Introduction	112
(b) Uniqueness of the Methyl Chloroform Gradient	113
(c) Trend Analysis of the Gradients, R_0 , of CCl_3F (F-11), CCl_2F_2 (F-12), CCl_4 and CH_3CCl_3	115
(d) Theoretical Investigation of the Changing Methyl Chloroform Gradient, R_0	119

Table of Contents (Continued)

5. (e) Interhemispheric Gradients and Sources in the Southern Hemisphere -- Short-Lived Trace Gases	136
(f) Conclusions	141
6. ACCUMULATION OF CH_3CCl_3 IN THE ATMOSPHERE	150
(a) Introduction	150
(b) Theoretical Analysis of Future CH_3CCl_3 Concen- trations	152
(c) Summary and Conclusions	159
PART II.	
RELATED TOPICS AND THEORETICAL TECHNIQUES	163
7. A STUDY OF CHClF_2 (F-22) IN THE ATMOSPHERE	164
(a) Introduction	164
(b) Review of the Data and the Global Averages	165
(c) The Global Time-Release and Budget of F-22	169
(d) Strengths of Natural Sources	173
(e) Conversion of CCl_2F_2 (F-12)	175
(f) Accuracy of Measurements and Release Estimates	181
(g) Summary and Conclusions	183
8. GLOBAL AND HEMISPHERICAL AVERAGES OF TRACE GASES	191
(a) Introduction	191
(b) High Latitude Measurements and Global Averages	193
(c) Tropospheric Averages Based on Detailed Latitudinal Measurements -- Latitudinal Polynomials	202

Table of Contents (Continued)

8.	(d) Trace Gases in the Stratosphere	208
	(e) Numbers of Molecules of Air in the Stratosphere and Troposphere	220
	(f) Summary and Conclusions	229
9.	SOURCE FUNCTIONS: SMOOTHING AND SPECTRAL ANALYSIS	236
	(a) General Ideas	236
	(b) Smoothing of Source Functions Described by Simple Exponentials	238
	(c) Complex Source Functions	240
	(d) Complex Source Functions: Fourier Analysis	242
	(e) Conclusions	247
10.	GLOBAL BOX MODELS: FORMULATION AND SOLUTIONS	250
	(a) General Ideas	250
	(b) Many-Box Theory	251
	(c) Simple Global Model	254
	(d) Two-Box Theories	255
	(e) Three-Box Theory	257
	(f) Four-Box Theories	259
	(g) Five-Box Theory	264
	(h) Six-, Seven-, and Eight-Box Theories	266
	(i) Graphical Summary	269
	(j) Conclusions	271

Table of Contents (Concluded)

11. CONCLUSIONS	272
(a) Review	272
(b) Environmental Action	282
SELECTED REFERENCES	285
APPENDIX I: DETAILS OF CALCULATIONS	292
(a) Chapter 2	293
(b) Chapter 3	301
(c) Chapter 4	307
(d) Chapter 5	327
(e) Chapter 6	344
(f) Chapter 7	346
(g) Chapter 8	354
(h) Chapter 9	358
APPENDIX II: SUMMARY OF COMMONLY USED MATHEMATICAL SYMBOLS	361
VITA	369

ABSTRACT
TOPICS IN THE BEHAVIOUR OF
ATMOSPHERIC TRACE GASES

Mohammad Aslam Khan Khalil, Ph.D.
Oregon Graduate Center, Beaverton, Oregon, 1979

Supervising Professor: R. A. Rasmussen

This dissertation is divided into two parts. The first part deals primarily with the lifetime, distribution, and implications of methyl chloroform (CH_3CCl_3) in the global environment. Part II deals with some theoretical considerations which support the calculations in Part I. The second part also contains a preliminary analysis of CHClF_2 (F-22) in the atmosphere.

The results of a budget analysis of CH_3CCl_3 imply a total global lifetime of between 7 and 10 years. The lifetime of 9 years is most consistent with the data. Similar analyses of CFCl_3 (F-11) and CCl_2F_2 (F-12) indicate that the lifetimes of these gases are greater than 20 years. The lifetime of CH_3CCl_3 due to HO radical interactions is consistent with average ground level HO densities of approximately $6-7 \times 10^5$ molecules/cm³. These are used to calculate the lifetimes of many other trace gases which are, or may become, important in understanding the global atmospheric environment. Most notably, the lifetimes of CH_4 ,

F-21, and F-22 turn out to be approximately 14, 3 and 23 years respectively. The long CH_4 lifetime has a variety of implications for CO production in the atmosphere as well as the budget of CH_4 . The data base used for the calculations is in general different from that used in other analyses discussed in the literature. Furthermore, new equations were derived to carry out the studies discussed in this work.

It was also found that the emissions history of CH_3CCl_3 shows cyclic fluctuations superimposed on the exponential growth. Including such fluctuations into the theory brought the observed growth of CH_3CCl_3 concentrations in the atmosphere in coincidence with the theoretically predicted growth rate. The observation that the ratio (R_0) of CH_3CCl_3 (concentration) in the northern and southern hemispheres has been changing was also properly explained by the cyclic fluctuations of the emissions. Thus in earlier years (before 1975) it is likely that there was a greater excess of CH_3CCl_3 in the northern hemisphere (compared to the southern hemisphere) than there is at this time. Other possible explanations of the changing ratio did not agree with observations. The theory used to study this ratio (R_0) was extended to derive a simple criterion for deducing the presence of significant southern hemisphere sources of trace gases. It was found that $\text{CH}=\text{CH}$ (acetylene), C_2H_6 , C_2H_4 , CO , COS , and several other relatively short-lived trace gases have southern sources.

In Part II one of the studies centered around the global analysis of CHClF_2 (F-22). Current global concentration of about 47 ppt was greater than could be explained by the accepted emissions estimates. Several explanations of the excess were offered. These included the possible slow conversion of F-12 to F-22 and sources other than direct F-22 emissions from the manufacture and use of this compound. Other aspects of Part II will not be discussed here.

The global measurements, on which all the theoretical considerations are based, were made by R. A. Rasmussen over the past five years.

CHAPTER 1. INTRODUCTION

"Deep in the human unconscious is a pervasive need for a logical universe that makes sense. But the real universe is always one step beyond logic." (Frank Herbert)

Today, environmental pollution linked to human activities manifests itself in more places, more forms and with a greater magnitude than ever before. The point has been reached where the possible future deterioration of the environment has seized the attention of rapidly increasing numbers of scientists as well as the society in general. This focus of attention is particularly acute in the highly industrialized nations of the world where most environmental pollution originates. The scientific study of the environment and its changes due to anthropogenic activity has already become extremely broad and occupies a large portion of the current scientific literature. It is becoming clear that the environment is changing, possibly towards a dangerous state for many forms of life on earth, including man. Global environmental pollution is just one aspect of the general problem, but it is particularly insidious. The studies I will report in this dissertation are directed towards some particular aspects of global environmental pollution.

There are many examples of global pollution caused by human activities. Some examples have received such widespread public attention that they have gone beyond the esoteric domains of current science to become general knowledge. This category includes global PCB (polychlorinated biphenyls) and DDT contamination. It includes the growing concern about the potentially dangerous effects from partial depletion of the strato-

spheric ozone layer. This depletion could be caused by continuing emissions of man-made fluorocarbons 11 and 12 (CFCl_3 and CF_2Cl_2), as well as other chlorine-containing gaseous emissions (e.g., CH_3CCl_3). The ozone layer is also threatened by growing use of nitrate fertilizers which add to the natural N_2O burden of the troposphere, which in turn yields NO and NO_2 in the stratosphere causing catalytic destruction of ozone (see Crutzen, 1971). Research on the fate of the stratospheric ozone layer has prompted many experimental and theoretical studies of the atmosphere itself as well as other long-lived chlorine-containing anthropogenic gases in the atmosphere. The study reported in this dissertation is one of these. The increases in the tropospheric burdens of CO_2 as well as F-11, F-12 and N_2O , from anthropogenic activities have also received considerable attention due to the concern that these gases will enhance the earth's greenhouse effect, leading to higher global temperatures and consequent changes in climate.

The total global environment is an extremely complex system with intricate connections among its components. These are many feedbacks and synergistic effects even in the stratospheric ozone problem (see for example: Groves et al., 1978; Groves and Tuck, 1979; Boughner, 1978; Chameides and Walker, 1975; and Yung et al., 1979). It is, therefore, difficult to isolate one trace gas for study. Nevertheless, in order to embark on a study of the global atmospheric environment, it is possible to delineate some steps. (1) First, the potentially dan-

gerous emissions have to be identified. Once identified, an assessment of the current state of affairs has to be made. This includes global measurements and evaluation of the emissions, past and present. Once we have a good grasp of the sources, sinks and lifetimes, these are coupled to the physical and chemical properties of the trace gas leading to an evaluation of the types of environmental perturbations it is capable of causing. It often happens that the worse effects of the trace gas are expected in the future. (2) Next, estimates have to be made regarding probable future emissions of these compounds. Then, the concentrations expected in the future can be quantified and the direct environmental effects can be evaluated. For example, various types of projections of the future uses of F-11 and F-12 are used along with information from (1) to tell us how much ozone depletion to expect in the future. (3) Lastly, the expected alterations of atmospheric composition are translated into ecological effects. For example, in the case of the ozone layer, one may calculate the expected effects on human health, or on crops and climate, based on the depletion of the ozone layer found in (2). Much of the work reported in this dissertation falls into step (1) with a few excursions into step (2). With this framework in mind, a preview of the dissertation is presented next.

The dissertation consists of two main parts. The primary subject of the first part is the trace gas methyl chloroform (CH_3CCl_3). Based

on current knowledge, it appears that CH_3CCl_3 is entirely man-made. It has been emitted into the atmosphere in ever-increasing amounts for nearly thirty years (about 1.1 billion lbs. were emitted in 1978). CH_3CCl_3 is an industrial degreasing solvent and is generally released to the atmosphere within a short time after production. The possible dangers of CH_3CCl_3 are similar to those from emissions of fluorocarbons 11 and 12, namely its contribution of stratospheric ozone depletion and enhancement of the greenhouse effect. It is one of several gases which contribute chlorine to the stratosphere by its UV photodissociation in the upper atmosphere. As such, it is just another straw on the camel's back. From a different scientific point of view, study of CH_3CCl_3 is capable of providing new information on atmospheric processes in general -- it serves as a test gas to obtain information which can be applied to other trace gases about which our knowledge is incomplete. There are several reasons why CH_3CCl_3 fits into this role. It has a source whose strength (emissions per unit time) and location are relatively well-known. Furthermore, its major sinks are few and strong enough to give it a lifetime of 7 - 10 years. This allows for studies of finer structure in its behaviour that would otherwise be impossible. Very long-lived trace gases, in general, require a long wait while the observational data base is built, before one can draw firm conclusions. Much shorter lived trace gases have highly variable concentrations, generally requiring greater spatial coverage of observations which are seldom available. The first two chapters contain an analysis of the life-

time of CH_3CCl_3 and its implications for the lifetimes of several other trace gases which are, or threaten to become, important in the study of the global atmospheric environment. Chapters 4 and 5 consider the effects of cyclic fluctuations in the emissions of gases to the atmosphere. The information which can be obtained by studying the inter-hemispheric differences in the abundances of trace gases is also considered in these chapters. This includes a criterion for deciding whether a trace gas has southern hemisphere sources. In all these considerations CH_3CCl_3 not only plays the role of an example, but the studies also reveal new information on the behaviour of CH_3CCl_3 itself. In the last chapter of Part I, attention is directed towards the possible future concentrations of CH_3CCl_3 . The studies provide information on sources, sinks and lifetimes of CH_3CCl_3 , which are all necessary ingredients in evaluating the future of CH_3CCl_3 . The theory which is developed is tailored to fit, as closely as possible, the nature of the selected data base.

It is no secret that global environmental studies contain many uncertainties. The risk of making sizeable errors in such analyses is always large. Generally, there are two major sources which contribute to this risk. First, there are uncertainties in the observational bases. This includes uncertainties in reaction rate constants, global measurements of ambient concentrations, and estimates of the global

sources. The second contributor to the risk of making errors is the theory used to tie observational knowledge into a consistent framework. This includes risks from oversimplification of the physical processes, but simplified theories require less observational information to yield results. Paying proper attention to details of the physical processes governing the atmospheric behaviour of trace gases leads to immensely complicated theories. Such theories are not only challenged on the ways by which the physical processes are incorporated, but they also require knowledge of many more physical variables none of which are accurately known. It also becomes increasingly difficult to arrive at and convey an intuitive understanding of the results. Furthermore, the choice of theoretical framework is also based on the nature of the questions one wants to answer and the data base available. In this dissertation attempts were made to weigh these factors. The resulting theoretical framework has the advantages of simplicity, solvability and compatibility with the available data, but the risk of errors could not be eliminated.

It should be pointed out that the steps discussed earlier each contains its own uncertainties as well as those propagated from the steps before. It becomes exceedingly difficult to accurately quantify future ecological change caused by anthropogenic activities.

As mentioned earlier, there is extensive current literature on the behaviour of anthropogenic trace gases and their dangers to our en-

vironment. This will be discussed where appropriate. Review and discussions of the greenhouse effect and other climatic changes due to anthropogenic activities may be found in Gribbin (1978), Ramanathan (1975) and Wang et al. (1976). The theory is discussed elegantly in Houghton (1977). Reviews of stratospheric ozone depletion can be found in Gutowsky (1976: NRC Report), Hudson (1977) and Johnston (1975). The CIAP monographs (see CIAP, 1975) are an extensive guide to techniques and information available before 1975.

PART I:

A STUDY OF METHYL CHLOROFORM
AND ITS IMPLICATIONS

CHAPTER 2. LIFETIME CALCULATIONS:

GLOBAL BUDGETS

(a) Introduction

There are two basic methods available for calculating the lifetimes of trace gases. One method is to consider the global budget. This method is usually described by the mass conservation equation which contains the relationship between the three fundamental variables: sources, ambient concentrations and the loss processes of the trace gas in question. All these variables are distributed in space and time, i.e., their values are functions of space-time variables. Dispersal of the trace gas is also included, but this is a physical variable of the atmosphere. Whenever any two of the variables (S , ξ , τ) are known, the third can be determined. Generally, the sources (magnitude and distribution) and the ambient concentration are determined experimentally and the lifetime chosen to balance the sources and the observed ambient concentrations.

This chapter contains the results of applying budget methods to CFCl_3 (F-11), CCl_2F_2 (F-12) and CH_3CCl_3 . Similar methods can be applied to other trace gases as well. The major emphasis of the work discussed here is on CH_3CCl_3 . For F-11 and F-12 the data required have to be much more detailed in order to properly apply the budget methods. Still, the data available are analyzed and conservative con-

clusions are drawn ($\tau > 20$ yrs). It should also be pointed out that the data used here are all part of a self-consistent series of measurements made by Rasmussen (personal communication) since January of 1975. The data are tabulated in Appendix I.

The second method of determining lifetimes does not require the knowledge of either emissions or ambient concentrations. This method delineates the sink mechanisms and then, using the available information, estimates the global effect of each sink mechanism. For example, when the loss of a trace gas in the troposphere is due entirely to reactions with HO radicals, the lifetime is sometimes estimated by $\tau = \{\bar{k} \overline{[HO]}\}^{-1}$ (\bar{k} is the reaction rate constant at the average tropospheric temperature, and $\overline{[HO]}$ the globally time-averaged HO radical density). Such a method will be discussed in detail for many trace gases in the next chapter (3).

The lifetime of a trace gas, along with the mechanisms (including products) which lead to the destruction of the trace gas, are the key ingredients determining the effects of the gas on the global environment. Furthermore, knowledge of the lifetime is an essential ingredient in determining the future accumulation of the trace gas and in general its future environmental effects.

(b) The Method of Global Averaging: Application to CH₃CCl₃, CFCl₃
(F-11) and CCl₂F₂ (F-12)

Part 1.

The type of budget method used to analyze the behaviour of a trace gas is, to a large extent, dictated by the type of data available on the sources and concentrations. The data used for this analysis have been obtained by Rasmussen (personal communication) over the past five years at remote sites ($\sim 45^\circ$, U. S. Pacific northwest, and $\sim 90^\circ$, south pole). These data are reported in the section of this chapter in Appendix I. The simplest way to obtain a lifetime is to consider a global average of the mass conservation equation given by:

$$\frac{d}{dt}\xi = S - \eta\xi \quad (2.1)$$

where ξ is the average mixing ratio, S the source strength in pptv per year and η is the reciprocal of the globally averaged effective lifetime. There are several ways to use eqn. (2.1). The following method is proposed as one possible way to evaluate the lifetime. Eqn. (2.1) is first rewritten as $d\xi = Sdt - \eta\xi dt$, then integrated, giving:

$$\Delta\xi = \xi(T) - \xi(0) = S_* - \eta\xi_* \quad (2.2)$$

$$\eta = 1/\tau$$

$$S_* = \int_0^T S(t)dt ; \quad \xi_* = \int_0^T \xi(t)dt \quad (2.3)$$

Therefore,

$$\tau = \frac{\xi_{*}}{S_{*} - \Delta\xi} \quad (2.4)$$

Note that S_{*} is the total release of the compound under consideration, between time 0 and time T. $\Delta\xi$ is the difference of the mixing ratio between measurements at time 0 and time T. ξ_{*} does not have a clear-cut intuitive meaning. In this analysis ξ is deduced from the measurements by:

$$\xi = \alpha \xi_T ; \quad \xi_T = \frac{1}{2} (\xi'_n + \xi'_s) \quad (2.5)$$

$$\alpha = \frac{N_T}{N_{\infty}} \left[1 + \zeta \frac{N_S}{N_T} \right] \quad (2.6)$$

$$\zeta = \xi_U / \xi_T \quad (2.7)$$

ξ_T is the average tropospheric mean mixing ratio of the trace gas. It is assumed to be given by $\frac{1}{2} (\xi'_n + \xi'_s)$ where ξ'_n are the measured mixing ratio at the high northern latitude location (here $\sim 45^{\circ}\text{N}$) and ξ'_s the high southern latitude mixing ratio (here $\sim 90^{\circ}\text{S}$). In Chapter 8 this equation is justified in detail. α transforms the tropospheric average mixing ratio, ξ_T , to the total global mixing ratio, ξ . ξ is the ratio of the total global burden (number of molecules) of a trace gas to N_{∞} (total no. of molecules of air in the troposphere and the stratosphere). Therefore, in eqns. (2.6) and (2.7), N_T is the number of molecules of air in the troposphere, N_S the number of molecules of air in

the stratosphere, and ξ_u is the mean concentration of the trace gas in the stratosphere. α is often very difficult to evaluate because it requires stratospheric measurements of the trace gases. Fortunately, the stratospheric burden of most trace gases of interest here makes a relatively small contribution to the lifetime. This is true as long as the total lifetime of the trace gas is due to tropospheric sinks as is the case for CH_3CCl_3 . (See Appendix I for α and ζ .)

$\Delta\xi$ is determined in the same way as ξ , and S is the source in number of molecules emitted per year divided by N_∞ ($= N_T + N_S$). Chapter 8 may be consulted for further details on N_S and N_T .

There are some nice features of eqn. (2.4) which ought to be mentioned. First, the knowledge of the source need only extend over the period from time 0 to T. The equation does not depend on the release history at times before measurements began (here $t = 0$ is at January 1975). Second, ξ_* is an integral of $\xi(t)$ which includes data over several years, so that ξ_* is not likely to be influenced by random measurement errors. Third, the lifetime is still susceptible to errors of absolute accuracy, but this is somewhat moderated because ξ appears in both the numerator (as ξ_*) and the denominator (as $\Delta\xi$). This method is suitable for calculating lifetimes when several years of discrete measurement data are available.

In this study, S_* is simply the sum of the emissions from 1/1975 to 1/1979 (0 to T) -- the first measurements were made in January 1975 and the last in this series (so far) were made in January 1979. ξ_* is

calculated by first deriving a functional form for $\xi(t)$ as $\xi(t) = \xi_0 e^{\beta t}$, ξ_0 and β are deduced from least squares fits of $\ln \xi$ as a function of time, where the ξ are known from measurements at January of each year since 1975. In this way the measurements of a trace gas at specific times during 0 - T are converted to a continuous function for integration in eqn. (2.3).

For CH_3CCl_3 the lifetime according to eqn. (2.4) is 8.5 years. The following table describes the results of the calculations:

Table (2.1): Lifetime of CH_3CCl_3 .

Conditions	Lifetime (Yrs.)
1. $\zeta = 0.2$	8.5
2. $\zeta = 0.25$	8.7
3. $\zeta = 1.0$	12
4. $\zeta = 0.2, \xi_1 = 0.9$	7
5. $\zeta = 0.2, S_1 = 1.15$	7
6. $\zeta = 0.2, \xi_1 = 0.9\xi$ and $S_1 = 1.15$	6

The first three conditions are related to the stratospheric burden of CH_3CCl_3 . Condition 3 is not possible because it implies that the CH_3CCl_3 mixing ratio is constant from the ground to the top of the stratosphere (stratopause, ~ 50 km). However, this is the longest lifetime calculated from the data. In condition 4, it is assumed that the measured numbers are consistently high by 10% (see Rasmussen, 1978),

and that the true ξ is 10% less than that derived from the data. In condition 5, it is assumed that the estimates of emissions are too low by 10%, and lastly, in condition 6, it is assumed that conditions 4 and 5 are present simultaneously.

From this analysis it appears that the lifetime of CH_3CCl_3 is between 7 and 9 years, with the value of 8.5 years as being the one most consistent with the data. Details of the calculations are given in Appendix I.

An analysis of CFCl_3 (F-11) by this method yields a lifetime of 56 years. If the measured numbers are too high by 10% or the source too low by 10%, the lifetime is 32 years.

In applying the method to CCl_2F_2 (F-12) it turned out that $S_* - \Delta\xi < 0$, implying that there was more F-12 around than could be expected from the release data. On the other hand, the excess is small, so that further speculations as to the cause of the excess are not appropriate without more data. If the source term assumed here is increased by 10% and the measurements reduced by 10%, the lifetime turns out to be 70 years; so one may say that $\tau_{\text{F-12}} \gtrsim 70$ years according to Rasmussen's time series of measurements and the source data.

The data for the emissions of CH_3CCl_3 is taken from Neely and Plonka (1978) and Neely and Farber (1979). The emissions data for CFCl_3 and CCl_2F_2 are taken from McCarthy et al. (1977) and Alexander Grant and Co. (1979). ζ can be deduced from the paper of Crutzen et al. (1978).

Part 2.

There is another simple method based on eqn. (2.1) which can be used to calculate the lifetimes. This method depends on solving eqn. (2.1) as:

$$\xi = \xi_0 e^{-\eta t} + \frac{a}{b + \eta} (e^{bt} - e^{-\eta t}) \quad (2.8)$$

The interpretations of ξ , η and S remain the same as before. ξ_0 is the mean mixing ratio (including troposphere and stratosphere) at $t = 0$ and the source is described by the function $S = ae^{bt}$. The (a) and (b) in the source function are derived by least squares fits to $\ln S$ as a function of time. The (a) is corrected slightly to derive a continuous version of S from discrete yearly estimates. The correction factors are derived and discussed in Chapter 9. For CH_3CCl_3 , (a, b) turned out to be (14.7 pptv/yr, 0.105/yr). Once again the source has to be known only for the period during which measurements were made, as long as there is no desire to theoretically determine ξ_0 . In this method several values of η are tried to see which one reproduces measured values the best. The results of the calculations for CH_3CCl_3 are given in Appendix I. These results (CH_3CCl_3) are plotted in Figure (2.1). The graph indicates that $\tau(\text{CH}_3\text{CCl}_3)$ is: $8 \text{ yrs} \leq \tau(\text{CH}_3\text{CCl}_3) < 10 \text{ yrs}$ and $\tau = 9 \text{ years}$ is in best agreement with the measurements. The 10-year lifetime predicts higher than measured concentrations for four of the five measurements, but the difference is not large. If inaccu-

rate, it is more likely that the measured values are too high compared to the true concentrations, so $\tau = 10$ years is not a good estimate. 8 - 9 years is most likely, and this is in agreement with the results of the last section. When the same calculations were repeated assuming that the measured mixing ratios are too high by 10%, the best lifetime predicted by eqn. (2.8) turned out to be 8 years.

F-11 and F-12 were not treated by this technique, because their lifetimes are long, and the predicted graphs bunch up so much that it is difficult to distinguish the best lifetime from a host of predicted graphs. In the next section more attention will be devoted to these compounds.

(c) The Method of Hemispherical Averages

Since the data on which the calculations of this chapter are based consisted of measurements in both northern and southern hemispheres, it is most appropriate to consider a theory with hemispherical averaging rather than global averaging. It should be pointed out that the global averaged theory has certain advantages over the hemispherically averaged theory. These will be discussed later. The theory with hemispherical averaging is written as (mass conservation equation):

$$\frac{d}{dt}\xi_n = S_n - \eta_n \xi_n - \eta_T(\xi_n - \xi_s) \quad (2.9)$$

$$\frac{d}{dt}\xi_s = -\eta_s \xi_s + \eta_T(\xi_n - \xi_s) \quad (2.10)$$

The assumptions made here are that there are no (or insignificant) southern hemisphere sources and that the average lifetime of the trace gas in the northern hemisphere is τ_n ($= 1/\eta_n$) and in the southern hemisphere it is τ_s ($= 1/\eta_s$). S_n are the emissions per unit time divided by $\frac{1}{2} N_\infty$ (rather than N_∞). τ_T ($= 1/\eta_T$) is the mean interhemispheric transport time. ξ_n and ξ_s , analogous to ξ of the last section, are the mean northern and southern hemisphere mixing ratios (including the troposphere and the stratosphere). These variables will be discussed again in more detail, particularly in Chapters 5, 8 and 10.

The formulation of the theory by eqns. (2.9) and (2.10) has the following technical problem (as opposed to the many philosophical problems): The measurements are at high latitudes and thus ξ (meas. 45°N) $\neq \xi_n$ and ξ (meas. -90°S) $\neq \xi_s$. In other words, the measured mixing ratio at the Pacific northwest location has to be corrected to not only take into account the lower stratospheric mixing ratio, but it also has to be corrected to take into account the decrease of the mixing ratio as one moves towards the equator. Similar statements apply to ξ_s . It is a typical feature of all trace gases released in the high ($> 30^\circ\text{N}$) northern latitudes that their mixing ratio declines with distance from about 30°N to 30°S before leveling off to a reasonably constant value (close to that observed at the south pole). More detailed independent latitudinal measurements of CH_3CCl_3 , CFCl_3 and CCl_2F_2 all suggest a simple latitudinal model which is discussed in detail in Chapter 8.

The result of this model is that the measured mixing ratios at remote high latitudes can be converted to hemispherical averages by the following equation:

$$\xi_n = b - \frac{(b - a)}{2\phi_0} (1 - \cos \phi_0) \quad (2.11)$$

$$\xi_s = a + \frac{(b - a)}{2\phi_0} (1 - \cos \phi_0) \quad (2.12)$$

$$\phi_0 \approx \pi/6 \text{ radians}$$

$$b = \xi \text{ (measured at } 45^\circ\text{N)}, a = \xi \text{ (measured at } -90^\circ\text{S)}.$$

With these assumptions in mind, it is now possible to construct solutions of eqns. (2.9) and (2.10) analogous to those discussed in the previous section.

The simplest solution is analogous to eqns. (2.2) - (2.4) and gives:

$$\Delta\xi_n = S_{n^*} - \eta_n \xi_{n^*} - \eta_T (\xi_{n^*} - \xi_{s^*}) \quad (2.13)$$

$$\Delta\xi_s = -\eta_s \xi_{s^*} + \eta_T (\xi_{n^*} - \xi_{s^*}) \quad (2.14)$$

or:

$$\tau_n = \frac{\xi_{n^*}}{S_{n^*} - \Delta\xi_n - \eta_T \delta\xi_{s^*}} \quad (2.15)$$

$$\tau_s = \frac{\xi_{s^*}}{\eta_T \delta\xi_{s^*} - \Delta\xi_s} \quad (2.16)$$

$$\delta\xi_{s^*} = \xi_{n^*} - \xi_{s^*} \quad (2.17)$$

$$\tau = \frac{\xi_n^* + \xi_s^*}{\eta_n \xi_n^* + \eta_s \xi_s^*} \quad (2.18)$$

The meanings of the symbols are obvious, but they are reiterated in Appendix II. τ in eqn. (2.18) is a composite total lifetime and is a weighted average of τ_n and τ_s .

A new variable, τ_T , has been introduced. Its value is not known precisely, but its main effect on the lifetime of CH_3CCl_3 is to distribute the sink strength over the hemispheres, rather than affect the total lifetime τ . Calculations for CH_3CCl_3 , based on equations (2.15) - (2.18) yield the results given in Table 2 below:

Table 2: CH_3CCl_3 Lifetimes in a Hemispherically Averaged Theory

		*	
τ_T (yrs)	1	1.2	1.4
τ (yrs)	8.5	8.5	8.5
τ_n (yrs)	27	12.3	8.9
τ_s (yrs)	4.4	6	8

It is not surprising that the total lifetime comes out the same as in the previous section. The interhemispheric lifetime of one year is very unlikely, because it predicts a difference between τ_n and τ_s which

cannot be explained by current knowledge. $\tau_T = 1.2$ or 1.4 yrs. are both reasonable and relatively small compared to previous estimates (see, for example, Chang and Penner, 1978). This will be discussed soon. If τ_T is taken to be 1.4 yrs, then the τ_n and τ_s are about the same. If τ_T is taken to be 1.2 yrs, then the lifetime of CH_3CCl_3 is about twice as large in the northern hemisphere as in the southern hemisphere. At this time I tend to favour the result of $\tau_T = 1.2$ yrs. There is a good possibility that the HO densities in the southern hemisphere are significantly higher than in the northern hemisphere. The most recent measurements of CO indicate a large difference (\sim factor of 2) between the two hemispheres, being higher in the northern hemisphere (Rasmussen, personal communication). CO is present in such large quantities that it can control the mean HO densities. Besides CO, some other gases, which destroy HO radicals, are probably present in higher concentrations in the northern hemisphere. These questions are discussed further in Chapter 3. Since HO is currently believed to be the main tropospheric sink of CH_3CCl_3 , it is possible that $\tau_n > \tau_s$ for this compound (as well as others which react with HO). There has also been a discrepancy in the τ_T deduced from CH_3CCl_3 measurements and that estimated from meteorological considerations. The τ_T based on CH_3CCl_3 has been large ($\tau_T = 1.8$ yrs: Chang and Penner, 1978) and τ_T based on meteorological considerations has been small ($\tau_T = 1$ yr: Newell et al., 1969). If one believes the meteorological estimate more, then the re-

sults of eqn. (2.15) and (2.16) for CH_3CCl_3 can be considered to be in favour of $\tau_n > \tau_s$. This isn't a strong case for this issue because of the many uncertainties involved and the sensitivity of τ_n and τ_s on τ_T ; nevertheless, it does help to create a certain amount of consistency in the overall picture.

The method analogous to that of eqn. (2.8) is discussed next. It is no longer an easy task to solve the equations (2.13) and (2.14).

The solutions can be written as:

$$\underline{\xi} = (P^{-1} e^{-\Lambda t} P) \underline{\xi}_0 + P^{-1} e^{-\Lambda t} \int_0^t e^{\Lambda t'} P \underline{S}(t') dt' \quad (2.19)$$

$$\Omega = \begin{bmatrix} (\eta_n + \eta_T) & -\eta_T \\ -\eta_T & (\eta_s + \eta_T) \end{bmatrix} \quad (2.20)$$

$$\underline{\xi} = \begin{bmatrix} \xi_n \\ \xi_s \end{bmatrix}, \quad P\Omega P^{-1} = \Lambda = \begin{pmatrix} \lambda_1 & 0 \\ 0 & \lambda_2 \end{pmatrix} \quad (2.21)$$

λ_1 and λ_2 are eigenvalues of Ω . All these equations will be discussed in greater detail in Chapters 6 and 10, so I will not go into the details here.

Taking into account α , eqns. (2.11) and (2.12) and several values for τ_n and τ_s , but keeping $\tau_T = 1.2$ years produced the results shown in Figure (2.2) for CH_3CCl_3 . The details of the calculations are given

in Appendix I. The figure shows that $\tau_T = 1.2$, $\tau_n = 12$, $\tau_s = 6$ (average lifetime $\tau = 8.5$ yrs) gave the best agreement with observations. The upper curves were based on $\tau_T = 1.2$, $\tau_n = 16$, $\tau_s = 8$ (all in years with the average lifetime $\tau = 11$ yrs); and the lower curves are for $\tau_T = 1.2$, $\tau_n = 8$ and $\tau_T = 4$ (average lifetime $\tau = 5$ yrs). (Note that the theoretical lines in best agreement with data are those from Table 2 with $(\tau_T, \tau_s, \tau_n) = (1.2, 12, 6)$, whereas the upper and lower lines are not based on the lifetimes discussed in Table 2 because those other lifetimes were not derived with $\tau_T = 1.2$ yrs.) It should be pointed out that there are other assumptions which will give just as good agreement as the $(\tau_T, \tau_n, \tau_s) = (1.2, 12, 6)$ curve. For example, $(\tau_T, \tau_n, \tau_s) = (1.4, 9, 8)$ will also be in good agreement. Regardless of these possibilities the total lifetime of $\tau = 8.5$ years would still have to be maintained.

CFCl_3 and CCl_2F_2 were also considered by this technique. Here it was assumed that $\tau_n = \tau_s$, which simplifies the theory considerably and yields:

$$\xi_n = \frac{1}{2} [A_o e^{-\eta t} + B_o e^{-(\eta + 2\eta_T)t}] + \frac{1}{2} \left[\frac{a_o}{\eta} (1 - e^{-\eta t}) + \frac{a_o}{(\eta + 2\eta_T)} (1 - e^{-(\eta + 2\eta_T)t}) \right] \quad (2.22)$$

$$\xi_s = \frac{1}{2} \left[A_o e^{-nt} - B_o e^{-(n + 2\eta_T)t} \right] + \frac{1}{2} \left[\frac{a_o}{n} (1 - e^{-nt}) - \frac{a_o}{(n + 2\eta_T)} (1 - e^{-(n + 2\eta_T)t}) \right] \quad (2.23)$$

$$A_o = \xi_{no} + \xi_{so}; \quad B_o = \xi_{no} - \xi_{so}, \quad S_n = a_o \quad (2.24)$$

The source S_n is assumed to be constant as implied by the release data (see references mentioned earlier).

In the analysis of F-11 and F-12 by this method there appeared to be little justification in trying to deduce the absolute lifetime. Again, this is because both are long-lived, and it is not possible to decide between the bunched up theoretically predicted lines for all lifetimes $> \sim 30$ years. Instead, it appeared worthwhile to explore the question: how low can the lifetimes of F-11 and F-12 be and still agree with the data? The results of the calculations suggested that a lifetime of F-11 or F-12 below 20 years could not be supported by our present knowledge of source strengths and the five years of measurements by Rasmussen (see Appendix I for data). Details of the calculations can be found in Appendix I. In Figure (2.3) the results are presented graphically. These are for CFC1_3 (F-11), but the behaviour of CCl_2F_2 (F-12) is essentially the same (in fact more emphatic). The dashed lines represent the mean northern and southern hemisphere mixing ratios of F-11. The lower cross-hatched regions represent the expected

concentrations if the lifetime was 10 years. The upper cross-hatched region represents the expected concentrations if the lifetime was 20 years. The lower limits of each region are for the best estimate of the emissions currently available. The upper limits of each region are the expected concentrations if the true source was in reality 20% higher than the initial estimate. It is apparent that even if there were sizeable errors in the source strength, a lifetime of less than or equal to 20 years is not consistent with the measured concentrations (actually this comment holds as long as $\delta\xi/\xi + \delta S/S \sim 0.2$). The case for this lower limit is strong.

There are other techniques also available for the analysis of the lifetimes of F-11 and F-12. These generally require a more detailed data base than is available for analysis in this chapter. It is anticipated that the Atmospheric Lifetime Experiment (ALE) will make significant progress towards determining the lifetimes of F-11 and F-12 (Cunnold et al., 1978).

(d) Conclusions

In this chapter a set of self-consistent data, collected by Rasmussen over five years, was analyzed to determine the budget lifetimes of CH_3CCl_3 , CFCl_3 (F-11) and CCl_2F_2 (F-12). Several related methods were used to accomplish this, and they all agreed. It was found that the lifetime of CH_3CCl_3 is 8 years (between 7 and 9 years). For CFCl_3

and CCl_2F_2 the results show that their lifetimes are greater than 20 years. The single numbers which can be considered most consistent with the data are $\tau(\text{CFC1}_3) \approx 50$ yrs and $\tau(\text{CCl}_2\text{F}_2) \geq 70$ yrs. It is not possible to put scientific confidence into these specific numbers because of the uncertainties in our knowledge of the emissions of F-11 and F-12 and because the data were not sufficiently detailed either in time or in space. There seems to be little doubt that F-11 and F-12 are long-lived trace gases. Both these fluorocarbons have been, and still are being, released in large quantities. Since 1975 the emissions have not risen according to most estimates, but the concentrations in the atmosphere have still been climbing at a rate of about 10% per year according to measurements (Appendix I). This feature in itself attests to long lifetimes. The possible detrimental effects of these gases on stratospheric ozone have been discussed extensively in the literature (see, for example, Hudson 1977). If the threat to the ozone layer becomes more solidly established, the releases of F-11 and F-12 (and perhaps CH_3CCl_3) will eventually have to be stopped or severely curtailed.

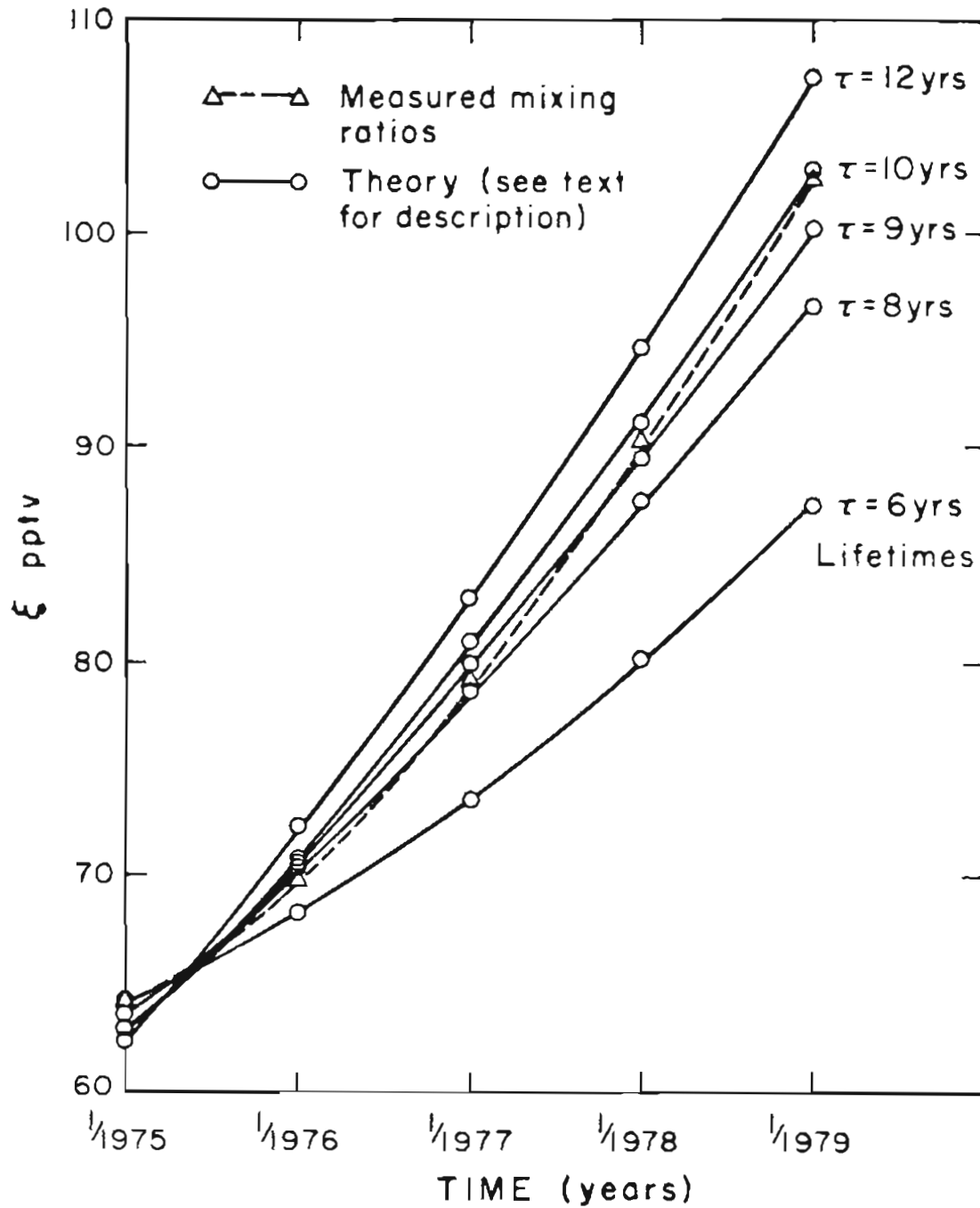


Figure (2.1): Theoretically predicted and measured concentrations of methylchloroform.

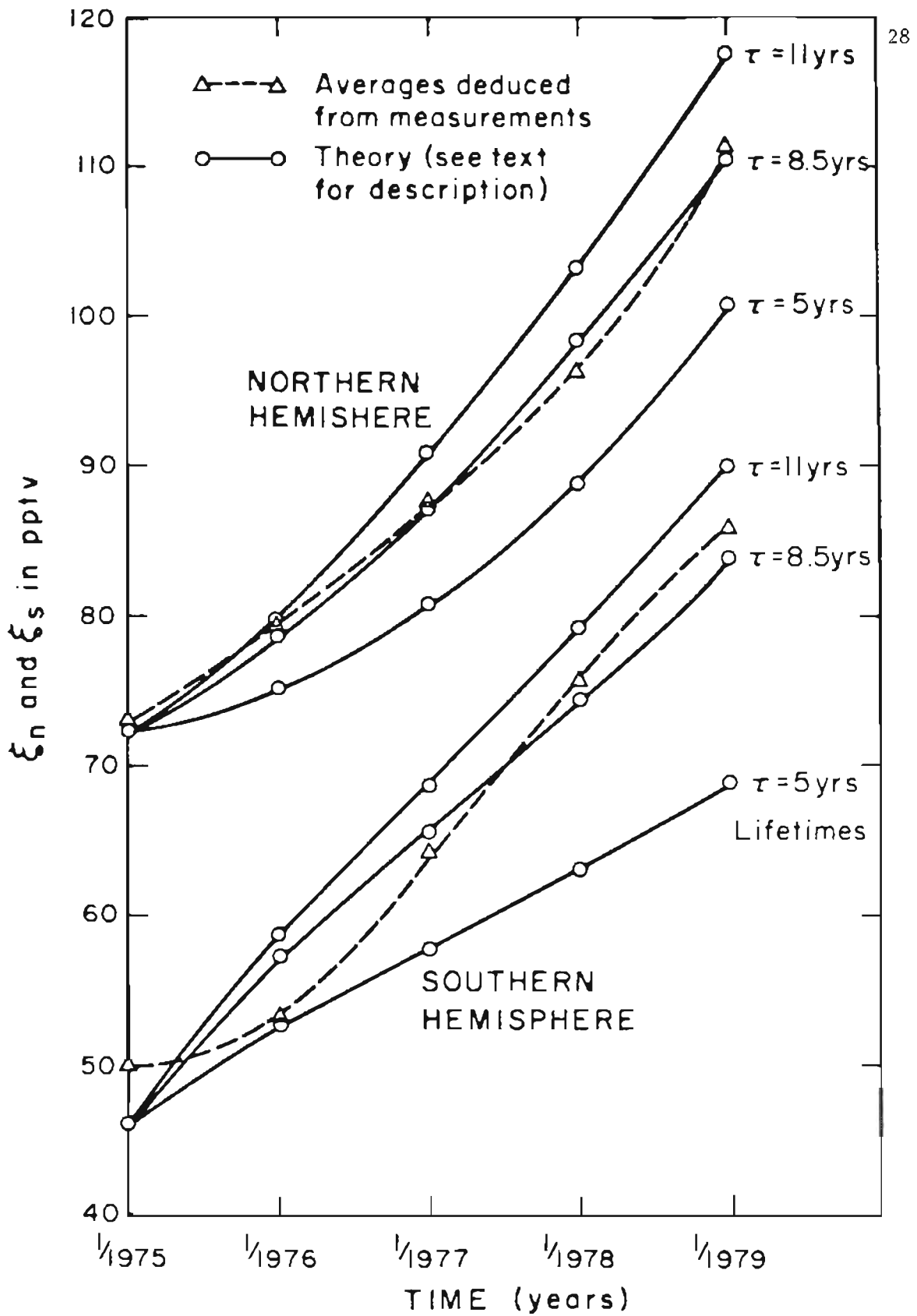


Figure (2.2): Predictions of a hemispherically averaged theory and measured concentrations of CH_3CCl_3

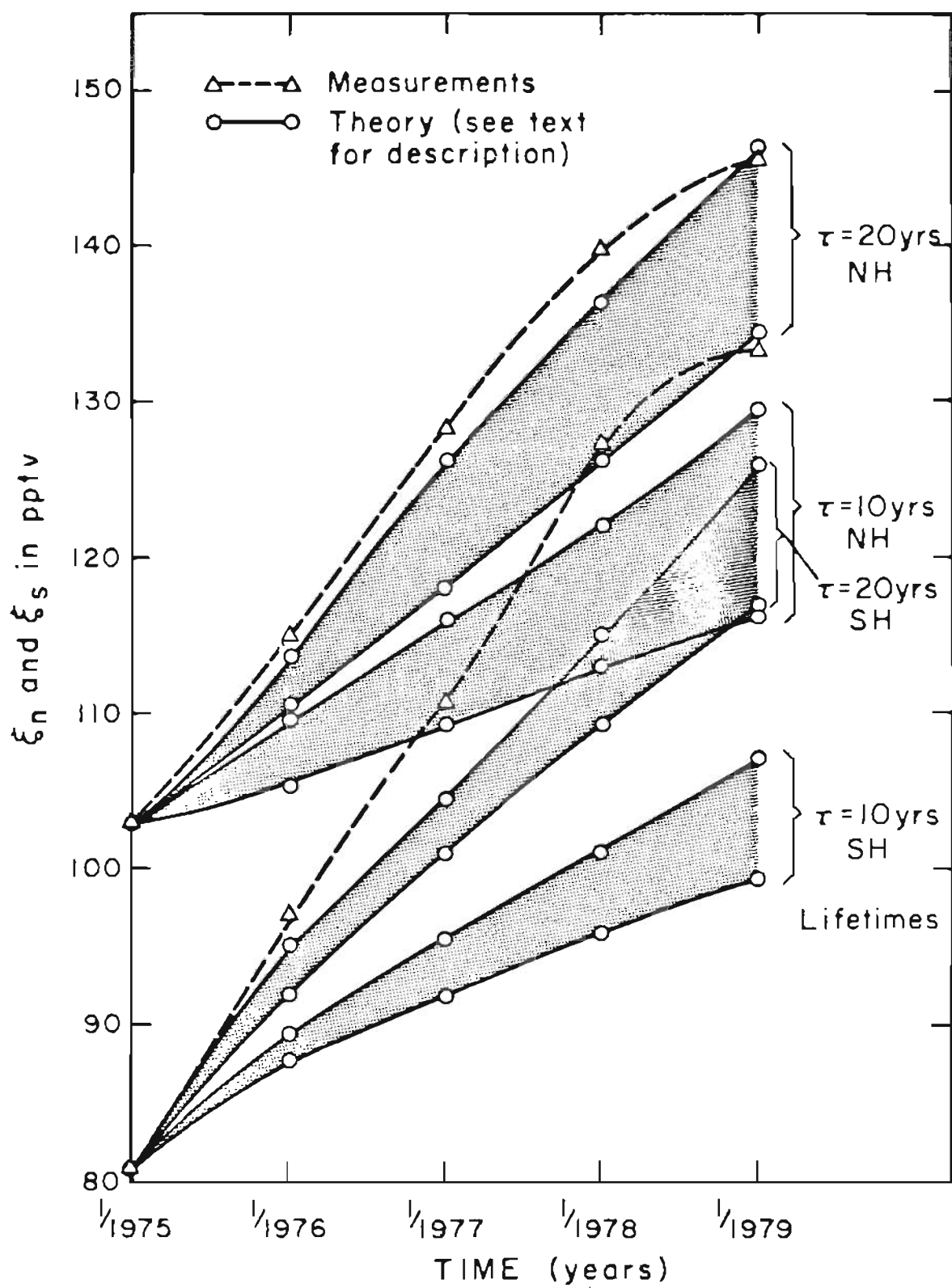


Figure (2.3): Comparison of measurements and theory for F-11

CHAPTER 3. LIFETIME CALCULATIONS: CHEMISTRY

(a) Introduction.

Many anthropogenic and natural gases released into the atmosphere undergo chemical reactions in the global environment, and are thus transformed into species which have completely different environmental behaviour. The fate or cycle of almost all trace gases and elements in the atmosphere is invariably mediated by many "chemical steps". This is indeed a very broad subject constituting much of atmospheric chemistry. This chapter deals with a small group of atmospheric trace gases which have a relatively simple but dominant transformation mechanism. This mechanism is the reaction of the trace gas with HO radicals in the atmosphere. Compared to the immense complexities of the chemistry of polluted urban air, the problem of determining the loss of a trace gas due to first order reactions with HO radicals in the atmosphere is simple from a chemical viewpoint, but is complicated by the irregular motions of the atmosphere.

There are many uncertainties in the calculation of global lifetimes of trace gases based on HO radical reactions, but the most important one is the current lack of information on the tropospheric distribution and absolute concentration of HO radicals. Even the yearly global mean and the mean ground level HO concentrations are not well known at this time. Because of this problem, the calculated global lifetimes of many important trace gases are only approximate and

the limits of reasonable values of the lifetimes are very large.

The next section deals with the methods of calculating global lifetimes of trace gases which react with HO radicals. The general equation describing the global lifetime is used to derive a simpler approximate equation. It is compared with other equations used in the current literature. In section (3.d), the general ideas which govern the HO density in the troposphere are reviewed and the budget, sources and sinks of CH_3CCl_3 are used to estimate the mean hydroxyl radical density. Based on these values, the lifetimes of several trace gases are calculated in section (3.c) and discussed in more detail when necessary.

(b) Hydroxyl Radical Sink of Trace Gases.

It is well known that reaction of many trace gases (particularly those containing hydrogen atoms) with hydroxyl radicals in the troposphere constitute a major sink. In many cases this is the only substantial tropospheric sink. The distribution of hydroxyl radicals in the troposphere, even when diurnally and seasonally averaged, is not well known at present. This situation will be discussed further in section (3.d). This section deals with lifetimes of trace gases based on their reaction with HO radicals in the troposphere. If reaction with HO radicals is the dominant sink, then the lifetimes calculated here are also approximately equal to the global lifetimes. The results of the section can be easily applied to calculating life-

times within smaller compartments of the troposphere.

It is instructive to first derive the general equation relating the global lifetime of a trace gas with the tropospheric concentration and distribution of hydroxyl radicals. Consider a localized region of the atmosphere within which the mass balance of the trace gas can be written as:

$$\frac{d}{dt} C(\underline{x}, t) = S(\underline{x}, t) - \eta(\underline{x}, t) C(\underline{x}, t) + T \quad (3.1)$$

where $C(\underline{x}, t)$ is the burden of the trace gas, inside the local volume, in molecules per unit volume. \underline{x} is the spatial variable denoting λ, ϕ, z (or r) (longitude, latitude, height). $\eta(\underline{x}, t)$ is the sink strength in this region.

$$\eta(\underline{x}) = K(\underline{x}) [\text{HO}](\underline{x}) = \frac{1}{\tau(\underline{x})} \quad (3.2)$$

The destruction of the trace gas as measured by the variable $\eta(\underline{x}, t)$ is a function of time of day and season. Since it is not practical (or perhaps even possible) to take into account the time behaviour of η , $\eta(\underline{x}, t)$ is replaced by $\eta(\underline{x})$ which represents a yearly averaged value. Replacing $\eta(\underline{x}, t)$ by $\eta(\underline{x})$, the time averaged value, may introduce considerable errors because the HO density is so variable in time. At present, however, there is little choice but to make this approximation, since it will take many years of measurements before $\eta(\underline{x}, t)$ can be defined. T is the transport contribution to the contents of the local region and $S(\underline{x}, t)$ is the source within the region (molecules/unit vol. emitted per unit time). Eqn. (3.1) can be integrated over any glo-

bal (as opposed to local) region. For simplicity, let us integrate eqn. (3.1) over the whole troposphere:

$$\frac{d\tilde{C}(t)}{dt} = \tilde{S} - \int_{V_T} \eta(\underline{x}) C(\underline{x}, t) dV_T + \int_{V_T} T dV_T \quad (3.3)$$

where $\int_{V_T} T dV_T$ is the effect of the stratospheric-tropospheric transport on the tropospheric burden, $\tilde{C}(t)$. The goal is to write eqn.

(3.3) as follows:

$$\frac{d}{dt} \tilde{C}(t) = \tilde{S} - \tilde{\eta} \tilde{C} - \int_{V_T} T dV_T \quad (3.4)$$

where $\tilde{\eta}$ is the reciprocal of the average lifetime of the trace gas in the troposphere. Thus, $\langle \tau \rangle = 1/\tilde{\eta}$ which is given by

$$\langle \tau \rangle = \frac{\tilde{C}(t)}{\int_{V_T} \eta(\underline{x}) C(\underline{x}, t) dV_T}$$

or

$$\langle \tau \rangle = \frac{\int_{V_T} \rho(\underline{x}) \xi(\underline{x}, t) dV_T}{\int_{V_T} \eta(\underline{x}) \rho(\underline{x}) \xi(\underline{x}, t) dV_T} \quad (3.5)$$

Eqn. (3.5) follows from the comparison of eqn. (3.3) with eqn. (3.4).

In eqn. (3.5) $C(\underline{x}, t)$ is rewritten as $\rho(\underline{x}) \xi(\underline{x}, t)$, where $\rho(\underline{x})$ is the density of air at \underline{x} and $\xi(\underline{x}, t)$ is the local mixing ratio of the trace gas at \underline{x} and time t . Since it is generally true that the background values of ξ (as well as the values of ρ and η) are approxi-

mately constant around latitude circles so that the longitude integration can be carried out yielding:

$$\langle \tau \rangle = \frac{\int_{-\pi/2}^{\pi/2} \int_0^{z_T} \rho \xi \cos\phi \, dz d\phi}{\int_{-\pi/2}^{\pi/2} \int_0^{z_T} \eta \rho \xi \cos\phi \, dz d\phi} \quad (3.6)$$

The derivation of eqn. (3.6) is carried out on a simplified basis, but it can be supported by more complex reasoning as well. Eqn. (3.6) is not new, but in general it has been ignored in the current literature.

The most common equation currently used for such calculations of lifetimes is given as follows: (see, for example, Davis et al., 1976; Watson et al., 1977).

$$\bar{\tau} = \frac{1}{\bar{K} [\overline{\text{HO}}]} \quad (3.7)$$

where \bar{K} is the rate constant at the average tropospheric temperature. For most trace gases of interest K is given by the Arrhenius equation of the form $K(T) = A \exp [-E/T]$ and so \bar{K} is $\bar{K} = A \exp [-E/\bar{T}]$ where \bar{T} is the average temperature of air in the troposphere. $[\overline{\text{HO}}]$ is the globally averaged HO concentration in the troposphere. There is no rigorous procedure for deriving eqn. (3.7). It is just assumed that $\eta(x) = K(x) [\text{HO}](x)$ in eqn. (3.3) can simply be replaced by $\bar{K} [\overline{\text{HO}}]$.

Jenq Sian Chang and F. Kaufman (1977a, 1977b) attempted to modify eqn. (3.7) to incorporate some of the features of the real atmosphere. It appears that their results are not physically justifiable, but they are a heuristic aid to developing the equations derived later in this section. The Chang-Kaufman approach is summarized next. They derived a global lifetime, let's call it $\bar{\tau}$, by eqn. (3.8) given below:

$$\bar{\tau} = \frac{1}{\bar{\eta}} ; \bar{\eta} = \frac{1}{z_T} \int_0^{z_T} K [\text{HO}] dz \quad (3.8)$$

$$K = A e^{-E/(T_0 - \ell z)} \quad (3.9)$$

Here T is converted to a function of z by $T = T_0 - \ell z$ where T_0 is the average ground level temperature of air over the whole earth, and ℓ is the average temperature lapse rate in the troposphere.

$$K \approx A e^{-E/T_0} \exp \left[-\frac{E\ell}{T_0^2} z \right]$$

$$K = K_0 e^{-\alpha z} ; \alpha = \frac{E\ell}{T_0^2} \quad (3.10)$$

Eqn. (3.10) follows from eqn. (3.9) by assuming

$$\frac{1}{T} = \frac{1}{T_0 - \ell z} \approx \frac{1}{T_0} + \frac{\ell z}{T_0^2} \quad (3.11)$$

which is just the Maclaurin series expansion of $[T_0 (1 - \ell z/T_0)]^{-1}$,

and is a very good approximation for the atmospheric values of ℓ , z_T and T_0 . (z_T is the average tropopause height). The HO concentration was taken to be:

$$[HO] = \overline{[HO]}_0 e^{-z/h} \quad (3.12)$$

where $\overline{[HO]}_0$ is the mean HO radical concentration at ground level. h was taken to be H or ∞ (where H is the scale height of air density). When $h = \infty$, it implies that the HO density is constant with height in the troposphere. With these assumptions eqn. (3.8) can be solved for $\bar{\tau}$ as:

$$\bar{\tau} = \frac{1}{K_0 \overline{[HO]}_0} \frac{\beta z_T}{(1 - e^{-\beta z_T})} \quad (3.13)$$

$$\beta = \alpha + \frac{1}{h} = \frac{E\ell}{T_0^2} + \frac{1}{h} \quad (3.14)$$

The main problem is that $\bar{\tau}$ is based on eqn. (3.8) which cannot be derived from basic principles. It takes into account the idea that HO concentration declines with height, and more importantly, that the reaction rate constant becomes slower with height, but it ignores the fact that the number of molecules of the trace gas per unit volume also declines with height. This physical problem is manifested by not weighting the average of τ by the density of air, ρ . No doubt eqn. (3.13) is a kind of average lifetime, but it does not necessarily correspond to the average lifetime which describes the destruction of a trace gas in the global troposphere. There are many ways to form an

average lifetime and the resulting numbers are different from each other. Only one average is appropriate for describing the average global destruction of trace gases by HO radicals (eqn. 3.6). For example, we can say that the lifetime at any location is $\tau(z) = 1/\eta(z)$, so that the average lifetime is $\bar{\tau}' = \frac{1}{z_T} \int_0^{z_T} \tau(z) dz$, then using $K = K_0 e^{-\alpha z}$; $[HO] = \overline{[HO]}_0 e^{-z/h}$ gives $\bar{\tau}' = [1/(K_0 \overline{[HO]}_0)] [(e^{\beta z_T} - 1)/\beta z_T]$. This is another type of average, different from that of Chang and Kaufman, but it too is inappropriate for describing the global HO sink.

The next step is to develop eqns. (3.6) and (3.7) so that they can be compared directly under the same assumptions for K and $[HO](\phi)$. Consider eqn. (3.6) first. In order to derive a workable equation from this, it is necessary to specify the latitudinal profile for the trace gas. Often the following function is a good approximation:

$$\xi = \begin{cases} a & -\frac{\pi}{2} \leq \phi \leq -\phi_0 \\ \frac{1}{2} (a + b) + \frac{(b - a)}{2\phi_0} \phi & \phi_0 < \phi < -\phi_0 \\ b & \phi_0 \leq \phi \leq \pi/2 \end{cases} \quad (3.15)$$

This profile is discussed further in chapter 8. $d\xi/dz \approx 0$ in the troposphere, and ϕ_0 is usually about $\pi/6$. If $\rho = \rho_0 e^{-z/H}$ and $[HO] = \overline{[HO]}_0(\phi) e^{-z/h}$, then eqn. (3.6) becomes:

$$\langle \tau \rangle = \frac{\Gamma H (1 - e^{-z_T/H})}{(1 - e^{-\Gamma z_T})} \frac{1}{k_0 \overline{[HO]}_0} \quad (3.16)$$

$$\text{where } \Gamma = \alpha + \frac{1}{H} + \frac{1}{h} \quad (3.17)$$

$$\overline{[HO]} = \frac{1}{2} \int_{-\pi/2}^{\pi/2} [HO]_0(\phi) \cos\phi \, d\phi \quad (3.18)$$

(Note that: $\int_{-\pi/6}^{\pi/6} [HO]_0(\phi) \phi \cos\phi \, d\phi = 0$ so that the $(b-a)/2\phi_0$ term

does not enter into eqn. (3.16). This is true as long as $[HO]_0(\phi)$ is symmetric about the equator, i.e., $[HO]_0(\phi) = [HO]_0(-\phi)$ for $-\pi/6 \leq \phi \leq \pi/6$.) Equation (3.16) is derived assuming that a single average air density scale height and lapse rate of temperature can be assumed throughout the atmosphere. It is assumed that h , H , ℓ , z_T , ρ_0 and k_0 are all independent of ϕ -- in reality they are not. Later we shall return to a reconsideration of some of these variables. Because of the symmetries assumed here, the values of ϕ_0 , a , and b do not enter into equation 3.16) for the lifetime.

In order to compare eqn. (3.16) with the usual equation (3.7), it is necessary to convert \bar{K} and $\overline{[HO]}$ in eqn. (3.7) to the same variables as those which define (3.16). \bar{K} is derived as follows:

$$\begin{aligned} T &= T_0 - \ell z \\ \langle T \rangle &= \frac{\int_0^{z_T} \rho T dz}{\int_0^{z_T} \rho dz} = T_0 - \ell \omega \end{aligned} \quad (3.19)$$

$$\omega = H - \frac{z_T}{(e^{z_T/H} - 1)} \quad (3.20)$$

$$K \approx K_0 e^{-\alpha\omega} ; \alpha = \frac{E\ell}{T_0^2} \quad (3.21)$$

Eqn. (3.21) is the usual assumption (see for example Watson et al., 1977). Deriving $\overline{[HO]}$ is difficult, because in practice it is more an intelligent guess than a calculation. Still, it should take the following form:

$$\overline{[HO]} = \frac{1}{z_T} \int_0^{z_T} \frac{1}{2} \int_{-\pi/2}^{\pi/2} [HO]_0(\phi) \cos\phi e^{-z/h} d\phi dz \quad (3.22)$$

$$\overline{[HO]} \approx \frac{h}{z_T} (1 - e^{-z_T/h}) \overline{[HO]}_0 \quad (3.23)$$

$$\overline{\tau} = \frac{z_T e^{\alpha\omega}}{h(1 - e^{-z_T/h})} \frac{1}{K_0 \overline{[HO]}_0} \quad (3.24)$$

Eqn. (3.24) is another version of eqn. (3.7) which is most commonly used. It is evident that eqns. (3.16) and (3.24) are different.

$$\overline{\tau} = \delta \langle \tau \rangle \quad (3.25)$$

$$\delta = \frac{z_T e^{\alpha\omega} (1 - e^{-\Gamma z_T})}{\Gamma H (1 - e^{-z_T/H}) h (1 - e^{-z_T/h})} \quad (3.26)$$

δ is the measure of how different $\overline{\tau}$ of eqn. (3.7) is from $\langle \tau \rangle$ of eqn. (3.6). Obviously δ depends in a complex way on the activation energy,

E' , so that agreement between $\bar{\tau}$ and $\langle\tau\rangle$ will be different for different trace gases. Similarly, one may define δ' so that

$$\bar{\tau} = \delta' \langle\tau\rangle \quad (3.27)$$

$$\delta' = \frac{\beta z_T (1 - e^{-\Gamma z_T})}{\Gamma H (1 - e^{-z_T/H})(1 - e^{-\beta z_T})} \quad (3.28)$$

δ' measures the difference between $\bar{\tau}$, the lifetime derived by Chang and Kaufman and the lifetime implied by eqn. (3.6). δ'' is defined by $\bar{\tau} = \delta'' \bar{\tau}$, $\delta'' = \delta'/\delta$. δ'' measures the difference between the simple averaged equation (3.7) and the lifetime derived by Chang and Kaufman. As examples five atmospheric trace gases were chosen with a wide range of activation energies: C_2H_6 , H_2 , $CHClF_2$ (F-22), CH_3CCl_3 , and C_2HCl_3 (trichloroethylene). C_2HCl_3 was chosen because its E' is negative (reaction with HO is faster at lower temperatures) -- this is somewhat rare for gases in the atmosphere. The results are summarized in the table (3.1) below:

Table (3.1): Comparison of Lifetimes
 $\langle\tau\rangle$, $\bar{\tau}$ and $\bar{\tau}$

Trace Gas	δ		δ'		δ''	
	$h=H$	$h=\infty$	$h=H$	$h=\infty$	$h=H$	$h=\infty$
C_2H_6	1.62	1.20	1.35	1.24	0.83	1.03
H_2	1.55	1.16	1.33	1.22	0.86	1.05
$CHClF_2$	1.41	1.09	1.29	1.17	0.92	1.07
CH_3CCl_3	1.37	1.07	1.28	1.15	0.93	1.07
C_2HCl_3	1.11	1.01	1.10	0.96	0.99	0.95

It was assumed that $T_0 = 288^\circ\text{K}$, $z_T = 12 \text{ km}$, $H = 9 \text{ km}$ and $\ell = 6.5^\circ\text{K/km}$. In general the three lifetimes agreed with each other for $h = \infty$ (scale height of HO). Most theoretical models do not support this assumption (see for example Atkinson et al., 1979; Crutzen et al., 1978; Crutzen and Fishman, 1977; Levy II, 1974; Penner et al., 1977; Warneck, 1975; Stewart and Hoffert, 1975). When $h = H$, the disagreement between $\langle\tau\rangle$ and $\bar{\tau}$ is quite large, so that $\bar{\tau}$ overestimates the lifetime by ~40% for CH_3CCl_3 and CHClF_2 . Similarly $\langle\tau\rangle$ is also in disagreement with $\bar{\tau}$, but to a slightly lesser extent. All three lifetimes agreed for trichloroethylene. The higher the activation energy is the bigger the disagreement; and reasonable agreement was achieved only for a gas with negative E^\ddagger . It is interesting that lifetime equation derived by Chang and Kaufman ($\bar{\tau}$) was in very close agreement with $\bar{\tau} = 1/\bar{K} [\overline{\text{HO}}]$, for all the gases studied and for both conditions ($h = \infty$ and $h = H$). So, there is little point in using $\bar{\tau}$ since it gives the same answer as the simpler equation $\bar{\tau} = 1/\bar{K} [\overline{\text{HO}}]$ which is commonly used. In their papers Chang and Kaufman (1977a, 1977b) calculated longer lifetimes than previously estimated. They assumed $[\overline{\text{HO}}]_0 = 1 \times 10^6$ molecules/cm³, but when they assumed $h = H$, it meant that $[\overline{\text{HO}}] \approx 5.5 \times 10^5$ molecules/cm³. It was because of this feature that they obtained longer lifetimes, and not because of the inclusion of temperature variation of the reaction rate constant. The δ , δ' and δ'' are so constructed as to be independent of the assumed global average of HO radical density ($[\overline{\text{HO}}]$) (also independent of K_0), so they reflect more accurately the model dependent effects.

This leaves equations (3.7) and (3.16) to choose from. The choice depends on the height variation of HO density. The faster the decline of HO concentration with height, the larger the δ will be. Many theoretical models give $h < H$, on the average, rather than $h > H$ (for example: $h \sim 8$ km for winter, and $h \sim 12$ km up to about 7 km height and $h \sim 4$ km above 7 km height to the tropopause, for the summer (Levy, 1974); $h \sim 8$ km (Penner et al., 1977), $h \sim 5$ km (Atkinson et al., 1978)) This will be discussed further in the next section (d). Since eqn. (3.16) is almost as simple as eqn. (3.7), it can be used in place of eqn. (3.7).

Clearly eqn. (3.16) is a rather simplified form of the more basic equation (3.6). Eqn. (3.16) can be improved by writing it as:

$$\langle \tau \rangle = \frac{H(1 - e^{-z_T/H})}{K_0 [\text{HO}]_0 G} \quad (3.29)$$

$$G = \int_0^{z_T} e^{-\beta z} g(z) dz; \quad \beta = \frac{E\ell}{T_0^2} + \frac{1}{H} \quad (3.30)$$

In eqn. (3.30), $g(z)$ is the function which describes the height variation of HO density so that $[\text{HO}]_0 = [\text{HO}]_0(\phi)g(z)$. Aside from the problem of knowing $g(z)$, the assumption regarding symmetry of the HO about the equator between $-\pi/6 < \phi < \pi/6$ may not be justified, in which case the "b" and "a" (concentrations of the trace gas) may also enter into the lifetime equation. The latitudinal variation of ℓ (lapse rate), K , and density scale height H as well as the changing tropopause height with ϕ may all be significant. There may be longitudinal variations in

both η and ξ which may become important in calculating $\langle \tau \rangle$. Furthermore, the details of the variability of η in time (during a year) may also be important. Such effects are likely to influence short-lived trace gases more than long-lived ones, and so in this study attention is primarily confined to trace gases with lifetimes $\gtrsim 3$ yrs. Eqn. (3.6) can be solved with the inclusion of many of these features, but the resulting equation is much more complicated compared to (3.16). Appendix I may be consulted for a slightly improved version of eqn. (3.16).

(c) Lifetimes of selected trace gases.

HO radicals in the troposphere can be estimated by various means. Some of the available methods are discussed in the next section. There are many uncertainties in the estimation of mean HO densities $\overline{[HO]}$ and $\overline{[HO]}_0$. In the next section CH_3CCl_3 is used to derive $[HO]$ and $[HO]_0$ with the result that values of $\overline{[HO]}_0$ are calculated to be between 3 and 6×10^5 molecules/cm³ (as the global mean, yearly ground level HO concentrations). Most calculations reported in the literature simply assume a fixed value of $\overline{[HO]}$ and thus give a particular lifetime for a trace gas. This looks good, but it hides the uncertainties. The calculations reported in this section give a range for the estimated lifetime, and the most probable value. Equation (3.16) is used to calculate the lifetimes assuming that $h = H$. Calculations assuming that $h > H$ ($h \sim \infty$) were also carried out but for these calculations $\overline{[HO]}_0$ is ta-

ken to be $2.1 - 4.2 \times 10^5$ molecules/cm³. (In this case $\overline{[HO]}_0 = \overline{[HO]}$ and Γ in eqn. (3.16) is $E\ell/T_0^2 + 1/H$.) The smaller values of $\overline{[HO]}_0$ assumed for $h \rightarrow \infty$ offset the effect of going from $h = H$ to $h = \infty$ in eqn. (3.16) and the resulting lifetimes are approximately the same under both assumptions. The rationale for adopting smaller $\overline{[HO]}_0$ values when $h \rightarrow \infty$ is evident from the discussion of the next section. Whether $h = H$ or $h = \infty$, the budget lifetime of CH₃CCl₃ remains unaffected. If we assume $h = H$, smaller values of $\overline{[HO]}$ suffice to explain the budget lifetime, if $h = \infty$, it requires larger values of $\overline{[HO]}$ (but smaller values of $\overline{[HO]}_0$) to explain the same lifetime.

Table (3.2) below summarizes the results for some trace gases.

Table (3.2): Lifetimes of Some Trace Gases
Due to HO Radical Interactions.

Trace Gas	Lifetime (yrs.)	Probable Lifetime (yrs.)	Trace Gas	Lifetime (yrs.)	Probable Lifetime (yrs.)
CH ₃ Cl	2.7-5.4	3.2			
CH ₂ Cl ₂	0.9-1.8	1.1	CH ₂ F ₂	24-48	30
CHFC1 ₂	4-9	5	CH ₂ FC1	3.7-7.4	4.5
CHF ₂ Cl	34-68	40	CH ₃ CHF ₂	2.6-5.2	3.2
CH ₂ ClF	3.2-6.6	4	CH ₃ CF ₂ Cl	36-72	44
C ₂ Cl ₄	0.8-1.6	1	CHFC1CF ₃	14-28	17
C ₂ HCl ₃	0.03-0.06	0.04	CHCl ₃	1.2-2.4	1.5
CH ₃ Br	3-518	3.6	COS		~ 2
CH ₄	20-40	25	H ₂ S	1-2 weeks	8 days
C ₂ H ₂	0.1-0.2	0.13			

The probable lifetime given in Table (3.2) is based on the assumption that the lifetime of CH_3CCl_3 due to HO interactions is 9 yrs. This is the most reasonable estimate based on the current data. The reaction rate constants for CH_2F_2 , CH_2FCl , CH_2Cl_2 , C_2H_2 , CH_3CHF_2 , $\text{CH}_3\text{CF}_2\text{Cl}$ and CHFClCF_3 are taken from Atkinson et al. (1978). The rate constants for the remaining species are taken from DeMore et al. (1979). The lower limits of the lifetime are true if the lifetime of CH_3CCl_3 with respect to HO interactions is ~ 7 yrs, and the upper limit is true if the CH_3CCl_3 lifetime with respect to HO interaction is ~ 14 yrs. Both limits are within the range of feasible lifetimes and as mentioned before $\tau_{\text{HO}}(\text{CH}_3\text{CCl}_3) = 9$ yrs. is used to calculate the single value in column 3.

The lifetimes that are shown here are generally longer than previous estimates. This is primarily due to the lower HO densities assumed here (which are justified in the next section). For the same $\overline{[\text{HO}]}$ the equation adopted for this study actually gives shorter lifetimes than the usual method of estimating lifetimes by $\bar{\tau} = \{\bar{K} \overline{[\text{HO}]}\}^{-1}$. It is very unlikely that more sophisticated theories, using the same HO densities as adopted here, can lower the calculated lifetimes by any significant amount (factor of two below the τ in col. 3 would be a significant amount).

The usually accepted lifetimes for CHFCl_2 (F-21) and CHF_2Cl (F-22) are ≤ 2 yrs and 15-25 yrs respectively. The calculation of this section give ~ 5 years and ~ 40 years for the lifetimes of F-21 and F-22. Currently available measurement data on these two compounds are simply

not sufficient to resolve this rather sizeable discrepancy. Let us take F-21 for further consideration. If the lifetime of F-21 is indeed ≤ 2 yrs, then it is possible that all the numbers in Table (3.2) may be too high. The method of eqn. (3.16) is not directly challenged by this discrepancy, but the HO concentrations adopted here would be so challenged. The case for the longer lifetime of F-21 can be strengthened by the following argument: Consider the more general equations (3.29) and (3.30) for F-21 and CH_3CCl_3 (MC)

$$\langle \tau \rangle_{\text{F-21}} = \frac{H (1 - e^{-z_T/H})}{K_o(\text{F-21}) [\text{HO}]_o G(\text{F-21})} \quad (3.31)$$

$$\langle \tau \rangle_{\text{MC}} = \frac{H (1 - e^{-z_T/H})}{K_o(\text{MC}) [\text{HO}]_o G(\text{MC})} \quad (3.32)$$

$$\frac{\langle \tau \rangle_{\text{MC}}}{\langle \tau \rangle_{\text{F-21}}} = \frac{K_o(\text{F-21}) G(\text{F-21})}{K_o(\text{MC}) G(\text{MC})} \quad (3.33)$$

$$G(\text{F-21}) = \int_0^{z_T} e^{-\beta(\text{F-21})z} g(z) dz$$

$$G(\text{MC}) = \int_0^{z_T} e^{-\beta(\text{F-21})z} g(a) dz$$

Since $\beta(\text{F-21}) = 0.204/\text{km}$ and $\beta(\text{MC}) = 0.225/\text{km}$, $G(\text{F-21}) \approx G(\text{MC})$ so that $\langle \tau \rangle_{\text{MC}} / \langle \tau \rangle_{\text{F-21}} \approx k_o(\text{F-21}) / k_o(\text{MC}) = 1.51$ ($T_o = 288^\circ\text{K}$). Now, if $\langle \tau \rangle_{\text{F-21}}$ is ≤ 2 yrs, then $\langle \tau \rangle_{\text{MC}}$ would have to be ≤ 3 yrs. These numbers are based on the generally accepted rate constants $K(\text{MC}) = 2.5 \times 10^{-12} \text{ exp}$

$[-1450/T]$ cm^3 per molecule-sec. and $K(\text{F-21}) = 1.5 \times 10^{-12} \exp$
 $[-1184/T]$ (DeMore et al., 1979). Note that the ratio in eqn. (3.33)
 is independent of the global hydroxyl radical concentration. (Another
 way to look at this is to use the usual eqn. $\bar{\tau} = 1/\bar{K} [\overline{\text{HO}}]$ so that
 $\bar{\tau}(\text{MC})/\bar{\tau}(\text{F-21}) = \bar{K}(\text{F-21})/\bar{K}(\text{MC}) = 1.64 \bar{T} = 266^\circ\text{K}$). So, if the $[\overline{\text{HO}}]$ esti-
 mate is raised to give $\langle\tau\rangle(\text{F-21}) = 2$ yrs, then $\langle\tau\rangle(\text{CH}_3\text{CCl}_3)$ will become
 at most about 3.2 yrs. This low value of $\langle\tau\rangle(\text{MC})$ is not supported by
 any budget analysis. The possible explanations for the discrepancy be-
 tween the often assumed 2 yr lifetime of F-21 and the ~ 5 yr lifetime
 calculated here are: (i) the true rate constant of F-21 reaction with
 HO is faster than the currently accepted values; (ii) the true CH_3CCl_3
 rate constant is slower than currently accepted, or (iii) both rate con-
 stants are correct but there is a bigger source of CH_3CCl_3 than cur-
 rently assumed and the $\langle\tau\rangle_{\text{MC}}$ is ~ 3 yrs and (iv) the lifetime of F-21
 is ~ 5 yrs. The second and third possibilities would both lead to the
 prediction of higher HO concentrations in the troposphere (to $[\overline{\text{HO}}] \sim$
 0.7×10^6 molecules per cm^3). It is unlikely that (iii) is the correct
 explanation, but (i) and (ii) are possible. If (i) is the explanation,
 then the remaining calculations in Table (3.2) are unaffected. There
 is some uncorroborated evidence for (i) in the measurements of Clyne
 and Hoyle (reported in Atkinson et al., 1978, and DeMore et al., 1979)
 who measured $K(\text{F-21}) = 4.75 \times 10^{-12} \exp [-1431/T]$. These measure-
 ments were made for $293^\circ\text{K} \leq T \leq 413^\circ\text{K}$, which is a higher range than
 that needed for tropospheric calculations. It is also possible that
 F-21 has other sinks than HO which could lower its global lifetime,

long lifetime of CH_4 implied here also affects the CO budget (see Bolin
 et al., 1979 for a review of the current status). The production of CO
 by a series of steps has been suggested. Such transformations can pro-

$[-1450/T]$ cm^3 per molecule-sec. and $K(\text{F-21}) = 1.5 \times 10^{-12} \exp$
 $[-1184/T]$ (DeMore et al., 1979). Note that the ratio in eqn. (3.33)
 is independent of the global hydroxyl radical concentration. (Another
 way to look at this is to use the usual eqn. $\bar{\tau} = 1/\bar{K} [\overline{\text{HO}}]$ so that
 $\bar{\tau}(\text{MC})/\bar{\tau}(\text{F-21}) = \bar{K}(\text{F-21})/\bar{K}(\text{MC}) = 1.64 \bar{T} = 266^\circ\text{K}$). So, if the $[\overline{\text{HO}}]$ esti-
 mate is raised to give $\langle\tau\rangle(\text{F-21}) = 2$ yrs, then $\langle\tau\rangle(\text{CH}_3\text{CCl}_3)$ will become
 at most about 3.2 yrs. This low value of $\langle\tau\rangle(\text{MC})$ is not supported by
 any budget analysis. The possible explanations for the discrepancy be-
 tween the often assumed 2 yr lifetime of F-21 and the ~ 5 yr lifetime
 calculated here are: (i) the true rate constant of F-21 reaction with
 HO is faster than the currently accepted values; (ii) the true CH_3CCl_3
 rate constant is slower than currently accepted, or (iii) both rate con-
 stants are correct but there is a bigger source of CH_3CCl_3 than cur-
 rently assumed and the $\langle\tau\rangle_{\text{MC}}$ is ~ 3 yrs and (iv) the lifetime of F-21
 is ~ 5 yrs. The second and third possibilities would both lead to the
 prediction of higher HO concentrations in the troposphere (to $[\overline{\text{HO}}] \sim$
 0.7×10^6 molecules per cm^3). It is unlikely that (iii) is the correct
 explanation, but (i) and (ii) are possible. If (i) is the explanation,
 then the remaining calculations in Table (3.2) are unaffected. There
 is some uncorroborated evidence for (i) in the measurements of Clyne
 and Hoyle (reported in Atkinson et al., 1978, and DeMore et al., 1979)
 who measured $K(\text{F-21}) = 4.75 \times 10^{-12} \exp [-1431/T]$. These measure-
 ments were made for $293^\circ\text{K} \leq T \leq 413^\circ\text{K}$, which is a higher range than
 that needed for tropospheric calculations. It is also possible that
 F-21 has other sinks than HO which could lower its global lifetime,

but that is a different issue altogether. As far as the current measurements of F-21 and F-22 are concerned, there are about 1-2 ppt of F-21 and ~ 47 ppt of F-22 in the atmosphere. Both these values are higher than can be explained on the basis of our current knowledge of their sources, so longer lifetimes are indicated (see also Chapter 7).

The long CH_4 (methane) lifetime is also at variance with the usually accepted value of 2-3 years based on the methane budget (see Walker, 1977; Seinfeld, 1975). It has been the prevalent belief that the only significant sink of CH_4 is its reaction with HO radicals. If this is true, then since the CH_4 reaction rate with HO is slower than the reaction rate of CH_3CCl_3 with HO, it implies that a 2-3 yr lifetime of CH_4 would lead to a CH_3CCl_3 lifetime of less than ~ 1 yr. Certainly the CH_3CCl_3 budget cannot support a lifetime this short. To resolve this difference between the CH_4 lifetimes, one has to either consider a much faster CH_4 sink other than HO reactions (implying that HO does not control the CH_4 budget) or one has to cut down substantially the estimated CH_4 source. Neither of these possibilities can be dismissed with information currently available. It is very difficult to accurately estimate the CH_4 source strength, and the current estimates may be in error. The interested reader is referred to the recent paper of Mayer et al. (1979) which reaches similar conclusions. The long lifetime of CH_4 implied here also affects the CO budget (see Bolin et al., 1979 for a review of the current status). The production of CO by a series of steps has been suggested. Such transformations can pro-

duce large amounts of CO ($1500 - 5000 \times 10^{12}$ g/yr, > 3 times the anthropogenic CO contribution). If CH₄ has a long lifetime with respect to HO radical reactions, then this source of CO could be much smaller (this conclusion was first reached by Warneck (1976)). On the other hand, there is no shortage of CO sources. The long CH₄ "HO lifetimes" cannot be denied on the basis of the CO budget because of the existence of so many sources and the uncertainties in their global strengths. The production of CO by transformations of C₅H₈ (isoprene) are currently being studied. The possible results of this evaluation could be that C₅H₈ would compensate for the CO production from CH₄. CH₄ may have other sinks than HO reactions which would reduce its global lifetime, but if such sinks are not related to HO, the discussion in this section will still be applicable without change. It is perhaps appropriate to conclude this discussion by stating that the CO, CH₄ budgets are not completely understood at this time, and the relative roles of these and other natural emissions on global HO densities are still undecided.

The three species CH₃CHF₂, CH₃CF₂Cl, and CHFClCF₃ are used as propellants and may come into greater use as F-11 and F-12 are removed from inessential uses. The environmental effects of increasing releases of these compounds have not yet been fully determined. The last two contain chlorine and are quite long-lived.

The effect of HO radicals on H₂S is minor compared to atmospheric

reactions with O, O₂, and O₃ (lifetime < ~ a day). For very short-lived species such as acetylene (C₂H₂), C₂HCl₃, and H₂S equations for $\langle \tau \rangle$ and $\bar{\tau}$ would require some modification to obtain more accurate results since their mixing ratios may decline with height and could vary longitudinally. These short-lived compounds are most affected by HO densities in the boundary layer.

For compounds whose "HO-lifetimes" are large (> ~ 15 yrs), the lifetime calculated from HO reactions may be significantly different compared to the total global lifetime because even weak sinks are effective (e.g., stratospheric photodissociation).

Many halocarbons also react with O(¹D) (e.g., F-21, F-22), with rate constants about four orders of magnitude faster than those for HO reactions, but this is overwhelmed by the smallness of the O(¹D) densities in the lower troposphere (~ 7-8 orders of magnitude smaller than HO density).

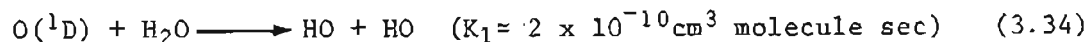
The sources and sinks for most of the compounds listed in Table (3.2) can be found in the references (Graedel, 1978).

(d) Estimates of Mean HO Radical Concentrations in the Troposphere.

It is apparent that the tropospheric HO radicals play a key role in the destruction of many atmospheric trace gases, both natural and anthropogenic. Indeed, the assessment of the relative dangers to the ozone layer from chlorine-containing trace gases of anthropogenic origin is often made on the basis of their reactivity with tropospheric

HO radicals (e.g., CH_3CCl_3). Aside from this aspect of tropospheric HO radicals, they are also believed to control the global distributions and budgets of many important atmospheric constituents, such as CO, CH_4 , SO_2 , NO_2 , and a variety of halocarbons. Consequently, considerable research efforts have been made, both in the measurement of HO radicals (Davis et al., 1976; Penner et al., 1976; and Campbell et al., 1979) and in theoretical estimates of HO concentrations and distribution (Warneck, 1975; Crutzen and Fishman, 1977; Levy, 1974; Penner et al., 1977; and Hov and Isaksen, 1979 (polluted air)).

The general reactions governing HO concentrations can be summarized as follows: The primary production mechanism for HO in the troposphere is the reaction of $\text{O}(^1\text{D})$ with H_2O :



The production of $\text{O}(^1\text{D})$ is photochemically controlled by the reactions $\text{O}_3 + h\nu \xrightarrow{\text{J}} \text{O}(^1\text{D}) + \text{O}_2$, $\text{O}(^1\text{D}) + \text{N}_2 \longrightarrow \text{O} + \text{N}_2$ and $\text{O}(^1\text{D}) + \text{O}_2 \longrightarrow \text{O} + \text{O}_2$ (Warneck, 1975). There are other processes that lead to additional HO production. These are reviewed by Levy II (1974) and Warneck (1975). Losses of HO radicals are dominated by their destruction from reactions with CO, CH_4 , and NO_2 . Various other losses are reviewed by Levy II (1974). Since the lifetime of HO is very short (\sim few seconds) a photostationary state results rather rapidly, thus

$$\frac{dn(\text{HO})}{dt} = P(t) - L(t) \approx 0 \quad (3.35)$$

$$L(t) \approx n(\text{HO}) Q(t) \quad (3.36)$$

$$n(\text{HO}) = \frac{P}{Q} \quad (3.37)$$

or

$$\begin{aligned} n(\text{HO}) = & \{ 2n[\text{O}(^1\text{D})] n(\text{H}_2\text{O}) K_1 + \\ & n(\text{HO}_2) n(\text{NO}) K_2 + n(\text{HNO}_3) J_1 + n(\text{HNO}_2) J_2 \\ & + 2n(\text{H}_2\text{O}_2) J_3 + n(\text{CH}_3\text{O}_2\text{H}) J_4 \} \div \{ n(\text{NO}_2) K_3 \\ & + n(\text{NO}) K_4 + n(\text{HNO}_3) K_5 + n(\text{CO}) K_6 \\ & + n(\text{H}_2\text{O}_2) K_7 + n(\text{H}_2) K_8 + n(\text{CH}_4) K_9 \\ & + n(\text{H}_2\text{C}=\text{O}) K_{10} + n(\text{CH}_3\text{O}_2\text{H}) K_{11} + n(\text{HO}_2) K_{12} \} \end{aligned} \quad (3.38)$$

where $n(x)$ is the density (molecules/unit vol.) of species x . Eqn. (3.38) is derived by Levy II (1974). The complete list of the loss and production reactions along with the rate constants are given in Levy's (1974) paper. In Warneck's study (1975), two production mechanisms are used: the $\text{O}(^1\text{D})$ reaction with H_2O and the conversion of HO_2 by the reactions $\text{HO}_2 + \text{NO} \rightarrow \text{HO} + \text{NO}_2$ and $\text{HO}_2 + \text{O}_3 \rightarrow \text{HO} + 2\text{O}_2$. Reaction of HO with NO_2 , CO , and CH_4 are the destruction mechanisms, leading to:

$$\begin{aligned} n(\text{HO}) = & \{ 2n[\text{O}(^1\text{D})]n(\text{H}_2\text{O})K_1 + n(\text{HO}_2)[n(\text{NO})K_2 + K_3n(\text{O}_3)] \} \div \\ & \{ K_3n(\text{NO}_2) + K_6n(\text{C}) + K_9n(\text{CH}_4) \} \end{aligned} \quad (3.39)$$

There may be other loss mechanisms of HO, which may be significant in reducing HO average concentrations in the atmosphere. Either eqn. (3.38) or eqn. (3.39) can be used to determine the approximate height and latitudinal variation of $n(\text{HO})$, by putting in the height and latitudinal variations of the molecules involved. Eqn. (3.39) is sufficient for most of the troposphere, but the inclusion of H_2 may be required. Ammonia ($\text{NH}_3 \sim 6$ ppb), HNO_3 (~ 10 ppb), H_2S , SO_2 , and CH_3Cl (~ 0.6 ppb) may also exert minor influences on HO densities especially in the lower troposphere.

In the boundary layer over large areas of the earth, compounds such as isoprene may be able to control the HO densities. Isoprene (C_5H_8), for example, has a reaction rate constant with HO of $6 - 8 \times 10^{-11}$ $\text{cm}^3/\text{molecule-sec}$. (more than 200 times faster than CO) and $\frac{1}{2} - 3$ ppb ambient concentrations have been reported (Rasmussen, private communication; see also Graedel, 1978; Zimmerman, 1979). In the first two kilometers of the atmosphere such compounds, in the absence of other HO production mechanisms, may lead to considerably diminished HO densities. Isoprene is just one example of very short-lived compounds which are emitted in incredibly large quantities by plants and seaweeds (the work on isoprene emissions by plants, pioneered by Rasmussen, Went, and Sanadze, is extensive and cannot be properly reviewed here, but the interested reader is referred to the publications of these authors). Up to now an evaluation of the effects of isoprene and similar species on the HO densities

in the boundary layer, has not been carried out. The implications for the global HO densities should be assessed (Appendix I contains further information on the sinks for HO).

Transport of HO in the troposphere is negligible because its lifetime is very short (\sim seconds). $n(\text{HO})$ rapidly approaches 0 as the night falls. $n(\text{HO})$ decreases sharply with increasing latitude, both through lowered H_2O density and through lower production of $\text{O}(^1\text{D})$. Similarly, the daily average of $n(\text{HO})$ is significantly lower in the winter than in summer because of increased solar zenith angle (which reduces intensity of UV needed to produce $\text{O}(^1\text{D})$), decrease in length of day and lower values of $n(\text{H}_2\text{O})$. The height profile is affected primarily by the balance between the increase of $\text{O}(^1\text{D})$ with altitude, and the sharp decline of $n(\text{H}_2\text{O})$ with altitude as well as the scaling of K_3 , K_6 and K_9 along with $n(\text{CO})$, $n(\text{CH}_4)$ and $n(\text{NO}_2)$. Consequently, $n(\text{HO})$ decreases with height, slowly in the first 5 km or so, then very rapidly up to the tropopause (Levy II, 1975; Walker, 1977). As mentioned earlier, some models predict sharper declines in $n(\text{HO})$ with height, throughout the troposphere, especially in low latitudes (see also Crutzen and Fishman, 1977). Latitudinally, $n(\text{HO})$ is believed to be higher at given southern hemisphere latitudes than the comparable northern hemisphere latitudes. Since CO is by far the strongest sink for HO because of its high ambient concentrations and relatively fast reaction with HO, the latitudinal distribution of CO (see for example Seiler and

Junge, 1970) controls the latitudinal distribution of HO. It is believed that there is a significant difference between CO concentrations in the two hemispheres, with more CO in the northern than southern hemisphere, partly due to increasing anthropogenic contributions. NO may also have a similar effect. The difference between the HO levels in the two hemispheres hinges on the CO levels, which are currently under experimental study. Concern has been expressed that increasing anthropogenic contributions to CO and CH₄ could lead to a lowering of tropospheric HO radical steady state concentrations. This could have dire consequences. The lifetimes of some undesirable trace gases (like CH₃CCl₃) can go up leading to serious environmental effects.

Since there are diurnal, seasonal and latitudinal variations of $n(\text{HO})$, the globally and yearly averages $n(\text{HO}) = \overline{n(\text{HO})} = \overline{[\text{HO}]}$ is much smaller than noontime tropospheric HO concentrations at low latitudes in bright sunshine. The problem of measuring tropospheric HO radicals is complex, partly because even the largest expected tropospheric concentrations are very small ($< \sim 0.4$ ppt). Davis et al. (1976) report $\sim 4 - 8 \times 10^6$ molecules/cm³ at 21 - 32°N latitude, at about noontime in October and at the altitude of ~ 7 km; Perner et al. (1976) report lower tropospheric $n(\text{HO})$ levels of $3 - 7 \times 10^6$ molecules/cm³ on bright days during August at $\sim 51^\circ\text{N}$. Closer to winter $n(\text{HO})$ dropped, often below detection limits. Campbell et al. (1979) have reported $n(\text{HO})$ at $\sim 3 \times 10^6$ molecules/cm³ on sunny July days at near noontime ($\sim 45^\circ\text{N}$

latitude). Most of their other measured values were considerably lower ranging from 0.3 to 1×10^6 molecules/cm³.

This completes the review of the general theory which can be used to estimate $\overline{[HO]}$ (global, yearly average) and the experimental data base which can also be used to estimate $\overline{[HO]}$. The problems associated with either approach are quite clear. The experimental values are too few, at only a few locations, and at only a few times per year. Their accuracy is not known. The experimental values at this time can be used only to check the consistency of the theoretically calculated HO concentrations for the conditions compatible with those under which measurements were made. The theoretical expressions derived above require a considerable amount of detailed knowledge of the distributions of trace gases such as CO, CH₄, and NO₂, as well as the knowledge of H₂O density. Furthermore, it requires knowledge of several photochemical rate constants as functions of time of year, cloudiness, etc.

Another method for deducing $\overline{[HO]}$ is to consider the atmospheric budget of some trace gas whose dominant loss in the troposphere is reaction with HO radicals. The procedure works as follows: (i) Determine the global lifetime of the trace gas by budget methods, i.e., by comparing the time release history of the gas with global measurements. (ii) If the main tropospheric loss is through HO reactions, then the tropospheric lifetime, $\bar{\tau}$, of the trace gas can be substituted into the equation $\overline{[HO]} = [\bar{K} \bar{\tau}]^{-1}$ to give $\overline{[HO]}$ or into eqn. (3.16) which is ex-

pected to be better, where K is the reaction rate constant. This method requires knowledge of the reaction rate constant (at atmospheric temperatures and pressures), the global distribution of the trace gas, and other possible sinks. Lovelock (1977) suggested CH_3CCl_3 (methylchloroform) as the trace gas suitable for such a study. Singh (1977a, 1977b) independently presented some calculations of $\overline{[\text{HO}]}$ based on CH_3CCl_3 . Other trace gases such as CO can also be used, but CH_3CCl_3 is exceptionally suited for such an analysis. Its source is believed to be strictly anthropogenic and accurately known (Neely and Plonka, 1978) and it doesn't have many competing sinks. The only problem is that its budget lifetime is not completely agreed upon since different experimental groups have arrived at significantly different assessments of its global burden at a given time. In the present study a range of possible values of $\overline{[\text{HO}]}$ will be calculated consistent with range of budget lifetimes of CH_3CCl_3 calculated by various researchers.

The global lifetime of CH_3CCl_3 is given by:

$$\eta = \eta_h + \eta_o + \eta_s \quad (3.40)$$

where $\eta_h = 1/\tau_h$ and τ_h is the global lifetime of CH_3CCl_3 due to heterogeneous reactions, most prominent of which are the sandy surface reactions or losses of CH_3CCl_3 in dust storms (Pierotti et al., 1978).

This sink is small but it does have its effects. We can indirectly estimate its global strength from the analysis in this section. $\eta_o =$

$1/\tau_{\text{HO}}$ where τ_{HO} is the global lifetime of CH_3CCl_3 with respect to hydroxyl radical reactions. $\eta_s = 1/\tau_s$ where τ_s is the effect of the stratospheric sink on the global concentration of CH_3CCl_3 . τ_s , τ_{HO} , and τ_h are all weighted lifetimes and so τ_{HO} is slightly different from the lifetime $\langle\tau\rangle_{\text{HO}}$ which can be deduced from eqn. (3.16). This will be discussed later. First τ_{HO} is written from eqn. (3.40) as:

$$\tau_{\text{HO}} = \frac{\tau}{1 - \alpha\tau} \quad (3.41)$$

where $\tau = 1/\eta$; $\alpha = \frac{1}{\tau_h} + \frac{1}{\tau_s}$

In Figures (3.1) - (3.2), τ_{HO} is plotted for a variety of assumptions regarding τ (which comes from budget methods) and τ_h and τ_s . It is assumed that τ_s is between 30 and 50 yrs. Methylchloroform has higher absorption cross sections for $186 \text{ nm} \leq \lambda \leq 226 \text{ nm}$ than do F-11 and F-12: $\sigma(\text{CH}_3\text{CCl}_3) > \sigma(\text{F-11}) > \sigma(\text{F-12})$ (DeMore et al., 1979). Consequently, its stratospheric lifetime is expected to be less than 50 yrs. (which is estimated for F-11). Theoretical profiles of the declining mixing ratios, with height, in the stratosphere are given in Crutzen et al. (1978) (for F-11, F-12, CH_3CCl_3 and other trace gases). τ_s between 30 and 50 years are, therefore, likely values for the stratospheric contribution to the global lifetime of CH_3CCl_3 . The "sand sink", τ_h , is taken to be from 10 years to 100 years. Clearly all three lifetimes, τ_h , τ_{HO} and τ_s compete with each other in the global lifetime τ (determined from budget methods). Thus the presence of τ_h and τ_s makes τ_{HO}

longer than one would otherwise imagine.

Figures (3.1) & (3.2) indicate that if the total global budget lifetime is 6 to 12 years, the stratospheric lifetime is 40 years and the τ_n is between 100 and ∞ years, then τ_{HO} is between 7.1 and 20 yrs. From the data considered here the most likely values of τ_{HO} are between 9 and 14 years. This would still keep the global lifetime between 8 and 10 years. The region marked by dashed lines in Figure (3.2) indicates this result.

It is, of course, τ_{HO} which determines the $\overline{[HO]}$ needed to explain the budget of CH_3CCl_3 . It was indicated before that τ_h , τ_s and τ_{HO} are weighted lifetimes.

$$\begin{aligned} \frac{1}{\tau} = & \frac{N_T}{N_T + \epsilon N_S} \frac{1}{\langle \xi \rangle_{HO}} + \frac{N_T}{N_T + \epsilon N_S} \frac{1}{\langle \xi \rangle_h} \\ & + \frac{N_S}{N_S + \frac{1}{\epsilon} N_T} \frac{1}{\langle \xi \rangle_s} \end{aligned} \quad (3.42)$$

where $\epsilon = \xi_u/\xi_T$, ξ_u is the mean stratospheric mixing ratio and ξ_T the mean tropospheric mixing ratio. N_S and N_T are the numbers of molecules of air in the stratosphere and the troposphere respectively. From eqn. (3.42) it is clear that the first term is $1/\tau_{HO}$, so that

$$\langle \tau \rangle_{HO} = \left[\frac{1}{1 + \epsilon \frac{N_S}{N_T}} \right] \tau_{HO} = a \tau_{HO} \quad (3.43)$$

ϵ is between 0 and 1. $\epsilon = 0$ indicates that there is almost no CH_3CCl_3 in the stratosphere due to (slow) mixing and fast destruction. $\epsilon = 1$ indicates that the mixing ratio of CH_3CCl_3 is constant with height in the stratosphere at the same value as in the troposphere. So, ϵ cannot be either 0 or 1. Values of ϵ from 0.2 - 0.5 are justifiable. Since N_S/N_T is small, $\langle \tau \rangle_{\text{HO}}$ does not depend very critically on ϵ and will be assumed to be 0.5 here. This gives $\langle \tau \rangle_{\text{HO}} = 0.9 \tau_{\text{HO}}$. From equation (3.16) $\overline{[\text{HO}]}$ can be written as:

$$\overline{[\text{HO}]} = \frac{\Gamma H^2 \left(1 - e^{-z_T/H} \right)^2}{z_T \left(1 - e^{-\Gamma z_T} \right) K_0} \cdot \frac{1}{a \tau_{\text{HO}}} \quad (3.44)$$

It is assumed that $[\text{H}]$ scales approximately as the density scale height of air in the troposphere. Using the values of τ_{HO} shown in Figure (3.1) and (3.2) yields the values of $\overline{[\text{HO}]}$ shown in Figures (3.3) - (3.5). H is taken to be 9 km, $z_T = 12$ km, $T_0 = 288^\circ\text{K}$ and $\ell = 6.5^\circ\text{K/km}$. Details of the calculations are given in Appendix I. The likely concentrations are enclosed by dashed lines in Figures (3.4) and (3.5). For τ_S between 40 and 50 years and τ_h between 100 yrs and ∞ $[\text{HO}]$ is between 1.8 and 3.4×10^5 molecules per cm^3 and the ground level global average is between 3 and 6×10^5 molecules per cm^3 ($\overline{[\text{HO}]_0}$).

Because $\overline{[\text{HO}]}$ not only has to explain CH_3CCl_3 concentrations, but also the budgets of other trace gases (like CO), it appears that the

"sand sink" lifetime cannot be smaller than about 50 yrs on the global basis. If it is smaller, then the globally averaged HO concentrations become too small. Even with a 6-year total lifetime for CH_3CCl_3 , with τ_h between 100 yrs and ∞ and $\tau_s = 40$ yrs, $\overline{[\text{HO}]}$ is $3.6 - 3.8 \times 10^5$ molecules/cm³. As a result of this analysis it can be concluded that $\tau_h > 50$ yrs, $\overline{[\text{HO}]}$ is between $1.8 - 3.4 \times 10^5$ molecules/cm³ and $\overline{[\text{HO}]}_0$ is between $3 - 6 \times 10^5$ molecules/cm³.

There are many uncertainties in such calculations and some of these will be reviewed now. First the rate constant K_0 , assumed here, may be too fast. DeMore et al. (1979) quote an uncertainty in E (for $K_0 = A \exp(-E/T_0)$) of $\pm 150^\circ\text{K}$. Taking the average $E + 150^\circ\text{K}$ gives 1600°K instead of 1450°K assumed here. This would slow down the reaction to about 0.6 of its former value ($K_{\text{new}} = 0.6K_0$), which would in turn require, approximately, 68% more HO radicals to achieve the same effect as that of the K_0 with $E = 1450^\circ\text{K}$. Therefore, all calculations such as those performed here are sensitive to the value of E in the rate constant. As mentioned before, the HO density height profile is also important for these calculations. If HO is constant with height to the tropopause, then eqn. (3.44) becomes:

$$\overline{[\text{HO}]}_{\text{new}} = \frac{\Gamma' H (1 - e^{-zT/H})}{(1 - e^{-\Gamma' zT})} \frac{1}{a\tau_{\text{HO}}} \quad (3.45)$$

$$\Gamma' = \frac{E\ell}{T_0^2} + 1/H$$

Keeping the other assumptions the same, $\overline{[\text{HO}]_{\text{new}}} \approx 1.28 \overline{[\text{HO}]}$ (eqn. 3.44) so that the average HO concentration required would be about 28% larger than estimated here, but the ground level average concentration required will be smaller, i.e., $\overline{[\text{HO}]_{\text{new}}} = 0.71 \overline{[\text{HO}]_0}$ (or $\sim 2 - 4 \times 10^5$ molecules/cm³ = $\overline{[\text{HO}]_{\text{new}}}$). Finally, the presence of other sources and sinks, as well as the uncertainties in determining the global release and budget from measurements, all contribute to the uncertainties in determining $\overline{[\text{HO}]}$ by this method. These problems cannot be resolved by simply invoking more sophisticated transport theories. On the other hand, direct experimental determination of $\overline{[\text{HO}]}$ in the troposphere will require many measurements at ground level and above, at several latitudes and longitudes, for several days or weeks at each site and continued for several years. At present it appears unlikely that the experimental measurements will give a more certain number for $[\text{HO}]$ (ϕ , z), $\overline{[\text{HO}]}$ or even $\overline{[\text{HO}]_0}$ (than obtained here) for many years to come.

It is desirable to measure trace gases other than CH_3CCl_3 which have similar characteristics, i.e., known source strengths, dominant HO sink and relative ease of measurement. In this way the values of $[\text{HO}]$ obtained by these other trace gases can be used to check the predicted concentrations based on CH_3CCl_3 . F-22 was a candidate for this role, but when measurements were made, it turned out that there was more of it in the atmosphere than could be accounted for by anthropogenic release. Thus, unless we can balance its budget precisely, it is not possible to use it for corroborative calculations (see Chapter 7).

Other possibilities include measuring the trace gases which control HO losses and production and then deduce HO concentrations indirectly.

(e) Conclusions

This chapter deals with the global lifetimes of trace gases which have a dominant atmospheric sink through their reactions with tropospheric hydroxyl radicals.

First some methods were discussed for evaluating the global lifetimes of trace gases with respect to hydroxyl radical interactions. A simple equation was proposed (eqn. 3.16) and some of its variations were discussed. This equation has a better physical basis than other equations used for evaluating global lifetimes, and is just as simple. The difference in the lifetimes predicted by this equation and the usual equations is dependent on how HO radical density scales with height and on the temperature dependence of the rate constant for the interaction of the trace gas under consideration, with HO radicals. The proposed equation generally predicts smaller lifetimes (by up to 60%) than the usual equations, assuming the same total global mean value of HO.

The overriding problem of estimating global lifetimes due to hydroxyl radical interactions is the current lack of information, both theoretical and experimental, on the distribution of HO radicals in the troposphere. Estimates of the global tropospheric average of HO were made using our current knowledge of the methylchloroform budget. This

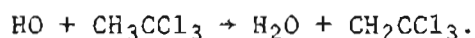
led to rather small average values. There are many uncertainties involved in such an assessment of mean HO density, including effects of other sources and sinks of CH_3CCl_3 , uncertainties in measurements and estimates of anthropogenic release and uncertainties in the reaction rate of CH_3CCl_3 with HO. The other available methods for determining HO concentrations were also discussed, but none of them are expected to predict HO concentrations with any better accuracy.

Using the equation developed in the beginning of the chapter and the HO concentrations determined from CH_3CCl_3 budget, the lifetimes of several trace gases were calculated. The lifetimes determined were generally higher than previous estimates. The particular example of CHCl_2F (F-21) was considered in more detail. The most logical conclusion seemed to be that the lifetime of F-21 is longer than previously estimated. The effects of smaller than previously expected HO densities on the CO and CH_4 global budgets was also discussed. It is possible that the current understanding of CH_4 and CO in the atmosphere will have to undergo significant revisions in the future in order to resolve some of the puzzles discussed in this chapter.

It also appears that the biggest contribution to the discrepancies between lifetimes calculated by different models are from different assumptions regarding the mean global HO density. True model dependent effects exist, but they are not as big. Until the uncertainties in the assessment of HO distribution in the troposphere can be reduced,

it is very difficult to put confidence into the calculated lifetimes. The methods discussed early in the chapter (eqn. (3.29)) and in the last section are more universal and would still be applicable even if the future estimates of HO concentrations have to be revised.

(f) Effects of the New (October 1979) Rate Constants for



After this chapter was written, two new studies were reported on the reaction of CH_3CCl_3 with HO radicals (Kurylo et al., 1979, and Jeong and Kaufman, 1979). Both these papers have just been published, side by side, in Geophysical Research Letters. The main findings of these papers are that the rate constant for the reaction of HO and CH_3CCl_3 is slower than previously reported. This was one of our fears when the work in sections (c) and (d) was being done. The reason given for the earlier faster rate constants is that olifinic impurities, CH_2CCl_2 in particular, affected the previous experiments, due to its extremely fast reaction with HO. Presumably, the new experiments used highly purified CH_3CCl_3 as a reactant.

I think that the work on the consequences of the earlier fast reaction rate was probably responsible for these new studies. The result is that now, with these new rate constants, the lifetime of CH_3CCl_3 can be long, but the lifetimes of other trace gases can be shorter than reported here (or by Graedel, 1978).

The preliminary study of the effects of the new rate constants is reported next. First, the probable new $\overline{[\text{HO}]}_0$ values are deduced. Since $\langle \tau \rangle_{\text{CH}_3\text{CCl}_3}$ deduced by budget methods is not altered by the new rate constants, eqn. (3.16), applied to CH_3CCl_3 , can be used to obtain:

$$\frac{\Gamma_*}{\Gamma} \frac{(1 - e^{-\Gamma Z T})}{(1 - e^{-\Gamma_* Z T})} \frac{K_0}{K_{0*}} = \frac{\overline{[\text{HO}]_{0*}}}{\overline{[\text{HO}]_0}} \quad (3.46)$$

$$\Gamma = \frac{E\ell}{T_0^2} + \frac{2}{H}, \quad \Gamma_* = \frac{E_*\ell}{T_0^2} + \frac{2}{H} \quad (3.47)$$

The $*$ indicates new values for these symbols (based on the new rate constant).

$$K = 2.5 \times 10^{-12} \exp(-1450/T) \quad (3.48a)$$

$$K_* = 5.4 \times 10^{-12} \exp(-1810/T) \quad (3.48b)$$

$$[K] = \text{cm}^3 / \text{molecule} - \text{sec.}$$

$$\overline{[\text{HO}]_{0*}} = 1.76 \overline{[\text{HO}]_0} \quad (3.49)$$

$$\langle \tau \rangle_* = 0.57 \langle \tau \rangle \quad (3.50)$$

Equations 3.49) and (3.50) are the approximate correction factors which can also be applied to figures (3.3) to (3.5). These reveal that ground level $\overline{[\text{HO}]}_0$ should now be around: $(0.5 - 1) \times 10^6$ molecules/ cm^3 , and the globally averaged $\overline{[\text{HO}]}$ should be between $3 \times 10^5 - 6 \times 10^5$ molecules/ cm^3 - probably nearer the upper limit or $\sim 6 \times 10^5$ molecules/

cm³. As a result, the most probable lifetimes, based on Rasmussen's five years of CH₃CCl₃ measurements (see Chapter 2), are modified to the following numbers:

Table (3.3). Revised Lifetimes of
Some Trace Gases

Trace Gas	Lifetime (yrs)	Trace Gas	Lifetime (yrs)
CH ₃ Cl	1.8	C ₂ H ₂	0.07
CHFC1 ₂	3	CH ₂ F ₂	17
CHF ₂ Cl	23	CH ₂ FC1	2.6
CH ₂ ClF	2.3	CH ₃ CHF ₂	2
CH ₃ Br	2.0	CH ₃ CF ₂ Cl	25
CH ₄	14	CHFC1CF ₃	10
CHCl ₃	0.9	COS	~ 1

The lifetime of F-21 turns out to be ~ 3 years and F-22 still has a lifetime of 23 years. The methane lifetime at 14 years is still much larger than 2-3 years. Thus, the previous discussion is still applicable.

In conclusion, the new rate constants of the CH₃CCl₃ + HO reaction moderate the radical changes in the lifetimes of other trace gases which were implied by the previous faster rate constant. Furthermore, these new rate constants imply that our previous understanding of trace gases and HO densities were better than the old rate constant led us to

believe. On the other hand, the new results do not resolve the question of long methane lifetimes and drastic changes in the CH_4 budget are still required to explain its lifetime. The $\text{CH}_4 + \text{HO}$ rate is still slower than the $\text{CH}_3\text{CCl}_3 + \text{HO}$ rate constant. Furthermore, it is no longer possible to use large HO densities to arrive at short CH_3CCl_3 lifetimes. It is much more probable now that the lifetime of CH_3CCl_3 is long, $\sim 8-10$ years, thus making it potent in the destruction of stratospheric ozone, if its release continues unabated (lifetimes of ~ 4 years were still being considered in some circles).

The reaction rate constants of other trace gases, as well as CH_3CCl_3 , are still in question, as they have always been. The effects of the new CH_3CCl_3 rate constants are currently under study and more detailed conclusions will be reported later.

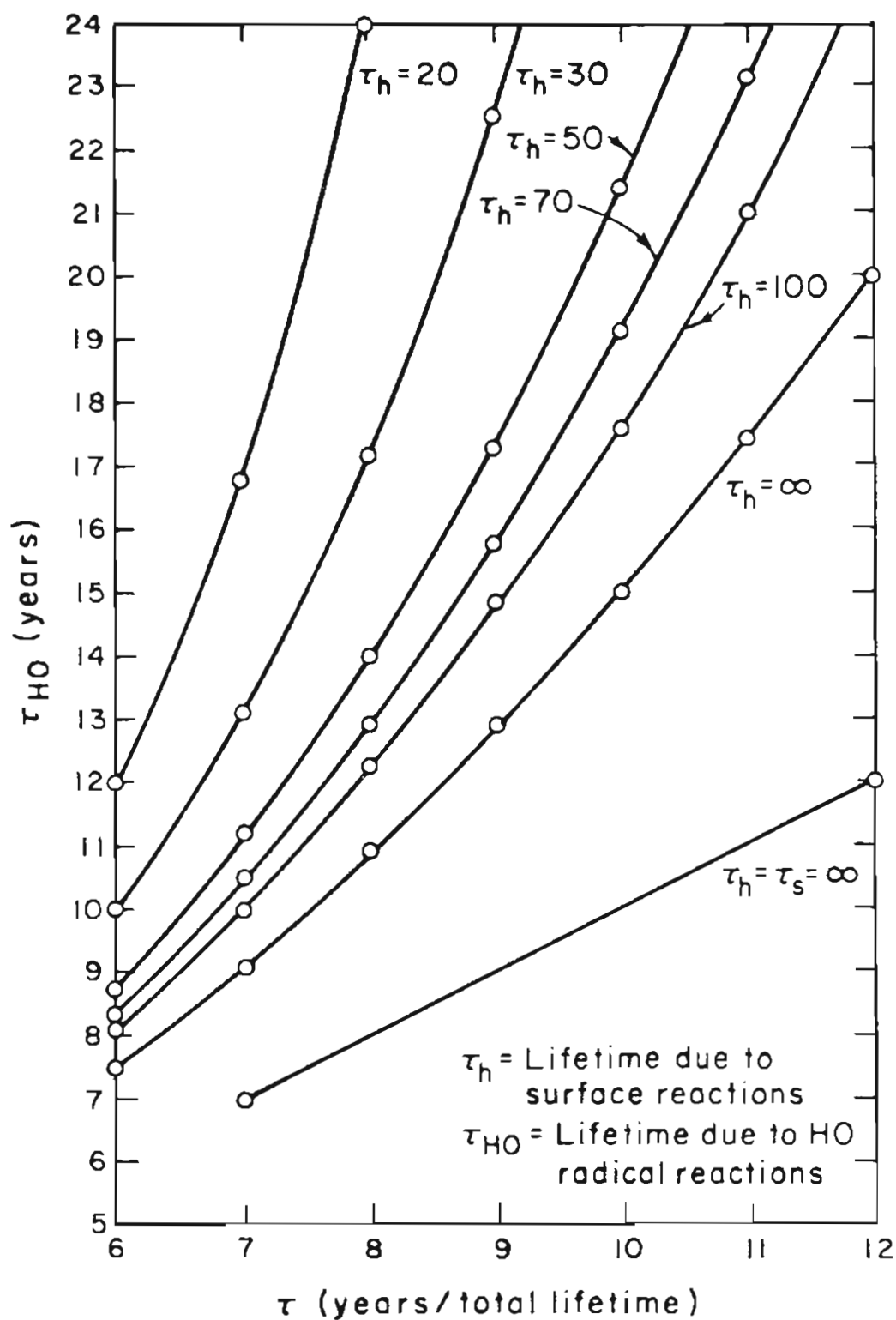


Figure (3.1a): The relationship between the total lifetime of CH_3CCl_3 and the component lifetimes ($\tau_s = 30$ years).

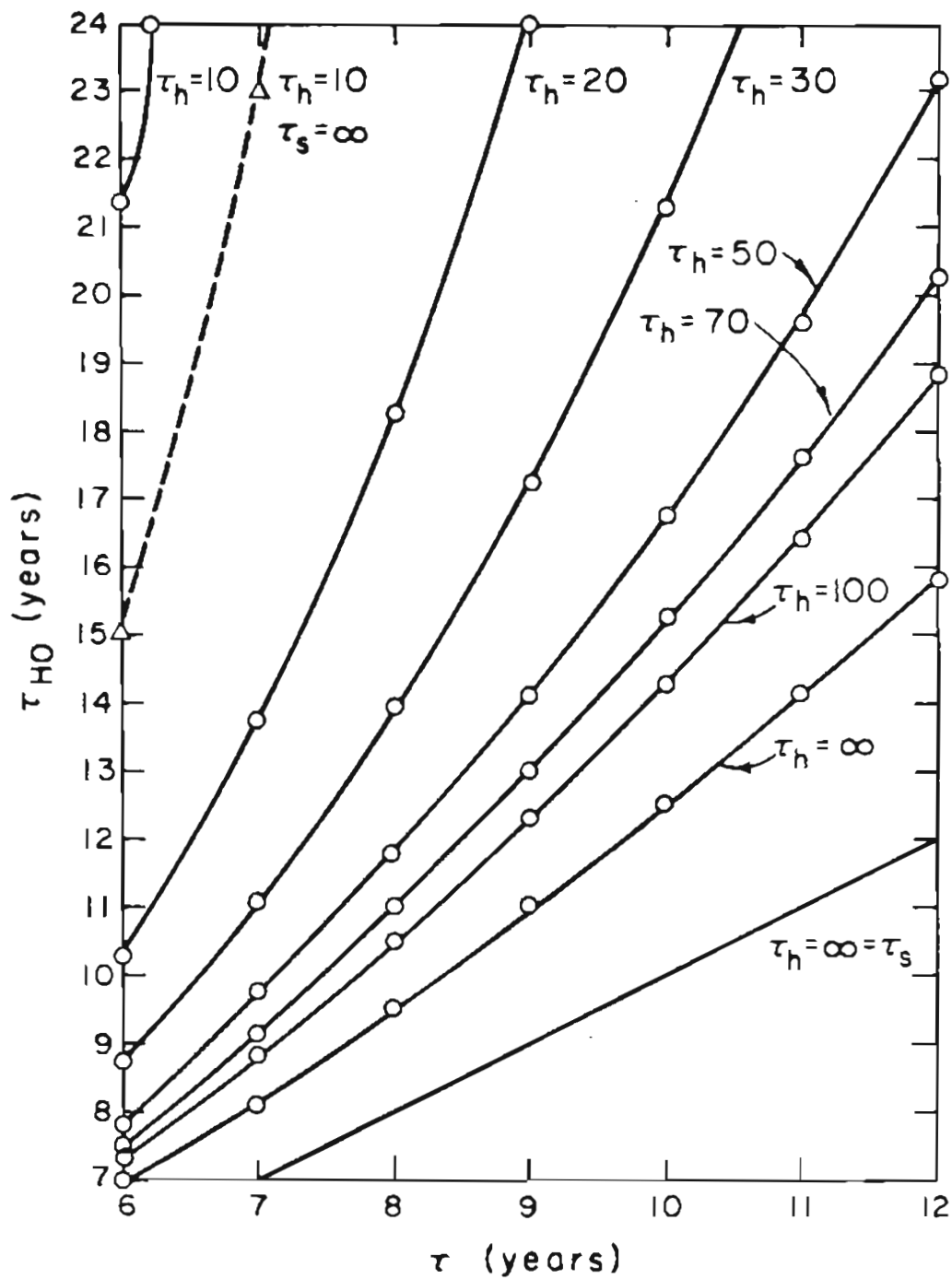


Figure (3.1b): The relationship between the total lifetime of CH_3CCl_3 and the component lifetimes ($\tau_s = 50$ years).

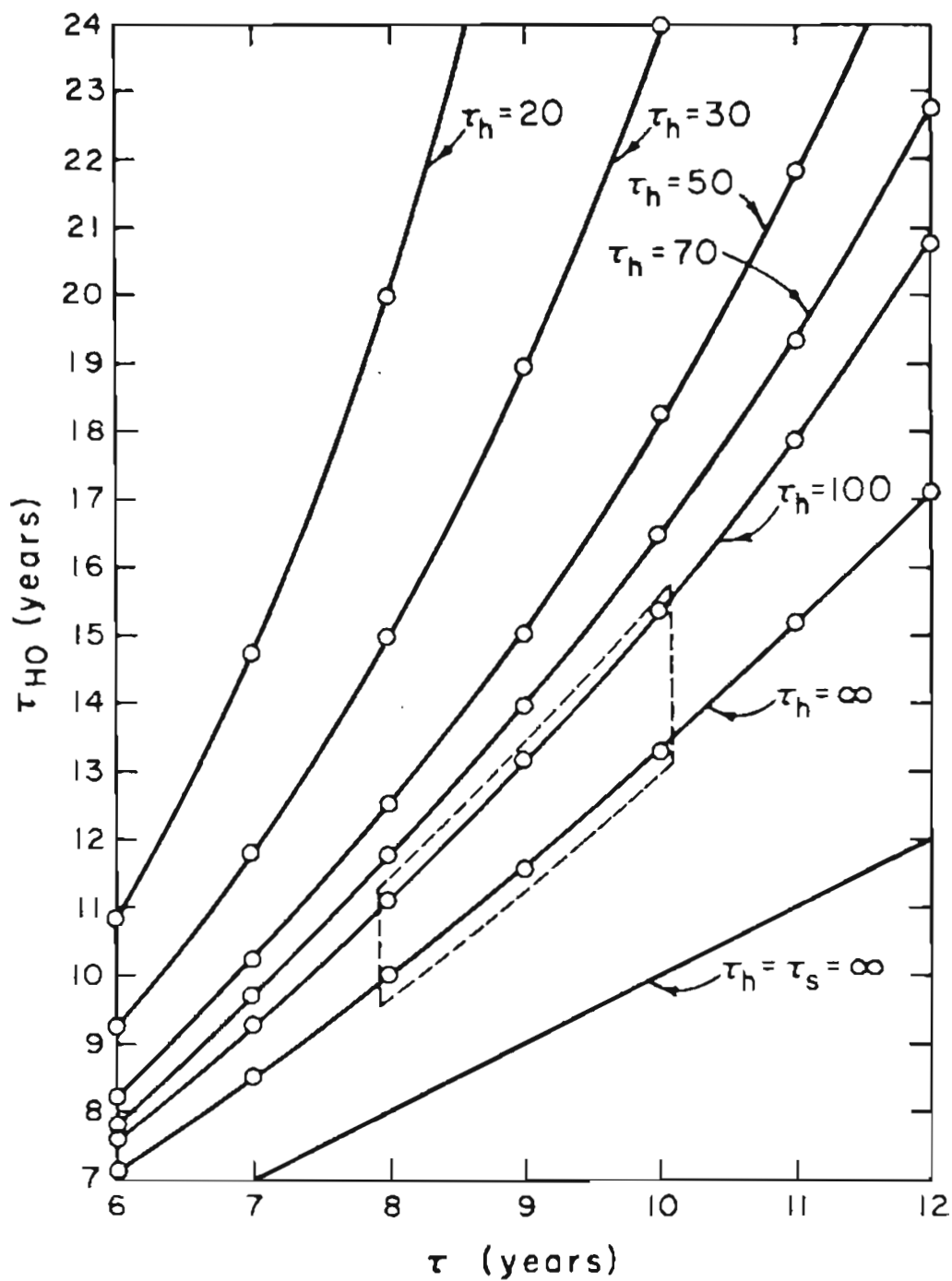


Figure (3.2): The relationship between the total lifetime of CH_3CCl_3 and the component lifetimes ($\tau_s = 40$ years).

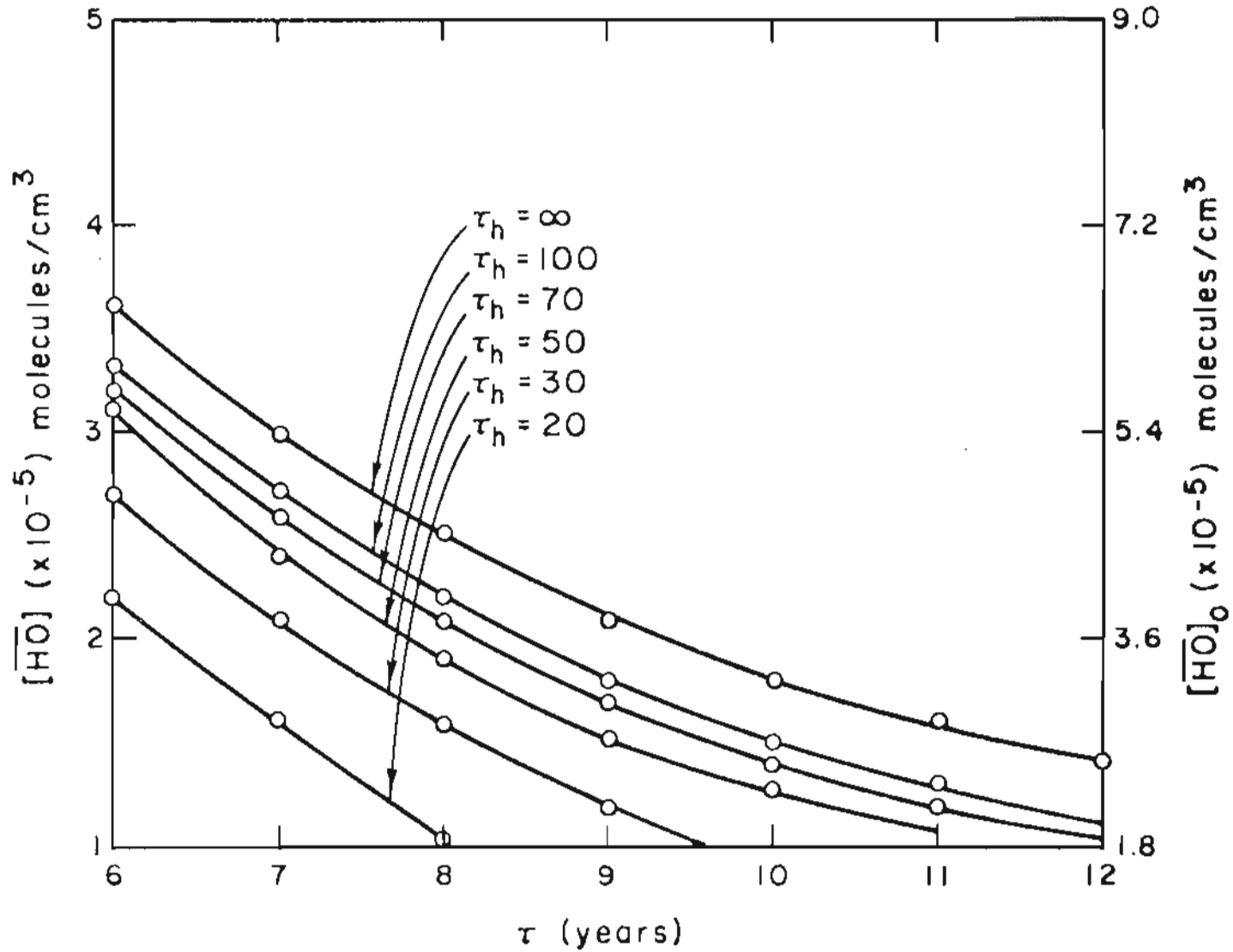


Figure (3.3): Average HO densities deduced from CH_3CCl_3 measurements ($\tau_s = 30$ years)

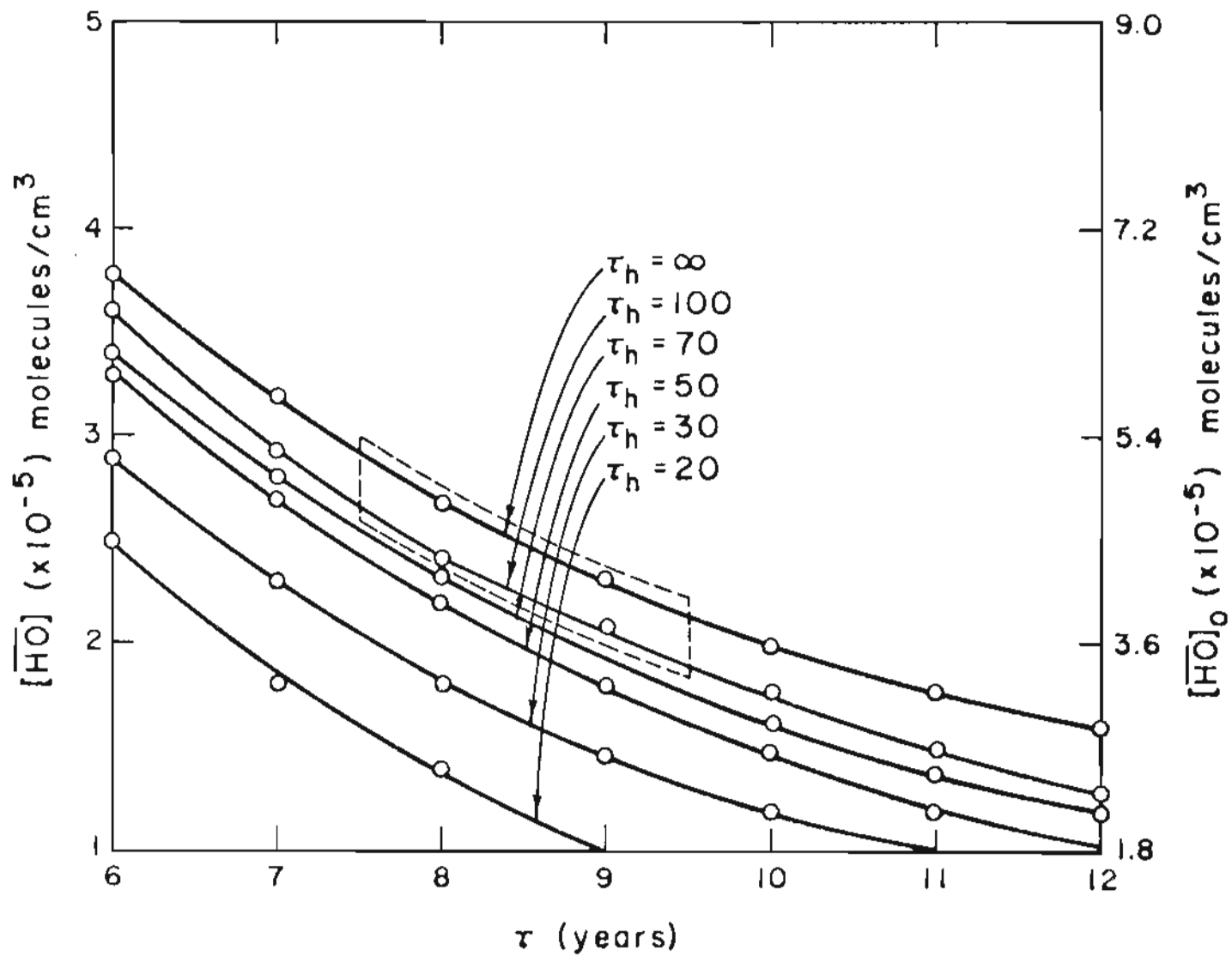


Figure (3.4): Average HO densities deduced from CH_3CCl_3 measurements ($\tau_s = 40$ years)

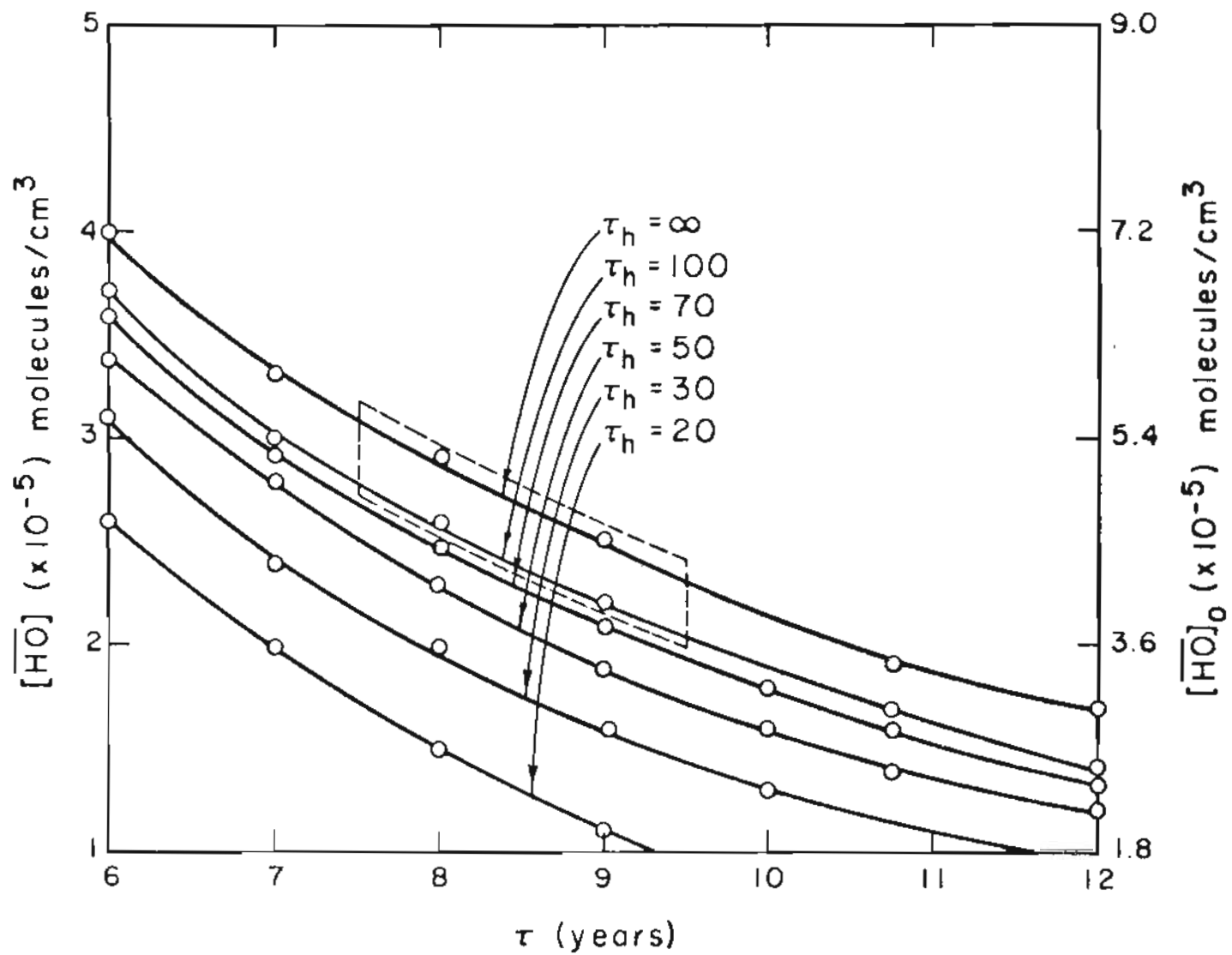


Figure (3.5): Average HO densities deduced from CH_3CCl_3 measurements ($\tau_s = 50$ years).

CHAPTER 4. AN ANALYSIS OF CYCLIC FLUCTUATIONS IN
THE GLOBAL SOURCE STRENGTHS OF TRACE GASES

(a) Introduction

As discussed in previous chapters, there is a class of long-lived atmospheric trace gases whose concentrations have been rising in recent years. This class includes many trace gases which are new to the earth's atmosphere and whose only source is man's surging industry. CFCl_3 (F-11), CCl_2F_2 (F-12), CH_3CCl_3 and CHClF_2 (F-22) are examples of accumulating trace gases with only anthropogenic sources. There is ample evidence to show the accumulation of the first three examples, and it can be inferred that F-22 is also accumulating since it belongs to this class and since rather high concentrations of F-22 have recently been detected (Rasmussen, 1979). CO and CO_2 are common examples of trace gases which are ordinarily present in the air, but to which human activities have been contributing increasing amounts. CH_3Br also belongs to this category, and may, therefore, be accumulating.

The rise in the atmospheric concentrations of these long-lived trace gases is intimately related to the rise in the anthropogenic contribution. For example, if the anthropogenic source rises exponentially, after a sufficiently long time, the atmospheric concentration also reflects an exponential rise with the same rate as the source term. In the theoretical analysis of trace gases such as F-11, F-12 and

CH_3CCl_3 it is justifiably assumed that the "sufficiently long time" has been achieved (Chang and Penner, 1978, Makide and Rowland, 1979; Singh, 1977). This time is a function of the rate of increase and the rate of removal of the compound by all terrestrial processes. It should also be kept in mind that the anthropogenic source of an atmospheric trace gas may be constant, but if the source strength is large and the lifetime long, the atmospheric concentration will still show a rise until a concentration ξ_s is reached where $\xi_s \approx S\tau$ (S = source strength in pptv per year and τ the lifetime in years).

Often the rising concentrations of trace gases result from exponentially rising anthropogenic sources. The causes behind exponentially rising anthropogenic sources are complex, but probably related to (exponentially) rising population, agriculture and industrialization (Meadows et al., 1973). It should be pointed out that growth of the production and release of any chemical cannot continue at a single exponential rate forever because there are limits to growth. In any case, when the carefully compiled estimates of the anthropogenic releases of F-11, F-12 and CH_3CCl_3 (as well as CO_2 ; Rust et al., 1979) are considered, it is found that they are described by exponential growth "on the average," at least for the period from the 1940's to now. Sometimes a sequence of exponential rates is used to describe the source term. For the particular case of CH_3CCl_3 the single exponential function ae^{bt} is always used in the literature (see for example Chang

and Penner, 1978), and it is a reasonable first approximation to the source term.

Later in this chapter we will see that the source term for CH_3CCl_3 is not adequately characterized by ae^{bt} ($t = 0$ around 1962). If b is written as $b = \langle b \rangle + b'$ where $\langle b \rangle$ is the "average" usually adopted value of b , and b' are fluctuations of the rate in the source term, then $\max |b'|$ actually exceeds $\langle b \rangle$. So CH_3CCl_3 is at least one example to which the analysis of this chapter can be applied. It will also be shown that the fluctuations b' affect both the calculated concentrations and lifetimes as well as (in the next chapter) lead to observable effects on the interhemispheric gradient of a trace gas. The large fluctuations b' , rapid increase in emissions and the high precision of time series of measurements all contribute to the observability of the effects of source fluctuations for the case of methylchloroform.

Many cyclical fluctuations are also superimposed on the exponential rise of CO_2 , but there the cyclic effects are of completely different origin from CH_3CCl_3 . The main exponential growth term in the observations of CO_2 at Mauna Loa Observatory could be due to anthropogenic activities since the rate of growth of the exponential term is close to the estimated production of CO_2 from fossil fuel burning. The recent article of Rust et al. (1979) presents evidence for several long-term cycles superimposed on the exponential growth and the well-known short term cycles.

Cyclically fluctuating sources are therefore present in the atmosphere for some trace gases. The treatment developed below investigates the expected behaviour of the concentration of a trace gas with cyclic source variations superimposed on an exponential function.

(b) Theoretically Predicted Concentrations of a Trace Gas with a Fluctuating Source.

Suppose that the source term for a trace gas is described by an exponential function, but superimposed on this function are cyclic variations of some frequency ω . In other words, the source is described by:

$$\ln S(t) = a + bt + \alpha \cos (\omega t + \phi) \quad (4.1)$$

or

$$S(t) = ae^{bt + \alpha \cos (\omega t + \phi)} \quad (4.2)$$

The global conservation equation can be written as

$$\frac{d\xi}{dt} = S(t) - \eta\xi \quad (4.3)$$

where ξ is the mean global concentration and $\eta = 1/\tau$ where τ is the total global average lifetime assuming that the destruction of the compound takes place by first order processes only. η is the strength of the sink; the smaller η is the less effective the sink is in removing the trace gas. The solution of (4.3) is:

$$\xi = \xi_0 e^{-\eta t} + e^{-\eta t} \int_0^t S(t') e^{\eta t'} dt' \quad (4.4)$$

If $S(t')$ is given by eqn. (4.2) and the value of α is small so that $\max |b'| = \alpha$ is small enough, then $S(t')$ can be written as

$$S(t) = ae^{bt} [1 + \alpha \cos (\omega t + \phi)] \quad (4.5)$$

If α is not small enough, the source term may be written directly as $S(t') = ae^{bt} [1 + \Delta_1(t)]$, or $\Delta_1(t) = \frac{S(t) - ae^{bt}}{ae^{bt}}$. This Δ_1 can then be approximated by a cosine function.

The integral in eqn. (4.4) can be solved using the techniques discussed in Chapter 9 or by other standard techniques. The result of Chapter 9 shows that the solutions can be formulated as follows:

$$\begin{aligned} & e^{-\eta t} \int_0^t e^{(b+\eta)t'} \cos (\omega t' + \phi) dt' \\ &= \frac{\omega}{\omega^2 + (b+\eta)^2} \left\{ e^{bt} \left[\sin (\phi + \omega t) + \frac{b+\eta}{\omega} \cos (\omega t + \phi) \right] \right. \\ & \quad \left. - \left[\sin (\phi) + \frac{(b+\eta)}{\omega} \cos \phi \right] e^{-\eta t} \right\} \end{aligned} \quad (4.6)$$

Substituting in eqn. (4.4), the predicted concentration at time t is:

$$\begin{aligned} \xi(t) &= \xi_0 e^{-\eta t} + \frac{a}{b+\eta} [e^{bt} - e^{-\eta t}] + \\ & \quad + \frac{\omega \alpha a}{\omega^2 + (b+\eta)^2} \left\{ e^{bt} f_0(\phi + \omega t) - e^{-\eta t} f_0(\phi) \right\} \end{aligned} \quad (4.7)$$

$$f_c(x) \equiv \sin(x) + \frac{b+\eta}{\omega} \cos(x) \quad (4.8)$$

Assuming that the source term is described by a single average exponential ignores the superimposed fluctuations given by $\cos(\omega t - \phi)$ in eqn. (4.2) and the resulting predicted concentration at time t is:

$$\lim_{\alpha \rightarrow 0} \xi(t) = \tilde{\xi}(t) = \left(\xi_0 - \frac{a}{b+\eta} \right) e^{-\eta t} + \frac{a}{b+\eta} e^{bt} \quad (4.9)$$

If the source is described by (4.2) or ae^{bt} for a long time (i.e., $t = 0$ is far enough in the past), then it is possible to drop terms containing $e^{-\eta t}$ since both ξ_0 and $a/(b+\eta)$ are small and counterbalance each other. ξ_0 and $a/(b+\eta)$ are small when most of the release has taken place after $t = 0$. Similarly, for the fluctuating source theory in eqn. (4.7), $[\xi_0 - a/(b+\eta) - f_0(\phi)]e^{-\eta t}$ may be neglected if it is small compared to $[a/(b+\eta)]e^{bt}$. Note that $f_0(\phi)$ is not a function of time.

$$\xi(t) = \tilde{\xi}(t) + \frac{\omega \alpha a}{\omega^2 + (b+\eta)^2} \{ e^{bt} f_0(\phi + \omega t) - e^{-\eta t} f_0(\phi) \} \quad (4.10)$$

Eqn. (4.10) summarizes the theoretical predictions of the atmospheric mean concentration (or total burden) when the source term is fluctuating (ξ) and when the fluctuations are disregarded ($\tilde{\xi}$).

In case the $e^{-\eta t}$ term can be dropped, eqn. (4.10) reduces to:

$$\xi(t) = \tilde{\xi}(t) \left[1 + \frac{\alpha \omega (b+\eta)}{\omega^2 + (b+\eta)^2} f_0(\phi + \omega t) \right] \quad (4.11)$$

where $\tilde{\xi}(t)$ is reduced to $[a/(b+\eta)e^{bt}]$ in eqn. (4.11). Usually, the source functions maintain the appropriate functional behaviour long

enough that eqn. (4.11) is applicable. The transitory term ($e^{-\eta t}$) can be dropped whenever the ratio of this term to the main growth term (e^{bt}) falls below some specified value ϵ (for example, 1% or $\epsilon = 0.01$), then eqn. (4.11) applies for all times $t > t_*$ where t_* is given by eqn. (4.12).

$$t_* = \frac{1}{b+\eta} \ln \left[\frac{1}{\epsilon} (g - 1) \right] \quad (4.12)$$

$$g = \xi_0 (b+\eta)/a \quad (\text{when } S = ae^{bt})$$

$$g = \left[\xi_0 - \frac{\omega \alpha a}{\omega^2 + (b+\eta)^2} f_0(\phi) \right] \left(\frac{b+\eta}{a} \right)$$

(when $S = ae^{bt} [1 + \alpha \cos(\omega t + \phi)]$)

(c) Effects of Source Fluctuations on Lifetime Calculations.

If cyclic source fluctuations are present but are ignored in the calculation of lifetimes by budget methods, then such calculated lifetimes could be in considerable error compared to the true lifetime. Generally the errors arising from neglecting source fluctuations are directly related to the size of the fluctuations given by α , and the period of the variations $T = 2\pi/\omega$. Inaccuracies are largest when α is large, but in such cases it is most likely that an investigator would recognize the deviation of the source term from a single exponential and take remedial steps. When α is small, it is easy to overlook its

existence and therefore its effect on lifetimes.

Suppose there is a trace gas whose source is actually described by eqn. (4.2) but the cyclic term is ignored and "on the average" S is taken to be $= ae^{bt}$. After a sufficiently long time of such release, the expected concentration is given by $\tilde{\xi}(t)$ (in eqn. (4.9)); or

$$\tilde{\xi}(t) = \frac{a}{b+\eta} e^{bt} \quad (4.13)$$

Suppose a measurement of the concentration is made at time t_0 and is found to be $\tilde{\xi}(t_0)$. Assuming the measurement to be ideally accurate, the lifetime can be calculated as:

$$\tau_0 = \frac{F}{b(1-F)} \quad (4.14)$$

$$F = \frac{\xi(t_0)}{R_T} \quad , \quad R_T = (a/b) e^{bt_0} \quad (4.15)$$

$$S_T = \int_0^{t_0} S(t') dt' = \frac{a}{b} (e^{bt_0} - 1) \quad (4.16)$$

For $t_0 \gg 0$, F is approximately the ratio of the measured burden at time t_0 to the total release up to time t_0 (assuming $S = ae^{bt}$). In the discussion of this section F will always be the quantity $\xi(t_0)/[\frac{a}{b} e^{bt_0}]$.

Assuming that the $f_0(\phi)$ term in eqn. (4.7) can be neglected, then the measured concentration (burden) at time t_* will be related to the true lifetime by eqn. (4.10); or as a solution of the following eqn.:

$$\frac{F}{b} = \left[\frac{1}{(b+\eta)} + \frac{\alpha \omega}{\omega^2 + (b+\eta)^2} f_0(\phi + \omega t_0) \right] \quad (4.17)$$

As one would suspect, the lifetime expression involves the value of $f_0(\phi + \omega t_0)$. If t_0 happens to be a time at which $f_0(\phi + \omega t_0) = 0$, then τ will be given by the expression (4.14). This reflects an accidental circumstance where the effects of the positive and negative fluctuations cancel, and the true lifetime will be the same as the lifetime calculated by ignoring the fluctuating term in the source function. On the other hand t_0 could be a time where $f_0(\phi + \omega t_0)$ takes on its extreme values, in which case the lifetime determined by eqn. (4.12) will be wrong by the maximum amount due to the fluctuations of the source term. Eqn. (4.17) can be solved for two special cases when $f_0(\phi + \omega t_0)$ takes on extreme values:

$$\begin{aligned} \omega^2 \gg (b+\eta)^2 \Rightarrow \\ \tau = \frac{F + \frac{\alpha b \epsilon}{\omega}}{b \left[1 - F - \frac{\alpha b \epsilon}{\omega} \right]} \end{aligned} \quad (4.18)$$

$$\omega^2 \ll (b+\eta)^2 \Rightarrow \quad \tau = \frac{F}{b[(1+\epsilon\alpha) - F]} \quad (4.19)$$

where $\epsilon = +1$ if t_0 is such that $f_0(\phi + \omega t_0)$ is minimum, and $\epsilon = -1$ if t_0 is such that $f_0(\phi + \omega t_0)$ is maximum.

There is one more point that should be stressed before concluding this section. When the source is fluctuating, the quantity F de-

fined as $\xi(t)/\frac{a}{b} e^{bt}$ will not be constant, but will be given by b times the right hand side of eqn. (4.17). So, if a series of measurements of the global concentrations is made and then τ is calculated for each time of measurement, say τ_k at times t_{ok} ($k = 1, \dots, n$), then $F(t_{ok}) = b[(b+\eta)^{-1} + f_o(\phi + \omega t_{ok}) (\omega^2 + (b+\eta)^2)^{-1}]$ and thus the $F(t_{ok})$ will be fluctuating. If eqn. (4.17) is used to determine the lifetime ($= 1/\eta$), then these fluctuations will exactly balance out and $\tau_1 = \tau_2 = \dots = \tau_n$. If the usual expression (4.12) is used, the calculated lifetimes τ_{ok} at t_{ok} will be different from each other, because $F(t_{ok})$ will be different at each time.

If the values of τ_o , calculated from a sequence of measurements of the concentration, are not all the same, then the expression (4.12) is at least philosophically unsatisfactory. Measured values of $\xi(t)$ used to calculate F show that F varies from year to year and therefore so does τ_{ok} . If the measurements were ideally accurate and had enough global coverage, then such a circumstance of a varying F would mean that the source term had significant fluctuating components. Real atmospheric measurements are far enough from this ideal that a changing τ_{ok} for a sequence of measurements is not in itself a proof of source fluctuations. Of course, a τ changing in time could be a real phenomenon if the sink mechanism is becoming stronger or weaker, but here only source fluctuations have been considered.

(d) An Analysis of the CH₃CCl₃ Source Function

Methyl chloroform is one anthropogenic trace gas in the earth's atmosphere which has a relatively well known release history. The data on yearly emissions were compiled by Plonka and reported with additional analysis relating to HO radicals in the paper by Neely and Plonka (1978). The release is reported from 1951 to 1976 in this paper. These emissions data have been used in all the analyses with the addition of the data for 1977 and 1978 (at 980 and 1100 million pounds respectively) supplied by Farber and Neely (1979). Figure (4.1) is a plot of $\ln S$ as a function of time. Here $S(t)$ is the release in millions of lbs.

Since it appears that CH₃CCl₃ has a lifetime of around 9 years as discussed in Chapter 2, much of the amount released prior to about 1963 would no longer be in the atmosphere by the time measurements of CH₃CCl₃ were made. More important reasons for neglecting releases prior to 1963 are that the total release up to that time is rather small compared to the huge amounts dumped into the atmosphere since then. Also the fact that there are counterterms in the predicted concentrations which tend to cancel ξ_0 (i.e., $(\xi_0 - \frac{a}{b+\eta})$) also reduces the importance of the source term before 1963. $\xi_0 \approx 9$ pptv and the term $a/(b+\eta)$ is also close to this number for both the exponential and fluctuating sources. Furthermore, the effects are reduced by the $e^{-\eta t}$ factor.

The analysis of Graedel and Allara (1976) led the authors to

conclude that formation of CH_3CCl_3 in the atmosphere is negligible. In the absence of any other plausible sources it is safe to assume that CH_3CCl_3 in the atmosphere results from direct anthropogenic release.

Most studies, therefore, consider the release from the early 1960's onwards and assume it to be given by an exponential function ae^{bt} up to the present. Values of b are about 0.153/yr, or a 15-16% per year increase since the early 1960's "on the average." There are many examples of studies using these assumptions (Chang and Penner, 1978; Singh, 1977; Makide and Rowland, 1979). As Figure (4.1) shown, the assumption of pure exponential function is not really valid. In the next section and in the next chapter domains where the deviations of the source function from an exponential can lead to significant effects will be discussed.

In Figure (4.2) the source function is plotted again on an expanded scale covering the years from 1963 to the present time. A straight line that fits best corresponds to a value of $b = 0.153/\text{yr}$ and $a = 2.62$ pptv (or 128 million lbs).

Using the numbers on which Figure (4.2) is based, it is possible to calculate the first remainder function $\Delta_1(t)$ by

$$\ln S(t) - \ln a - bt = \Delta_1(t) \quad (4.20)$$

This function $\Delta_1(t)$ is plotted in Figure (4.3). Since it is periodic, a cosine function is fitted to it, giving:

$$\Delta_1(t) = \alpha_0 + \alpha \cos(\omega t + \phi) + \Delta_2(t) \quad (4.21)$$

where $\Delta_2(t)$ is the second remainder function. The function $\Delta_2(t)$ is plotted in Figure (4.4) on the same scales as Figure (4.3).

The first remainder function expresses the magnitude of deviation of the "true" source function $S(t)$ from ae^{bt} . It says that if it is assumed that $S(t) = ae^{bt}$, the error between the true $S(t)$ and ae^{bt} will be $\exp[\Delta_1(t)]$ at time t . Similarly, the second remainder function gauges the error between the true source function and the assumption that $S(t) = a \exp(bt) \exp[\Delta_1(t)]$. The process can be continued, but here Δ_2 is sufficiently small in most of the years before 1972 that it can be assumed to be "noise" -- the source term is not known to arbitrary accuracy. After 1972, there appears to be another cycle, which will be considered in the next section. Although this cycle has small amplitude and more rapid frequency, it appears at a crucial time in the release history.

A rough assessment of the relative goodness of fit of ae^{bt} and $a \exp[bt + \Delta_1(t)]$ can be made by looking at the average deviations of the two functions from the "true" $S(t)$. The mean deviation calculated

by $1/(N+1) \sum_{i=0}^N |\ln S(t_i) - (a + bt_i)|$ and $1/(N+1) \sum_{i=0}^N |\ln S(t_i) -$

$(a + bt_i) - \alpha \cos(\omega t_i + \phi)|$ gives the values 0.12 and 0.04 respectively. The Δ_2 cycle after 1972 has not been included in these numbers. Thus, on the average, ae^{bt} deviates from the true source func-

tion by a little over 12% and a $\exp [bt + \alpha \cos (\omega t + \phi)]$ deviates from the true source function by only 4% based on the last 16 years of source data.

It therefore appears that a cyclic variation exists in the source term of CH_3CCl_3 , with a period of about 6.7 years (ω , α and ϕ are found to be 0.94/yr, 0.21 and 2.38 radians respectively). α_0 in eqn. (4.21) is 0.025 and is simply absorbed in $\ln a$, and is not a new constant. Details of the calculations are given in Appendix I.

It is impossible to predict if this cycle would continue beyond the present time. In fact, it appears that there will be a general decline in the production and release of CH_3CCl_3 in the future (partly because its production has caught up to demand, partly because of limits to growth, and probably because legislation to restrict emissions is being considered by the EPA).

The value of α indicates that the slope of $\ln S$ has fluctuations bigger than the mean value ($\alpha = 0.21$, $b = 0.153$). The value of $\omega = 0.94$ indicates that for a global average model, $\omega^2 \gg (b + \eta)$ and the corrected phase ϕ' makes recent times the worst for ignoring source fluctuations.

(e) A Look at $\Delta_2(t)$ in the CH_3CCl_3 Source Function

In general $\Delta_2(t)$, as shown in Figure (4.4), is small in its absolute value, but it is worst for some of the years following 1972.

Since a lot of release took place during this period, it seems worthwhile to look into the cycle which appears during this period. In Figure (4.5) this cycle is isolated.

The Δ_2 plotted in Figure (4.5) is constructed as follows:

$$S = ae^{bt} [1 + \alpha \cos (\omega t + \phi) + \Delta_2] \quad (4.22)$$

so that

$$\Delta_2(t) = \frac{S}{ae^{bt}} - 1 - \alpha \cos (\omega t + \phi) \quad (4.23)$$

This is approximately the same as

$$\Delta_2(t) = \ln S - (\ln a + bt) - \alpha \cos (\omega t + \phi) \quad (4.24)$$

which was discussed earlier. Eqn. (4.23) is chosen over (4.24) to eliminate the effects of making the approximation $\exp [\alpha \cos (\omega t + \phi)] \approx 1 + \alpha \cos (\omega t + \phi)$ in Δ_1 . There are also other ways of computing Δ_2 , but in the end they are all more or less the same. Figure (4.5) also shows the function:

$$\Delta_2 = \alpha_* + \tilde{\alpha}_* \cos (\omega_* t + \phi) \quad (4.25)$$

where $\alpha_* = -0.01$, $\tilde{\alpha}_* = 0.11$, $\omega_* = 1.57 = \pi/2$ rad/yr and $\phi_* = 5.1$ radians with $t = 0$ at 1/72. The third remainder function is: $\Delta_3 = \Delta_2$ [in eqn. (4.23)] - $(\alpha_* + \tilde{\alpha}_* \cos (\omega_* t + \phi_*))$. The mean deviation of Δ_2 during these years was about 0.072 and it is reduced to about 0.012 when Eqn. (4.25) is subtracted, i.e., the mean deviation expressed in Δ_3 is

only 1.2%. The agreement between the release estimates and the cyclic source function is improved in all years except 1978; thus, it is better to use this cycle only for the six years (1972-1977). Even with this restriction, the cycle will have an effect on predicted concentrations for times beyond 1978.

This additional feature of the source term can be added to the theoretical equations derived in section (b) for the Δ_1 -cycle. The resulting additional term follows from the same analysis as that used for the Δ_1 - cycle.

$$\xi = \hat{\xi}(t) + H(t - T) e^{-\eta t} \int_0^t A e^{bt} \Delta_2(t) dt \quad (4.26)$$

where $\hat{\xi}(t)$ is the value predicted by the analysis in section (b) for the Δ_1 -cycle, and $A = ae^{bT}$ where T adjusts the time scales used in the previous section to those which describe the Δ_2 -cycle. ($T = 9$ yrs)
 $H(t - T)$ is 0 for $t < T$ and +1 for $t \geq T$. The integral in the second term is:

$$\begin{aligned} & e^{-\eta t} \int A e^{bt} [\alpha_* + \tilde{\alpha}_* \cos(\omega_* t + \phi_*)] dt \\ &= \frac{A\alpha_*}{b+\eta} (1^{bt} - e^{-\eta t}) + \frac{\omega_* A \tilde{\alpha}_*}{\omega_*^2 + (b+\eta)^2} \{ e^{bt} [\sin(\omega_* t + \phi_*) \\ &+ \frac{b+\eta}{\omega_*} (\cos(\omega_* t + \phi_*))] - \\ &e^{-\eta t} [\sin \phi_* + \frac{b+\eta}{\omega_*} \cos \phi_*] \} \end{aligned}$$

The parameters ϕ_* and $\tilde{\alpha}_*$ were adjusted according to the results of Chapter 9. Figures illustrating the source fluctuations for CFCl_3 (F-11), CCl_2F_2 (F-12), and CHClF_2 (F-22) are included in Appendix I.

(f) Comparison of Theory and Observations.

In order to demonstrate the behaviour of the theory with fluctuations, the α , ϕ and a are adjusted to obtain a smoothed source function corresponding to the function derived from the discrete emission estimates (see Chapter 9). The results are ($\alpha \rightarrow 0.22$, $\phi \rightarrow 1.91$ radians, $a \rightarrow 2.42$ pptv for the theory with $S = ae^{bt}$, and $a \rightarrow 2.49$ pptv for the fluctuating source theory which requires the addition of α_0 . (See Appendix I.) It should also be noted that time is taken to be zero at 1963; thus, at $t = 1$ the smoothed source term (4.2) predicts the emissions of 1963. So $t = 1$ corresponds to the start of 1964.

The behaviour of eqn. (4.7) and the usual theory eqn. (4.9) are compared in Figure (4.6). In this figure ξ_0 is derived from the source data of Neely and Plonka (1978) for the years prior to 1963 and found to be about 9 pptv. A lifetime of 10 years is assumed for the comparison. The Δ_2 -cycle has been ignored since it takes effect only over the last few years.

In Figure (4.7) the two theories of Eqn. (4.7) and (4.26) are plotted with the same values of α' , ω , ϕ' , and a' as in Figure (4.6), but with two alterations. First, the Δ_2 -cycle has been included in the

theoretical expression, and second, the lifetime has been readjusted.

In this figure the time series data of Rasmussen (1979) are used to compare the predictions of the two theories (the observed values are indicated by triangles (Δ)). The lifetime chosen for the simple source theory is $\tau = 12.8$ years. This is the optimum value so that the least squares deviation between the observations and the simple source theory are (approximately) minimized. For the fluctuating source theory, $\tau = 11.8$ years. This value is also close to that required for minimizing the deviations between the observations and fluctuating source theory. It was pointed out in Section (4.c) that the predictions of lifetimes would be different for the two theories. Here the difference is not significant. (This is partly due to the presence of α_0 in the equation for $\Delta_1(t)$). Figure (4.8) indicates the deviation between observations and the two theories given by $\delta\xi/\xi = |1 - \xi_p/\xi_m|$ (100%) where ξ_m is the measured concentration and ξ_p is the predicted concentration. The mean deviation for the predictions using $S = ae^{bt}$ is 4% and that using the $\alpha' \cos(\omega t + \phi')$ cycle is about 2½%. Inclusion of the Δ_2 -cycle brings the mean deviation down to 1.6%.

Considering all the arguments that can be made, it is not possible to present an irrefutable case for favouring either theory over the other. From the results of this analysis it is possible to make a reasonable case for the fluctuating source theory.

Prediction of the trend (slope of $\ln \xi(\text{observed})$) is the main

variable to be compared. For the simple source theory the predicted slope is just $b = 0.153/\text{yr}$. Systematic inaccuracies of the data simply change the value of τ needed to obtain the best agreement, thus affecting the intercept of the prediction eqn., $\ln \xi = \hat{a} + b\tau$ and not the slope. The fluctuating source theory predicts a non-linear time behaviour, but can be linearized over a few years at a time. It too predicts trends that are not expected to be very sensitive to absolute accuracy. Because of these characteristics, the prediction of the trend by the two theories is an appropriate variable to consider, and τ can be regarded as a free adjustable parameter which absorbs systematic inaccuracies (see Appendix I for further discussion of this point.) τ is the only free parameter and all the rest of the constants, ω , ϕ' , a' , α' , b , $\tilde{\alpha}_*$, ϕ_* and ω_* , are determined from the source statistics.

The least squares slope of the observed concentrations is $0.12/\text{yr}$. The simple source theory predicts a slope of $0.153/\text{yr}$ based on 16 years of source data. This value is too high, a fact that is visible in Figure (4.8). The shape of this graph for the simple source theory is typical of an overestimated slope. For the fluctuating source theory the fluctuations are such that they improve the agreement between theory and observations by raising the concentrations where the simple source theory predicts low values and lowering the concentrations where the simple source theory predicts values that are too high. Thus, the ω , α' , ϕ' , b , a' , ω_* , ϕ_* and $\tilde{\alpha}_*$ derived from the emissions data are

just right to moderate the slope to a lower value (compared to 0.153/yr) in addition to giving better absolute agreement between theory and experiment. In fact, the linear approximation to the fluctuating source theory gives a slope of 0.13/yr which is very close to the least squares value for the observed data. It appears that the theory with the fluctuating source terms is better at explaining the observations than the simple theory. The case for this statement can be strengthened by a statistical analysis as shown in the next section.

Details of all the calculations presented in this section are given in Appendix I.

(g) Analysis of the CH₃CCl₃ Observed Time Series Using Non-Parametric Statistics.

In order to make a better case that the usual theory assuming $S = ae^{bt}$ is not adequate at explaining the observed concentrations over the last five years, one may employ the distribution free Theil test of slope to the $\ln \xi_m(t_i)$, where $\xi_m(t_i)$ are the observed global concentrations at time t_i .

The distribution free Theil test for the slope of a regression line is based on Kendall's K-statistic (Hollander and Wolfe, 1973). The observable is $\ln \xi_i$ given at times t_i such that $t_1 < t_2 < \dots < t_n$.

$$Y_i = \tilde{\alpha} + \beta t_i + \epsilon_i, \quad i = 1, \dots, n \quad (4.27)$$

ϵ_i 's come from the same continuous population and are assumed to be mutually independent. The one-sided hypothesis to be tested is:

$$H_0: \beta = \beta_0 \text{ (specified)} \quad (4.28)$$

versus the alternative that $\beta < \beta_0$ (or $\beta > \beta_0$). To do this, one defines $D_i = Y_i - \beta_0 t_i$ and calculates

$$C = \sum_{i < j}^n \delta(D_j - D_i) \quad (4.29)$$

where

$$\delta(x) = \begin{cases} 1 & x > 0 \\ 0 & x = 0 \\ -1 & x < 0 \end{cases} \quad (4.30)$$

The lowest level of significance, α , at which the hypothesis (H_0) can be rejected is limited by the number of observations n , which in our case is 5. The lowest level of significance at which H_0 can be rejected turns out to be $\alpha = 0.008$, and this value will be adopted here. Therefore, H_0 is to be rejected in favour of $\beta < \beta_0$ if $C \leq -K(\alpha, n) = -K(0.008, 5)$; and similarly for the test of H_0 versus the alternative $\beta > \beta_0$, H_0 must be rejected for $C \geq K(\alpha, n) = K(0.008, 5)$.

One can note that H_0 can be rejected in favour of the alternative $\beta < \beta_0$ at the lowest α if (and only if) β_0 is such that $D_1 > D_2 > \dots > D_n$. Similarly for the test of H_0 versus $\beta > \beta_0$, H_0 can be re-

jected at the lowest level of significance, if and only if the slope β_0 is such that $D_1 < D_2 < \dots < D_n$. Obviously these are stringent requirements.

First the hypothesis:

$$H_0 : \beta = 0.15/\text{yr}.$$

is tested versus the alternative $\beta < 0.15/\text{yr}$. Calculations of C show that $C = -10$. Considering the tabulated values of the Kendall's K -statistic, one finds that the hypothesis $H_0 : \beta = 0.15/\text{yr}$ must be rejected in favour of $\beta < 0.15/\text{yr}$ at the $\alpha = 0.008$ level.

Similarly on the lower side, the hypothesis $H_0 : \beta = 0.07/\text{yr}$ versus the alternative $\beta > 0.07/\text{yr}$ can be rejected at the 0.008 level of significance. In the case of CH_3CCl_3 , the analysis suggests that the value of β , in the observed growth given by $\tilde{\alpha}e^{\beta t}$, is very unlikely to be bigger than 0.15/yr or less than 0.07 yr. Intuitively, the probability that due to random errors the true slope is any specific value, 0.15/yr or bigger, is ≤ 0.008 . By choosing the lowest possible value of α I have made it as difficult as possible to reject the hypothesis H_0 , yet was forced to do so. (The probability of making a type I error has been made as small as possible.) The single source model of $S = ae^{bt}$ predicts the slope to be $b = 0.15/\text{yr} - 0.16/\text{yr}$ and therefore fails to predict the observed growth rate.

A usual alternative to the statements expressed above is to calculate the confidence interval for the slope. The calculation of the

distribution free confidence interval based on the Theil test is described by Hollander and Wolfe (1973). The 91% confidence interval is (β_L, β_U) and turns out to be (0.103/yr, 0.133/yr). This means that the probability that the slope is between 0.103/yr and 0.133/yr is 91%. The Theil estimator for the slope (Hollander and Wolfe, 1973) gives the slope of 0.124/yr which is close to the least squares value. Details of the calculations are given in Appendix I.

The theory with the cyclic terms in the source function predicts a non-linear relationship between $\ln \xi$ and time; thus it cannot be directly tested by this method. On the other hand, the period of observations covers a short enough time that the predicted concentration function of the fluctuating source theory can be linearized. It then gives a slope of about 0.131/yr. This cannot be rejected by testing the two sided hypothesis $H_0: \beta = 0.13/\text{yr}$ versus $\beta \neq 0.13/\text{yr}$. Such a result is to be expected since this predicted value of the slope is so close to the least squares value of the observed concentrations.

The analysis of this section leads to four broad alternatives:

- (1) The true value of the overall slope of the $\ln S$ term as a function of time is less than that derived from the emissions data.
- (2) The true concentrations in the atmosphere have been rising faster than Rasmussen's data indicate.
- (3) A combination of the effects stated in (1) and (2) is present,
- (4) that the known fluctuations of the source term from its mean exponential behaviour have an effect on atmospheric concentrations which is manifested in the time series of observations.

In my opinion, the first three alternatives are unlikely for the following reasons: The growth rate is not sensitive to constant systematic errors. If the true source term was $S_{\text{true}} = (1 + \epsilon_s) S(t)$, so that the emissions data are systematically too low, then this would affect the intercept but not the slope of the predicted function $\ln \xi = \ln \left(\frac{a}{b+\eta} \right) + bt$. $\left(\ln \frac{a}{b+\eta} + \ln \frac{a(1+\epsilon_s)}{b+\eta} \right)$. Similarly, if the measurements are too high (or low) due to calibration problems, once again the slope would be unaffected. On the other hand, it is possible that atmospheric variability (non-systematic) can account for the smaller slope (than 0.15/yr) found by using Rasmussen's data. It is also more probable that the emissions data have too small a slope compared to the true source, which makes the predictions of the simple source theory (with $S = ae^{bt}$) even worse. Such a situation is possible because it is easy to accidentally miss records of sales and inventories or overlook production by smaller companies and other countries. The Theil test used here tests only the slope or the growth rate and is independent of the intercept. The third alternative mentioned above is subject to the same reservations and would also require the coincidental occurrence of two unlikely events.

The simple source theory can only be resurrected by the introduction of ad hoc hypotheses regarding long term biases in the source term or observed concentrations, otherwise the simple source theory fails to predict atmospheric concentrations. It is possible that such

effects have taken place in reality, and therefore, the simple source theory is correct in principle. On the other hand, the current knowledge of the source term over 16 years, and the observed concentrations over 5 years, is completely consistent with the fluctuating source theory. Even if there are constant systematic biases in the observed concentrations or the source term, the simple source theory will fail and the fluctuating source theory will continue to be consistent.

One point which is appropriate here is the effects of possible systematic biases in the observational data. Since there is a possibility that the observed values are high, if each number is reduced by some factor (say 10%), the consequent change in the value of τ needed to fit the fluctuating source theory to data will cause a change in the relative magnitudes of the predicted fluctuations. This is an effect of the non-linearity of the fluctuating source theory and thus the effects of the cycles would have to be reevaluated. Indeed, the predicted slope will change. In contrast, the slope predicted by the simple source theory would not be affected. These comments also apply to the analogous theories which have two or more "boxes". (Further comments can be found in Appendix I.)

For the particular case of CH_3CCl_3 , which has been considered here, there are alternative methods of taking the source fluctuations into account, which can give at least as good, or even better agreement between theory and experiment. The main point to be kept in mind

is that these methods are based on the source term which is not described by the simple term ae^{bt} over a long time, but are simply alternative ways of looking at the fluctuations. Two such methods are discussed below: First, one may start with the solution of (4.3) given by (4.4) and take the discrete limit by assuming that

$$S(t) = \sum_{k=0}^t S(k) \delta(t-k) \quad (4.31)$$

so that (4.4) becomes ($\delta(t-k)$ is the Dirac delta function):

$$\xi(t) = \sum_{k=0}^t S(k) e^{-\eta(t-k)} \quad (4.32)$$

where $S(k)$ is the release in the k -th year. By using eqn. (4.29), $\xi(t)$ can be calculated for any sequence of years. The results of this method will take the "exact" source function into account rather than an approximation such as that of eqn. (4.5). In reality this method would also be taking source fluctuations into account in the same way as the fluctuating source theory developed here. It is, however, very tedious to calculate the right τ to reproduce the data and no physical insights about the functional form of $\xi(t)$ are gained.

Since the observational data for CH_3CCl_3 are available for only the last few years during which period the source behaved very much like $S = a'e^{b't}$ (where $b' = 0.083/\text{yr}$ rather than the long term value of $0.15 - 0.16/\text{yr}$), one may use the solution of eqn. (4.3) given by:

$$\xi = \frac{a'}{b'+\eta} [e^{b't} - e^{-\eta t}] + \xi_0 e^{-\eta t} \quad (4.33)$$

ξ_0 is the concentration at 1/1975. During 1975-1979 the residual function $\Delta_1(t)$ (eqn. 4.20) is approximately linear with a negative slope. Such a method would apply for only short periods, and it also requires the independent knowledge of ξ_0 . Again, though this method is good for CH_3CCl_3 , its applicability to more general situations is limited. The purpose of the work developed in this chapter was to explore more general ideas and CH_3CCl_3 was considered in detail only as an example.

(h) Summary and Conclusions

The main results of this chapter are reviewed below:

(1) The effects of the source fluctuations on globally averaged concentrations are reflected in the magnitude of the term $\alpha (b' + \eta) / [\omega^2 + (b + \eta)^2]^{\frac{1}{2}}$ compared to 1.

(2) When lifetimes are small and the rate of increase large enough so that $(b + \eta)^2 \gg \omega^2$, then the amplitude of the predicted fluctuations in the concentration are approximately equal to α . For the other extreme when $\omega^2 \gg (b + \eta)^2$ the effects are moderated so that the effect on predicted concentrations is smaller than the magnitude of source fluctuations.

(3) The maximum (or minimum) of the predicted concentration occurs after a delay period relative to the maximum (or minimum) of the smoothed source function. The delay period may be calculated using the following equations:

$$\begin{aligned}
 t_* &= t_0 + \frac{1}{\omega} \arctan \frac{\omega}{b+\eta} \\
 t_* &= t_0 + \frac{1}{\omega} \frac{\pi}{2} ; \omega/b+\eta \gg 1 \\
 t_* &= t_0 \quad \omega/b+\eta \ll 1
 \end{aligned}
 \tag{4.34}$$

where t_0 is the time at which a maximum of the source term ($S(t)$) occurs and t_* is the time at which this source maximum leads to a maximum of concentration. The smoothing transformation may affect a part of this delay period.

(3) Finally, CH_3CCl_3 was considered as an example of a compound with a varying source function. The cycles of source fluctuations over the last 16 years were demonstrated. It is probable that these cycles will not continue, but new cycles may emerge. Although the analysis of the methylchloroform source cycles is applicable to all theories used to analyze the atmospheric concentrations of this compound, only very simple theoretical examples were used in this chapter. These examples were designed to explain the growth of CH_3CCl_3 in the atmosphere based on the time series data of Rasmussen. The results are generalizable to more complex models. The fluctuating source theory developed here is exactly solvable and demonstrates the features discussed in (1) and (2) above. It also predicted the correct growth rate of CH_3CCl_3 whereas the analogous theory without source fluctua-

tions failed to adequately predict the slope of the growth trend (in $\ln \xi$).

In general the cycles in the methylchloroform source function are expected to yield new insights into atmospheric processes and test the consistency of the time series data.

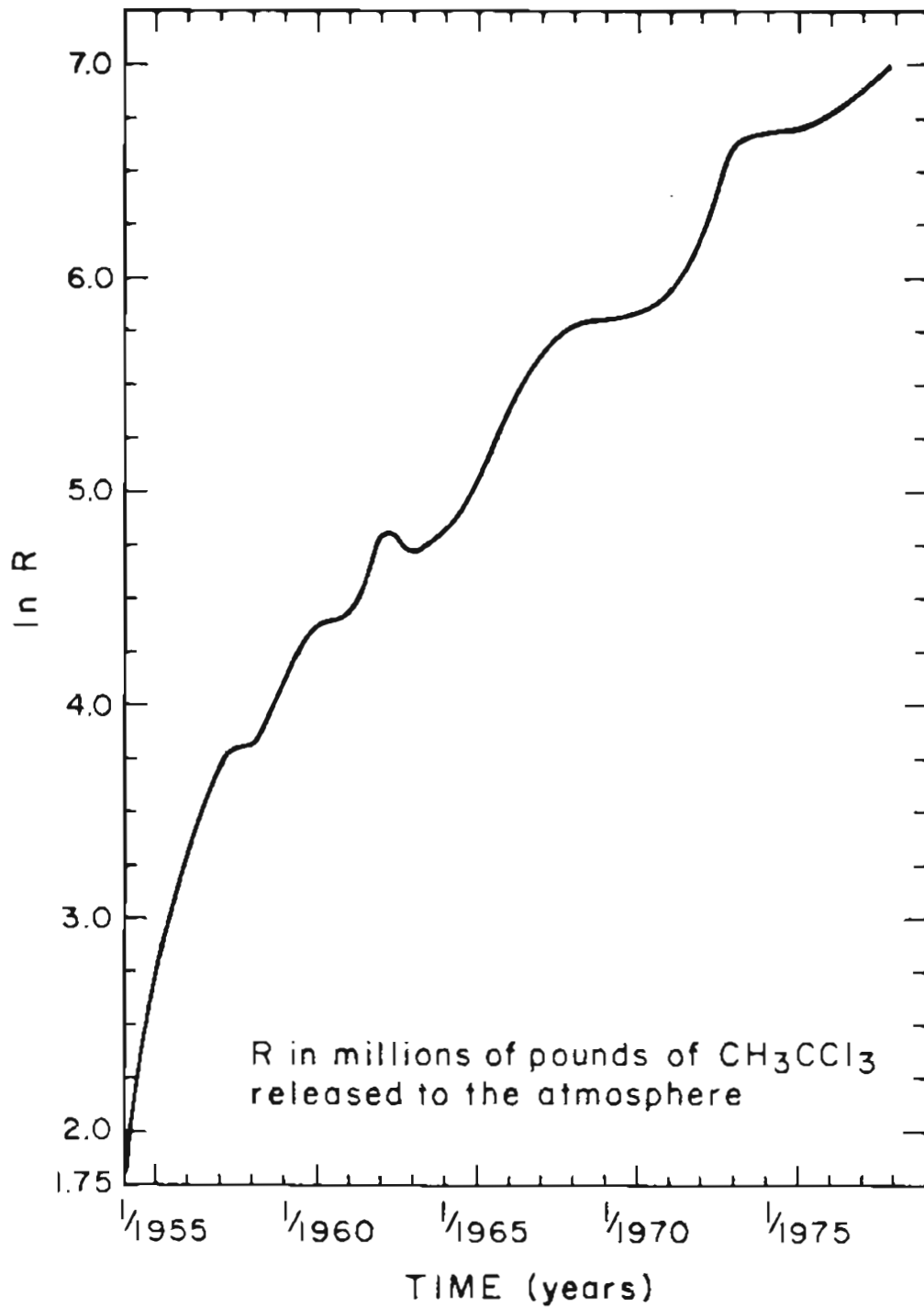
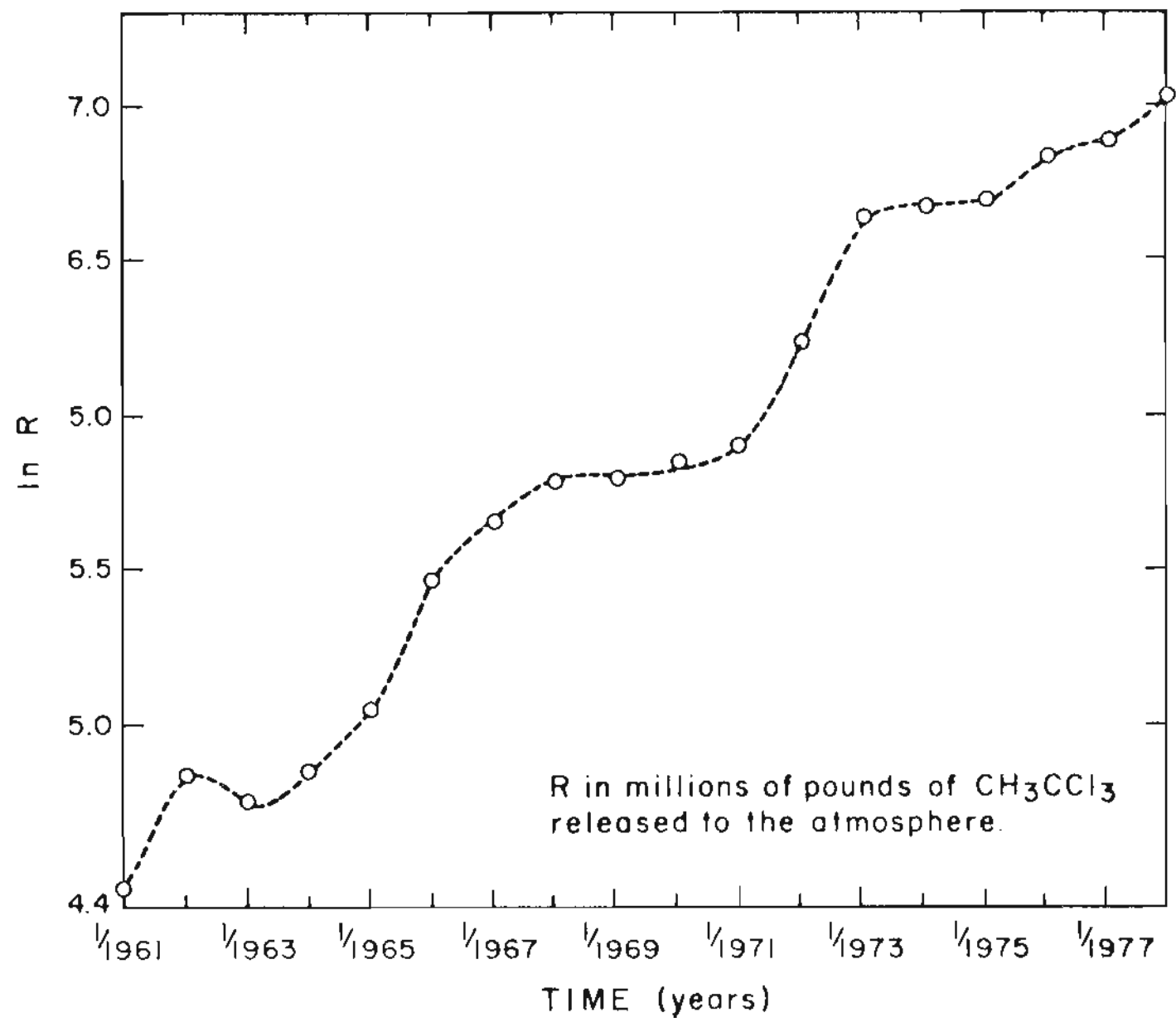


Figure (4.1): Time variation of the global source strength of CH_3CCl_3 .

Figure (4.2): Time variation of global CH_3CCl_3 emissions (1961-1978).



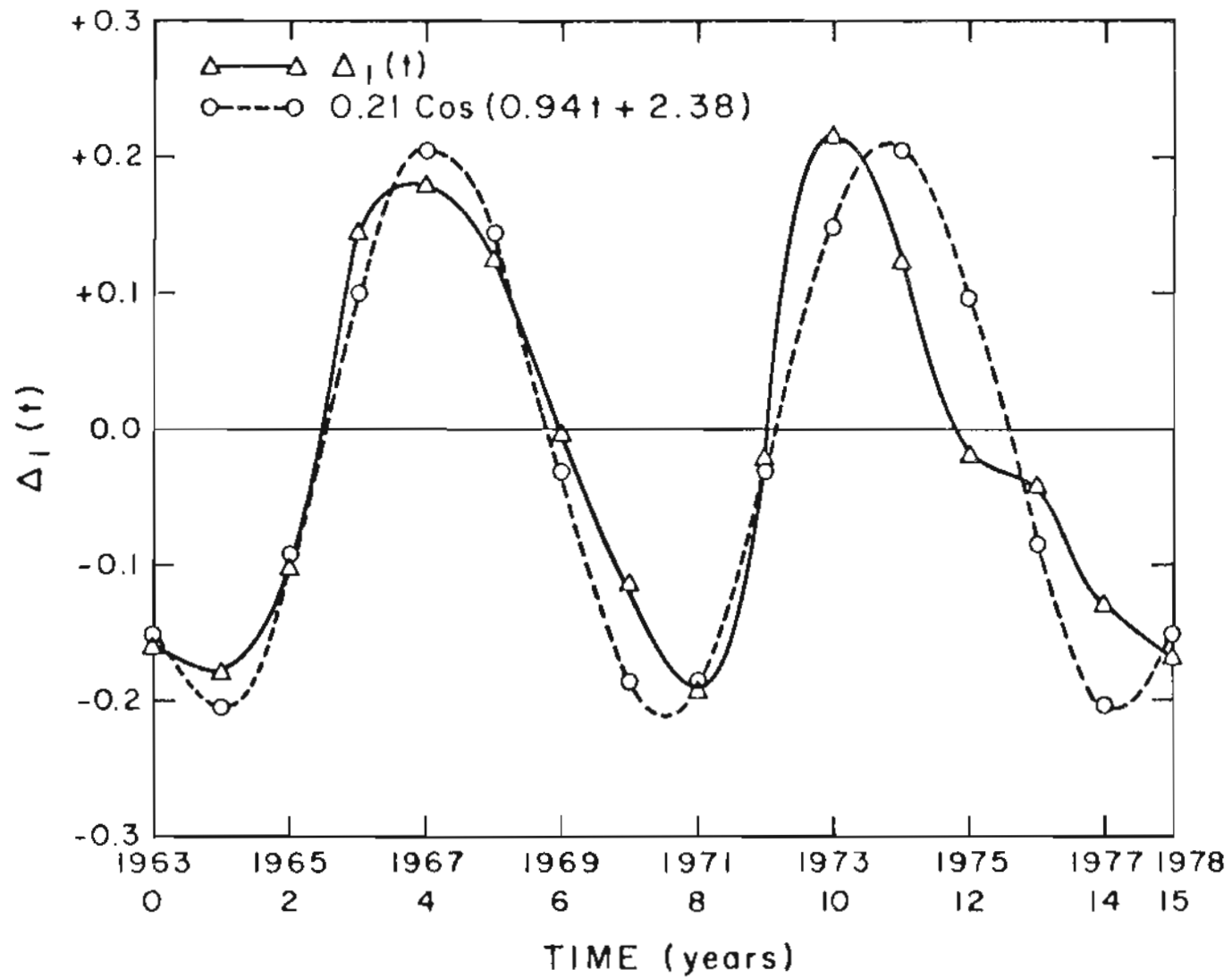


Figure (4.3): The Δ_1 cycle in the global emissions of methylchloroform.

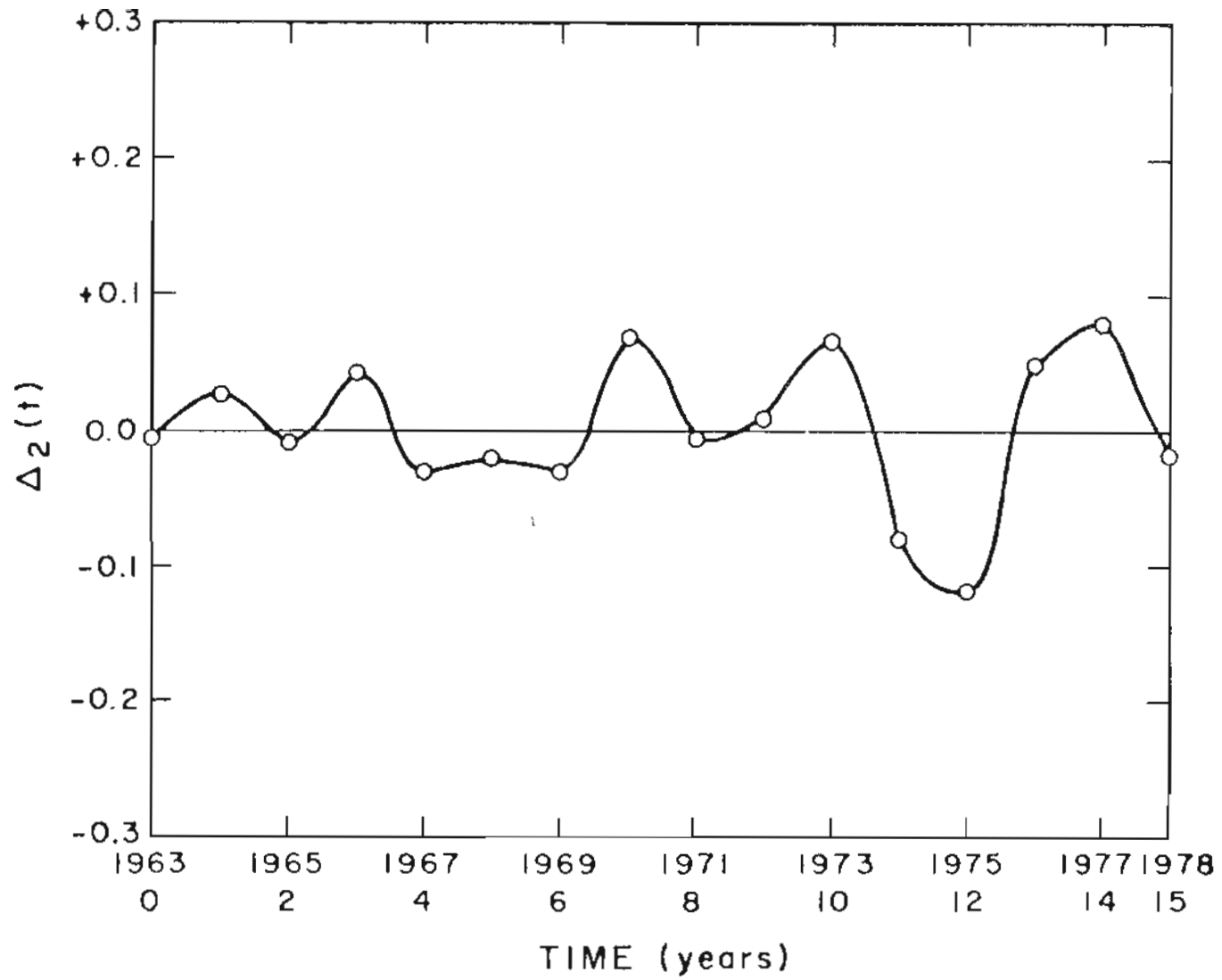


Figure (4.4): The Δ_2 cycle in the global emissions of methylchloroform.

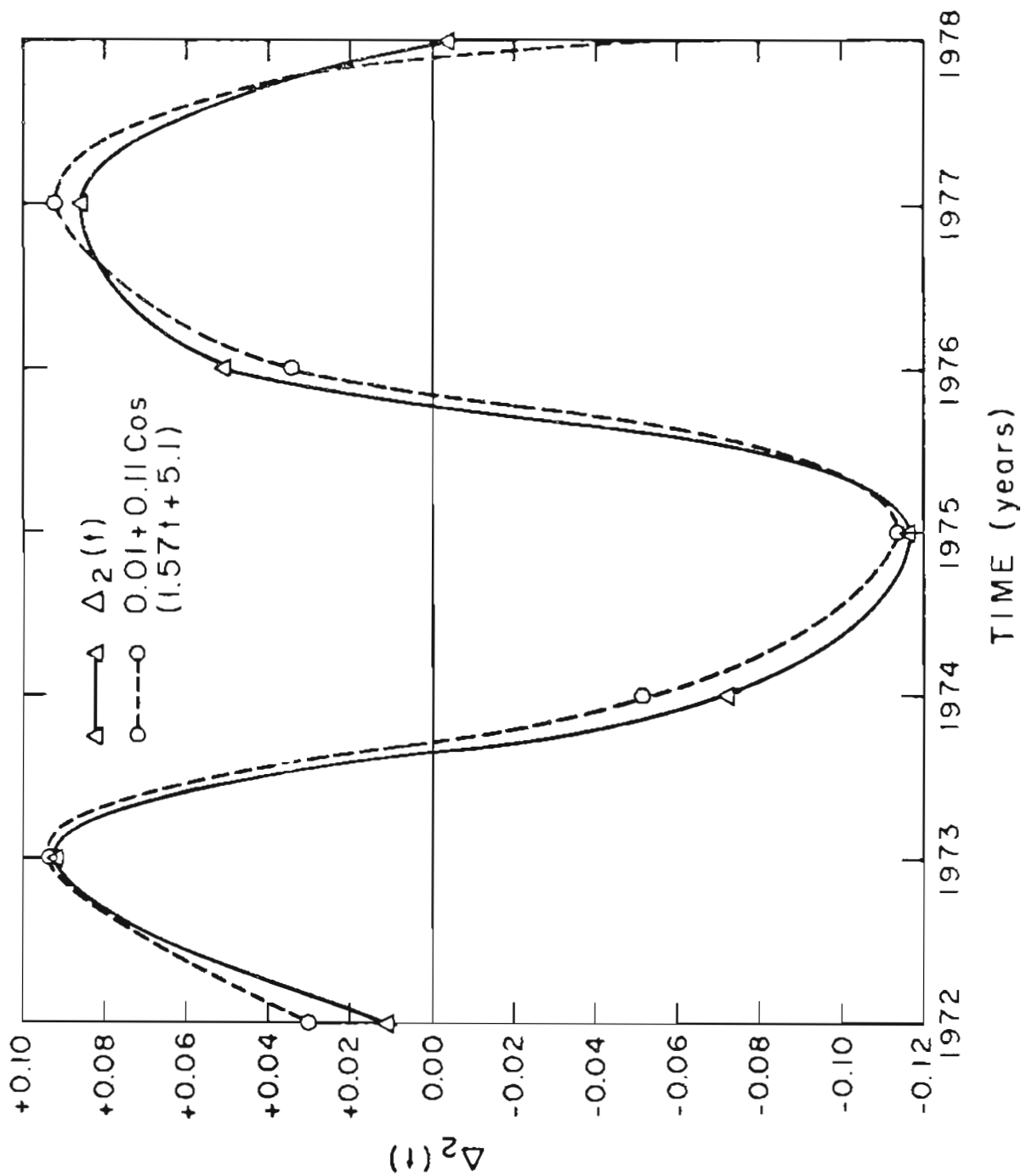


Figure (4.5): A model for the Δ_2 cycle in the global emissions of CH_3CCl_3 .

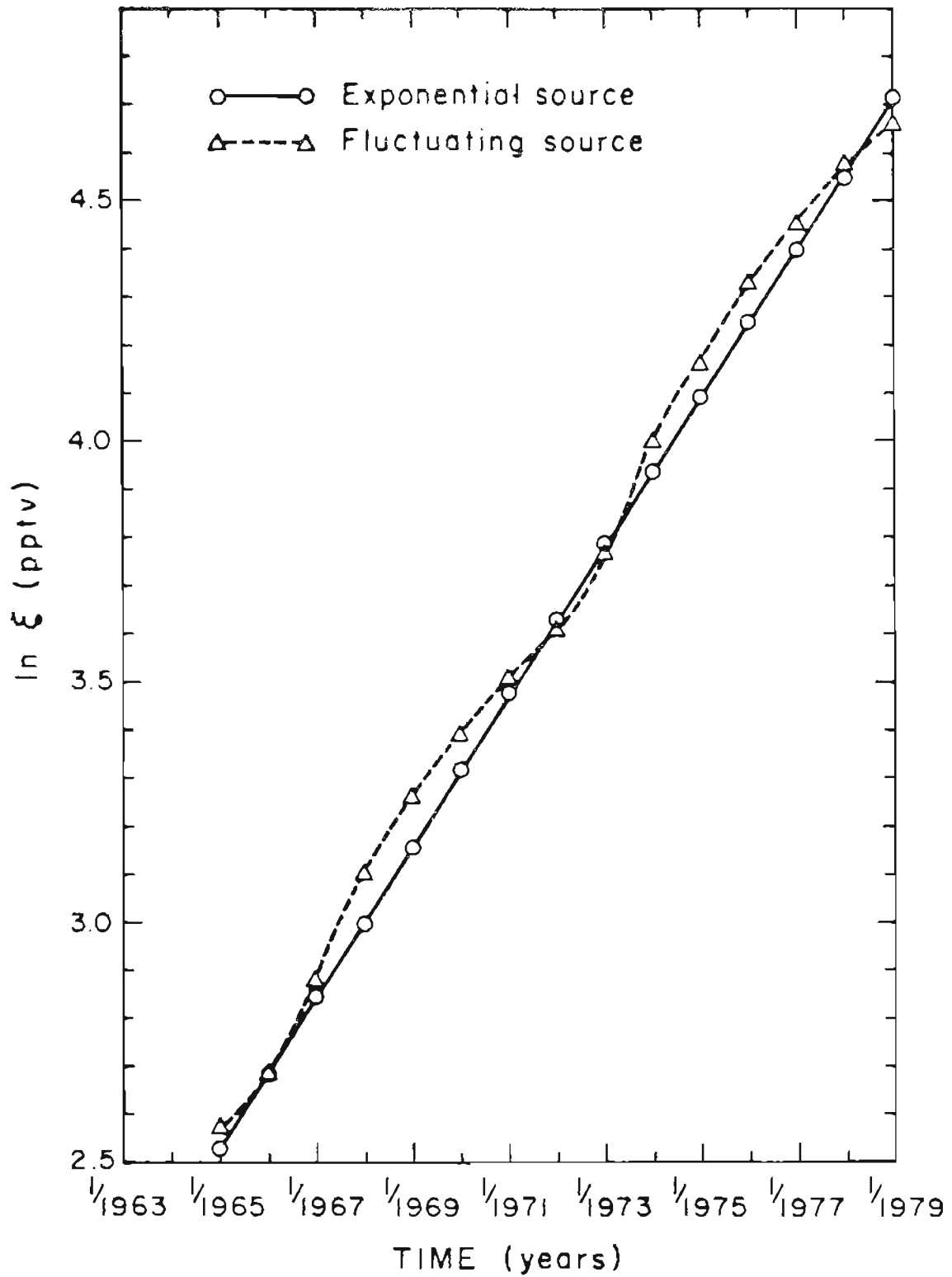


Figure (4.6): Comparison of the predictions of theories with fluctuating and exponentially rising sources.

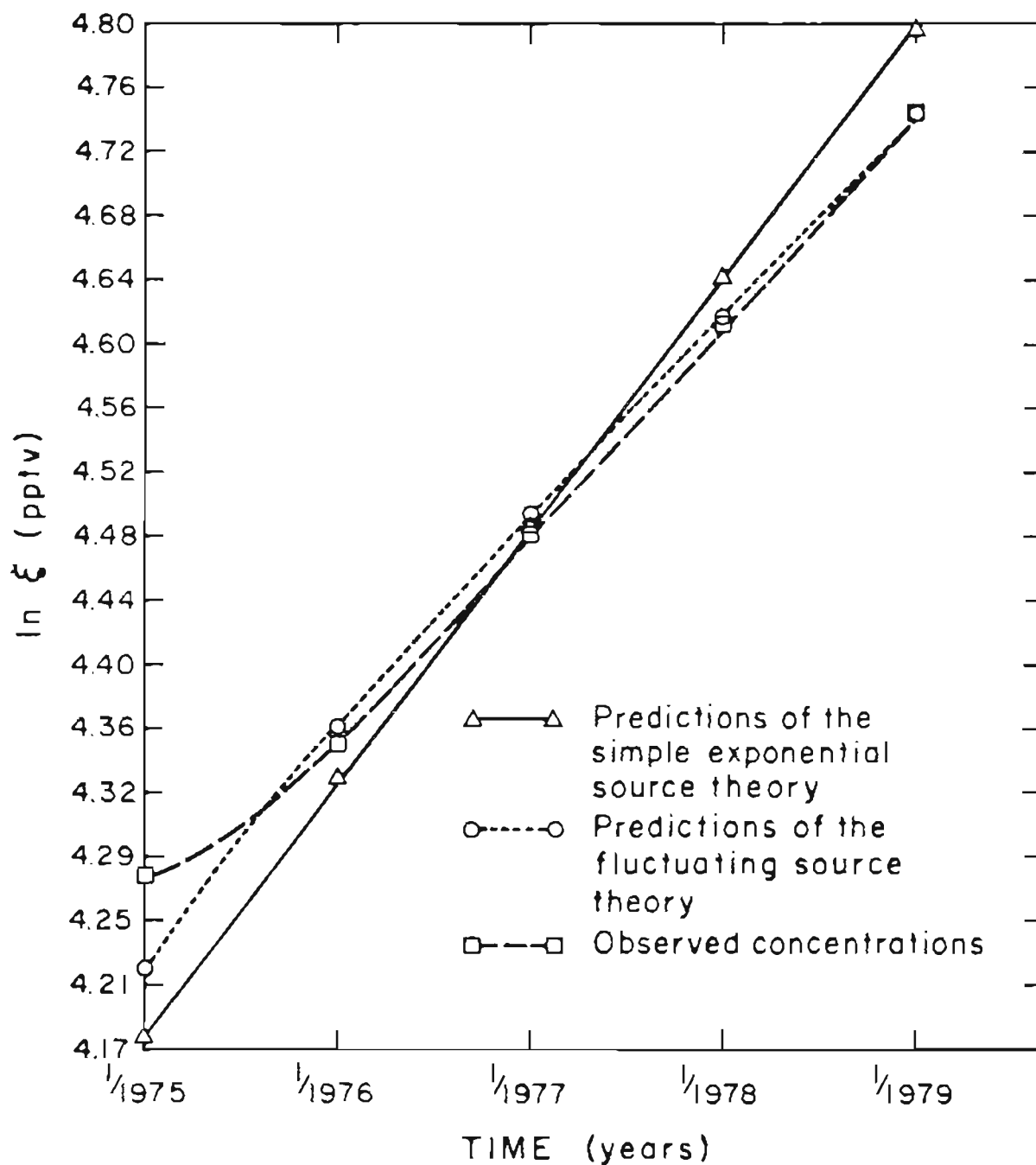


Figure (4.7): A comparison of observed concentrations of CH_3CCl_3 with two theories.

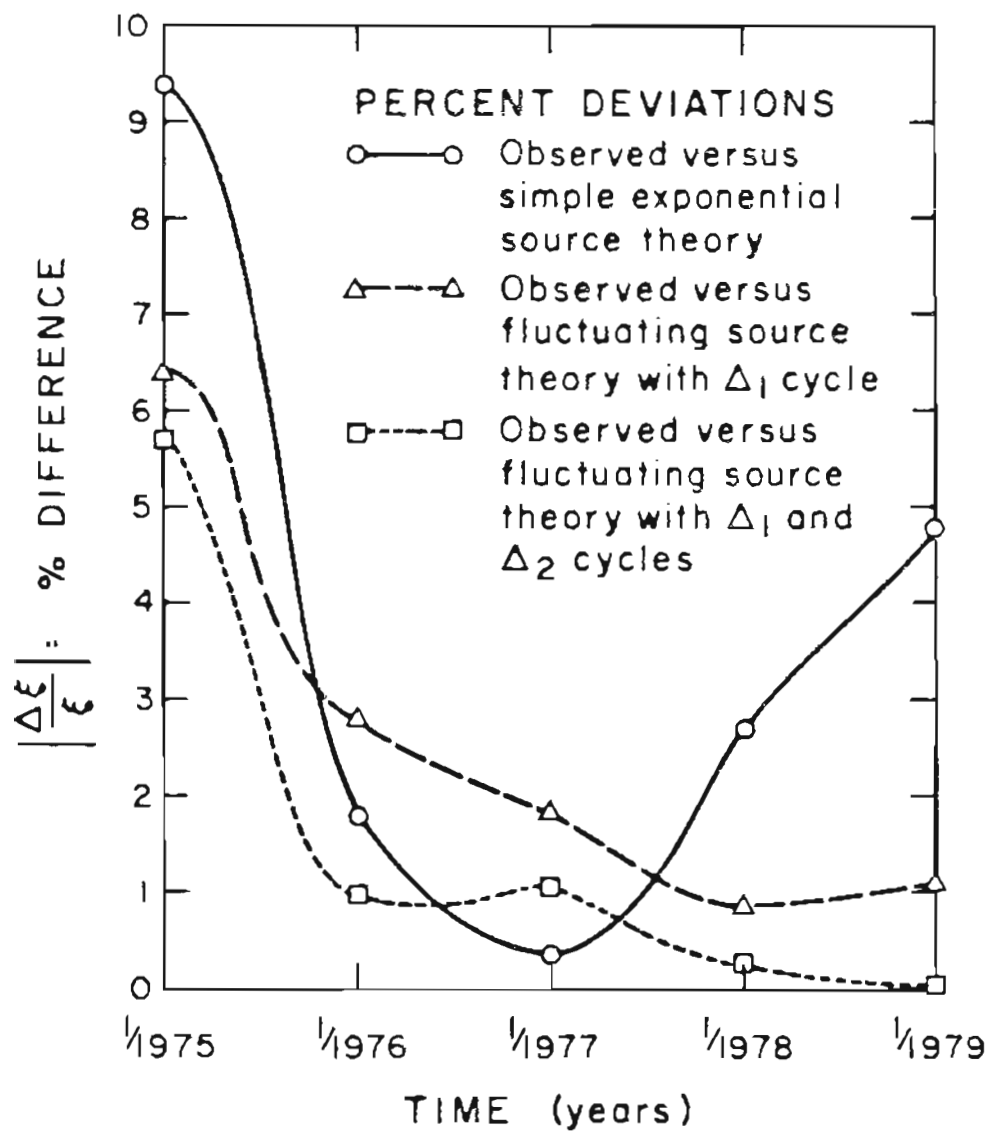


Figure (4.8): Differences between the observed and theoretical global concentrations of methylchloroform.

CHAPTER 5: SOURCES AND INTERHEMISPHERIC GRADIENTS:
APPLICATIONS TO CH_3CCl_3 AND OTHER TRACE GASES

(a) Introduction

The presence of a hemispherical gradient has been experimentally demonstrated for many trace gases. It has also been observed that the ratio of the concentrations, determined by remote northern hemisphere and south pole measurements of some trace gases, changes with time. In this chapter a case is made that, at least for CH_3CCl_3 , such changes of the gradient are real and can be understood on the basis of source fluctuations. The general idea extends to the current and future observations of other trace gases as well. As will soon become apparent, the quantification of this idea is beset by many difficulties. For some short-lived species the gradient can also be used to establish the existence of sources in the southern hemisphere. A criterion for southern hemisphere sources, based on observed gradients, will also be established in this chapter.

There are two types of "gradients" in general use, defined as follows:

$$R = \int_0^{\pi/2} \int_0^{z_T(\phi)} \rho \xi_n(\phi, z, t) \cos \phi \, dz d\phi \bigg/ \int_{-\pi/2}^0 \int_0^{z_T(\phi)} \rho \xi_s(\phi, z, t) \cos \phi \, dz d\phi$$

whereas

$$R_0 = \xi_n(\pi/4, 0, t) \bigg/ \xi_s(-\pi/2, 0, t)$$

where ξ_n and ξ_s are the usual mixing ratios. When the

maximum variations of $\xi(\phi, z, t)$ are small taken over all latitudes (ϕ), then $R \approx R_0$. The time series of data available, on several anthropogenic trace gases, gives R_0 and not R , whereas R drives the transport of trace gases from the northern to southern hemispheres, at least within the framework of hemispherically averaged two-box theories.

(b) Uniqueness of the Methylchloroform Gradient

Methylchloroform is exceptionally suited for the study of gradients because R_0 is large, and the lifetime of intermediate value. The large value of R_0 allows the source fluctuations to have large absolute effects on the gradient. The long atmospheric lifetimes allows transport to control the changes in the gradient, R_0 , otherwise the atmosphere effectively buffers source fluctuations and the effects are washed out. In order to discuss these ideas more quantitatively, it is necessary to adopt a simple model. The best suited compounds whose gradients allow observable changes are those which satisfy the following assumptions: (1) They are of anthropogenic origin, (2) with sources primarily in the northern (or southern) hemisphere. (3) Their lifetimes should be long (compared to interhemispheric transport times). (4) There are no significant differences between the sink strengths in the two hemispheres, and (5) that the emissions have been growing rapidly (exponentially, on the average). It is well known that under these conditions, with the source given by ae^{bt} , the hemispherically averaged mass conservation equations give a constant value of R after a sufficiently long time of release:

$$R = [1 + (b + \eta) \tau_T] \quad (5.1)$$

where b is the rate in the source term $S = ae^{bt}$; τ_T is some effective interhemispheric transport time.

If assumption (1) is relaxed, it becomes very difficult to assess the source term accurately. Usually if assumption (1) is relaxed, assumption (2) has to be given up also. If there are sources in both hemispheres, the gradient becomes much smaller (e.g., N_2O , CO_2 ; exception: CO). If (3) is relaxed, some new measured trace gases become available. Examples include C_2H_4 , C_2Cl_2 , CH_2Cl_2 , $CHCl_3$, and C_2HCl_3 , the measurements of which have been reported by Singh (1979). The gradients of these gases are not transport-controlled. Assumption (4) allows simpler analytical results to hold, but it is not as necessary as the other requirements outlined above. Assumption (5) makes the gradient R bigger. If $b = 0$, $R = 1 + \eta\tau_T$, and we then have to deal with small changes of a small number. Very long lifetimes also lower the gradient, since $\eta \rightarrow 0$. This is the case for F-11 and F-12.

Methylchloroform satisfies all of these assumptions with the possible exception of (4) (Chang and Penner, 1978). As long as lifetimes of CH_3CCl_3 are only slightly different in the two hemispheres, the effect on R_0 is expected to be small. Aside from these good properties of CH_3CCl_3 , there are practical considerations. CH_3CCl_3 is one of the few compounds whose source strength is well known and for which a rea-

sonably long time series of measurements exists. Its gradient R is among the highest of all the known long-lived trace gases.

(c) Trend Analysis of the Gradients, R_0 , of CCl_3F (F-11), CCl_2F_2 (F-12), CCl_4 , and CH_3CCl_3 .

Statistical tests can be applied to the time series of measurements of F-11, F-12, CCl_4 , and CH_3CCl_3 to see if there are any trends (Mann, 1945; Hollander and Wolfe, 1976; Edwards, 1976). The Theil test which was discussed in the previous chapter is applied to F-11, F-12, and CCl_4 . The more standard statistical analysis, based on the t-test, is carried out for CH_3CCl_3 . For the purposes of comparison the t-test is also carried out for F-11 and CCl_4 . The main reason for abandoning the Theil test for CH_3CCl_3 is that the theoretically expected trend of R_0 for CH_3CCl_3 is non-linear based on source fluctuations. Over the period of observations, the theoretical values of R_0 can be approximated by a linear function. But the Theil test overemphasises the departures from linearity. In this case the comments of Brase and Brase (1978) are applicable. They state: "The disadvantages are that they (non-parametric methods) tend to waste information and tend to result in acceptance of the null hypothesis more often than they should; non-parametric tests are sometimes less sensitive than other tests." In the particular case of CH_3CCl_3 , even if the t-test fails to support a linear trend, a time variation can still be present

in some non-linear form.

The model is:

$$R_{oi} = \tilde{\alpha} + \beta t_i + \epsilon_i \quad (5.2)$$

and the hypothesis to be tested is $H_0: \beta = 0$ versus the alternative $H_1: \beta < 0$ for each of the four trace gases mentioned above. The data and results are tabulated below. The details of the calculations are in Appendix I.

Table (5.1) Interhemispheric Gradients, R_o ,
of F-11, F-12, CCl_4 , and CH_3CCl_3 .

t	Yr.	R_o			
		CCl_4	CCl_3F	CCl_2F_2	CH_3CCl_3
1	1/1975	1.08	1.39	--	1.67
2	1/1976	1.10	1.22	1.17	1.72
3	1/1977	1.13	1.21	1.16	1.53
4	1/1978	1.25	1.14	1.15	1.38
5	1/1979	1.04	1.12	1.15	1.42

Table (5.2) Tests of Trends in the
Interhemispheric Gradient R_0

	CCl_4	CCl_3F	CCl_2F_2	CH_3CCl_3
H_0 :	$\beta = 0$	$\beta = 0$	$\beta = 0$	$\beta = 0$
Alternative	$\beta \neq 0$	$\beta < 0$	$\beta < 0$	$\beta < 0$
Theil test				
c	+ 2	- 10	- 5	--
α	0.1	0.025	0.025	--
result	accept H_0	reject H_0	accept H_0	--
t-test				
t	0.24	- 4.1	--	- 3.35
α	0.05	0.025	--	0.025
result	accept H_0	reject H_0	--	reject H_0

The results given in Table (5.2) show that trends are probable in the gradients of F-11 and CH_3CCl_3 .

Another way to look at the trend in the gradient of CH_3CCl_3 is to establish that $\ln \xi_s$ and $\ln \xi_n$ as linear functions of time have statistically significant differences in their slopes. In other words, if ξ_s (concentration at the south pole) = $a_s \exp[b_s t]$ and ξ_n (concentration in the Pacific northwest) = $a_n \exp[b_n t]$, it is desirable to establish that $b_n - b_s < 0$ so that

$$R_0(\text{observed}) = \frac{a_n}{a_s} e^{(b_n - b_s)t} \quad (5.3)$$

$$\approx \frac{a_n}{a_s} (1 - |b_n - b_s| t)$$

Eqn. (5.3) then says that the slope of the gradient R_0 is

$$-\frac{a_n}{a_s} | b_n - b_s |.$$

The hypothesis to be tested is $H_0: \beta_n - \beta_s = 0$ versus the alternative $H_1: \beta_n - \beta_s < 0$. Computational details are presented in Appendix I. The methods used in the calculations can be found in Edwards (1976). The level of significance was fixed as $\alpha = 0.01$ and the results are that $t = -3.42$ with 6 degrees of freedom. The critical t value is $t = -3.143$. Since our t is less than this, H_0 is rejected at the $\alpha = 0.01$ level. In these computations $b_n = 0.011/\text{yr}$ and $b_s = 0.153/\text{yr}$, $b_n - b_s = -0.054/\text{yr}$.

The least squares slope for R_0 is $b_* \approx -0.084/\text{yr}$. The 90% ($1 - \alpha = 0.9$) symmetric confidence interval for the slope, based on the t -statistic is $(b_{*U}, b_{*L}) = (-0.025/\text{yr}, -0.143/\text{yr})$. Note that from eqn. (5.3) the slope of the gradient, b_* , is not just the difference of the slopes of $\ln \xi_n$ and $\ln \xi_s$. It should also be noted that the 90% confidence interval for the slope is quite wide. This can be partially explained by the assumption of linearity for R_0 , when in fact there may be physical mechanisms that can account for the non-linearity.

Encouraged by the results of this section, some possible mechanisms for the changing gradient can now be considered.

(d) Theoretical Investigation of the Changing Methylchloroform Gradient, R_0

The main mechanism which succeeds in explaining the shape and values of the CH_3CCl_3 gradient function R_0 is the cyclic source fluctuation discussed in the last chapter. There are various available methods to introduce the source fluctuations to construct the theoretical expression for R_0 . The more physically exact the theory is, the more information it needs to specify the internal variables such as transport times and sink strengths. Several possible theoretical constructions were explored to account for the changing gradient R_0 . These methods are, more or less, equivalent, though some are more physically satisfactory than others. The common feature that all these methods required was the cyclic fluctuations found in the analysis of the CH_3CCl_3 source function.

Considering the results to be presented here, it appears likely that the measured values of the CH_3CCl_3 gradient behave the way they do because of the cyclic fluctuations of the source. Without source fluctuations the gradient is predicted to be constant at the mean value.

The simplest idea that can be used is to assume that the concentrations observed at the south pole (SP) at time t are due to the source strength at some earlier time $t' = t - t_*$ where t_* is the delay time. It is assumed that an overwhelmingly large portion of the CH_3CCl_3 content in the south polar cell is from the northern hemis-

pheric sources. This assumption is in keeping with the generally accepted belief that there are no significant sources of CH_3CCl_3 in the southern hemisphere. When CH_3CCl_3 is transported from the northern hemisphere, it undergoes more mixing with the somewhat "cleaner" air of the southern hemispheric troposphere, and some of it is also destroyed by atmospheric HO radicals and any other sinks that may be present. It is expected that the sink mechanisms are very weak in the polar cell since the mean yearly average of HO radicals is small there. The actual amount of CH_3CCl_3 which reaches the polar cell is, therefore, a function of the mechanisms discussed above. These mechanisms still leave the rate of increase at the south pole equal to the rate of increase in the northern hemispheric concentrations, but with a time shift of t_* . The value of t_* is bigger than the interhemispheric transport time since material has to be transported not only across the low equatorial latitudes, but all the way to the south pole. The upshot of this discussion is that

$$R_0 = a \frac{\xi_n(t)}{\xi_r(t-t_*)} \quad (5.4)$$

where a is some proportionality constant. Considering only the Δ_1 cycle discussed in the previous chapter:

$$R_0 \approx \tilde{R}_0 \frac{[1 + \sigma f_0(\phi' + \omega t)]}{[1 + \sigma f_0(\phi' + \omega t - \omega t_*)]} \quad (5.5)$$

$$\sigma = \frac{\omega \alpha' (b + \eta)}{\omega^2 + (b + \eta)^2}$$

In Fig. (5.1) R_0 of eqn. (5.5) is plotted for various values of t_* . All the variables in $f_0(\phi + \omega t)$ and $f_0(\phi + \omega(t-t_*))$ are from the source data and are the same values used in the last chapter. Details of the calculations are in Appendix I.

It appears that eqn. (5.5) is in very good agreement with the measured changing gradient. The frequency of the Δ_1 cycle is just right to explain the observed behaviour of R_0 . It is also possible to obtain better agreement between eqn. (5.5) and the observed values of R_0 by increasing ω (in Δ_1) which is justified since during the period of interest ω is a little higher than 0.94 radians/yr. This changes α' and ϕ' as shown in eqns. (9.14) - (9.16) of Chapter 9. Taking the Δ_2 cycle into account does not make a significant difference here. These possibilities may be explored further if desired. For this study the values of all the parameters except \tilde{R}_0 and t_* in (5.5) are determined from the source data and this theoretical expression is considered to explain the shape of the changing gradient function of a sufficient degree of accuracy.

Equation (5.5) was derived, based on rather simplified ideas. It

For the Δ_1 cycle and the main exponential growth term in the source function:

$$R_o = \tilde{R}_o \frac{[1 + \sigma f_o(\phi' + \omega t)]}{[1 + \sigma f_o(\phi' + \omega t - \omega t_*)]} \quad (5.5)$$

$$\sigma = \frac{\omega \alpha' (b + \eta)}{\omega^2 + (b + \eta)^2}$$

In Fig. (5.1) R_o of eqn. (5.5) is plotted for various values of t_* . All the variables in $f_o(\phi + \omega t)$ and $f_o(\phi + \omega(t-t_*))$ are from the source data and are the same values used in the last chapter. Details of the calculations are in Appendix I.

It appears that eqn. (5.5) is in very good agreement with the measured changing gradient. The frequency of the Δ_1 cycle is just right to explain the observed behaviour of R_o . It is also possible to obtain better agreement between eqn. (5.5) and the observed values of R_o by increasing ω (in Δ_1) which is justified since during the period of interest ω is a little higher than 0.94 radians/yr. This changes α' and ϕ' as shown in eqns. (9.14) - (9.16) of Chapter 9. Taking the Δ_2 cycle into account does not make a significant difference here. These possibilities may be explored further if desired. For this study the values of all the parameters except \tilde{R}_o and t_* in (5.5) are determined from the source data and this theoretical expression is considered to explain the shape of the changing gradient function of a sufficient degree of accuracy.

Equation (5.5) was derived, based on rather simplified ideas. It

turns out that the form of equation (5.5) follows from all theories where the mass conservation equation is spatially averaged over any given scale. But in all cases the fluctuations of the source term must be included, otherwise the observed changes of the gradient R_0 cannot be properly explained. Consider, first, a two-box theory, which is discussed in more detail in Chapter 10 as a special case. It is no longer necessary to postulate the delay time t_* . The role of t_* is taken by $\tau_* = 1/\eta_*$ where τ_* is the so-called interhemispheric transport time. This theory is expressed by the equations (5.6) and 5.7):

$$\dot{\xi}_n = S_n - \eta \xi_n - \eta_* (\xi_n - \xi_s) \quad (5.6)$$

$$\dot{\xi}_s = -\eta \xi_s + \eta_* (\xi_n - \xi_s) \quad (5.7)$$

It is assumed that the lifetimes are not significantly different in the two hemispheres. The solutions of (5.6) and 5.7) are:

$$\xi_n = \frac{1}{2} [\Omega(n, t) + \Omega(n + 2\eta_*, t)] \quad (5.8)$$

$$\xi_s = \frac{1}{2} [\Omega(n, t) - \Omega(n + 2\eta_*, t)] \quad (5.9)$$

$$\Omega(x, t) = e^{-xt} \int_0^t S(t') e^{xt'} dt' \quad (5.10)$$

For the Δ_1 cycle and the main exponential growth term in the source function:

$$\Omega(x, t) \approx \frac{ae^{bt}}{b+x} \left[1 + \frac{(b+x)\alpha\omega}{\omega^2 + (b+x)^2} \left(\sin(\phi + \omega t) + \frac{b+x}{\omega} \omega(\phi + \omega t) \right) \right]$$

From eqns. (5.8) and (5.9) the gradient R, discussed in Section (5.a) can be written as:

$$R = \frac{\xi_n}{\xi_s} \approx \frac{\left(\frac{1}{b+\eta} + \frac{1}{b+\eta+2\eta_*} \right) + \left(\frac{\alpha'\omega}{\omega^2+(b+\eta)^2} f_o + \frac{\alpha'\omega}{\omega^2+(b+\eta+2\eta_*)^2} g_o \right)}{\left(\frac{1}{b+\eta} - \frac{1}{b+\eta+2\eta_*} \right) + \left(\frac{\alpha'\omega}{\omega^2+(b+\eta)^2} f_o - \frac{\alpha'\omega}{\omega^2+(b+\eta+2\eta_*)^2} g_o \right)} \quad (5.11)$$

$$R = \frac{Y_n + Z_n}{Y_s + Z_s} \quad (5.12)$$

$$f_o = \sin(\phi' + \omega t) + \frac{b+\eta}{\omega} \cos(\phi' + \omega t) \quad (5.13)$$

$$g_o = \sin(\phi' + \omega t) + \frac{b+\eta+2\eta_*}{\omega} \cos(\phi' + \omega t) \quad (5.14)$$

where Y_n , Z_n , Y_s and Z_s are the terms inside the parentheses () in eqn. (5.11). R can be rewritten as

$$R = \bar{R} \left[\frac{1 + Z_n / Y_n}{1 + Z_s / Y_s} \right] \quad (5.15)$$

$$\bar{R} = \frac{Y_n}{Y_s} = [1 + (b+\eta)/\eta_*] \quad (5.16)$$

Eqn. (5.16) is the same as eqn. (5.1), so that the gradient R is the usual gradient \bar{R} with the fluctuating term represented by $[1 + A_z/Y_n] [1 + Z_s/Y_s]^{-1}$. Eqn. (5.15) can be rewritten as:

$$R = \bar{R} \left[\frac{1 + a_0 \sin(\omega t + \phi) + a_1 \cos(\omega t + \phi)}{1 + b_0 \sin(\omega t + \phi) + b_1 \cos(\omega t + \phi)} \right] \quad (5.17)$$

The primes on ϕ 's and α 's will be dropped for notational convenience, but their presence will be implicitly assumed.

Later it will be shown that eqn. (5.17) is generally true for all theories, regardless of the scale of the spatial average (number of boxes). The only requirement is that the source term contains a Δ_1 term. Recall that a source with a Δ_1 term is $S = ae^{bt} [1 + \alpha \cos(\omega t + \phi)]$. Different theories may, however, predict different values of \bar{R} , a_0 , a_1 , b_0 , and b_1 .

For the two-box theory it has already been shown that \bar{R} is given by eqn. (5.16), and with some patience a_0 , a_1 , b_0 , and b_1 can be shown to be:

$$a_0 = \frac{\alpha \omega (b+\eta) (b+\eta+2\eta_*) \{ [\omega^2 + (b+\eta)^2] + [\omega^2 + (b+\eta+2\eta_*)^2] \}}{2 [\omega^2 + (b+\eta)^2] [\omega^2 + (b+\eta+2\eta_*)^2] [b+\eta+\eta_*]} \quad (5.18)$$

$$a_1 = \frac{\alpha (b+\eta) (b+\eta+2\eta_*) \{ [\omega^2 + (b+\eta+2\eta_*)^2] (b+\eta) + [\omega^2 + (b+\eta)^2] (b+\eta+2\eta_*) \}}{2 [\omega^2 + (b+\eta)^2] [\omega^2 + (b+\eta+2\eta_*)^2] [b+\eta+\eta_*]} \quad (5.19)$$

$$b_0 = \frac{2\alpha\omega (b+\eta+\eta_*) (b+\eta) (b+\eta+2\eta_*)}{[\omega^2+(b+\eta)^2][\omega^2+(b+\eta+2\eta_*)^2]} \quad (5.20)$$

$$b_1 = \frac{\alpha(b+\eta) (b+\eta+2\eta_*) [(b+\eta+2\eta_*) (b+\eta) - \omega^2]}{[\omega^2+(b+\eta)^2][\omega^2+(b+\eta+2\eta_*)^2]} \quad (5.21)$$

In this case the value of \bar{R} is predicted by the theory in terms of simpler variables. In Fig. (5.2) the values of R_0 predicted by this theory are plotted for several values of the transport time τ_* . All other variables are essentially the same as those found from the source analysis given in the previous chapter. Details of the calculations are given in Appendix I.

It is important to note that the two-box theory does not directly predict R_0 but instead it gives equations for R . (The differences between R and R_0 were pointed out in section (a) of this chapter, and will be discussed further in Chapter 8.) In order to compare the values of the gradient R , derived here with the observed values of R_0 , R was transformed into R_0 by the equation

$$R_0 = [R(1 - \frac{\alpha}{2\phi_0}) - \frac{\alpha}{2\phi_0}] [1 - \frac{\alpha}{2\phi_0} (1+R)]^{-1} \quad (5.22)$$

$$\alpha = (1 - \cos\phi_0)$$

where ϕ_0 is the latitude beyond which the concentration almost stops changing with latitude. The value of ϕ_0 was taken as $\pi/6$ determined

from independent global data for CH_3CCl_3 , F-11 and F-12. In these calculations ω was taken to be 0.9 radians per year.

In summary, the obvious approximations that can contribute to disagreement between theory and observations are: (1) an average transport time τ_* is used; (2) the theory calculates R which has to be converted to R_0 since observations are only for R_0 ; (3) northern and southern hemispheres lifetimes are assumed to be the same and constant; (4) Δ_2 -cycle is neglected, and finally (5) transient terms of the form $\alpha_1 e^{-\lambda_1 t}$ and $\alpha_2 e^{-\lambda_2 t}$ are assumed to be negligible (λ_1 and λ_2 are eigenvalues of the matrix M where $M_{11} = (\eta + \eta_*) = M_{22}$; $M_{12} = M_{21} = -\eta_*$, so that $\lambda_1 = \eta$, $\lambda_2 = \eta + 2\eta_*$). The most serious difficulties within the framework of this theory are probably due to the oversimplification of atmospheric transport. Considering these factors, the agreement between theory and observations is very good as shown in Fig. (5.2). It is especially noteworthy that the shape of the gradient is described very well. More extensive calculations also indicate that the values of R_0 are sensitive to changes in several of the variables involved. It is clear from the figure that the function $R_0(t)$ is sensitive to the interhemispheric transport time τ_* . R_0 is also sensitive to ω and ϕ . The good agreement between theory and observations indicates that the values of these parameters determined from independent source data are very close to those required to explain the observations optimally. So it is probable that the source variations are real and are manifested in the observed R_0 as a function of time.

In order to avoid some of the problems discussed above, a four-box theory was used to investigate the changing methylchloroform gradient. This theory divides the troposphere into four pieces of approximately equal air masses. The divisions are along latitude circles. Some of the details of this theory are discussed in Chapter 10, and will be briefly reviewed here. The northern and southern hemispheres are subdivided into two sections each at 30°N and 30°S latitudes respectively. Very approximately, this is a reasonable division to approximate the barriers to meridional transport (Barry and Chorley, 1968). Figure (5.3) illustrates the general features of the theory. Note that the transport times between the two northern hemispheric boxes and the two southern hemispheric boxes are assumed to be equal. The lifetimes in the boxes on either side of the equator are also assumed to be equal. The lifetimes in the northernmost and southernmost boxes are also equal, but longer than the boxes on either side of the equator. This feature is needed to reflect the smaller HO concentrations in these boxes. The theory is defined by the system of equations:

$$\frac{d\underline{\xi}(t)}{dt} = \underline{S}(t) - M\underline{\xi}(t) \quad (5.23)$$

$\underline{\xi}(t)$ is a (vector) 4x1 matrix, representing the concentrations in each of the four boxes. $S(t)$ is also a 4x1 matrix representing the sources in each box. M is a 4x4 matrix representing the transport between boxes and the destruction within each box.

$$M = \begin{bmatrix} (\eta + \eta_T + \eta_0) & -\eta_T & -\eta_0 & 0 \\ -\eta_T & (\eta + \eta_T + \eta_0) & 0 & -\eta_0 \\ -\eta_0 & 0 & (\eta + \eta_0) & 0 \\ 0 & -\eta_0 & 0 & (\eta + \eta_0) \end{bmatrix} \quad (5.24)$$

The solution to eqn. (5.23) is:

$$\underline{\xi} = P^{-1} e^{-\Lambda t} \int_0^t e^{\Lambda t'} P \underline{s}(t') dt' \quad (5.25)$$

where Λ is the matrix: $\Lambda_{ij} = \lambda_i \delta_{ij}$ and δ_{ij} is the Kronecker delta.

P is a 4x4 matrix which is defined by the following relationship:

$$PMP^{-1} = \Lambda \quad (5.26)$$

Equations (5.25) and 5.26) are discussed in more detail in Chapter 10.

λ_i are the eigenvalues of M . In the case under consideration λ_i are:

$$\lambda_{\left(\frac{1}{2}\right)} = \frac{1}{2}(\eta + 2\eta_T + 2\eta_0 + \bar{\eta}) \pm \frac{1}{2}[(\eta + 2\eta_T - \bar{\eta})^2 + 4\eta_0^2]^{\frac{1}{2}} \quad (5.27)$$

$$\lambda_{\left(\frac{3}{4}\right)} = \frac{1}{2}(\eta + 2\eta_0 + \bar{\eta}) \pm \frac{1}{2}[(\eta - \bar{\eta}) + 4\eta_0^2]^{\frac{1}{2}} \quad (5.28)$$

Here $4\eta_0^2$ is usually $\gg (\eta - \bar{\eta})^2$, therefore

$$\lambda_3 \approx \frac{1}{2}(\eta + \bar{\eta}) + 2\eta_0; \quad \lambda_4 \approx \frac{1}{2}(\eta + \bar{\eta}) \quad (5.29)$$

The matrix P is given explicitly in Appendix I as are the details of the numerical calculations on which the rest of the discussion, in this section, is based.

This theory predicts R_0 directly and there is no need to use eqn. (5.22). This result is based on the observation that there is no significant change in the concentration with latitude in the northernmost and southernmost boxes (boxes 3 and 4). The equations for the gradients of CH_3CCl_3 are of the form given by eqn. (5.17):

$$R_0 = \bar{R}_0 \frac{1 + a_0 \sin(\omega t + \phi) + a_1 \cos(\omega t + \phi)}{1 + b_0 \sin(\omega t + \phi) + b_1 \cos(\omega t + \phi)} \quad (5.30)$$

and then the Δ_2 -cycle is included:

$$R_0 = \bar{R}_0 \frac{1 + a_0 \sin(\omega t + \phi) + a_1 \cos(\omega t + \phi) + a_2 \sin(\omega_* t + \phi_*) + a_3 \cos(\omega_* t + \phi_*)}{1 + b_0 \sin(\omega t + \phi) + b_1 \cos(\omega t + \phi) + b_2 \sin(\omega_* t + \phi_*) + b_3 \cos(\omega_* t + \phi_*)} \quad (5.31)$$

The values of all the symbols a_0 , a_1 , a_2 , a_3 , b_0 , b_1 , b_2 , b_3 and \bar{R}_0 are completely determined by the source data and the transport and lifetime coefficients. The values of the a's, b's and \bar{R}_0 are very complicated functions of η , η_T , $\bar{\eta}$, ω , ω_* , ϕ , ϕ_* and b (the rate of the exponential source term), so these will not be discussed here but can be found in Appendix I.

The results of the analysis using this theory are shown in Figures (5.4) and (5.5). The assumptions under which these calculations

were made are as follows: For Figure (5.4) $\eta = 0.12/\text{yr}$, $\bar{\eta} = 0.08/\text{yr}$, $\eta_T = 1.14/\text{yr}$, and η_0 is varied so that $\eta_0 = 5.0/\text{yr}$ (curve 1), 4.0 (curve 2) and 3.5 (curve 3). The observed values are given by the triangles (Δ). The calculations of Figure (5.4) are based on the Δ_1 -cycle only and calculated from eqn. (5.30). The source is assumed to be divided up between boxes 1, 2 and 3. The major source is $S_3 = 0.8S$ where $S = ae^{bt}(1+\Delta_1)$; $S_1 = (0.1)(ae^{bt}) = S_3$. This assumes that the main sources are in the northernmost box (beyond 30°N). Figure (5.5) is based on exactly the same assumptions as curves 1 and 2 of Figure (5.4) except that the effect of the Δ_2 cycle is added. The Δ_2 cycle is added with the simplifying approximation: $S = ae^{bt}(1+\Delta_1+\Delta_2)$. The values of the η 's can be converted to the more familiar τ 's (η 's = $1/\tau$'s). The results of the conversion are $\eta = 0.12/\text{yr} \leftrightarrow \tau = 8.3 \text{ yrs} = \text{lifetime of } \text{CH}_3\text{CCl}_3 \text{ in boxes 1 and 2}$, $\bar{\eta} = 0.08/\text{yr} \leftrightarrow \bar{\tau} = 12.5 \text{ yrs} = \text{lifetime in boxes 3 and 4}$. $\eta_0 = 5/\text{yr} \leftrightarrow 2.4 \text{ months} = \text{transport time between boxes 2 and 3}$. $\eta_T = 1.14$ corresponds to $\tau_T = 320 \text{ days}$ (see Newell et al., 1969).

The changing gradient of CH_3CCl_3 can be characterized by two main variables which are convenient for the discussion of the agreement between theory and experiment. First in the mean gradient \bar{R}_0 which would be expected if no source fluctuations were present; and the second is the depth of the variation given by

$$\delta_R = R_0(\text{max}) - R_0(\text{min}) \quad (5.32)$$

For equations of the type represented by (5.17):

$$\delta_R \approx 2[(a_0 - b_0)^2 + (a_1 - b_1)^2]^{1/2} \bar{R}_0 \quad (5.33)$$

Eqn. (5.33) holds when a_0 , b_0 , a_1 and b_1 are all small ($\ll 1$).

To obtain the correct value of \bar{R}_0 is very easy because there are enough uncertainties in η_T (or η_* for the 2-box theory) and in τ (the lifetime). Obtaining the proper depth δ_R is much more complicated. The 2-box theory does not have as much depth as the 4-box theory, and the 4-box theory with the Δ_2 term has better depth than the 4-box theory without the Δ_2 term. The 4-box theory with the Δ_2 term is in excellent agreement with the observed \bar{R}_0 for all years except 1976. It can be concluded that the fluctuating source theory explains the observed changes in the CH_3CCl_3 gradient. The gradient would be predicted to be constant at the mean value \bar{R}_0 (depending on η and η_T) if the source fluctuations are ignored.

Many additional calculations were also carried out with the 4-box theory described in this section. These calculations investigated the effects of changing the variables about which we do not have precise knowledge. The results of these calculations are deferred to Appendix I, but the general conclusions will be discussed here. It is common knowledge that "speeding up the chemistry" (shorter lifetimes) results in larger gradients \bar{R}_0 , and "speeding up the transport" results in

smaller gradients R_o . If we believe that the gradient is constant, then only \bar{R}_o has to be explained and the interplay of the transport and chemistry allows a very wide range of choices of η_T , η_o (or η_* of the 2-box theory) and τ to accomplish this. If, on the other hand, the gradient is changing as in the case studied here and is due to the fluctuations of the source, then this possible range of choices for the transport and lifetime variables is reduced. The depth δ_R being large requires that there be a delay of response in the southern hemisphere concentrations compared to the northern hemisphere concentrations. The gradient will change the most if the southern hemisphere concentration is on the downswing when the northern hemisphere concentration is on the upswing and vice versa. This is expressed in the eqn. (5.17) by making a_o , a_1 big and at the same time making b_o and b_1 small (negative if possible). When the transport is made long by the desire to obtain greater depth δ_R , the lower bound of τ (and $\bar{\tau}$), the lifetime, is increased substantially in order to get a low enough value of \bar{R}_o to be representative of the observations. If the lifetime is increased too much, the fluctuations tend to be further dampened as discussed in previous chapters, thus decreasing the depth δ_R . On the other hand, if the lifetime is lowered, the fluctuations become more prominent, thus increasing δ_R , but the faster transport times required to reproduce \bar{R}_o lead to a simultaneous decrease in δ_R . Therefore, δ_R depends on both the lifetimes and the transport in a complicated way.

These features are implicit in the equations of this chapter and are also present in the results given in Appendix I.

The results in Figure (5.3) and (5.4) are based on reasonable assumptions regarding the properties of CH_3CCl_3 in the atmosphere and the distribution of its sources. In order to draw firm conclusions about the lifetime, it is still necessary to calculate ξ_3 and ξ_4 and compare these to the observed time series data (given in Appendix I). Approximate calculations show that the assumptions on which Figures (5.3) and (5.4) are appropriate for reproducing the observations. It appears that $\tau \approx 8 - 10$ yrs based on the gradient and its changes.

It is also believed that the south pole measured value of CH_3CCl_3 in January 1975 may be too high. These were the first measurements and the detector temperature was lower than in subsequent measurements. This implies that the measured gradient in 1975 should be higher than reported. This would be consistent with the general features of all the theories discussed here because in all of them the maximum value of R_0 occurs in 1975. Some attention was also devoted to possible alternative explanations of the changing gradient which do not involve the fluctuating source. (1) It is possible that the changing gradient is an accidental manifestation of atmospheric variability and measurement errors. This is not probable, but it is possible. There may be seasonal effects which differ from year to year, adding to the uncertainties in using measured values for studying the

changing gradient. The numbers used in the gradient arise from many measurements over a month or so (for some years, hundreds of numbers are used to obtain the average), so that the standard error of the measurements is reduced. Also the atmospheric variability is mostly averaged out in a monthly mean. (2) The transient terms are also too small to give such a large change in the gradient. (3) Finally, calculations were made assuming that there are southern hemispheric sources that have increased at a rate different from that of the northern hemispheric sources. Suppose that $S_n = \alpha_n e^{b_n t}$ and $S_o = \alpha_s e^{b_s t}$ are the source functions in the northern and southern hemispheres respectively. Within the framework of a 2-box theory the gradient can be easily shown to be:

$$R = [1 + (b_n + n)\tau_*] \left[\frac{1 + \frac{\alpha_s}{\alpha_n} \frac{\eta_T (b_n + n) (b_n + n + 2\eta_*)}{(b_n + n + \eta_*) (b_s + n) (b_s + n + 2\eta_*)} e^{(b_s - b_n)t}}{1 + \frac{\alpha_s}{\alpha_n} \frac{(b_s + n + \eta_*) (b_n + n) (b_n + n + 2\eta_*)}{(b_s + n) \eta_* (b_s + n + 2\eta_*)} e^{(b_s - b_n)t}} \right] \quad (5.34)$$

It is assumed that the lifetime in the two hemispheres is approximately the same. Since the same function of time, namely $\exp [(b_s - b_n)t]$ appears in both the numerator and denominator, the variation of the gradient is never very large. Furthermore, if it is assumed that the southern hemispheric sources are small compared to the northern hemispheric sources, then $\alpha_s/\alpha_n \ll 1$ and b_s is close to b_n , in which case

the change of R with time is very small and unobservable. Obviously if $b_n = b_s$, $R = [1 + (b_n + \eta) \tau_*]$ in eqn. (5.34). The difference of lifetimes in the two hemispheres, by themselves, do not give the gradient R , variability with time. It is a general result of the 2-box theory, with different lifetimes in the northern and southern hemispheres, that the asymptotic gradient (gradient after transient terms $a_* e^{-\lambda_1 t}$, $b_* e^{-\lambda_2 t}$ have become negligible) is a function only of the southern hemispheric lifetime and not the northern hemispheric lifetime, or $R = [1 + (b + \eta_s) \tau_*]$, regardless of the lifetime in the northern hemisphere.

This treatment doesn't exhaust all possibilities, but within reason it appears that the fluctuations of the sources are necessary to explain the changing gradient.

The τ_* in 2-box theories is a parameter which must take into account both the transport from the regions north of 30°N as well as the transport across the equator. This is true for species whose primary sources are of industrial origin (e.g., F-11, F-12, CH_3CCl_3 , etc.). When the sources of a trace gas are more evenly distributed throughout the northern hemisphere, then the transport of these gases from the latitudes beyond 30°N is not as important and thus a smaller τ_* suffices to explain their gradients. In 2-box theories the τ_* can, therefore, depend on the source distribution and can have different values for different trace gases.

Earlier in section (5.c) there was an indication that the gradient of F-11 may also be changing. This was not pursued further in the present study, but a couple of comments can be made. The change in this gradient is small over the years and does not seem to have a structure similar to CH_3CCl_3 . The lifetime of F-11 is long, so source fluctuations are damped; furthermore, its source fluctuations are not as cyclic as CH_3CCl_3 , and lastly, its release has become almost constant in recent years. It is, therefore, more difficult to formulate a theory for this compound, but the changing gradient could be due to these complicated features in its source function.

(e) Interhemispheric Gradients and Sources in the Southern Hemisphere
-- Short-Lived Trace Gases.

For short-lived trace gases the interhemispheric gradients R or R_0 are large. Intuitively we know that if the measured gradient of any trace gas with intermediate or short lifetime is close to unity, then there must be sources in both hemispheres. This idea is quantified and a reasonably sensitive criterion is developed to decide whether there are southern hemispheric sources of a trace gas, based on measured gradients.

For this analysis, it is most convenient to use the simplest applicable theory, which is the 2-box model. As already discussed, the gradient R is given by

$$R = [1 + (b + \eta) \tau_*] \quad (5.35)$$

assuming that the sources are all in the northern hemisphere and that the source term is given by ae^{bt} . If the source is constant, $b = 0$. This eqn. (5.35) for R is valid after the transient terms have died out. The time it takes for this to happen (beginning at the point when release is first started) is relatively short if the lifetime is short. Specifically $\lambda_1 t, \lambda_2 t \gg 0$, $\lambda_1 = \eta$, $\lambda_2 = \eta + 2\eta_*$. If τ is short, η is very large and $\lambda_1 t, \lambda_2 t$ quickly become large, damping out all terms $e^{-\lambda t}$ within a short time.

The main idea is to derive the equation for the smallest (closest to 1) possible value of the gradient R which can be expected if the sources are only in the northern hemisphere. This is denoted by R_{\min} . In case the measured gradient, R_m , is smaller than this ($R_m < R_{\min}$), then the assumption of only northern hemisphere sources is deduced to be incorrect and there must be sources in the southern hemisphere. If $R_m > R_{\min}$, then southern hemisphere sources are unlikely. This idea will be refined a little further as we proceed.

Only relatively short-lived trace gases will be considered so that η is large (recall that $\eta = 1/\tau$). In most cases b is expected to be ≥ 0 , but its value won't matter much because $\eta \gg b$, so the first simplification is to drop b and thus $R = [1 + \eta\tau_*]$. When the primary sink is reaction with atmospheric HO radicals, $\eta \approx \bar{K} [\overline{\text{HO}}]$. Two R_{\min} 's be defined:

$$R_{\min}^{(1)} = (1 + \bar{K}[\overline{\text{HO}}] \tau_{*0}) \quad (5.36)$$

$$R_{\min}^{(2)} = (1 + 4\bar{K}[\overline{\text{HO}}] \tau_{*0}) \quad (5.37)$$

$\overline{[\text{HO}]} = 2 \times 10^5$ molecules/cm³ = minimum of the yearly global mean average HO density.

$$\tau_{*0} = 0.75 \text{ years}$$

For trace gas with other primary sinks or combinations of sinks, $K \overline{[\text{HO}]}$ is replaced by $\eta_{\min} = 1/\tau_{\max}$. $R_{\min}^{(1)}$ represents the lowest limit of R consistent with current knowledge of mean HO radical densities in the atmosphere, and interhemispheric transport time τ_* . $R_{\min}^{(2)}$ doubles the values of $[\text{HO}]$ to $2[\text{HO}]$ and doubles the τ_{*0} to $2\tau_{*0}$, or in general it raises the minimum expected η_{\min} to $4\eta_{\min}$. The criterion for southern hemisphere sources then becomes:

$$\text{If } R_m \leq R_{\min}^{(1)} \Rightarrow \text{sources in the southern hemisphere} \quad (5.38a)$$

$$R_{\min}^{(2)} > R_m > R_{\min}^{(1)} \Rightarrow \text{undecideable, but southern hemisphere sources are unlikely or small} \quad (5.38b)$$

$$R_m \geq R_{\min}^{(2)} \Rightarrow \text{most probably there are no southern hemisphere sources} \quad (5.38c)$$

Considering eqns. (5.36) and (5.37), it is possible to convert this criterion (eqn. (5.38)) into graphical form. If R is plotted as a function of η , $R_{\min}^{(1)}$ and $R_{\min}^{(2)}$ define a cone. $\eta_{\min} = \bar{K} \overline{[\text{HO}]}$ can be calculated for a given trace gas. If R_m lies below the cone at $\eta = \eta_{\min} = \bar{K} \overline{[\text{HO}]}$, one concludes that there are southern hemisphere sources.

If R_m lies in the cone for this η_{\min} , no strong conclusion can be drawn, and if R_m lies above the cone, then southern hemispheric sources are very unlikely. The strongest conclusion is drawn when R_m lies below the cone.

Figure (5.6) is such a graph and the following trace gases are included in it as examples: CHCl_3 , CH_3Cl , CH_2Cl_2 , C_2Cl_4 , C_2H_6 , C_2H_2 , C_2H_4 , CHCl_2F , CO , CH_4 , COS and CS_2 .

The sources of information used to obtain the locations of these trace gases on Fig. (5.6) are as follows: (1) The calculations of η_{\min} were carried out using the rate constant data reported by Atkinson *et al.* (1978) and DeMore *et al.* (JPL, 1979). (2) The global measurement data yielding the gradients are from Rasmussen (personal communication) and Singh (1978, 1979). Additional information on η_{\min} was obtained from Graedel (1978). Graedel (1978) also discusses in detail the sources of several of these trace gases as well as their lifetimes and chemistry. For the calculations based on rate constant data, the average temperature in the lower atmosphere was taken to be 266°K.

The results of the figure are that $\text{CH} \equiv \text{CH}$, C_2H_6 and C_2H_4 as well as CO , CH_4 , CH_3Cl , COS and CS_2 must have southern sources. CH_2Cl_2 and C_2Cl_4 are not decideable, whereas CHCl_2F (F-21) is unlikely to have southern sources. In this graph, the underlined locations are for Rasmussen's measurements, and the rest are Singh's measurements. The

CH₄, CO, C₂H₄, COS and CS₂ lifetimes, necessary to locate these trace gases on the graph, were taken directly from Graedel (1978). The leftmost location of C₂H₂ is based on the lifetime calculated from measured value of the rate constant for C₂H₂+ HO → products (Atkinson et al., 1978). This is also consistent with the lifetime given by Graedel (1978). The rightmost location of C₂H₂ is based on the Arrhenius expression for this reaction. The location of C₂H₂ with a double underline is the measurement of Robinson (1979), and it too falls below the cone. Robinson (1979) also discusses the latitudinal distribution of acetylene in his paper but does not draw any conclusions about possible southern hemisphere sources. The arrows on the graph indicate that the true locations of these trace gases on this graph are farther out along the direction of the arrows. For example, η for C₂H₄ is 195 (Graedel, 1978), but since the graph doesn't go that far, the arrow is used to indicate this. In the cases of CHCl₃ and CHCl₂F measured concentrations only give lower limits of the gradient.

In case these compounds have other sinks, the lifetime can only go down, in which case their locations on the graph move to the right. The case for southern hemisphere sources becomes stronger as the location of the trace gas on this graph is moved to the right. The undecidable gases could also move into the region below the cone.

Clearly, there are straightforward generalizations of the criterion discussed here. One need not restrict attention to only those trace gases that have HO-dominated sinks. The $\bar{K} \overline{[HO]}$ in eqns. (5.36)

and (5.37) can simply be replaced by the smallest expected values of η regardless of the types of sinks which lead to it. Secondly, relatively longer-lived species can be included, but then the value of b has to be restored in eqns. (5.36) and (5.37). With some effort the cone can also be shrunk so that more definite conclusions can be drawn about more of the trace gases.

For any trace gas with a finite lifetime and gradient of 1 or less, there must be southern sources as expected. All these will lie below the cone. CH_3Cl , CH_3Br , CH_3I , N_2O and CCl_4 are examples of such trace gases.

In summary, the criterion for the existence of southern sources is formulated as follows: It is assumed that there are sources only in the northern hemisphere and then the smallest value of R that can be consistent with this assumption is derived. If $R = [1 + (b + \eta)\tau_*]$, this minimum theoretically expected gradient is obtained by taking the smallest reasonable value for the transport time, τ_* , and the upper limit of the lifetime (minimum η). If the measured gradient is still smaller than this minimum expected value, then it can only be explained by southern sources.

(f) Conclusions

The principal results of this chapter can be divided into three classes.

(i) First statistical tests were performed on the measured time

series of the gradients of CCl_3F , CCl_2F_2 , CCl_4 and CH_3CCl_3 . The conclusions drawn from these tests were that it is likely that the decline, in the gradients of CCl_3F and CH_3CCl_3 , is significant. The gradient of CH_3CCl_3 as a function of time was picked for detailed study, so a further statistical test was performed to see if the slope of $\ln \xi_n$ (log base e of the northern hemisphere measured time series) and the slope of $\ln \xi_s$ were significantly different. The test showed that the slopes are very probably different, thus supporting the idea of a changing gradient.

(ii) A detailed study was undertaken to explain the changes in the gradient of CH_3CCl_3 based on the fluctuations of the source term. These fluctuations were discussed in the previous chapter. To start the investigation, a simple delay idea was considered. It was postulated that the south pole concentrations respond, after a delay, to the fluctuations of the source which is concentrated in the northern hemisphere above 30°N . The success of this idea in explaining the changing gradient led to two more rigorous studies. In the first one the troposphere was divided into the northern and southern hemisphere tropospheres. The transport of CH_3CCl_3 and its atmospheric chemistry were specified in simplified form by transfer times and lifetimes. The fluctuations were added to the source term. The agreement between this theory and observations was good, but it led to the suspicion that a more exact explanation could be constructed based on the same idea of

fluctuating sources, but with more refined assumptions regarding the global behaviour of CH_3CCl_3 . The problems associated with the 2-box theory were reviewed. Both this 2-box theory and the next more refined theory automatically introduced the delays in the response of the south pole concentrations with respect to fluctuations of the sources in the northern hemisphere.

The next step involved the construction of a 4-box theory, which is summarized in section (5.d). The main problems that were encountered in the application of this theory to CH_3CCl_3 were related to our ignorance of the source distribution and transport times. Using reasonable assumptions regarding these variables, the agreement between theory and observations turned out to be very good.

The results of the analysis indicated that the changing gradient, if it is a real change, is most probably due to the cyclic fluctuations of the source term.

(iii) Finally, a criterion was developed to detect southern hemisphere sources of trace gases, based on the measured gradient. This criterion, though easily generalizeable, was developed in detail for short-lived species and applied to the measured gradients of several trace gases. The criterion is strongest when it indicates that there are southern hemisphere sources. It was found that several of the trace gases studied very probably have southern hemisphere sources.

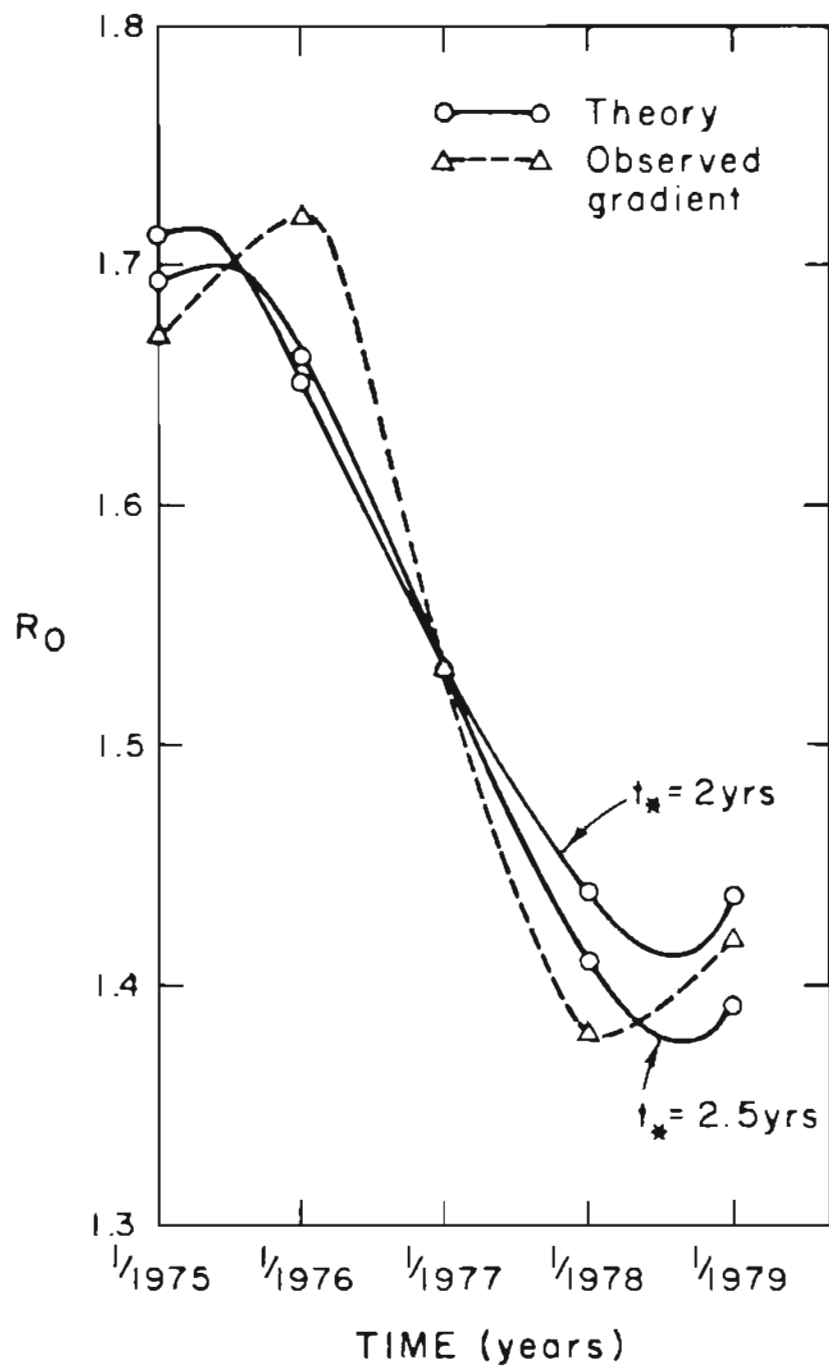


Figure (5.1): Comparison of the observed CH_3CCl_3 gradient with a simple delay theory.

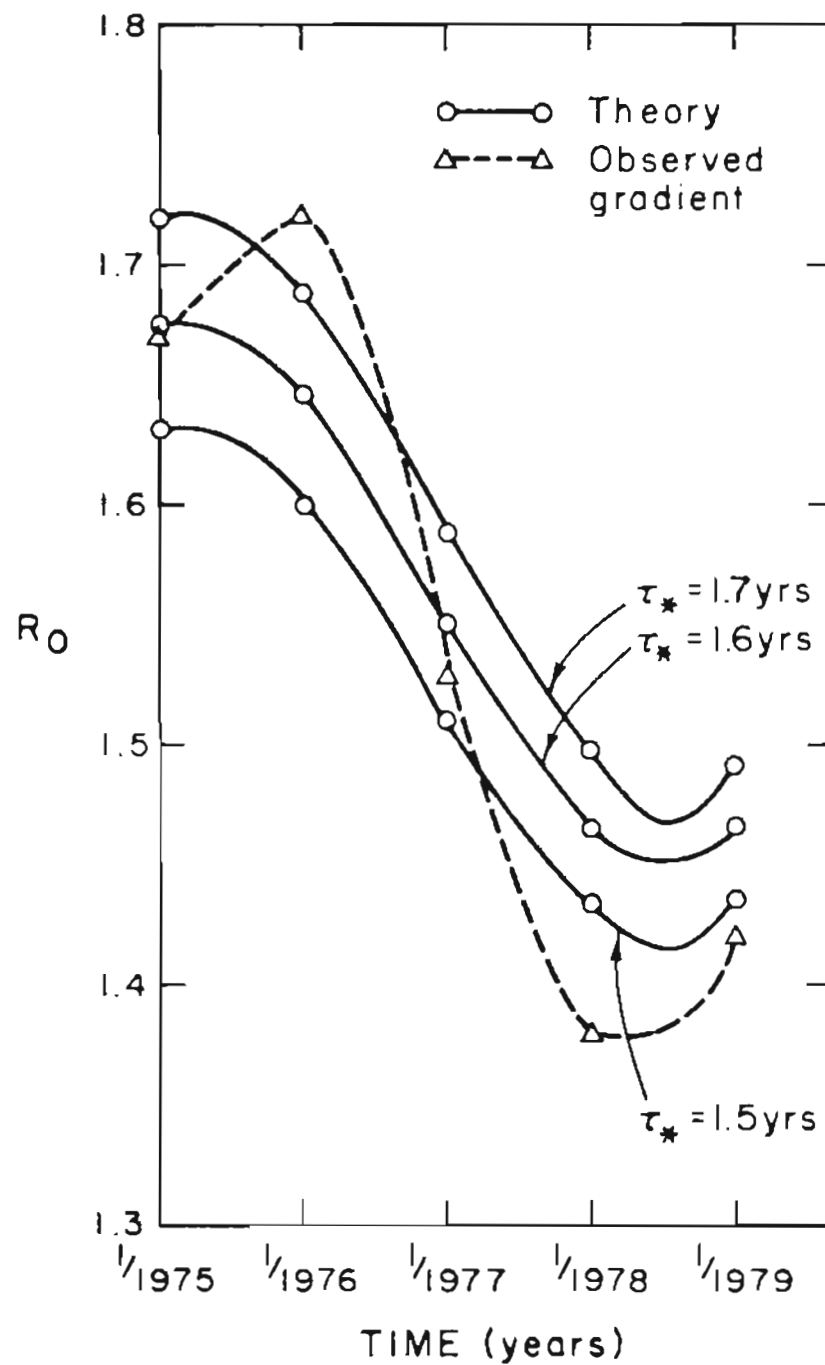


Figure (5.2): The observed methylchloroform gradient and the two box theory.

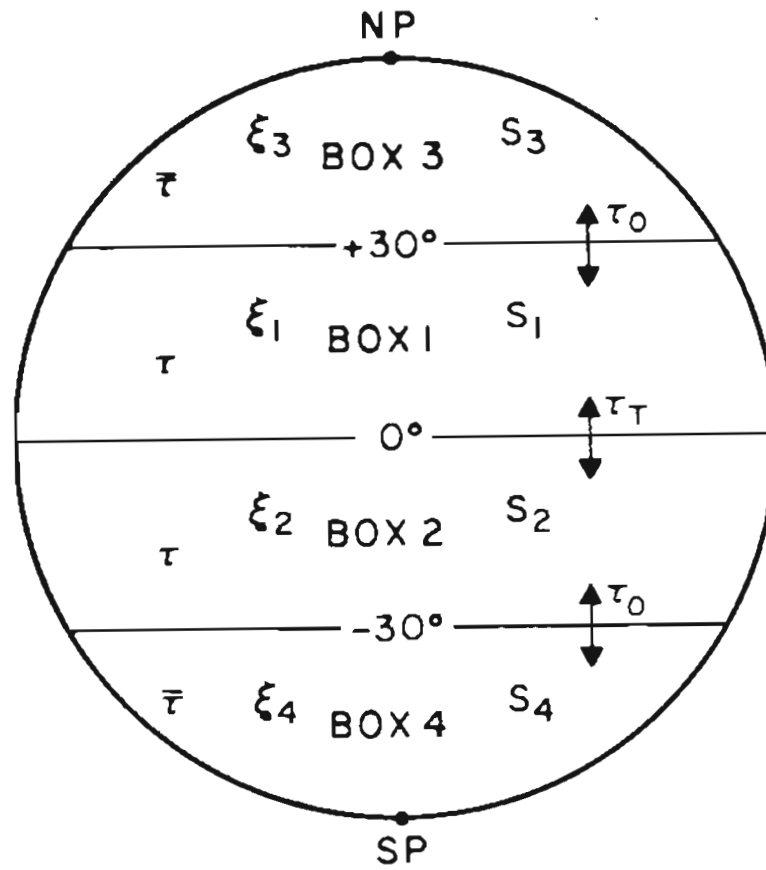


Figure (5.3): A picture of the four box theory.

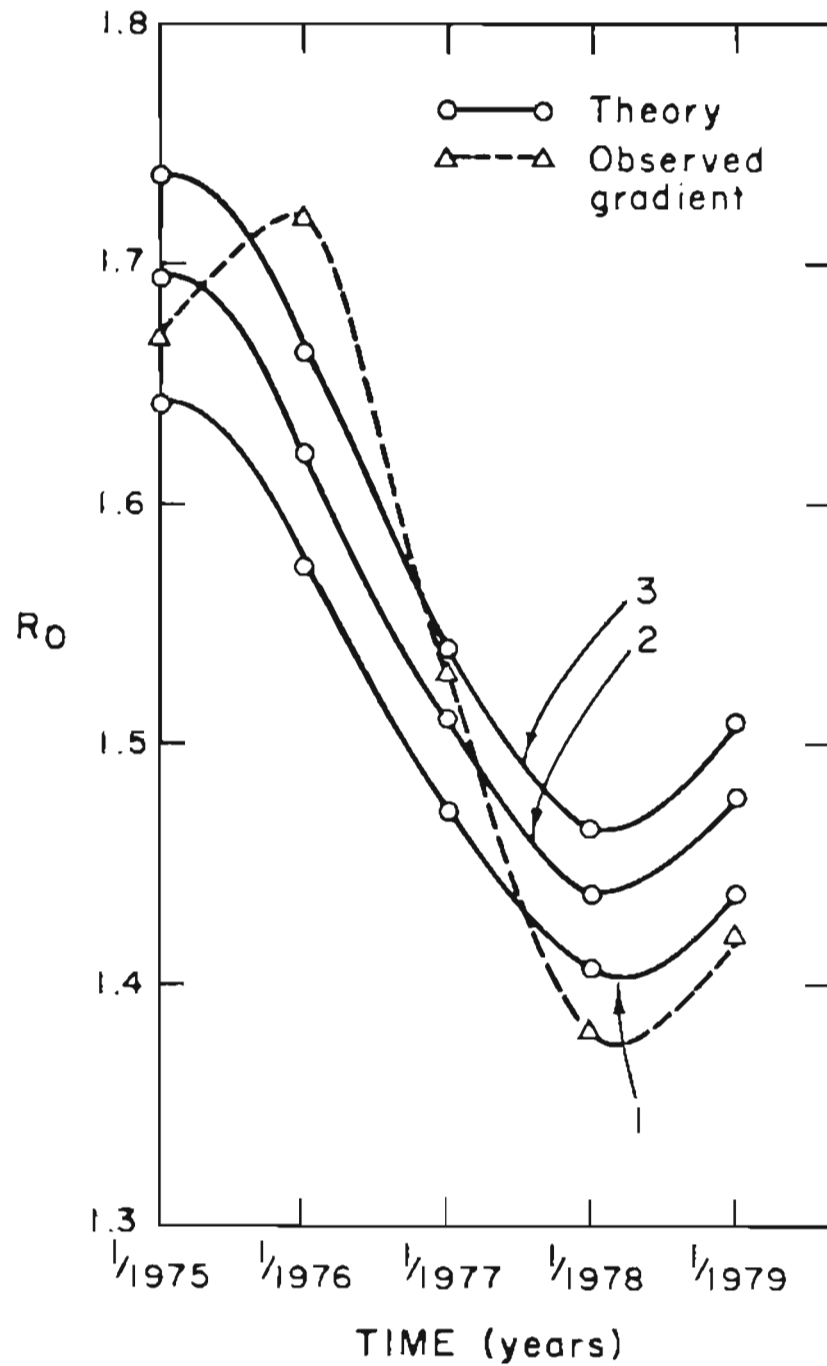


Figure (5.4): The observed methylchloroform gradient and the four box theory.

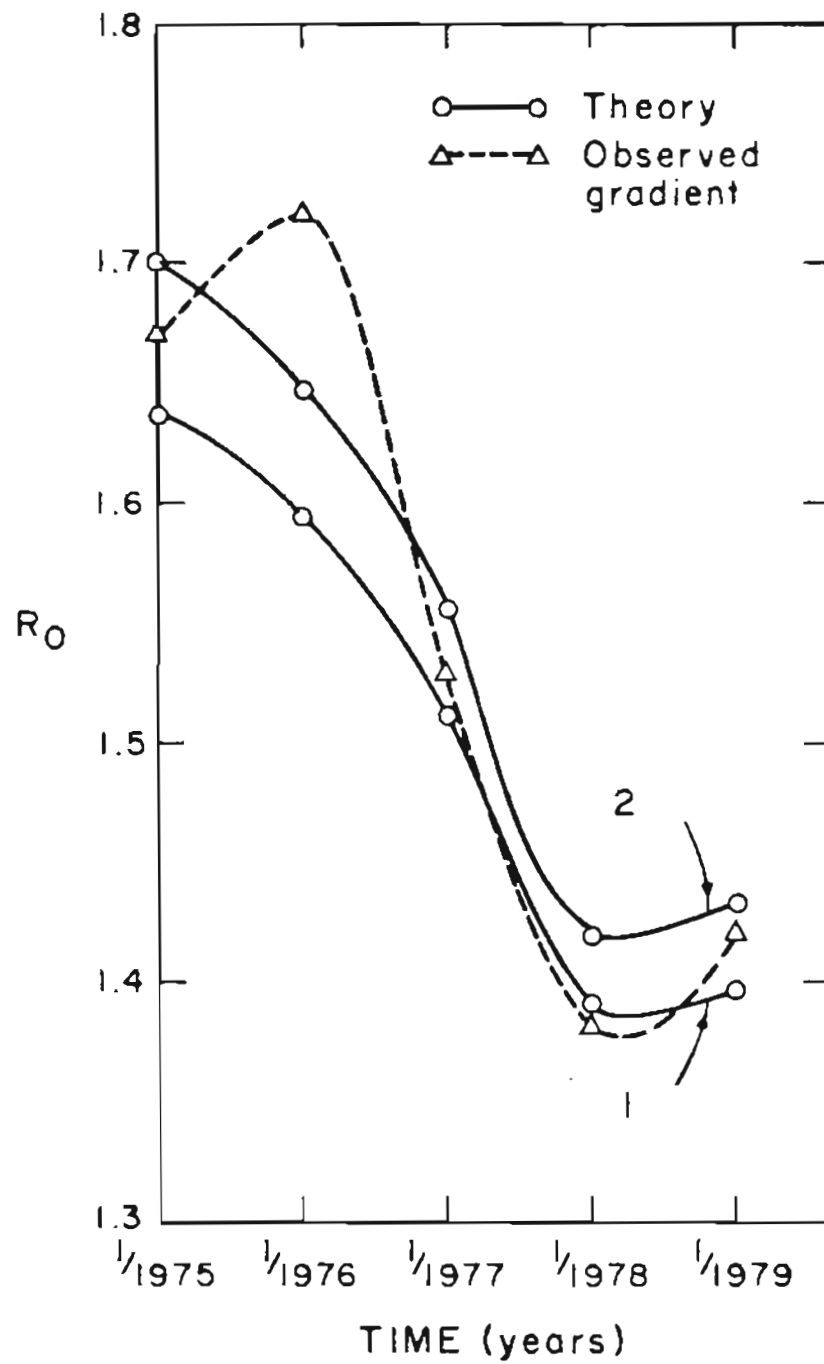


Figure (5.5): The observed methylchloroform gradient and the four box theory with the Δ_1 and Δ_2 cycles.

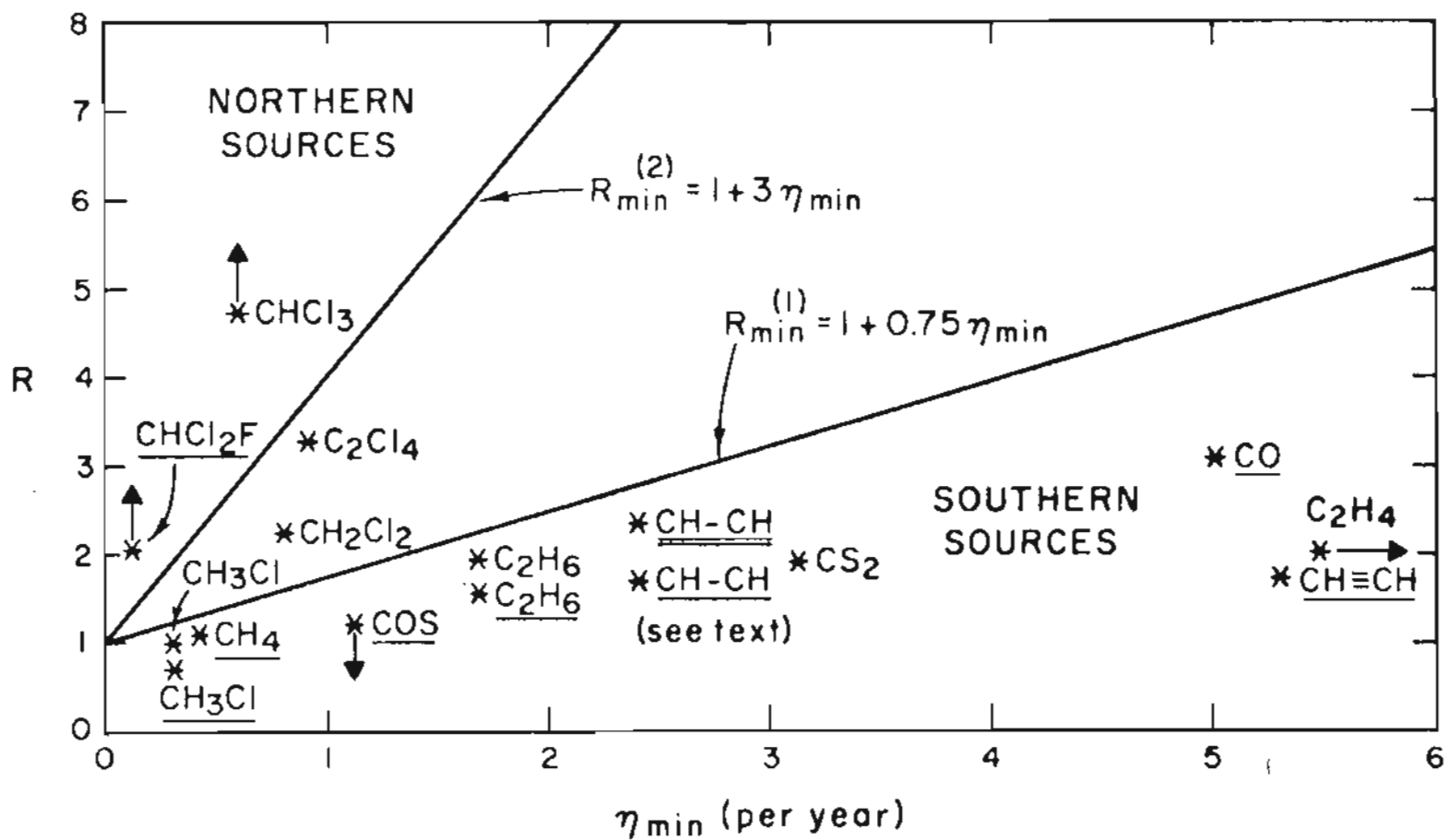


Figure (5.6): A diagram illustrating evidence for southern hemisphere sources of some atmospheric trace gases.

CHAPTER 6: ACCUMULATION OF CH_3CCl_3
IN THE ATMOSPHERE

(a) Introduction

In this chapter investigations of possible future concentrations of CH_3CCl_3 are reported and discussed. Several possible scenarios are considered which indicate that CH_3CCl_3 concentrations could become two to four times higher than they are today (~ 115 pptv).

Chlorine containing anthropogenic trace gases have been implicated in the destruction of the stratospheric ozone layer (see for example Molina and Rowland, 1974). The fluorocarbons CFCl_3 (F-11) and CCl_2F_2 (F-12) have become the focus of this threat to the global environment of our future. The main case against methylchloroform is the same as that against F-11 and F-12. CH_3CCl_3 will reduce the current concentrations of stratospheric ozone, and it can also lead to the enhancement of the atmospheric greenhouse effect, thus raising the global temperature of the atmosphere. The infrared absorption bands of CH_3CCl_3 are similar to those of F-11 and F-12 between 8-16 μm (Thompson, 1974).

There are two key variables which determine the threat of CH_3CCl_3 to the future environment. These are: (i) the ambient concentrations of CH_3CCl_3 in the troposphere, which will result from continuing or increasing emissions, and (ii) the photodissociation characteristics of CH_3CCl_3 in the stratosphere. These variables are important for the assessment of the dangers of any trace gas in the same class as

F-11, F-12 and CH_3CCl_3 .

There are differences between the dangers of continued emissions of CH_3CCl_3 and the continued releases of F-11 and F-12. It is well known that CH_3CCl_3 has tropospheric sinks, the most prominent being the reactions with tropospheric hydroxyl (HO) radicals. The implications of this sink are: (i) for equal amounts (number of molecules/yr) of releases of CH_3CCl_3 and F-11 or F-12, CH_3CCl_3 is safer because many of the CH_3CCl_3 molecules are destroyed by HO and have nothing to do with the destruction of the ozone layer. (ii) If releases of CH_3CCl_3 are cut down or stopped, its tropospheric concentrations will decline more rapidly than F-11 and F-12, so that the detrimental environmental effects of CH_3CCl_3 can be contained over a relatively shorter time scale than the effects of F-11 and F-12.

These points, favourable to CH_3CCl_3 , have the clear danger of tranquilizing us into a false sense of security. Already huge quantities of CH_3CCl_3 are being released into the atmosphere. In fact, more CH_3CCl_3 has been released per year, during the last couple of years, than either F-11 or F-12. It appears that soon CH_3CCl_3 releases, per year, will exceed the combined releases of F-11 and F-12, per year (by mass). The lifetime of CH_3CCl_3 is short compared to F-11 and F-12, but it is not so short as to make it comfortably safe. Consequently the tropospheric concentrations of CH_3CCl_3 have been rising rapidly ($\sim 10 - 12\%$ per year). The current tropospheric concentrations of CH_3CCl_3

are probably a very minor threat to the ozone layer, and have virtually no effect on the earth's greenhouse effect. But these concentrations will continue to rise and will make CH_3CCl_3 more and more prominent in the perturbation of the ozone layer due to anthropogenic activities. Once its tropospheric concentrations rise high enough to significantly affect the ozone layer, it will still take a decade or more to nullify its effects, even if all further release is stopped.

(b) Theoretical Analysis of Future CH_3CCl_3 Concentrations

There is no definite method by which one can predict the future concentrations of CH_3CCl_3 , or of any other atmospheric trace gas, resulting from anthropogenic activity. All that can be done is to guess the source strengths of the future and estimate their effects. The factors which will control future emissions are many, which include the state of the economy, the demand for CH_3CCl_3 (which can diminish because of limits of growth), and possible governmental restrictions on releases.

The theory adopted for this study consists of two (hemispherical) boxes. It is, of course, possible to construct more sophisticated theories, but it appears that this theory is adequate considering our current knowledge of CH_3CCl_3 concentrations in the atmosphere. The general theory is discussed in other chapters, as well as in Chapter 10. It is stated by the following (matrix) equation.

$$\frac{d}{dt} \begin{bmatrix} \xi_n \\ \xi_s \end{bmatrix} = \begin{bmatrix} S_n \\ 0 \end{bmatrix} - \begin{bmatrix} (\eta_n + \eta_T) - \eta_T & \\ -\eta_T & (\eta_s + \eta_T) \end{bmatrix} \begin{bmatrix} \xi_n \\ \xi_s \end{bmatrix} \quad (6.1)$$

The solution of eqn. (6.1) is:

$$\underline{\xi} = P^{-1} e^{-\Lambda t} P \underline{\xi}_0 + P^{-1} e^{-\Lambda t} \int_0^t e^{\Lambda t'} P \underline{S}(t') dt' \quad (6.2)$$

$$\underline{\xi} = \begin{pmatrix} \xi_n \\ \xi_s \end{pmatrix} \quad (6.3)$$

$$P = \begin{bmatrix} \eta_T / (a - \lambda_1) & 1 \\ \eta_T / (a - \lambda_2) & 1 \end{bmatrix} \quad (6.4)$$

$$P^{-1} = \begin{bmatrix} 1 & -1 \\ \frac{-\eta_T}{(a - \lambda_2)} & \frac{\eta_T}{(a - \lambda_1)} \end{bmatrix} \frac{(a - \lambda_1)(a - \lambda_2)}{\eta_T(\lambda_1 - \lambda_2)} \quad (6.5)$$

$$a = \eta_n + \eta_T; \quad c = \eta_s + \eta_T \quad (6.6)$$

$$\lambda_1 = \frac{1}{2}(a + c) + \frac{1}{2} [(a - c)^2 + 4\eta_T^2]^{\frac{1}{2}} \quad (6.7)$$

$$\lambda_2 = \frac{1}{2}(a + c) - \frac{1}{2} [(a - c)^2 + 4\eta_T^2]^{\frac{1}{2}} \quad (6.8)$$

The result is that:

$$\begin{aligned} \xi_n = \frac{1}{(\lambda_1 - \lambda_2)} \left\{ [(a - \lambda_2) \xi_{on} + \frac{(a - \lambda_1)(a - \lambda_2)}{n_T} \xi_{os} \right. \\ \left. - Q_{1n}] e^{-\lambda_1 t} + [- (a - \lambda_1) \xi_{on} - \frac{(a - \lambda_1)(a - \lambda_2)}{n_T} \xi_{os} \right. \\ \left. + Q_{2n}] e^{-\lambda_2 t} + Q_{3n} \right\} \end{aligned} \quad (6.10)$$

$$\begin{aligned} \xi_s = \frac{1}{(\lambda_1 - \lambda_2)} \left\{ [- n_T \xi_{on} - (a - \lambda_1) \xi_{os} + Q_{1s}] e^{-\lambda_1 t} + \right. \\ \left. [n_T \xi_{on} + (a - \lambda_2) \xi_{os} - Q_{2s}] e^{-\lambda_2 t} + Q_{3s} \right\} \end{aligned} \quad (6.11)$$

If in the future, the source is constant at some level, say a_0 (pptv/yr), then

$$Q_{1n} = \frac{a_0}{\lambda_1} (a - \lambda_2) \quad (6.12)$$

$$Q_{2n} = \frac{a_0}{\lambda_2} (a - \lambda_1) \quad (6.13)$$

$$Q_{3n} = \frac{a_0 (a - \lambda_2)}{\lambda_1} - \frac{a_0 (a - \lambda_1)}{\lambda_2} \quad (6.14)$$

$$Q_{1s} = \frac{a_0 n_T}{\lambda_1} \quad (6.15)$$

$$Q_{2s} = \frac{a_0 n_T}{\lambda_2} \quad (6.16)$$

$$Q_{3s} = -a_0 n_T \left[\frac{1}{\lambda_1} - \frac{1}{\lambda_2} \right] \quad (6.17)$$

If, in the future, the source continues to rise at some rate so that

$$S_n = a_0 e^{\tilde{b}t}, \text{ then:}$$

$$Q_{1n} = \frac{a_0}{(\tilde{b} + \lambda_1)} (a - \lambda_2) \quad (6.18)$$

$$Q_{2n} = \frac{a_0}{(\tilde{b} + \lambda_2)} (a - \lambda_1) \quad (6.19)$$

$$Q_{3n} = a_0 \left[\frac{(a - \lambda_2)}{(\tilde{b} + \lambda_1)} - \frac{(a - \lambda_1)}{(\tilde{b} + \lambda_2)} \right] \quad (6.20)$$

$$Q_{1s} = a_0 n_T \frac{1}{(\tilde{b} + \lambda_1)} \quad (6.21)$$

$$Q_{2s} = a_0 n_T \frac{1}{(\tilde{b} + \lambda_2)} \quad (6.22)$$

$$Q_{3s} = -a_0 n_T \left[\frac{1}{(\lambda_1 + \tilde{b})} - \frac{1}{(\lambda_2 + \tilde{b})} \right] e^{\tilde{b}t} \quad (6.23)$$

$$\eta_n = 1/\tau_n, \quad \eta_s = 1/\tau_s, \quad \eta_T = 1/\tau_T \quad (6.24)$$

τ_n , τ_s are the lifetimes of CH_3CCl_3 in the northern and southern hemispheres (including both the stratosphere and the troposphere). τ_T is the interhemispheric transport time. λ_1 and λ_2 are eigenvalues of the matrix in the second term of eqn. (6.1). It is assumed that there are no significant sources in the southern hemisphere. ξ_{n0} , ξ_{s0} are the

values of the CH_3CCl_3 mixing ratios, averaged over the northern and southern hemispheres, at time zero which is January 1979. $\xi_n(t)$ and $\xi_s(t)$ are the predicted future concentrations.

Figures (6.1) and (6.2) show the main results of the calculations. The numerical results, from which these figures are constructed, are given in Appendix I. Further details of the calculations can also be found in Appendix I. The results shown in Figures (6.1) and (6.2) are discussed next. Figure (6.1) shows the expected northern hemisphere mean tropospheric concentrations and Figure (6.2) the southern hemisphere mean tropospheric concentrations.

The conditions chosen to calculate these curves (Figures (6.1) and (6.2)) are as follows: $\xi_{onT} = 130$ pptv and $\xi_{osT} = 100$ pptv. These are the mean tropospheric mixing ratios in the northern and southern hemispheres during January 1979 and are determined from the measurements of Rasmussen. ξ_{onT} and ξ_{osT} are based on the results of Chapter 8, and the measurements are tabulated in Appendix I corresponding to Chapter 2. The equations (6.1) - (6.24) refer to the expected concentrations over the whole hemispheres which include the troposphere and the stratosphere. In calculating the expected concentrations, ξ_{on} and ξ_{os} were assumed to be 112 pptv and 86 pptv respectively. These numbers correspond to $\zeta \equiv \xi'_s / \xi'_T = 0.25$ (ξ'_s and ξ'_T are the stratospheric and tropospheric mean mixing ratios). The equations give $\xi_n(t)$ and $\xi_s(t)$ which were divided by $\alpha = 0.862$ (corresponding to $\zeta = 0.25$) to obtain the tropospheric mean concentrations.

τ_T is taken to be 1.2 yrs and τ_n is taken to be $2\tau_s$. In curve (2) $(\tau_n, \tau_s) = (12, 6)$ yrs, in (3) $(\tau_n, \tau_s) = (7, 4)$, in (1) $(\tau_n, \tau_s) = (20, 10)$. Curves marked (1), (2) and (3) correspond to the expected future concentrations in the troposphere if the source remains constant and equal to its 1978 value (which was 1.1 billion lbs/yr). Curves marked (4) and (5) reflect the expected concentrations if the source strength continues to increase at 8% per year or $S = (1.1 \times 10^9 \text{ lbs/yr}) \exp [0.08 t]$. If the source term is going to grow, an 8% growth per year is a conservative estimate. In the past the CH_3CCl_3 source has grown faster than 8%/yr (average of $\sim 15\%$ per yr for the past twenty years).

If the source continues to grow at $\sim 8\%$ per year, the emissions in about 9 years will be double of the 1978 value of 1.1 billion lbs. per year. If the emissions do rise to ~ 2.2 billion lbs/yr and then remain at this level, the future concentrations of CH_3CCl_3 in the atmosphere will rise to 1/2 ppbv. The asymptotic limit of how high the CH_3CCl_3 concentrations can go are given by eqn. (6.10), (6.11) with:

$$\xi_{n*} = Q_{3n}, \quad \xi_{s*} = Q_{3s} \quad (6.25)$$

With constant release at 1.1×10^9 lbs/yr, $\xi_{nT*} \approx 220$ pptv and $\xi_{sT*} \approx 185$ pptv, and with constant release at 2.2×10^9 lbs/yr, $\xi_{nT*} \approx 450$ pptv, $\xi_{sT*} \approx 380$ pptv. If the source is not constant in the future, but continues to rise, then there is no steady state limit.

Table (6.1) below summarizes the results:

Table (6.1): Expected Tropospheric Concentrations

(a) Source Constant at 1978 Emissions.

Time	ξ_{nT} (pptv)	ξ_{sT} (pptv)
1/1979	130	100
1989	195	160
1999	213	177

(b) Source Continues to Rise at 8%/Yr.

1/1979	130	100
1989	306	236
1999	685	530

(c) Source Rises at 8%/Yr, then Becomes Constant at Twice 1978 Emissions.

1/1979	130	100
1989	306	236
1999	400	350
later	~ 450	~ 380

Numbers based on $\tau \approx 8.5$ yrs, curves (2) and (5).

Curves (2) and (5) are the most likely possibilities, based on the most likely lifetime of CH_3CCl_3 as deduced in Chapter 2. The table above is based on this lifetime.

It should be stressed that the numbers derived here are hemispherical tropospheric averages. The actual concentrations at high northern latitudes (PNW $\sim 45^\circ\text{N}$) will be higher than ξ_{nT} and the concen-

trations at the high southern latitudes (e.g., SP or Tasmania sites) will be lower than ξ_{ST} . By invoking the results of Chapter 8, the entire latitudinal profile expected in future years can be constructed by using the values of ξ_{NT} and ξ_{ST} derived here.

(c) Summary and Conclusions

The future concentrations of CH_3CCl_3 were calculated in this chapter. If the emissions of CH_3CCl_3 remain at the 1978 levels of 1.1 billion lbs/yr, then in ten years the tropospheric concentrations will be 60% higher than in January 1979 ($\xi_{NT} \approx 200$ pptv, $\xi_{ST} \approx 160$ pptv). Beyond the first ten years the concentrations of CH_3CCl_3 will not rise much -- ultimately reaching about 220 pptv and 180 pptv for the northern and southern tropospheres respectively. If emissions continue to rise at $\sim 8\%/yr$, the tropospheric concentrations could rise to more than double the January 1979 values within a decade. If the source stops increasing at that stage, the subsequent concentrations of CH_3CCl_3 could reach four times the January 1979 values.

It appears that in the future (next 20 years) CH_3CCl_3 concentrations could easily double, and if the emissions continue to increase, CH_3CCl_3 concentrations could quadruple.

The effect of CH_3CCl_3 on stratospheric ozone is still under investigation (see McConnell and Schiff, 1978; Crutzen et al., 1978). In any case the two to four times higher concentrations of CH_3CCl_3 in the

future will make it much more significant in ozone depletion.

The results of the calculations shown here lead me to the opinion that CH_3CCl_3 emissions should be restricted -- at least held at the 1978 levels -- while studies of its effects are being carried out.

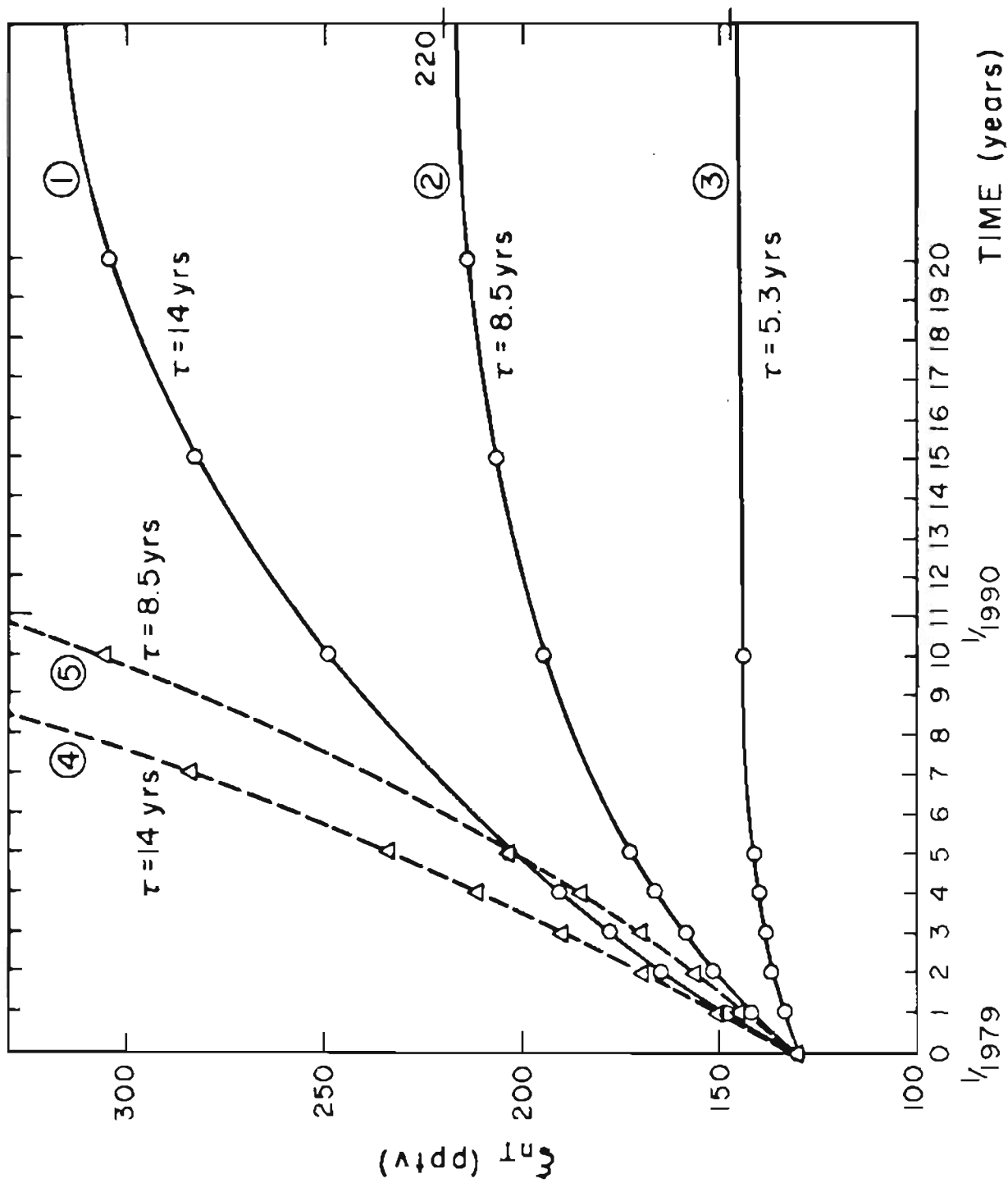
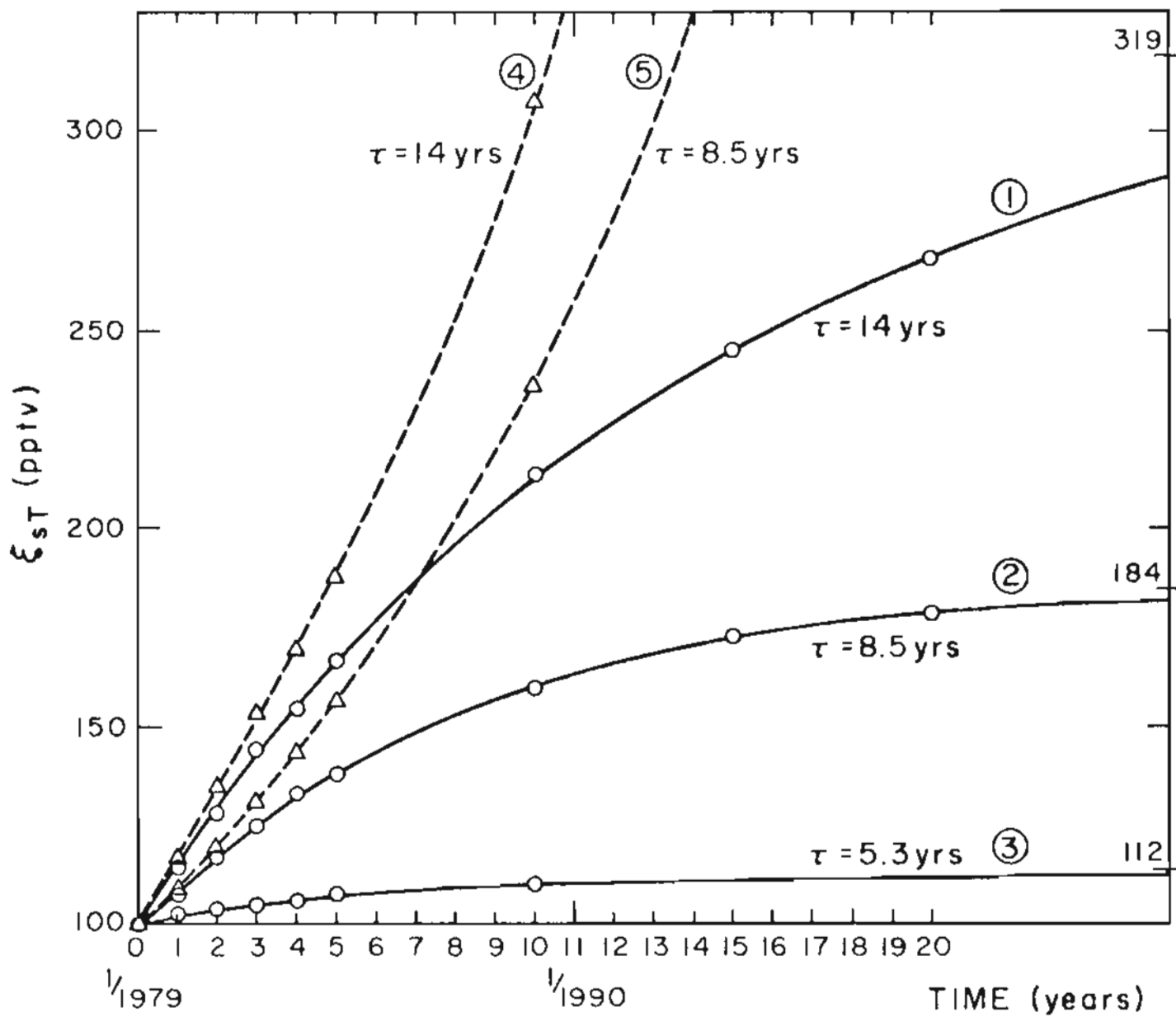


Figure (6.1): Predicted mean northern hemisphere (troposphere) concentrations of methylchloroform.

Figure (6.2): Predicted mean southern hemisphere (troposphere) concentrations of methylchloroform.



PART II:

RELATED TOPICS AND THEORETICAL TECHNIQUES

CHAPTER 7. A STUDY OF CHClF_2 (F-22) IN THE ATMOSPHERE(a) Introduction

CHClF_2 (F-22) has been measured recently (Rasmussen, 1979), in the earth's atmosphere. These measurements were made using GC/MS techniques and are shown in Figure (7.1). The observed concentrations are significantly higher than expected on the basis of anthropogenic release (McCarthy et al. 1977; Alexander Grant & Co. 1979).

A wide spectrum of possible explanations for the observed F-22 concentrations are reported in the chapter. It should be stated from the onset that there are several puzzles in the small amount of data currently available. It is, therefore, necessary that the measurements of Rasmussen be replicated and more data be obtained before any definitive statements can be made.

After a review of the observational data the remaining sections are devoted to looking at additional sources of CHClF_2 . The four possibilities that will be considered here are that (i) the measured values are inaccurate, (ii) the release estimates are too low, (iii) there are natural sources - perhaps volcanic emissions (Graedel, 1978), and (iv) F-12 (CCl_2F_2) is converted to F-22 in the earth's environment. The magnitudes of these mechanisms, necessary to account for the excessive F-22, are also obtained.

(b) Review of the data and the global averages

Based on the measurements shown in Figure (7.1), the first quantity that has to be determined is the globally averaged concentration or the total global burden. The simplest procedure is to obtain the globally averaged mixing ratio, $\bar{\xi}$, and the globally averaged tropospheric mixing ratio, $\bar{\xi}_T$. These are given by:

$$\bar{\xi}_T = \frac{1}{2} (a + b) \quad (7.1)$$

$$\bar{\xi} \approx \bar{\xi}_T \epsilon \quad (7.2)$$

where (a) represents the average mixing ratio at the South Pole or high southern latitudes; (b) is the mixing ratio at high northern latitudes, which are represented by the Adrigole, Cape Meares (Oregon), Canary Islands and Harwell sites. In Eq. (7.2) ϵ is the factor ($\sim 0.8 < \epsilon < 1$) which takes into account the (lower) stratospheric average mixing ratio (see the next chapter). This gives $\bar{\xi}_T \approx 47$ pptv; ($a = 41$ pptv, $b = 52$ ppt) $\bar{\xi} \approx 42-43$ pptv. These estimates of the global average exclude the Adrigole measurements, which are probably too high to represent the true background F-22 mixing ratios at high ($>30^\circ$) northern latitudes (see Kerr 1979). Inclusion of the Adrigole data on an equal footing with the rest of the northern hemisphere measurements, increases the global average and the tropospheric average. It also increases the interhemispheric gradient to uncomfortably high values.

The values of a and b chosen above, on the basis of the measurements can be checked for consistency by considering the interhemispheric gradients R and R_o (see Chapter 5). In figure (7.1) the solid

line represents a latitudinal profile whose shape is typical of long lived trace gases as discussed in the previous chapters. The resulting gradients of F-22 are $R_0 = 1.27$ and $R = 1.2$. Since $R = [1 + (b' + \eta) \tau'_t]$, the value of $R (= 1.2)$ is consistent with a lifetime of about 30 years, a growth rate of 15-16% per year (b') and the interhemispheric transport time (τ'_t) of about one year. It is probable that 52 ppt is a slight underestimation of the high latitude northern hemispheric mixing ratio, and therefore the global tropospheric mixing ratio of 47 pptv = $\bar{\xi}_T$ may be a slight underestimate. In any case, the values chosen for a , b , and the global tropospheric mixing ratio $\bar{\xi}_T$ are in general consistent with the expected interhemispheric gradient, and therefore constitute good estimates of the global concentration based on the observations.

The rate constant of the reaction $\text{CHClF}_2 + \text{HO} \rightarrow \text{CClF}_2 + \text{H}_2\text{O}$ is quite temperature sensitive but it is unlikely to be faster than $\sim 4 \times 10^{-15}/\text{sec}$ (298 K) at globally averaged atmospheric temperatures (DeMore 1979, Atkinson et al. 1979). This means that the global lifetime of F-22 is of the order of 15-30 years due to HO interactions. The relatively long lifetime coupled with the average exponential growth rate of anthropogenic release at 15-16% per year (1968-1975 - see Appendix I Chap. 4) with $\sim 95\%$ of the release in the northern hemisphere (Alexander Grant and Co., 1979) should make the gradient R_0 between 1.2-1.4. Since it is very likely that there are sources of F-22 other than the direct anthropogenic release, the equation for

$R = [1 + (b' + \eta) \tau'_T]$ may not be strictly valid. On the other hand, it is likely that a significant portion of the global burden at the time of measurements (5/79) is due to direct antropogenic release, so there is cause for concern only if the gradient R deviates significantly from $R = [1 + (b' + \eta) \tau'_T]$, because this should be the approximate gradient. There are several other assumptions which can be made, but ultimately they all give similar mixing ratios when averaged over the whole atmosphere. Thus the globally averaged mixing ratio is

$$\bar{\xi} = \bar{\xi}_T \epsilon = \frac{1}{2} (a + b) \epsilon = 47 \epsilon \text{ pptv} \quad (7.2)$$

$$\epsilon = \frac{N_T}{N_\infty} \left[1 = \frac{N_S}{N_T} \langle f \rangle \right] \quad (7.3)$$

$$\xi_S = \xi_T f(z); Z_T < Z < Z_S \quad (7.4)$$

$$\langle f \rangle_\rho = \frac{\int_{Z_T}^S \rho_S(z) f(z) dz}{\int_{Z_T}^S \rho_S(z) dz} \quad (7.5)$$

where $\bar{\xi}_T$ is the average tropospheric mixing ratio, Z_T and Z_S are the heights of the tropopause and the stratopause, $f(z)$ is some function which describes the stratospheric vertical mixing ratio of F-22 (or any other trace gas under consideration); $N_\infty = N_S + N_T$, N_S and N_T are the numbers of molecules of air in the stratosphere and the troposphere respectively. ξ_S and ξ_T are the mixing ratios of F-22 in the stratosphere and the troposphere. Equations (7.2) - (7.5) are valid

for the latitudinal profile shown by the solid line in Fig. (7.1) and under the assumption that there is some mean tropopause height Z_T and that $f(z)$ is approximately independent of latitude. Further details regarding these equations will be developed in the next chapter.

$$0 < \langle f \rangle_\rho < 1 \quad (7.6)$$

When $\langle f \rangle_\rho = 0$, it means that there are no molecules of F-22 in the stratosphere. If $\langle f \rangle_\rho = 1$, it implies that the mixing ratio of F-22 is constant with height in the stratosphere, with the same value it has in the troposphere, at any latitude. Both these limits are unrealistic, the first implying extremely rapid destruction in the stratosphere thus reducing the total global lifetime (to ~ 10 yrs. and the second is improbable because the anthropogenic source of the compound has been rising exponentially and vertical transport beyond Z_T is slow. Since data are not available on the photo-dissociation cross sections for F-22, nor are there any stratospheric measurements, it is very difficult to estimate $\langle f \rangle_\rho$ accurately. Fortunately, the total effect of the stratospheric burden is not very large and reasonable assessments of F-22 can still be made without precise knowledge of $\langle f \rangle_\rho$. Thus, if 47 ppt is accepted as the tropospheric average, then the global average is $38 \text{ ppt} < \bar{f} \leq 47$ with the lower limit corresponding to $\langle f \rangle_\rho = 0$, and the upper limit to $\langle f \rangle_\rho = 1$.

Summary: Considering the measurements of F-22 given by Fig. (7.1), a latitudinal profile was constructed which is consistent with

the measurements and also consistent with the interhemispheric gradient, R_0 , of F-22. The global tropospheric average of 47 ppt was deduced. This value is on the lower side of the range consistent with the observations.

(c) The global time-release and budget of F-22

In Fig. (7.2) of this chapter, the release of F-22 is shown as a function of time from 1968-1975, and the production is shown from 1968-1978. The release is very close to an exponential with a growth rate of 0.158/yr. (McCarthy et al. 1976). It is assumed here that the release continued to grow at the same rate between 1975-present, as it did between 1968-1975. This will be discussed again later on in the chapter. The figure for F-22, corresponding to Chapter 4, shows the release since 1950.

One may assume that both the stratospheric and tropospheric lifetimes of F-22 are infinite, thus resulting in the highest possible anthropogenic contribution to the current burden. This yields the global burden based on measurements of about 45 pptv based on Eq. (7.2) with $\epsilon = 0.96$ where $\langle f \rangle_\rho \approx \frac{N_S}{N_T} [1 + b\tau_{ST}]$. This equation is based on a two box theory dividing the atmosphere into the troposphere and the stratosphere. The total release up to 5/1979 is approximately 532.7×10^9 gm, where the exponentially rising release is added to that of McCarthy et al.'s (1977) estimate of release up to 1975. This divided by N_∞ yields an average global mixing ratio

of about 35 ppt. This implies a 28% excess or about 150 billion gr. extra in the atmosphere after subtracting the total estimated anthropogenic release from 1931 to 5/1979, and assuming that all the anthropogenic contribution is still in the atmosphere.

There are several possibilities that can explain this difference, and these are listed below: (1) The measured values are inaccurate, and the true background concentrations are substantially smaller than measured. (2) The release estimates may be too low. (3) There are natural sources, perhaps volcanic, which contribute the remainder. (4) There is a slow conversion of F-12 to F-22. These four possibilities will be explored further in the remainder of this chapter. It should be kept in mind that the difference between the present F-22 burden based on the measured concentrations (Fig. 7.1) and the anthropogenic component is probably much larger than 28% which is discussed above. The lifetime of F-22 is not infinite, and therefore, the anthropogenic component is likely to be substantially smaller than 35 pptv.

In order to quantify the possible explanations of the observed F-22 concentrations, it is necessary to develop some theory which provides the values of $\bar{\xi}$ at the time measurements were made (5/1979) as a function of the global lifetime of F-22. The following method is adopted:

$$\frac{d}{dt} \bar{\xi}_T = S - \eta \bar{\xi}_T - \eta_T \frac{N_S}{N_T} (\bar{\xi}_T - \bar{\xi}_u) \quad (7.7)$$

$$\frac{d}{dt} \bar{\xi}_u = -\bar{\eta} \bar{\xi}_u + \eta_T (\bar{\xi}_T - \bar{\xi}_u) \quad (7.8)$$

where $\bar{\xi}_T$ and $\bar{\xi}_u$ are the mean mixing ratios of F-22 in the global troposphere (T) and the stratosphere (u - upper atmosphere) respectively. η and $\bar{\eta}$ are the reciprocals of lifetimes of F-22 in the troposphere and the stratosphere. η_T is the reciprocal of the stratospheric-tropospheric exchange time. N_S and N_T are the numbers of molecules of air in the stratosphere and the troposphere respectively. S is the total number of molecules of F-22 released per year divided by N_T . Let $C_T = \bar{\xi}_T N_T$, $C_u = \bar{\xi}_u N_S$, then the average global lifetime is: $\tilde{\eta} = \frac{C_T}{C} \eta + \frac{C_u}{C} \bar{\eta}$ with $C = C_T + C_u$. $\tilde{\eta}$ is not constant unless C_T/C and C_u/C are both constant; so defining a global lifetime is an idealization of the real situation. Equations (7.7) and (7.8) can be written as:

$$\frac{d}{dt} \vec{\xi} = \vec{S} - M \vec{\xi} \quad (7.9)$$

$$M = \begin{bmatrix} \eta + \eta_T \frac{N_S}{N_T} & -\eta_T \frac{N_S}{N_T} \\ -\eta_T & (\bar{\eta} + \eta_T) \end{bmatrix} \quad (7.10)$$

The solution is:

$$\vec{\xi} = P^{-1} e^{-\Lambda t} \int_0^t e^{\Lambda t'} P S(t') dt' \quad (7.11)$$

$$P M P^{-1} = \Lambda = \begin{pmatrix} \lambda_1 & 0 \\ 0 & \lambda_2 \end{pmatrix}$$

λ_1 and λ_2 are eigenvalues of M . $S(t')$ is taken to be the function

in Eq. (7.12) (McCarthy et al.; 1977).

$$S(t') = a e^{bt'} \quad (7.12)$$

Time	S(t).	
(1/1950) $0 \leq t < 10$ (1/1960):	$0.01e^{0.32t}$	(7.13a)

(1/1960) $0 \leq t' < 8$ (1/1968):	$0.234e^{0.187t'}$	(7.13b)
------------------------------------	--------------------	---------

(1/1968) $0 \leq t'' < 11.4$ (5/1979):	$1.206e^{0.158t''}$	(7.13c)
--	---------------------	---------

In Eqns. (7.13) the release within any period between t and $t + \delta t$ is given by $\int_t^{t + \delta t} S(t)dt$; and the result is in pptv in the troposphere. The tropospheric box contains all the sources so by Eq.(7.7) the source in 10^6 kg/yr is converted to pptv in the troposphere (with 8.69×10^{43} molecules of air ~ see Chap. 8). The methods of Chap.9 have also been applied in obtaining Eqns. (7.13).

One of the most desirable features of the theory expressed by Eqns. (7.7) and (7.8) is that it predicts the expected tropospheric average mixing ratio $\bar{\xi}_T$ based on the antropogenic source strength $S(t)$. It, therefore, allows direct comparison of the calculated average mixing ratio in the troposphere with that obtained from the tropospheric measurements shown in Fig. (7.1) (as $\frac{1}{2} (a + b)$).

In Fig. (7.3) the results of the calculations based on (7.7) and (7.8) are shown for various assumptions regarding the lifetimes of F-22 in the troposphere (τ) and the stratosphere ($\bar{\tau}$). Fig. (7.3) shows $\bar{\xi}_T$. The complete details of the calculations including the expected $\bar{\xi}_U$ and the global average $\bar{\xi}$ are shown in Appendix I. The

dashed enclosed region in Fig. (7.3) indicates the most likely values of $\bar{\xi}_T$ which can be explained by the antropogenic source, η_T is taken to be 0.58/yr (Reiter, 1975).

In general it is clear that there is a substantial amount of F-22 in the atmosphere that cannot be explained on the basis of the accepted antropogenic release of F-22.

(d) Strengths of Natural Sources

The excess of F-22 present in the atmosphere can be accounted for by some small natural source. The strength of the source is a function of the tropospheric and stratospheric lifetimes of F-22. On the simplest level the natural source strength can be estimated by assuming a constant output which has been operative over a long time (several lifetimes). The linearity of Eqns. (7.7) and (7.8) allows separation of the natural source and the contribution from the antropogenic source. Therefore, one may write the equations for the natural contribution as:

$$S_* - \eta \bar{\xi}_{T*} - \eta_T \frac{S}{N_T} (\bar{\xi}_{T*} - \bar{\xi}_{*S}) = 0 \quad (7.14)$$

$$- \bar{\eta} \bar{\xi}_{u*} + \eta_T (\bar{\xi}_{T*} - \bar{\xi}_{u*}) = 0 \quad (7.15)$$

where $d\bar{\xi}_{T*}/dt = d\bar{\xi}_{*u}/dt = 0$.

In these equations (7.14), (7.15), S_* is the source strength of the natural contribution (in pptv/yr or g/yr) and $\bar{\xi}_{T*}$, $\bar{\xi}_{u*}$ are the contributions of this source to the observed mixing ratio at this time.

Equations (7.14) and (7.15) can be solved to give:

$$\bar{\xi}_{T^*} = \frac{(\bar{n} + \eta_T) S_*}{\eta(\bar{n} + \eta_T) + \bar{n}\eta_T \frac{N_S}{N_T}} \quad (7.16)$$

$$\bar{\xi}_{U^*} = \frac{\eta_T S_*}{\eta(\bar{n} + \eta_T) + \bar{n}\eta_T \frac{N_S}{N_T}} \quad (7.17)$$

Eqn. (7.16) and Eqns. (7.7) - (7.13) can be used to estimate S_* as given by the following equation.

$$S_* = \left[\bar{\xi}_T^{(o)} - \bar{\xi}_T(\eta, \bar{n}) \right] \eta \left[1 + \frac{\bar{n}}{\eta} \frac{\eta_T}{\bar{n} + \eta_T} \frac{N_S}{N_T} \right] \quad (7.18)$$

where $\bar{\xi}_T^{(o)}$ is the observed tropospheric mixing ratio (~ 47 pptv), $\bar{\xi}_T(\eta, \bar{n})$ is the solution of Eqn. (7.7) (see Appendix I or Fig. 7.3) as a function of η, \bar{n} at the time measurements were made. It is assumed that $\bar{\xi}_{T^*} = \bar{\xi}_T^{(o)} - \bar{\xi}_T(\eta, \bar{n})$ so that the natural contribution is the difference of the anthropogenic contribution and the observed mixing ratio. S_* in grams is given by $(S_*(\text{pptv}) N_T M) / N_O$, where N_O is Avogadro's number, M the molecular weight of F-22 and N_T the number of molecules of air in the troposphere.

Taking the tropospheric lifetime of 15-30 yrs and a stratospheric (average) lifetime of 7-20 yrs implies that a constant natural source of 12-22 billion grams per year would yield the

observed global average mixing ratio of F-22 when added to the estimated anthropogenic source. This is a significant contribution which would imply that the natural source exceeded the anthropogenic source until about 10- 14 years ago.

It is difficult to point to a particular new source of F-22, other than the direct release. Graedel (1978) includes volcanoes as a source of both F-21 and F-22, and refers to the work of Stoiber et al. (1971). In this paper no quantitative estimates are given as to how much F-21 or F-22 was detected in the volcanic emissions investigated. In fact, the F-21 and F-22 peaks in the typical chromatogram given in their paper, are nonexistent. Prof. Rasmussen detected significantly enhanced F-21 and F-22 concentrations in aluminum manufacturing plant plumes (personal communication). It is possible that the processes involved in aluminum manufacturing contribute, at least part of the excess F-22 in the atmosphere. It appears that the explanation of the excess F-22 is likely to be a complicated combination of a variety of sources.

(e) Conversion of CCl_2F_2 (F-12)

It is well known that CFCl_3 (F11) and CCl_2F_2 (F12) have been released into the atmosphere in huge quantities. The atmospheric burden of these fluorocarbons is believed to be purely anthropogenic. The total release of F-11 up to the present is about 4.8 trillion grams and the total release of F-12 has been even larger at about

6.7 trillion grams (McCarthy et al. 1977, Alexander Grant & Co., 1979). The possible dangers from the accumulation of these trace gases to the earth's environment, as it is today, are also well known and have been highly publicized in recent years. Primary effects include the destruction of the earth's ozone layer and an enhancement of the greenhouse effect both of which can lead to a myriad of perturbations to the global environment. In the process of assessing the impact of these fluorocarbons, considerable attention has been directed towards finding possible tropospheric sinks for these compounds. Such sinks could reduce the possible environmental dangers these compounds pose. All attempts at finding significant tropospheric sinks have been unsuccessful. One possible sink considered for F-11 was its conversion to F-21. F-11 and F-21 differ in molecular structure only by a substitution of a hydrogen atom for a chlorine atom. This is the same relationship which exists between F-12 and F-22. In any case, if F-11 could convert to F-21 in the earth's environment, then this conversion would be an effective sink of F-11 because F-21 is destroyed rather rapidly (3-4 yrs; see Atkinson et al. 1979, Demore et al. 1979, Graedel, 1978) in the atmosphere due to its reaction with atmospheric HO radicals. This possibility was further highlighted by the observations of Ausloos et al. (1977) in laboratory experiments in which F-21 was detected when F-11 was irradiated with uv light ($\lambda < 400$ nm) in the presence of sand. It is still not completely

clear if the results can be extrapolated to the natural environment (see Glasgow et al. 1977). If F-11 is converted to F-21, it could take place through some heterogeneous process on the earth's deserts. F-21 has not been produced in any significant quantities (Glasgow et al. 1978); so its presence in the atmosphere could give support to the idea of such transformations unless other sources were identified. Recent measurements of F-21, however, have shown very small concentrations in the atmosphere (1-4 ppt; Rasmussen 1979, Singh 1979). So, it is still possible that a very small amount of F-11 is converted heterogeneously to F-21 but it is not a significant sink.

The analogous possibility can be considered for the conversion of F-12 to F-22. At the start two statements should be made and emphasized. First, it is not possible to make a convincing case, based on the currently available information, that F-11 and F-12 either do or do not convert to F-21 and F-22 respectively in the environment. Second, even if they do convert, the process is too slow to reduce the possible dangers of F-11 and F-12 accumulating in the atmosphere. Furthermore, even if F-12 converted in reasonably significant quantities to F-22, it could still pose similar threats to the global environment because, unlike F-21, F-22 has a rather long lifetime (~ 20 yrs) in the troposphere, and would therefore be exported to the stratosphere where its behavior could be similar to that of F-12.

There are basically two reasons why the conversion of F-12 to F-22 is especially significant to the problem of explaining the high F-22 concentrations measured in the troposphere. First, as mentioned, F-12 has been released in very large quantities and second the relatively long atmospheric lifetime of F-22 implies that even a small conversion (per year) would lead to a large effect due to accumulation. Both of these factors indicate that even if only minute fractions of the F-12 global burden are converted to F-22 every year, the conversion would still significantly elevate the present F-22 global burden, above that which can be accounted for by direct F-22 emissions. In order to explain the difference between the observed F-22 global burden, and that expected on the basis of direct emissions of F-22, such small conversion rates are required that they would not be easily detectable in the F-12 measurements.

The simplest way to formulate the possible contribution of F-12 to the atmospheric burden of F-22 is as follows:

$$\frac{d}{dt} \bar{\xi}_o = S_o - \eta_o \bar{\xi}_o \quad (7.19)$$

$$\frac{d}{dt} \bar{\xi}_x = -\tilde{\eta} \bar{\xi}_x + \tilde{\eta}_c \bar{\xi}_o \quad (7.20)$$

$$\begin{aligned} \eta_o &= \eta_c \alpha_T \frac{N_T}{N_\infty} + \left(\eta'_r \alpha_T \frac{N_T}{N_\infty} + \eta_s \alpha_u \frac{N_S}{N_\infty} \right) \\ &= \tilde{\eta}_c + \tilde{\eta}_r; \left(\tilde{\eta}_c = \eta_c \alpha_T \frac{N_T}{N_\infty} \right) \end{aligned} \quad (7.21)$$

$$\alpha_{\left(\frac{T}{u}\right)} = \bar{\xi}_o \left(\frac{T}{u}\right) / \bar{\xi}_o \quad (7.22)$$

In these equations, $\bar{\xi}_0$ is the global mixing ratio of F-12, η_0 is the reciprocal of the total global lifetime of F-12, $\bar{\xi}_*$ is the mixing ratio of F-22 resulting from the conversion of F-12 to F-22, $\tilde{\eta}$ is the reciprocal of the total global lifetime of F-22, $\tilde{\eta}_c$ is the reciprocal of the lifetime of F-12 with respect to conversion to F-22, and $\tilde{\eta}_r$ is the reciprocal of the lifetime of F-12 due to all other removal processes. The subscripts (T) and (u), as before, indicators of the tropospheric and stratospheric values of the function they appear with. The solution of Eqn. (7.20) is:

$$\bar{\xi}_*(t) = \tilde{\eta}_c \int_0^t \int_0^{t'} S(\tilde{t}) e^{-\eta(t'-\tilde{t})} e^{-\tilde{\eta}(t-t')} \tilde{t} dt dt' \quad (7.22)$$

Eqn. (7.22) is derived by regarding $\tilde{\eta}_c \bar{\xi}_0$ as a source of F-22, $S_*(t')$, then from Eqn. (7.20) $\bar{\xi}_*(t)$ is $\int_0^t S_*(t') \exp[-\tilde{\eta}(t-t')] dt'$. Since $\tilde{\eta}_c \bar{\xi}_0 = \tilde{\eta}_c \int_0^t S_0(\tilde{t}) \exp[-\eta_0(t'-\tilde{t})] dt$ from which Eqn. (7.22) follows. The function for the source strength of F-12 over the years is plotted in the figure for F-12 of Appendix I corresponding to Chapter 4 (McCarthy et al., 1977):

$$S_0(\tilde{t}) = a e^{b\tilde{t}} \quad (7.23a)$$

$$(1/1947) \quad 0 \leq \tilde{t} < 27(1/1974); \quad S_0(\tilde{t}) = 0.786 e^{0.121\tilde{t}}$$

$$(1/1974) \quad 27 \leq \tilde{t} < 32.4(5/1979); \quad S_0(\tilde{t}) = 19.5 \quad (7.23b)$$

$S_0(\tilde{t}) N_\infty$ = number of molecules of F-12 released per year, $S_0(\tilde{t})$ in Eqns. (7.23) is in pptv, in the whole atmosphere.

Equation (7.22) is solved and the results are presented in Figure (7.5). Details of the calculations, as well as the solution

of Eqn. (7.22) and the numbers used in Fig. (7.5) are given in Appendix I. Figure (7.5) shows $\bar{\xi}_*$ as a function of total global lifetime of F-22 ($\tilde{\tau} = 1/\tilde{\eta}$) when it is assumed that the conversion rate of F-12 is $\tilde{\eta}_c = 0.0125/\text{yr}$, $0.01/\text{yr}$, $0.0075/\text{yr}$ or $0.005/\text{yr}$. $\Delta\bar{\xi}_*$ is the excess of F-22 in the atmosphere. It is the difference of the global mixing ratio obtained from observations (Fig. 7.1; see also Appendix I) and the mixing ratio which is expected on the basis of direct emissions (Fig. 7.3). $\tilde{\tau}_r$ is taken to be 90 yrs (Hudson, 1977).

The results shown in Fig. (7.5) can be interpreted as follows: If the global lifetime of F-22 is between 15-50 yrs then the excess of F-22 now present in the atmosphere can be accounted for by the conversion of F-12 to F-22 with the rate of conversion between 0.0125/yr and 0.0075/yr. This result follows from the points at which the $\Delta\bar{\xi}_*$ curve crosses the $\bar{\xi}_*(t_*)$ curves. If the lifetime of F-22 is quite a bit smaller than 18 years, then a faster than 0.0125/yr conversion will be needed to explain the excess. This also means that the lifetime of F-12 with respect to conversion should be between 80-133 yrs to account for the excess (as long as the lifetime of F-22 ≥ 15 yrs). If the lifetime of F-22 is ~ 20 yrs then a 90 yr lifetime of F-12 with respect to conversion of F-12 is necessary to account for the excess. If the lifetime of F-22 is smaller than 20 years a faster conversion of F-12 is needed to account for the excess. Even though the conversion rates of

F-12 required to explain the excess F-22 are small (1-2% per yr) it is clear that they are of the same order of magnitude as the lifetime of F-12 due to stratospheric losses. In order to account for the excess F-22 on the basis of F-12 conversion alone requires that this sink for F-12 be of approximately the same strength as the stratospheric sink (or perhaps even stronger) thus reducing the total global lifetime of F-12 from ~ 90 yrs to ~ 50 yrs. It is likely that the excess is not entirely due to F-12 conversion but is a result of a combination of sources.

It is also likely that if conversion of F-12 is taking place and it takes place on desert surfaces or in dust storms, then the main loss of F-12 and gain of F-22 will be in the northern hemisphere.

(f) Accuracy of Measurements and Release Estimates

It is possible that the excess of F-22, as calculated earlier, is due to inaccuracies of either the measurements or the release estimates (or both).

If the measurements are accurate, it is quite unlikely that more detailed latitudinal observations would be enough to lower the global average so that it would coincide with the amount expected from the direct emissions data. On the other hand it is possible that the measurements are not accurate. Absolute accuracy is very crucial to all budget analyses. If the measurements are inaccurate, they would have to be too high, in absolute accuracy, by about 35-40% to account for the excess. This is evident from the predicted

mixing ratio for F-22 lifetimes of 15-20 yrs. After recent checks on the accuracy of measurements, it is unlikely that the accuracy of the measurements is as far off as 35-40%.

It is also possible that the release estimates of F-22 are inaccurate. There could be inaccuracies in either the estimates of McCarthy et al. (1977) or in the extrapolation of the release beyond 1975, assumed here. For F-22 this is a rather more difficult question to resolve. Unlike F-11, F-12 and CH_3CCl_3 , a large fraction of F-22 is unreleased. For example, up to 1975 about 85% of F-11 and about 87% of F-12 that had been produced before 1975, had been released. In contrast only 41% of the F-22 produced up to 1975 had been released (McCarthy et al. 1977). Since F-22 is not released very rapidly after production, it is more difficult to calculate the yearly release. The data on the production is much more accurate than the estimate of release, and so, in the case of F-22 certainly more than enough of it has been produced to account for the global burden as calculated from Rasmussen's (1979) observations reported in Fig. (7.1). Still the total source strength would have to be about 35% higher than McCarthy et al.'s estimates in order to account for the excess of F-22 observed. If the rate of increase of the emission since 1968 was $ae^{0.22t}$ instead of $ae^{0.158t}$, then there would be no excess F-22 present in the atmosphere that couldn't be accounted for by the direct emissions. A 27% higher rate of increase (than that of McCarthy et al., 1976) has to be assumed to account for the

excess and this higher rate must persist over more than 11 years. These calculations are based on a 20 year total global lifetime of F-22. If F-22 lifetimes are smaller, an even faster rate of increase of emissions would have to be assumed to get the same results. Again this is possible, but it is not at all clear as to how probable it is. The release in years before 1968 does not contribute much to the present burden, so the only way to explain the excess based on release estimate errors is by considering the releases after 1968.

The main conclusion that can be drawn from this analysis is that it is possible that inaccuracies of measurements or release estimates can account for the excess F-22 observed in the atmosphere. It is also evident that the inaccuracies would have to be substantial if they are to account for the excess.

(g) Summary and Conclusions

Recent tropospheric observations of CHClF_2 (F-22), made by Rasmussen (1979) were considered in this chapter. The direct anthropogenic release estimates of McCarthy et al. (1977) were used to calculate the global and tropospheric mixing ratios of F-22 that should have existed at the time of measurements. It turned out that even if all the F-22 ever emitted, based on McCarthy et al.'s (1977) estimates, was still in the atmosphere, it would fall short of the amount of F-22 in the atmosphere calculated from Rasmussen's (1979) measurements.

In order to explain the apparent excess of F-22 in the atmosphere, several possibilities were considered. (i) It was assumed that there is an approximately constant natural source that contributes the extra burden. Taking into account the likely range of lifetimes of F-22 in the atmosphere, it was shown that the strength of the natural source should be about 12-22 billion grams per year. If this is the explanation of the excess F-22 then the natural source would have exceeded the anthropogenic source until about 10 years back. (ii) Another possibility, which was explored, was that F-12 may convert to F-22 by some heterogeneous process. This idea is analogous to that of F-11 converting to F-21 which has been discussed in the literature. It was found that a conversion rate of about 0.0125/yr to 0.0075/yr would be sufficient to explain the excess if the lifetime of F-22 is $\geq \sim 15$ yrs. This implies that one would hardly be able to detect the effect of conversion on the atmospheric concentration of F-12 but it would still have a substantial effect on the atmospheric F-22 concentrations. The reasons why such small conversion rates of F-12, are sufficient to account for the excess are that F-12 has been released in very large quantities; and its total global lifetime is long. Also, F-22 is not readily destroyed, so the amount converted stays in the atmosphere year after year. On the other hand, since the stratospheric sink of F-12 is weak, even these small conversion rates become competitive with the stratospheric sink of F-12. (iii) The

possibilities that the measurements are inaccurate or that the release estimates are too low, were also considered. It appears that there would have to be substantial errors in the measurements or release estimates to account for the excess. Nevertheless, it is not possible to discount these explanations, with the information currently available.

Most of the calculations reported here are based on idealization of the real atmosphere. More sophisticated theoretical considerations may reveal alternate explanations. Furthermore, it is possible that all the explanations considered here may be operating simultaneously, each at a much weaker level than calculated in this chapter.

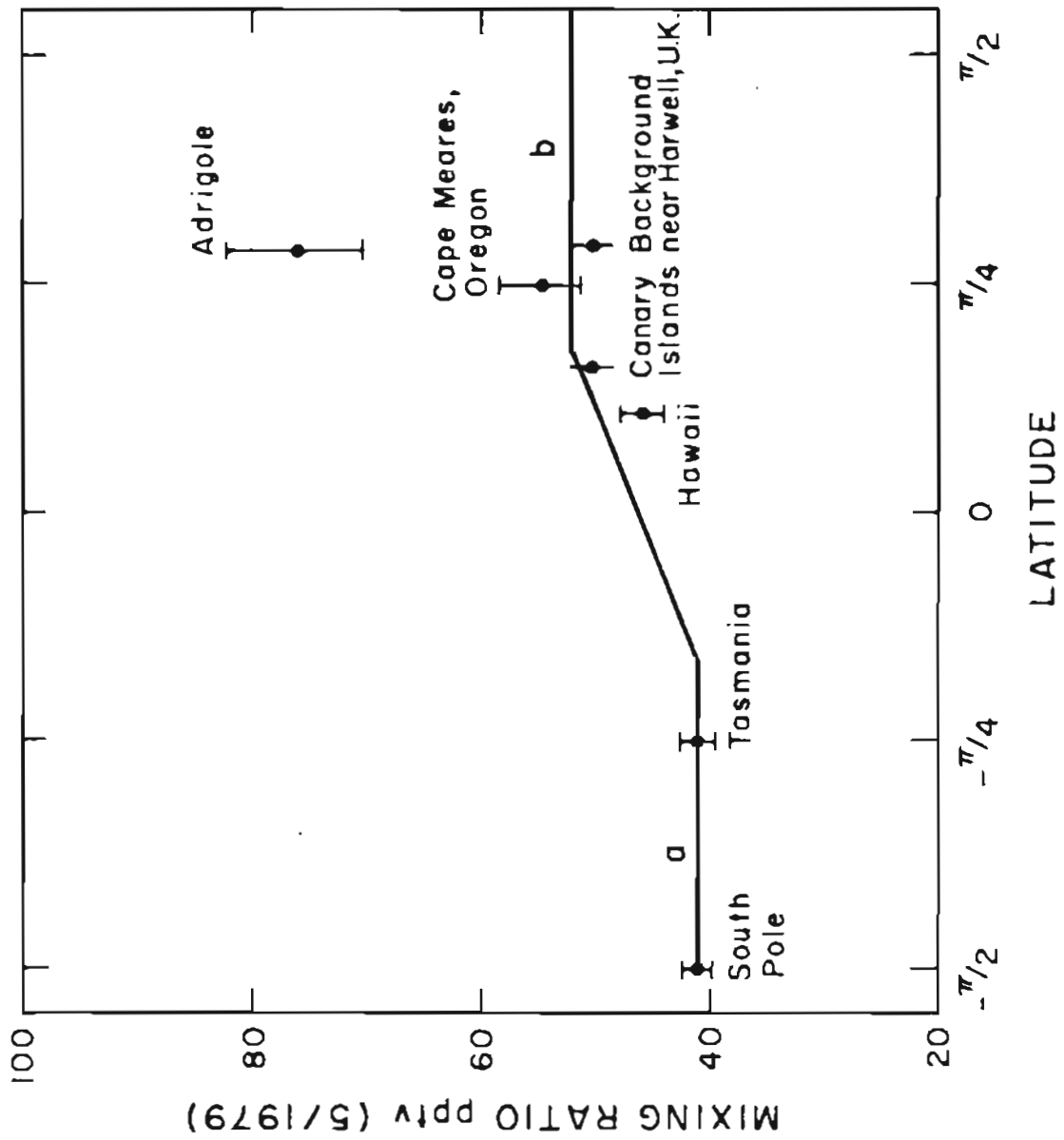


Figure (7.1): Global measurements of CHClF₂(F-22) in the atmosphere.

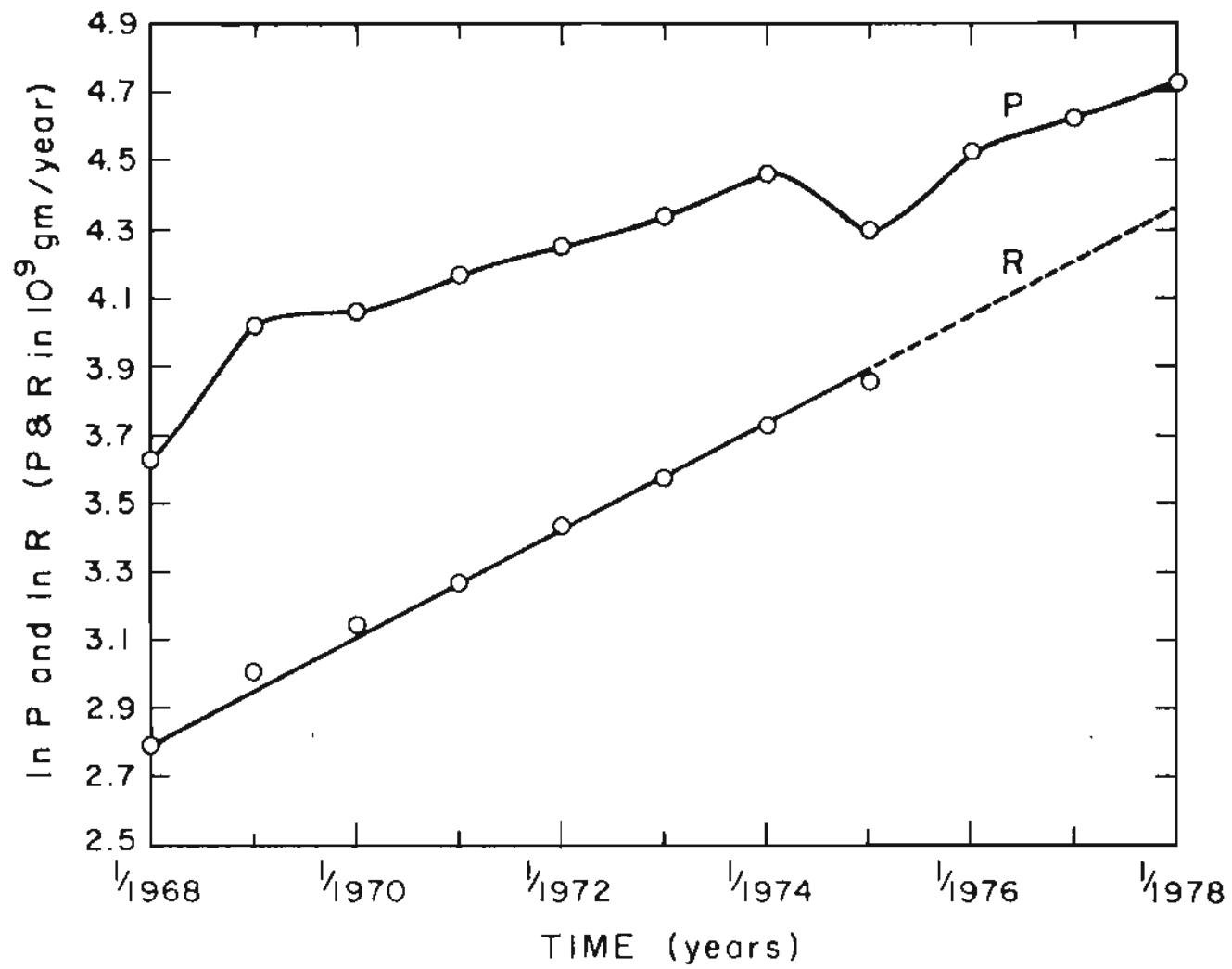


Figure (7.2): Production and release history of CHClF_2 (F-22)
 (From McCarthy et.al. 1977).

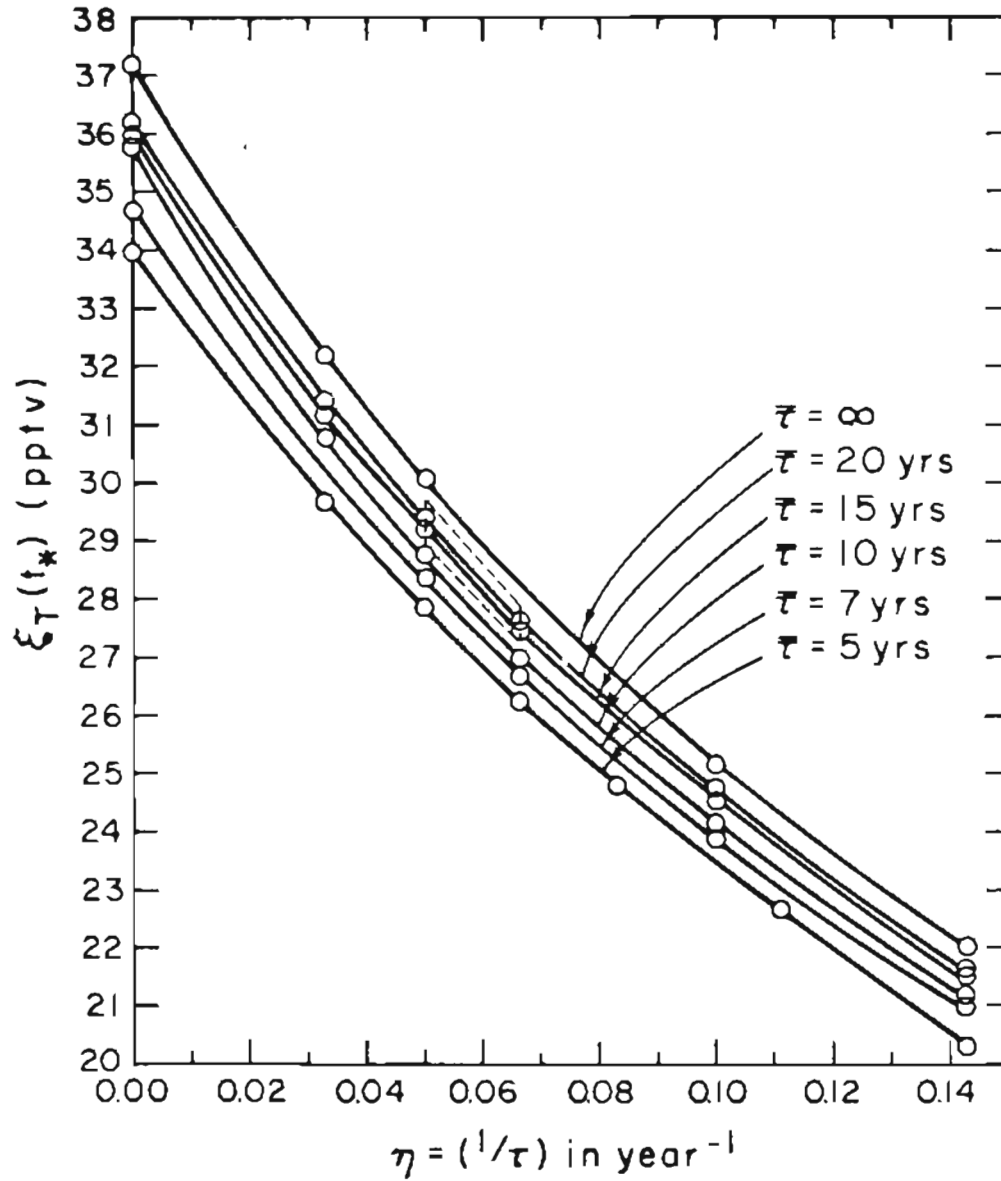


Figure (7.3): Concentrations of CHClF₂ (F-22) expected on the basis of direct anthropogenic release. Based on various assumptions regarding the lifetimes ($\bar{\tau}$ = stratospheric lifetime and τ = tropospheric lifetime).

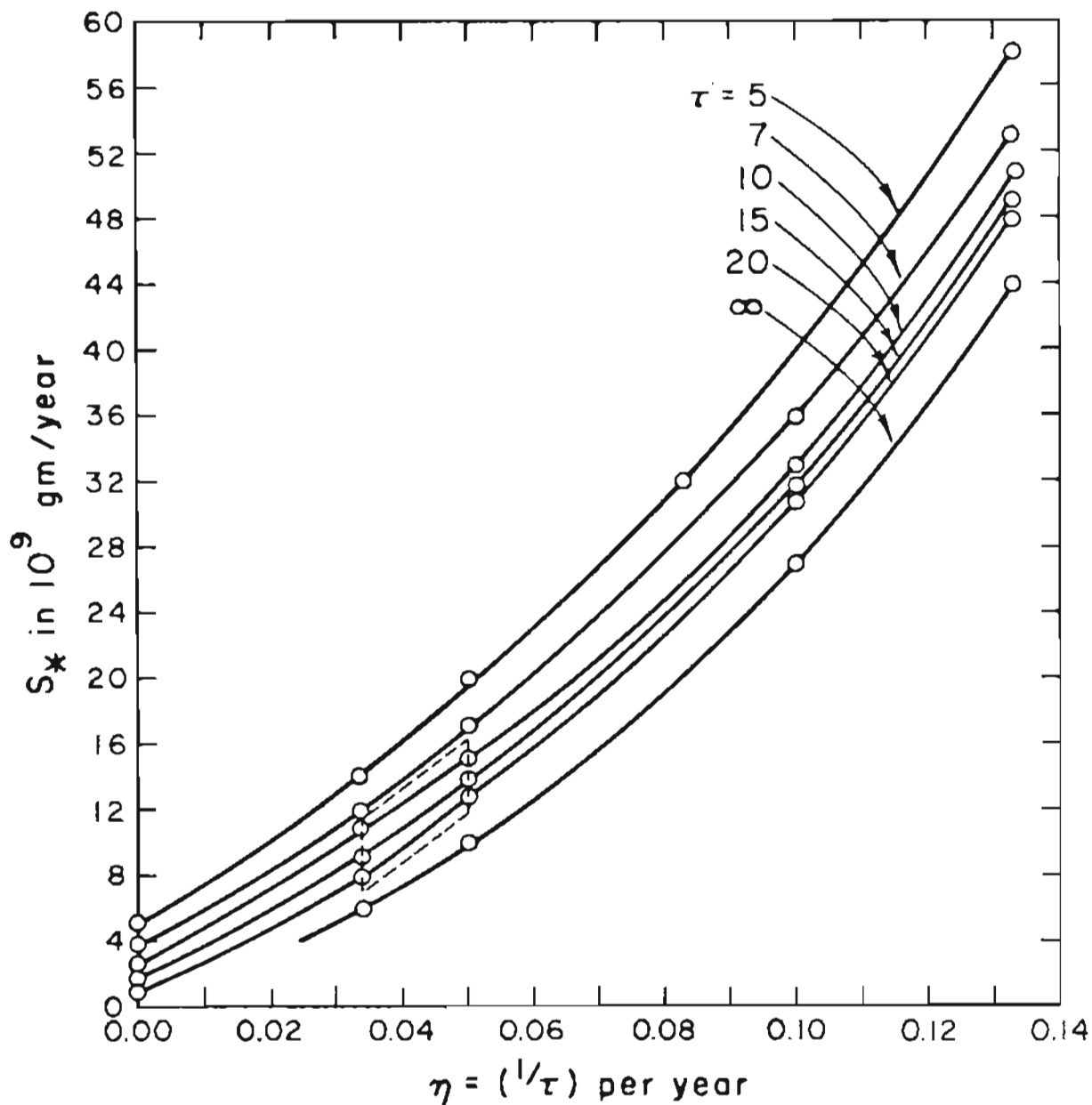


Figure (7.4): The strength of the source, other than direct emissions of F-22, needed to account for the excess F-22 present in the atmosphere.

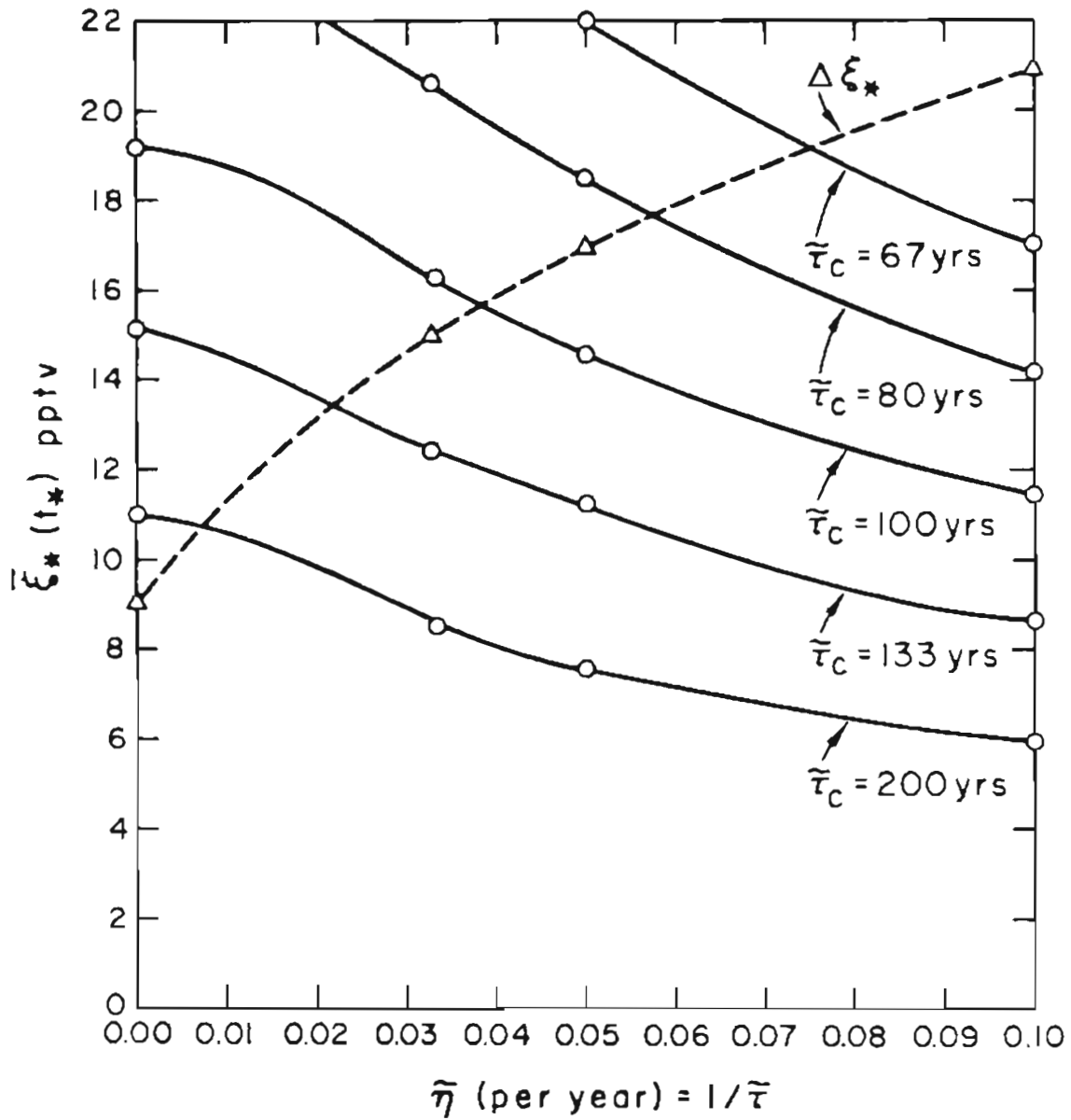


Figure (7.5): Conversion of F-12 to F-22, based on various assumptions regarding the total lifetime of F-22 ($\bar{\tau}$) and the lifetime of F-12 with respect to conversion ($\bar{\tau}_c$).

CHAPTER 8. GLOBAL AND HEMISPHERICAL AVERAGES
OF TRACE GASES

(a) Introduction

Often the theoretical treatment of trace gases is carried out using spatial averages of these trace gases within specified cells of the troposphere and the stratosphere. The reasons for simplifying the theory to such forms has already been discussed. Principally, these methods, using averages, compensate for the lack of detailed knowledge of the general circulation of the earth's atmosphere and detailed global measurements. Furthermore, the solvability of the resulting equations provides physical insights which are difficult to achieve in numerical solutions.

There are various approximations that can be made in transforming the observations into proper averages compatible with the requirements of the theory being constructed. This chapter deals with several such approximations and the reasons behind them. Theoretical methods are developed to more accurately calculate the burdens and average mixing ratios within specified atmospheric cells. In this way, the effects of neglecting a variety of atmospheric features can be assessed.

The next section deals with trace gases which have a significant gradient between the northern and southern hemispheres. It shows that under reasonable assumptions about the atmosphere, background measurements at high northern and southern latitudes are uniquely suited to give accurate global tropospheric averages of mixing ratios (or concen-

trations). Coupled with information from more detailed observations, the higher latitude measurements can also be used to derive hemispherical averages (in the troposphere) or average mixing ratios over spatial regions covering only half a hemisphere.

Section (8 .c) deals with the situation when more detailed concentration data are available as functions of latitude. The average mixing ratios are then expressed in terms of the coefficients of polynomials (usually of the fourth order) which are used to describe the latitudinal distribution of trace gases. Often global observations are expressed as $\xi(\phi) = \alpha_0 + \alpha_1\phi + \alpha_2\phi^2 + \alpha_3\phi^3$, where ϕ is the latitude. It is also shown that a small part of the global data (at high latitudes) can be used to obtain essentially the same values for the hemispherical or global averages as the complete data.

In section (8 .d) the effect of the destruction of trace gases in the stratosphere is discussed. The formulation of global box theories or theories with two or more boxes is also considered.

Later the numbers of molecules of air in the appropriate tropospheric cells, as well as the whole troposphere and the stratosphere, are calculated. Although other calculations exist for the total number of molecules of air in the troposphere and the stratosphere, these quantities are now knowable to arbitrary accuracy. In fact, these numbers are not only dependent on time of year but probably fluctuate from year to year even when averaged over a year's time. These quantities play an important role in determining the average mixing ratio of a trace gas in any atmospheric box.

(b) High Latitude Measurements and Global Averages.

It is well known that many trace gases have a non-constant latitudinal distribution. This is especially applicable to man-made compounds released into the atmosphere, primarily in (the northern half of) the northern hemisphere. CH_3CCl_3 , CFCl_3 and CF_2Cl_2 are obvious examples. In this section, simple mathematical ideas are used to demonstrate how measurements at one or two crucial places on the earth can be used to obtain global tropospheric average concentrations of these species. Complete global averages, as the reader will recall, define instantaneous global burdens, which can be used to calculate lifetimes and other characteristics of these trace gases. Complete global averages include the presence of the trace gases in the stratosphere.

Often, the mixing ratio of a long-lived trace gas is constant with height in the troposphere. It is also approximately zonally constant (constant with respect to longitude) barring small polluted urban regions. This is especially true when concentrations or mixing ratios are averaged over a month or so, which is usually done. The only strong variations of the mixing ratio (in the monthly average for example) are expected to occur along latitudes and above the tropopause. These variations are due to the properties of the general circulation of the earth's atmosphere. Transport is rapid around each latitude circle, but certain regions pose barriers to north-south mixing. The most prominent of these barriers is in the vicinity of the

equator with the strong Hadley cells convergence limiting exchange of air. Other weaker but similar barriers exist at analogous locations where other general circulation cells converge. The seasonal variations of trace gas concentrations, and the longitudinal variability of concentrations do produce uncertainties in estimated global burdens. These can be assessed only after more data become available. The mixing ratio of many trace gases is constant with height in the troposphere. The temperature inversion at the tropopause presents the major barrier for further upward transport. Vertical mixing beyond the tropopause is slow. When the trace gas reaches even higher altitudes, it may be more rapidly destroyed by the larger uv fluxes present. This depends on the properties of the trace gas. Therefore, the mixing ratio can undergo rapid decline with height in the stratosphere. For trace gases that have strong tropospheric sinks, such as reactions with HO or other radicals, the mixing ratio may decline with height even in the troposphere. The magnitude of the decline is a direct function of the rapidity of the atmospheric reaction. In this study it will be assumed that the mixing ratio is constant with height in the troposphere. The equations become simpler and less abstract by assuming this, but the feature of changing mixing ratio with height can be easily incorporated into the equations if the need arises.

In most cases of long- or medium-lived ($\tau > \sim 2$ yrs) species, whose primary sources are direct emissions in the northern hemisphere,

the tropospheric latitudinal distribution is to a very good approximation described by the picture in Figure (8 .1). The mixing ratio is high and relatively constant in the mid to high northern latitudes $\phi > \sim 30^\circ$ to 40° , then the mixing ratio declines through the ITCZ and continues to decline as one goes well into the southern hemisphere, finally reaching a relatively low constant value beyond $\phi < \sim -30^\circ$ to -40° . This can be seen in the global observations of several groups (Rasmussen, personal communication; Makide and Rowland, 1979; Singh, 1979). It should also be noted that most of the sources of CH_3CCl_3 , F-11, F-12 as well as most other trace gases of industrial origin are beyond 30°N , thus further increasing the gradient to look like the picture in Fig. (8.1). A little later some actual data on CH_3CCl_3 will also be discussed in detail.

Consider first the tropospheric averages of the mixing ratio. Suppose that the latitudinal distribution is described by some function of the following form:

$$\xi(\phi, t) = \xi(0, t) + f(\phi, t) \quad (8.1)$$

where $f(\phi)$ is any odd function of ϕ ($f(-\phi) = -f(\phi)$). The latitudinal profile in Fig. (8 .1) is a simple example of eqn. (8 .1). The total number of molecules of the given species is:

$$\begin{aligned}
 C &= \int_0^{2\pi} \int_{-\pi/2}^{\pi/2} \int_R^{z_T(\phi)+R} \xi(\phi) \rho(\phi, z) r^2 dr \cos \phi d\phi d\lambda \\
 &= \int_V \xi \rho dV
 \end{aligned} \tag{8.2}$$

and the globally averaged mixing ratio is

$$\langle \xi \rangle = \frac{C}{N_T} = \frac{\int_V \xi \rho dV}{\int_V \rho dV} \tag{8.3}$$

$$N_T = \int_V \rho dV = \int_0^{2\pi} \int_{-\pi/2}^{\pi/2} \int_R^{R+z_T(\phi)} \rho r^2 dr \cos \phi d\phi \tag{8.4}$$

In eqn. (8 .2), $z_T(\phi)$ is the latitude dependent tropopause height, R the radius of the earth and λ is the longitudinal angle. Let us assume that the northern and southern hemispheres are symmetric so that $z_T(-\phi) = z_T(\phi)$ (see Reiter, 1975). Consider eqn. (8.2) as:

$$C = \int_V \xi(0) \rho dV + \int_V f \rho dV \tag{8.5}$$

$$C = \xi(0) \int_V \rho dV + \int_0^{2\pi} \int_{-\pi/2}^0 \int_R^{z_T(\phi)+R} f \rho dV + \int_0^{2\pi} \int_0^{\pi/2} \int_R^{R+z_T(\phi)} f \rho dV \tag{8.6}$$

By the symmetry of the hemispheres $z_T(-\phi) = z_T(\phi)$ $\rho(-\phi, z) = \rho(\phi, z)$;
 $dV(-\phi) = -dV(\phi)$. It is easy to see that the second and third integrals
 have the same magnitude but opposite signs so that

$$C = \xi(0)N_T \quad (8.7)$$

$$\langle \xi \rangle = \xi(0) = \frac{1}{2}[\xi(\tilde{\phi}) + \xi(-\tilde{\phi})] \quad (8.8)$$

where $\tilde{\phi}$ is any latitude. So the global average is a simple average of
 two concentrations measured at $\tilde{\phi}$ and $-\tilde{\phi}$ in latitude. The situation is
 even simpler when $\xi(\phi)$ assumes the form in Figure (8.1). In case
 $\xi(\phi)$ is like Fig. (8.1):

$$\xi(\phi) = \begin{cases} a & -\frac{\pi}{2} \leq \phi < -\phi_0 \\ \frac{1}{2}(a+b) + \frac{1}{2} \frac{(b-a)}{\phi_0} \phi & -\phi_0 \leq \phi \leq \phi_0 \\ b & \phi_0 < \phi \leq \pi/2 \end{cases} \quad (8.9)$$

so that

$$\langle \xi \rangle = \frac{1}{2} (a+b) \quad (8.10)$$

"a" can be measured at any latitude higher than ϕ_0 and "b" can be meas-
 ured at any latitude below $\phi = -\phi_0$.

The time series of measurements made by Rasmussen at two locations -- the remote Pacific Northwest site (PNW 45°N) and at the south pole (-90°) -- can be used to calculate the global tropospheric average, simply as $\langle \xi \rangle = (\frac{1}{2}) (\xi_{\text{PNW}} + \xi_{\text{SP}})$. Furthermore, hemispherical averages can also be computed from just these pairs of measurements, as long as it is accepted that the latitudinal distribution is similar to that shown in Fig. (8.1).

In practice there are several sources of error; particularly (i) the latitudinal distribution deviates from the antisymmetric function $f(\phi)$. (ii) The hemispheres could have antisymmetries in $\rho(\phi)$ and $z_T(\phi)$, and (iii) $\xi(\phi)$ may have complicated time behaviour including seasonal effects due to transport.

Based on the idea of eqn. (8.9) the hemispherical averages of trace gases can be inferred even when full latitudinal coverage is not available. Consider the example where measurements exist at high latitudes so that a and b are measured. This is the case for the time series measurements of CH_3CCl_3 discussed previously. The hemispherical averages can then be calculated based on a, b and ϕ_0 (eqn. 8.9).

$$\langle \xi \rangle_n = \frac{\int_0^{\pi/2} \int_R^{z_T(\phi)+R} \xi(\phi) \rho(r) r^2 dr \cos\phi d\phi}{\int_0^{\pi/2} \int_R^{z_T(\phi)+R} \rho(r) r^2 dr \cos\phi d\phi} \quad (8.11)$$

$$\langle \xi \rangle_s = \frac{\int_{-\pi/2}^0 \int_R^{z_T(\phi)+R} \xi(\phi) \rho(r) r^2 dr \cos\phi d\phi}{\int_{-\pi/2}^0 \int_R^{z_T(\phi)+R} \rho(r) r^2 dr \cos\phi d\phi} \quad (8.12)$$

In these equations integration over λ has been carried out.

Eqns. (8.11) and (8.12) can be simplified if $z_T(\phi)$ is taken as a constant average tropopause height; and ρ is assumed to be independent of ϕ . With these approximations:

$$\langle \xi \rangle_n \approx \int_0^{\pi/2} \xi(\phi) \cos\phi d\phi$$

$$\langle \xi \rangle_s \approx \int_{-\pi/2}^0 \xi(\phi) \cos\phi d\phi$$

These can be solved to give:

$$\langle \xi \rangle_n = b - \frac{(b-a)}{2\phi_0} (1 - \cos \phi_0) \quad (8.13)$$

$$\langle \xi \rangle_s = a + \frac{(b-a)}{2\phi_0} (1 - \cos \phi_0) \quad (8.14)$$

Equations (8.13) and (8.14) will usually be sufficient for many applications. The value of ϕ_0 is usually around $\pi/6$ radians.

Eqns. (8.13) and (8.14) can be used to derive the relationship between the gradient R and R_0 . These are discussed in the first section of chapter 5.

$$R = \frac{\langle \xi \rangle_n}{\langle \xi \rangle_s} ; \quad R_0 = \frac{b}{a} \quad (8.15)$$

$$R_0 = \left[\frac{R \left(1 - \frac{\alpha}{2\phi_0} \right) - \frac{\alpha}{2\phi_0}}{1 - \frac{\alpha}{2\phi_0} (1 - R)} \right] \quad (8.16)$$

where $\alpha = (1 - \cos\phi_0)$. Eqn. (8.16) was used in chapter 5 to discuss the variation of the gradient R_0 in time due to the fluctuations of the source. When the two-box theory was used, the small calculated gradient R had to be expanded to obtain calculated values of R_0 which could be compared to observations. The four-box theory automatically gave R_0 . In other words, the gradient $R_0 = b/a$, which has been measured for many years for CH_3CCl_3 , F-11, and F-12, has to be converted to R by (8.16) before it can be used in two-box theories. Similarly the two-box theories deal with $\langle \xi \rangle_n$ and $\langle \xi \rangle_s$ and not with the directly measured time series data at the Pacific Northwest sight and the south pole. For the case of a compound with as large a gradient as CH_3CCl_3 , using a , b , and R_0 instead of the proper variables $\langle \xi \rangle_s$, $\langle \xi \rangle_n$ and R can lead to distortions in the lifetimes and gradients predicted by the two-box theory (see discussion in Chang and Penner, 1978).

With these ideas in mind, it is also possible to deduce the concentrations that should have existed at other latitudes even though measurements were only made at two high latitude locations. All that has to be done is to evaluate the integrals over smaller spatial ranges

and all concentrations can be computed from a , b , and ϕ_0 . Of course the results are approximate, but in the absence of data at the missing latitudes, they can be used. These calculations are simple generalizations of the situation already discussed in this section, so they won't be given in detail here.

When detailed global measurements, over many latitudes, are available, it is possible to compute the global and hemispherical averages based on the detailed data and also on the simple ideas presented in this section. This comparison lends strong support to the applicability of the equations given in this section.

(c) Tropospheric Averages Based on Detailed Latitudinal Measurements
-- Latitudinal Polynomials.

From ocean cruises and aircraft flights measurements have been made of several trace gases. These measurements give almost continuous data on the ground level mixing ratio of a trace gas as a function of latitude. Figures (8.2) - (8.4) give Rasmussen's global measurements of F-11, F-12 and CH_3CCl_3 during 1976-1978. Similar measurements have also been reported by Singh et al. (1979) for F-11, F-12, CH_3CCl_3 and several other trace gases. Makide and Rowland (1979) have reported CH_3CCl_3 measurements from 25 ground-based locations, most of which were at $\phi > + \pi/6$ radians and $\phi < - \pi/6$ radians.

It is customary to report the results of such observations with a fourth order polynomial in latitude so that the mixing ratio at any latitude ϕ is given by:

$$\xi(\phi) = \alpha_0 + \alpha_1\phi + \alpha_2\phi^2 + \alpha_3\phi^3 \quad (8.17)$$

One of the principal reasons for obtaining a function like (8.17) is to be able to compute global and hemispherical averages, as well as R. It is of interest to find out how well the values of such averages, obtained by the use of the polynomial, agree with the values obtained by the simple methods of the previous section.

First, let us consider the evaluation of the hemispherical and global averages by the polynomials.

$$\langle \xi \rangle_n^{(p)} = \frac{2\pi}{\frac{1}{2}N_T} \int_0^{\pi/2} \int_R^{R+z_T(\phi)} \left[\sum_{k=0}^3 \alpha_k \phi^k \right] \rho(r) r^2 \cos\phi \, dr d\phi \quad (8.18)$$

$$\langle \xi \rangle_s^{(p)} = \frac{2\pi}{\frac{1}{2}N_T} \int_{-\pi/2}^0 \int_R^{R+z_T(\phi)} \left[\sum_{k=0}^3 \alpha_k \phi^k \right] \rho(r) r^2 \cos\phi \, dr d\phi \quad (8.19)$$

$$\langle \xi \rangle^{(p)} = \frac{1}{2} \left[\langle \xi \rangle_s^{(p)} + \langle \xi \rangle_n^{(p)} \right] \quad (8.20)$$

$$N_T = \int_V \rho \, dV = 2\pi \int_{-\pi/2}^{\pi/2} \int_R^{R+z_T(\phi)} \rho(r) r^2 \cos\phi \, dr d\phi$$

$\langle \xi \rangle_n^{(p)}$ denotes the average northern hemisphere mixing ratio obtained by the use of the polynomial (superscript (p) is used to indicate the polynomial). $\langle \xi \rangle_s^{(p)}$ indicates the southern hemisphere average mixing ratio and $\langle \xi \rangle^{(p)}$ the global average. The global average is always $(\frac{1}{2}) [\langle \xi \rangle_n + \langle \xi \rangle_s]$ as long as the two hemispheres are regarded as symmetrical with respect to $z_T(\phi)$ and $\rho(z, \phi)$.

The approximations made to derive eqns. (8.13) and (8.14), namely $z_T(\phi)$ is set equal to some constant average value and ρ is not a function of ϕ , imply that eqns. (8.18) - (8.20) can be simplified to:

$$\begin{aligned} \langle \xi \rangle_n^{(p)} = & \alpha_0 + \alpha_1 \left(\frac{\pi}{2} - 1 \right) + \alpha_2 \left[\left(\frac{\pi}{2} \right)^2 - 2 \right] \\ & + \alpha_3 \left[\left(\frac{\pi}{3} \right)^3 - 3\pi + 6 \right] \end{aligned} \quad (8.21)$$

$$\langle \xi \rangle_n^{(p)} = \alpha_0 + 0.5708\alpha_1 + 0.4674\alpha_2 + 0.4510\alpha_3$$

$$\langle \xi \rangle_s^{(p)} = \alpha_0 - \alpha_1 \left(\frac{\pi}{2} - 1 \right) + \alpha_2 \left[\left(\frac{\pi}{2} \right)^2 - 2 \right] - \alpha_3 \left[\left(\frac{\pi}{2} \right)^3 - 3\pi + 6 \right] \quad (8.22)$$

$$\langle \xi \rangle_s^{(p)} = \alpha_0 - 0.5708\alpha_1 + 0.4674\alpha_2 - 0.4510\alpha_3$$

$$\langle \xi \rangle^{(p)} = \alpha_0 + \alpha_2 \left[\left(\frac{\pi}{2} \right)^2 - 2 \right] \quad (8.23)$$

$$\langle \xi \rangle^{(p)} = \alpha_0 + 0.4674\alpha_2$$

In these equations α_0 , α_1 , α_2 , and α_3 have the following units: $[\alpha_0] = \text{pptv}$, $[\alpha_1] = \text{pptv/degree radian}$, $[\alpha_2] = \text{pptv/(degree radian)}^2$ and $[\alpha_3] = \text{pptv/(degree radian)}^3$. Equations (8.21) - (8.23) are most commonly used.

The following table (8.1) shows the hemispherical and global averages computed by the two methods represented by equations (8.21) - (8.23) and (8.13) and (8.14). These values are for data shown in figures (8.2] - (8.4].

Table (8 .1) Average Tropospheric
Mixing Ratios of CH_3CCl_3 (pptv)

	$\langle \xi \rangle_n$	$\langle \xi \rangle_n^{(p)}$	$\langle \xi \rangle_s$	$\langle \xi \rangle_s^{(p)}$	$\langle \xi \rangle$	$\langle \xi \rangle^{(p)}$
1976	109	108	78	84	94	96
1977	107	107	86	89	97	98
1978	121	120	95	94	108	107

Here $\langle \xi \rangle_n$, $\langle \xi \rangle_s$ and $\langle \xi \rangle$ are the appropriate hemispherical and global averages computed from eqns. (8.13) and (8.14) and using only a small part of the data around $\pi/4^\circ\text{N}$ and $-\pi/2$ degrees south; whereas $\langle \xi \rangle_n^{(p)}$, $\langle \xi \rangle_s^{(p)}$ and $\langle \xi \rangle^{(p)}$ are the same quantities calculated from the full data using the polynomial and equations (8.21) - (8.23).

Similar calculations can easily be made for F-11 and F-12 from figures (8.2) - (8.4). It is clear that the agreement between the two methods is extremely good -- especially for the global average.

A few words of caution are needed here. The table above and figures (8.2) to (8.4) are given as illustrative examples to show the typical structure of latitudinal distributions of trace gases. The common features are visible in these figures. These data are reported here in a form that can only be characterized as preliminary. Data collected on ocean cruises and aircraft flights conducted at somewhat different times during the year have all been put together under one graph for the year quoted. This was done to reproduce full latitudinal coverage. Consequently, conclusions cannot be drawn from

the increases represented here without further consideration of the times of the year at which measurements were made. Currently, the data are being separated and reevaluated so that several latitudinal profiles can be abstracted for each year, where each profile represents data taken within a short period of time. The results of the analysis will be reported elsewhere in the near future. For the purposes of the analysis given here, the data are used just to show that a small segment of it can yield hemispherical and global averages just as well as the full data with the polynomial.

Once it is established that the latitudinal profile of a trace gas with northern sources is similar to that shown in Figure (8.1), the hemispherical and global means of concentrations or mixing ratios can be evaluated with data only from the remote northern hemisphere (such as the Pacific Northwest) and southern hemisphere (such as the south pole or Tasmania) measurements. It is always good to have lots of data at every latitude, but if one is interested only in hemispherically averaged concentrations, then measurements at two locations, one each in high northern and southern latitudes, will do almost as well.

Appendix I contains polynomial coefficients and other details of the calculations given in this section.

It is possible to look upon the polynomial as a power series approximation to the solution of the species conservation equation. With some effort, the theoretical α_0 , α_1 , α_2 , and α_3 can be derived. One possible procedure for doing this can be deduced from the references (Fink and Klais, 1978, Czeplak and Junge, 1974).

The methods discussed in this section are approximate. It has been assumed that $\rho(r)$, the air density, is not a function of latitude. It has also been assumed that one can define an average tropopause height which suffices for the calculations of hemispherical and global averages of mixing ratio in the troposphere. It is expected that these are good approximations in that they accurately reproduce the hemispherical and global averages. The dependence of ρ on ϕ comes from the dependence of scale height on latitude. The tropopause height z_T also changes both with season and with latitude. A reasonable time averaged function for $z_T(\phi)$ is:

$$z_T(\phi) = \begin{cases} h_0 & |\phi| \leq \pi/6 \\ h_1 - \alpha|\phi| & \pi/6 < |\phi| < \pi/2 \end{cases} \quad (8.24)$$

where $h_0 \approx 16$ km, $h_1 \approx 14$ km and $\alpha \approx 3.82$ km per radian of latitude. The obvious effect of this function is that the concentration of a trace gas in the region of the troposphere from $0 - \pi/6$ radians of latitude should be weighted more heavily (than $\frac{1}{2}$) compared to the con-

centration in the region from $\pi/6 - \pi/2$ radians, when computing the hemispherical average. Similar statements apply to the global average and the southern hemisphere average.

Some of the questions discussed above can be considered further with the aid of the results of the next section.

(d) Trace Gases in the Stratosphere.

Medium and long-lived trace gases found in the troposphere are often present in the stratosphere as well. The mass conservation equations when averaged over the whole atmosphere or hemispherical pieces must include this extra burden. On the other hand, it is also true that the numbers of molecules of these trace gases, present in the whole stratosphere, are small compared to numbers present in the troposphere. This is because of two reasons. First, the density of "air" in the stratosphere is small, and second, because most trace gases such as F-11, F-12 and CH_3CCl_3 do not survive for very long in the stratosphere due to the high solar ultraviolet present in the stratosphere, and vertical mixing is slow.

Expressions for the total northern and southern hemisphere average mixing ratios are:

$$\langle \xi \rangle_n = \frac{1}{N_{\infty n}} \left\{ \int_0^{2\pi} \int_0^{\pi/2} \left[\int_R^{R+z_T(\phi)} \xi_T(r, \phi, \lambda, t) \rho_T(r, \phi, \lambda, t) r^2 dr \right. \right. \\ \left. \left. + \int_{R+z_T}^{\infty} \xi_U(r, \phi, \lambda, t) \rho_U(r, \phi, \lambda, t) r^2 dr \cos \phi d\phi d\lambda \right] \right\} \quad (8.25)$$

$$\langle \xi \rangle_s = \frac{1}{N_{\infty s}} \left\{ \int_0^{2\pi} \int_{-\pi/2}^0 \left[\int_R^{R+z_T} \xi_T \rho_T r^2 dr + \right. \right. \\ \left. \left. \int_{R+z_T}^{\infty} \xi_U \rho_U r^2 dr \right] \cos \phi d\phi d\lambda \right\} \quad (8.26)$$

$$\langle \xi \rangle = \frac{1}{N_{\infty}} \int_0^{2\pi} \int_{-\pi/2}^{\pi/2} \left[\int_R^{R+z_T} \xi_T \rho_T r^2 dr + \right. \\ \left. \int_{R+z_T}^{\infty} \xi_U \rho_U r^2 dr \right] \cos \phi d\phi d\lambda \quad (8.27)$$

From these expressions, it follows that $\langle \xi \rangle_n N_{\infty n}$ represents the total number of molecules of the trace gas in question, in the northern tro-

posphere, stratosphere, and beyond. Similar comments apply to $\langle \xi \rangle_s$, $N_{\infty s}$ and $\langle \xi \rangle N_{\infty}$ (which is the total number of molecules of the trace gas in the whole atmosphere). R is the radius of the earth.

$\xi_T(r, \phi, \lambda, t)$ is the mixing ratio of the trace gas at ϕ , r , λ , and t , in the troposphere, ρ_T is the space-time density of air in the troposphere. Similarly, $\xi_u(\phi, r, \lambda, t)$ is the mixing ratio of the trace gas in the stratosphere (upper atmosphere) and ρ_u the density of air in the stratosphere.

In order to determine the true values of $\langle \xi \rangle_n$, $\langle \xi \rangle_s$, and $\langle \xi \rangle$ one must have measured values of the mixing ratio at a large number of points within the troposphere and the stratosphere. Since there are severe practical limitations to obtaining a large number of measurements within a small interval of time, we have to resort to filling the gaps in our (observational) knowledge of the mixing ratio with theoretical ideas which have been deduced from the observations of the atmosphere in general. For example, it can sometimes be assumed that $(\partial/\partial\lambda)\xi_T$ and $(\partial/\partial\lambda)\xi_u$ are zero; i.e., the gases are zonally well mixed. Similarly, based on other observations it can also be assumed that ξ_o is constant with height up to $r = R + z_T(\phi)$. (These assumptions should be verified experimentally, at least once. Generally one would expect them to hold for relatively long-lived species.)

The stratosphere extends from $R + z_T(\phi)$ to some height $r = R + z_{\infty}$, where z_{∞} is the height of the stratopause. Beyond z_{∞} there are

very few molecules of air in the atmosphere, and even fewer molecules of the trace gases with ground level sources. Therefore, the upper limit of ∞ in the integrations with respect to r , in equations (8.25) - (8.27) can be safely replaced by $R + z_\infty$. Now, z_∞ is also a function of time and latitude, just like $z_T(\phi)$ (Reiter, 1975). But, to a good approximation z_∞ can be assumed constant at 50 km. This height is so high that small changes in it do not affect the $\langle \xi \rangle_n$, $\langle \xi \rangle_s$, and $\langle \xi \rangle$ to any significant degree. On the average, it is also appropriate to assume that $N_{\infty n} = N_{\infty s} = \frac{1}{2} N_\infty$. This implies that the total number of molecules of air in the northern and southern tropospheres and stratospheres are the same and equal to half the total number of molecules of air in the atmosphere.

Lastly, it is reasonable to assume that:

$$\int_R^{R+z_T} r^2 \rho \xi \, dr \simeq R^2 \int_0^{z_T} \rho(z) \xi(z) \, dz \quad (8.28)$$

With all these approximations equations (8.25) - (8.27) become:

$$\begin{aligned} \langle \xi \rangle_n \simeq & \frac{4\pi R^2}{N_\infty} \left[\int_0^{\pi/2} \int_0^{z_T(\phi)} \rho_T \xi_T \, dz \cos\phi \, d\phi \right. \\ & \left. + \int_0^{\pi/2} \int_{z_T(\phi)}^{z_\infty} \rho_u \xi_u \, dz \cos\phi \, d\phi \right] \quad (8.29) \end{aligned}$$

$$\langle \xi \rangle \simeq \frac{4\pi R^2}{N_\infty} \left[\int_{-\pi/2}^0 \int_0^{z_T(\phi)} \rho_T \xi_T dz \cos\phi d\phi + \int_{-\pi/2}^0 \int_{z_T}^{z_\infty} \rho_U \xi_U dz \cos\phi d\phi \right] \quad (8.30)$$

$$\langle \xi \rangle \simeq \frac{2\pi R^2}{N_\infty} \left\{ \int_{-\pi/2}^{\pi/2} \left[\int_0^{z_T} \rho_T \xi_T dz + \int_{z_T}^{z_\infty} \rho_U \xi_U dz \right] \cos\phi d\phi \right\} \quad (8.31)$$

These three equations may be used in the two-box and global theories.

In order to look at the effects of the stratospheric content of trace gases, some more simplifying assumptions can be made. Let us go back to the simplifying assumption that z_T can be represented by some average tropopause height. Furthermore, it may be assumed that

$$\xi_U = \xi_T e^{-\alpha(z - z_T)} \quad (8.32)$$

$$\rho_U = \rho_T(z_T) e^{-(z - z_T)/h_U} \quad (8.33)$$

where α and h_U are constants; h_U is the appropriate density scale height of air in the stratosphere. The value of $\alpha > 0$ in eqn. (8.32) signifies the departure of the stratospheric mixing ratio from a constant value; it also shows that the density of the trace gas scales

with a faster decline with height than the density of air. Eqns. (8.29 - (8.31) become:

$$\langle \xi \rangle_n \approx \langle \xi \rangle_{nT} \frac{N_T}{N_\infty} \left[1 + \frac{1}{h_u \alpha + 1} \frac{N_s}{N_T} \right] \quad (8.34)$$

$$\langle \xi \rangle_s \approx \langle \xi \rangle_{sT} \frac{N_T}{N_\infty} \left[1 + \frac{1}{h_u \alpha + 1} \frac{N_s}{N_T} \right] \quad (8.35)$$

$$\langle \xi \rangle \approx \langle \xi \rangle_T \frac{N_T}{N_\infty} \left[1 + \frac{1}{h_u \alpha + 1} \frac{N_s}{N_T} \right] \quad (8.36)$$

where $\langle \xi \rangle_{nT}$, $\langle \xi \rangle_{sT}$, and $\langle \xi \rangle_T$ are the tropospheric averages defined in the previous section. N_T and N_s are the total numbers of molecules of air in the troposphere and the stratosphere respectively. If $\alpha = 0$, implying that there is no change of the mixing ratio with height, then $(N_T/N_\infty) [1 + (h_u \alpha + 1)^{-1} (N_s/N_T)]$ becomes 1, and thus there is no difference between the global and hemispherical averages computed in the troposphere and with the inclusion of the stratosphere. This conclusion remains valid even when several of the approximations made to derive (8.34) - (8.36) are relaxed. In the other limit, if $\alpha \rightarrow \infty$, the effect of the stratosphere is most severe for the calculation of global and hemispherical averages. This is to be expected because $\alpha \rightarrow \infty$ implies a zero lifetime for the trace gas in the stratosphere.

There are several, seemingly equivalent, ways in which one can look at the effects of the stratosphere. Here, only very simple formulations will be considered to clarify some of the questions regarding the calculations of lifetimes by budget methods. Consider first a two-box hypothesis where one box is the troposphere and the other box the stratosphere. The complete mass conservation equation can then be written as:

$$\frac{d}{dt} \langle \xi \rangle_T = S - \eta \langle \xi \rangle_T - \eta_T \frac{N_S}{N_T} (\langle \xi \rangle_T - \langle \xi \rangle_U) \quad (8.37)$$

$$\frac{d}{dt} \langle \xi \rangle_U = -\bar{\eta} \langle \xi \rangle_U + \eta_T (\langle \xi \rangle_T - \langle \xi \rangle_U) \quad (8.38)$$

The brackets $\langle \rangle$ will be dropped from here on for the sake of notational convenience. These two equations account for the total number of molecules of the trace gas. Where $\eta_T = 1/\tau_T$ and τ_T here is the average stratospheric-tropospheric transport time. These equations are derived as follows: Multiply (8.37) by N_T and (8.38) by N_S to get:

$$\frac{d}{dt} C_T = \tilde{S} - \eta C_T - \eta_T \left[\frac{N_S}{N_T} C_T - C_U \right] \quad (8.39)$$

$$\frac{d}{dt} C_U = -\bar{\eta} C_U + \eta_T \left[\frac{N_S}{N_T} C_T - C_U \right] \quad (8.40)$$

where C_T and C_U are the total number of molecules of the trace gas in

the troposphere and the stratosphere. Adding these equations gives:

$$\frac{d}{dt} C = \tilde{S} - \eta C_T - \bar{\eta} C_U \quad (8.41)$$

Here $\tilde{S} = S N_T$ which is the total number of molecules released per unit time. Equation (8.41) says that the change in C - the total number of molecules of a trace gas in the entire atmosphere is equal to the source per unit time, less the numbers of molecules destroyed in the troposphere and the stratosphere per unit time. Consider eqns. (8.39) and (8.40) when τ_T is the time for complete exchange of mass between the boxes, then the total number of molecules of air that go into the stratosphere in time τ_T is N_S , thus carrying $N_S \xi_T / \tau_T = \frac{N_S}{N_T} C_T / \tau_T$ molecules of the trace gas per unit time. During the same time N_S molecules of stratospheric air are returned to the troposphere, which bring $N_S \xi_U / \tau_T = C_U / \tau_T$ molecules of the trace gas per unit time. Equation (8.37) follows by dividing C_T by N_T to obtain ξ_T and C_U by N_S to obtain ξ_U . Eqn. (8.38) follows similarly, from eqn. (8.40).

Let us return to eqns. (8.37) and (8.38). These equations can be solved explicitly for all times. It is much easier to consider their solutions in the asymptotic time limit when ξ_T / ξ_U is almost constant with time. In that case the tropospheric equation becomes:

$$\frac{d}{dt} \xi_T = S - \eta \xi_T - \eta_T \frac{N_S}{N_T} (1 - \zeta) \xi_T \quad (8.42)$$

where $\zeta = \xi_u/\xi_T = \text{constant}$. ξ_T will be

$$\xi_T = ae^{bt} \left[b + \eta + \eta_T \frac{N_S}{N_T} (1 - \zeta) \right]^{-1} \quad (8.43)$$

ζ depends on η_T and $\bar{\eta}$ and is $[1 + (b + \bar{\eta}) \tau_T]^{-1}$, where it has been assumed that the source is rising exponentially as ae^{bt} .

If a simple tropospheric box theory has been used, the equation would have been $(d/dt) \xi_T = S - \eta_{*T} \xi_T$ with the (asymptotic) solution

$$\xi_T = \frac{ae^{bt}}{b + \eta_{*T}} \quad (8.44)$$

so that the sink strength found by using only the tropospheric box would be approximately given by:

$$\eta_{*T} = \eta + \eta_T \frac{N_S}{N_T} (1 - \zeta) \quad (8.45)$$

The lifetime found by considering only the troposphere would be τ_{*T} which is a combination of the tropospheric lifetime, τ , and the stratospheric term given by $\eta_T (N_S/N_T) (1 - \zeta)$. The true global lifetime is neither τ nor τ_{*T} , but $\tilde{\tau} = 1/\tilde{\eta}$:

$$\tilde{\eta} = \frac{C_T}{C} \eta + \frac{C_u}{C} \bar{\eta} \quad (8.46)$$

where $C = C_T + C_n$ = total number of molecules of the trace gas in the entire atmosphere. There are some special cases in which η_{*T} and $\tilde{\eta}$ are equal, i.e., when the lifetime determined by considering only the troposphere is the same as the true global lifetime. If $\bar{\eta} \rightarrow \infty$, implying very rapid destruction in the stratosphere so that none of the molecules of the trace gas that enter the stratosphere ever return, then it is easy to check that $\frac{C_u \bar{\eta}}{C} \rightarrow \eta_T N_s / N_T$; $(C_T \rightarrow C) \zeta \rightarrow 0$ so that $\eta_{*T} \rightarrow \tilde{\eta}$ according to eqns. (8.45) and (8.46).

In real situations

$$\tau \geq \tilde{\tau} \geq \tau_{*T} \quad (8.47)$$

(recall that $\eta = 1/\tau$, $\tilde{\eta} = 1/\tilde{\tau}$ and $\eta_{*T} = 1/\tau_{*T}$). Eqn. (8.47) is based on the assumption that $\bar{\eta} \geq \eta$ or that $\tilde{\tau}$ (stratospheric lifetime) is $\leq \tau$ (tropospheric lifetime). In case $\bar{\eta} \leq \eta$, then $\tilde{\tau} \geq \tau$

Similar conclusions can be drawn from eqn. (8.34) - (8.46). First by comparing eqn. (8.36) to ζ one can deduce the value of α , in terms of the mean (effective) stratospheric-tropospheric transport time τ_T and the stratospheric lifetime $\bar{\tau}$. The result is:

$$\alpha = \frac{1}{h_u} (b + \bar{\eta}) \tau_T \quad (8.48)$$

Alternatively, the τ_T in this expression can be determined from the knowledge of α , b and $\bar{\eta}$. This is the effective stratospheric-tropospheric transport time. If most of the stratospheric air, which is ex-

changed yearly with the troposphere, comes from the lower stratosphere, then this air will bring back a lot of molecules of the trace gas. τ_T should be adjusted to simulate this situation.

By using eqn. (8.36), one can also determine the effect of ignoring the stratospheric sink in global budget methods: Let us rewrite (8.36) as $\langle \xi \rangle = \langle \xi \rangle_T (N_T/N_\infty) \epsilon$: The tropospheric budget is formulated by solving

$$(d/dt) \langle \xi \rangle_T = S/N_T - \eta_{*T} \langle \xi \rangle_T$$

If $S = ae^{bt}$, then

$$\langle \xi \rangle_T = \frac{ae^{bt}/N_T}{b + \eta_{*T}} \quad (8.49)$$

after a long time of release at the exponential rate. When the entire global budget is considered, the following equation is valid:

$$(d/dt) \langle \xi \rangle = S/N_\infty - \tilde{\eta} \langle \xi \rangle$$

with the analogous solution

$$\langle \xi \rangle = \frac{ae^{bt}/N_\infty}{b + \tilde{\eta}} \quad \text{or} \quad \frac{ae^{bt}/N_\infty}{b + \tilde{\eta}} = \langle \xi \rangle_T \frac{N_T}{N_\infty} \epsilon$$

$$\langle \xi \rangle_T = \frac{ae^{bt}/N_T \epsilon}{b + \tilde{\eta}} \quad (8.50)$$

Comparing eqns. (8.49) and (8.50) yields

$$\tilde{\eta} = \frac{\eta_{*T}}{\epsilon} + b \left[\frac{1 - \epsilon}{\epsilon} \right] \quad (8.51)$$

Equations (8.49) and (8.50) imply that $\epsilon(b + \tilde{\eta}) = (b + \eta_{*T})$. Since $\epsilon \geq 1$, $b + \tilde{\eta} \leq b + \eta_{*T}$, or $\tilde{\eta} \leq \eta_{*T}$ so that $\tau \geq \tau_{*T}$. In either case it turns out that the true global lifetime is bigger than the lifetime determined by considering just the troposphere. $\epsilon \rightarrow 1$ when $\tilde{\eta} \rightarrow \infty$ and only then does $\tilde{\eta} \rightarrow \eta_{*T}$.

It is true that much of the discussion above has been based on averages over very large spatial domains, but it is obvious that similar results would also hold for models with many boxes.

The results of these calculations show that for long-lived species whose mixing ratio is constant with height in the troposphere, the stratospheric burden may have a significant effect on the lifetimes obtained by budget methods. The magnitude of the effect depends on the ratio N_s/N_∞ where N_s and N_∞ are the numbers of molecules in the stratosphere and the whole atmosphere. The magnitude of the effect also depends on the lifetime of the compound in the stratosphere. The shorter the stratospheric lifetime, the bigger the effect on the total lifetime and the discrepancy between the true tropospheric sink strength and that estimated by neglecting the stratospheric burden altogether. Thus, for a proper budget calculation, it is not only necessary to know the

burden in the troposphere, but one also needs to know the burden in the stratosphere.

For particular applications, such as those of CH_3CCl_3 in determining the average atmospheric HO concentrations it seems that the HO concentration must be even lower, because the loss of molecules of CH_3CCl_3 in the stratosphere is dominated by a different mechanism, namely solar ultraviolet fluxes, for which CH_3CCl_3 has a large interaction cross-section.

It is of interest to calculate N_s and N_T as accurately as possible for the estimation of the magnitude of the stratospheric sink. It may also be necessary to incorporate the latitudinal variation of the tropopause height in numerical calculations.

(e) Numbers of Molecules of Air in the Stratosphere and Troposphere

It is of considerable importance to have good estimates of the number of molecules of air in the troposphere and the stratosphere, as well as in smaller cells of the atmosphere. These quantities are necessary ingredients in the theoretical formulations of theories with global or hemispherical averages. For continuous transport and chemical theories the same problem persists in terms of $\rho(r, \phi, \lambda, t)$ which enters the partial differential equations. Specifically, for theories which employ global or smaller scale averages, the estimates of the global (or smaller scale) burdens, deduced from atmospheric measure-

ments, depend on these numbers. In addition to uncertainties in the measured mixing ratios, the uncertainties in the number of molecules in the troposphere and the stratosphere can introduce significant errors in the calculation of lifetimes. The longer-lived the species is, and the faster the sources have been increasing, the more important these numbers become to the calculations of lifetimes.

In principle, the problem is almost trivial. If N_S and N_T are the numbers of molecules of air in the stratosphere and the troposphere, then:

$$N_T = \int_{V_T} \rho dV \quad (8.52)$$

$$N_S = \int_{V_S} \rho dV \quad (8.53)$$

$$N_\infty = \int_{V_\infty} \rho dV \quad (8.54)$$

$$\tilde{N}_\infty = N_S + N_T \quad ; \quad dV = r^2 dr d\lambda \cos\phi d\phi \quad (8.55)$$

The ranges of integration over V_T , V_S and V are as follows: $0 \leq \lambda \leq 2\pi$, $-\pi/2 \leq \phi \leq \pi/2$ in all cases but the limits of integration for r (height) vary. For V_T , $R + \bar{z}_0(\phi) \leq r \leq R + z_T(\phi)$, for V_S , $R + z_T(\phi) \leq r \leq R + z_S(\phi)$, and for V_∞ , $R + z_0(\phi) \leq r \leq \infty$, $R + z_0(\phi) \approx R$. In these equations $\rho = \rho(\lambda, \phi, r)$ is the appropriately time averaged den-

sity of air molecules at λ , ϕ and r . Because of the atmospheric temperature structure, the earth's rotation, and the gravitational field, ρ changes in a complex manner, particularly with r . In these equations $z_T(\phi)$ is the tropopause height at latitude ϕ . $z_T(\phi)$ is also a function of time of year. R is the mean radius of the earth. $z_o(\phi)$ describes the height of the land above sea level. Since the pressure above the earth's surface declines rapidly with height due to the gravitational field of the earth, the height $z_o(\phi)$ is important only in evaluating the mean global surface level pressure \bar{p}_E . $z_o(\phi)$ makes no significant contribution in the integrals when it comes with R . The inexact knowledge of ρ , $\bar{z}_o(\phi)$, and $z_T(\phi)$ are the main obstacles to evaluating N_T , N_S and N_∞ .

In the present analysis $z_T(\phi)$ will be assumed to be described by the following function (Reiter, 1975):

$$z_T(\phi) = \begin{cases} h_o & |\phi| \leq \pi/6 \\ h_1 - \alpha\phi & \pi/6 < |\phi| \leq \pi/2 \end{cases} \quad (8.56)$$

$h_o = 16$ km, $h_1 = 14$ km, $\alpha = 3.82$ km/per degree radian. $z_S(\phi)$ is assumed to be constant at 50 km (Reiter, 1975). $z_o(\phi)$ is assumed to be represented by a mean effective elevation of 0.236 km = \bar{z}_o (Verniani, 1966).

Verniani (1966) has carried out a very careful study of the problem of determining N_∞ , where the height integration goes up to 100 km above R . Verniani's procedure and results will be adopted in this section to calculate N_s and N_T . There are several methods available for these calculations and a variety of atmospheric data can be used. Some of the alternate methods may be more exact, but it is expected that the numbers obtained here will be adequate for most applications to the budgets of long-lived trace gases.

In Verniani's method, eqn. (8.54) is expressed as:

$$\int_{m_a} g \, dm_a = \int_s p_E \, dS \quad (8.57)$$

$$m_{(\alpha)} = \sum_{i=1}^N (\bar{p}_i S_i - \bar{p}_{i+1} S_{i+1}) \frac{1}{\bar{g}_i} \quad (8.58)$$

In equations (8.58) and (8.59) the symbols are defined as follows: \bar{p}_i is the mean pressure at height h_i ($h_1 = h$), S_i is the surface area of a sphere with radius $R + h_i$ and \bar{g}_i is the average gravitational field strength in the shell between spheres with radii $h_i + R$ and $R + h_{i+1}$. In eqn. (8.59) only two surfaces are used; where $h = h_1$ and $h + \delta h = h_N$, and $\bar{g}_{(\alpha)}$ is the average gravitational field between h and $h + \delta h$. $m_{(\alpha)}$ is the mass of the atmosphere between heights h and $h + \delta h$ above the earth. Eqn. (8.59) differs negligibly from (8.58) because g does

not change much within the heights considered here, i.e., up to the stratopause (z_s).

The gravitational field strength varies with latitude and height.

$$g_0(\phi) = a(1 + b \sin^2\phi - c \sin^2 2\phi)$$

$$\bar{g}_0 = \int_0^{\pi/2} g_0(\phi) \cos\phi \, d\phi$$

$$\bar{g}(z) = \bar{g}_0 \frac{R^2}{(R+z)^2} - 2\omega^2 z \left(1 - \frac{z}{R}\right)$$

$$\bar{g}(\alpha) = \frac{\int_{m(\alpha)} \bar{g}(z) \rho \, dV}{\int_{m(\alpha)} \rho \, dV}$$

In these eqns. $g_0(\phi)$ is the surface level gravitational field at latitude ϕ (b and c are small). \bar{g}_0 is ground level, latitudinally averaged gravitational field strength and $\bar{g}(z)$ is the latitudinally averaged field strength as a function of height. ω is the angular velocity of the earth.

The main results of Verniani that are used here are his estimates of \bar{p}_E , \bar{g}_0 and eqn. (8.59). Taking into account the average elevation of the land, Verniani estimates \bar{p}_E to be 984.0 mb. \bar{g}_0 is derived to be 979.76 cm/sec².

One fast and easy way to calculate N_∞ is to assume that there is only one shell between radii $R + z_0$ to $R + 100$ km, and that $\bar{p}_{100} S_{100} \ll \bar{p}_E S_E$, $\bar{g}(z) \approx \bar{g}$, so that

$$m_{\infty} \approx \bar{p}_E S_E / \bar{g}_0; N_{\infty} = \frac{\bar{p}_E S_E}{g_0 \bar{\mu}} N_0 \quad (8.60)$$

where $\bar{\mu}$ is the mean molecular weight of the molecules that make up the air and N_0 is Avagadro's number. Eqn. (8.60) gives $m_{\infty} = 5.123 \times 10^{21}$ gm and $N_{\infty} = 1.065 \times 10^{44}$ molecules of air. Eqn. (8.60) is the most common way in which m_{∞} and N_{∞} are usually calculated (see for example Walker, 1977). The differences arise from the assumptions of \bar{p}_E and to a lesser extent $\bar{g}_{(\alpha)}$. Verniani's final numbers are $m_{\infty} = 5.136 \times 10^{21}$ gm and $N_{\infty} = 1.068 \times 10^{44}$ molecules. In applications these numbers may also have to be corrected for the water vapour content of the atmosphere.

To calculate N_S and N_T the following procedure is adopted: The atmosphere is divided into three shells: the first covering $R + \bar{z}_0$ to height $R + \bar{z}_0 + H_1$; the second covering heights $R + \bar{z}_0 + H_1$ to $R + \bar{z}_0 + H_2$; and the third covering heights from $R + \bar{z}_0 + H_2$ to $R + \bar{z}_0 + H_3$. H_1 is taken to be 8 km, H_2 is 16 km, and H_3 is 50 km. All the mass in the first shell belongs to the troposphere. Most of the mass in the second shell is also tropospheric, and all the mass of the third shell lies in the stratosphere. The distribution of the mass in the second shell between the troposphere and the stratosphere is calculated below:

$$f_{(2)} = \frac{\int_{-\pi/2}^{\pi/2} \int_{R+H_1}^{R+z_T(\phi)} \rho(r) r^2 dr \cos\phi d\phi}{\int_{-\pi/2}^{\pi/2} \int_{R+H_1}^{R+H_2} \rho(r) r^2 dr \cos\phi d\phi} \quad (8.61)$$

$f_{(2)}$ is the fraction of molecules in the second shell that belongs in the troposphere. It is easy to show that approximately $f_{(2)}$ is given by:

$$f_{(2)} = \left\{ 1 - \frac{1}{2} \exp \left[- \frac{(h_0 - H_1)}{H} \right] - \exp \left[- \frac{(h_1 - H_1)}{H} \right] \left[\frac{H^2}{H^2 + \alpha^2} \right] \right. \\ \left. \left[\exp \frac{\pi\alpha}{2H} - \left(\frac{1}{2} + \frac{\sqrt{3}\alpha}{2H} \right) \exp \frac{\pi\alpha}{6H} \right] \right\} \left\{ 1 - \left[\exp - \frac{(H_2 - H_1)}{H} \right] \right\}^{-1} \quad (8.62)$$

With these approximations the masses of the troposphere and the stratosphere are:

$$m_T = \frac{1}{\bar{g}_{(1)}} (\bar{p}_E S_E - \bar{p}_{H_1} S_{H_1}) + \frac{f_{(2)}}{\bar{g}_{(2)}} (\bar{p}_{H_1} S_{H_1} - \bar{p}_{H_2} S_{H_2}) \quad (8.63)$$

$$m_s = \frac{1}{\bar{g}_{(3)}} (\bar{p}_E S_E - \bar{p}_H S_H) - m_T \quad (8.64)$$

$$N \begin{pmatrix} s \\ T \end{pmatrix} = \frac{m \begin{pmatrix} s \\ T \end{pmatrix} N_0}{\bar{\mu}} \quad (8.65)$$

In eqn. (8.62), H is the average scale height in the region from $r = R + \bar{z}_0 + H_1$ to $r = R + \bar{z}_0 + H_1$. The results of the numerical calculations are summarized in Table (8.2) below. Additional information on the data used is given in Appendix I. These numbers are based on the model atmosphere given by Houghton (1977). The pressures at each height (H_1 , H_2 or H_3) are first averaged over the seasons of the year, then weighted as:

$$\bar{p}_i = \int_0^{\pi/2} \langle p_i \rangle \cos\phi \, d\phi \quad (8.66)$$

where $\langle p_i \rangle$ is the time average over the year, of pressure at height H_i ($i = 1, 2, 3$). It is assumed that the two hemispheres are symmetric. If the U. S. Standard Atmosphere (1962) is used, the results may be slightly different (see, for example, Neiburger et al., 1973). In these calculations $\bar{g}_{(i)}$ is taken to be \bar{g}_0 and partially compensated by taking \bar{p}_i at the geopotential heights. The value of $\bar{g}_{(i)}$ is not very different from \bar{g} within the region of the atmosphere: $0 < z < H_3$ (see also Verniani, 1966). It is possible to do more exact calculations, avoiding some of the simplifications made here.

Table (8.2): Mass and the Number of Molecules
of Air in Various Compartments of the Atmosphere

Mass: ($\times 10^{-21}$ g)

M_T	M_s	M_{nT}	M_{ns}	M_{nTa}	M_{nTb}	M_{nsa}	M_{nsb}	\tilde{M}_∞
4.180	0.939	2.090	0.470	1.141	0.949	0.139	0.331	5.119

Number of Molecules ($\times 10^{-43}$)

N_T	N_s	N_{nT}	N_{ns}	N_{nTa}	N_{nTb}	N_{nsa}	N_{nsb}	\tilde{N}_∞
8.690	1.951	4.345	0.976	2.372	1.973	0.288	0.688	10.641

In Table (8.2) the subscript $_{nTa}$ refers to the region of the troposphere between the latitudes 0° and 30° , and $_{nTb}$ refers to the region between 30° and 90° . N_{nsa} is the number of molecules of air in the stratosphere between 0° and 30° (north or south) and N_{nsb} the number in the stratosphere between 30° and 90° (latitude). It is assumed that the southern hemisphere is symmetric with respect to the northern hemisphere, so that $N_{nT} = N_{sT}$, $N_{ns} = N_{ss}$, $N_{nTa} = N_{sTa}$, $N_{nTb} = N_{sTb}$, $N_{nsa} = N_{ssa}$, $N_{nsb} = N_{ssb}$, where the first subscript stands for northern (n) or southern (s) hemisphere, the second subscript stands for the troposphere (T) or the stratosphere (s), and when there is a third subscript, it represents the regions from $0-30^\circ$ (a) and $30^\circ-90^\circ$ (b). Between H_1 and H_2 a mean density scale height of 8 km was used in the ratio $f(2)$ (eqn. 8.61). The average densities computed at H_1 and H_2 from the

model atmosphere, and the direct calculation of the number of molecules

in the shell between $R' + H_1$ and $R' + H_2$, by $2\pi \int_{R'_1+H_1}^{R'+H_2} \int_{-\pi/2}^{\pi/2} \rho(r)r^2 dr$

$\cos\phi d\phi$ are both consistent with this scale height ($R' = R + \bar{z}_0 \approx R$).

The relatively large value of $N_s/N_T \approx 0.22$ can make a considerable contribution to the global average lifetime.

(f) Summary and Conclusions

This chapter deals with the methods of taking into account all the regions of the atmosphere where trace gases abound. The main ideas are illustrated by simplified theoretical models which show the magnitude of the effects of trace gases in various parts of the atmosphere.

It was shown that a couple of high latitude tropospheric measurements of a trace gas can be used to obtain approximate hemispherical average mixing ratios or burdens, and are particularly suited to global averages. These facts are a consequence of the latitudinal and vertical structure of the earth's atmosphere. As an example, measurements of CH_3CCl_3 with complete global coverage were used to compute the hemispherical and globally averaged mixing ratios of this trace gas. Next all the latitudinal data were discarded, except those for a few degrees around 45°N and 90°S . Using the equations developed

here, the hemispherical and global averages of CH_3CCl_3 were calculated using this much reduced data set and found to be indistinguishably close to the results obtained from the full data set. Thus, reasonably accurate assessments of the atmospheric properties and global distribution of relatively long-lived trace gases can be made using measurements at only a couple of remote high latitude regions of the earth. This should not be construed to mean that detailed global measurements coverage is not important. It is usually very difficult to obtain accurate global data covering all latitudes over a relatively short time. It is also difficult to build up a data base with compatible measurements year after year. With current capabilities it is more realistic to conduct careful measurements at fixed points on the earth, and these can provide accurate information about the trace gases under study, when used in conjunction with any type of theoretical model. Detailed latitudinal measurements have many unique applications, which can add significantly to our understanding of atmospheric transport and chemistry.

The contribution of the stratosphere to the budgets and lifetimes of trace gases was considered in section (8.d). The lifetimes determined without including the stratosphere are not representative of physical total or tropospheric lifetimes even if the molecules are not destroyed in the stratosphere. The effect of the stratosphere on the global lifetime calculations depends on the ratio N_S/N_T -- the ratio

of molecules of air in the stratosphere and the troposphere. This ratio was calculated using the model atmosphere given by Houghton (1977) and found to be about 0.22. The approximate numbers of molecules of air in various compartments of the atmosphere were also calculated.

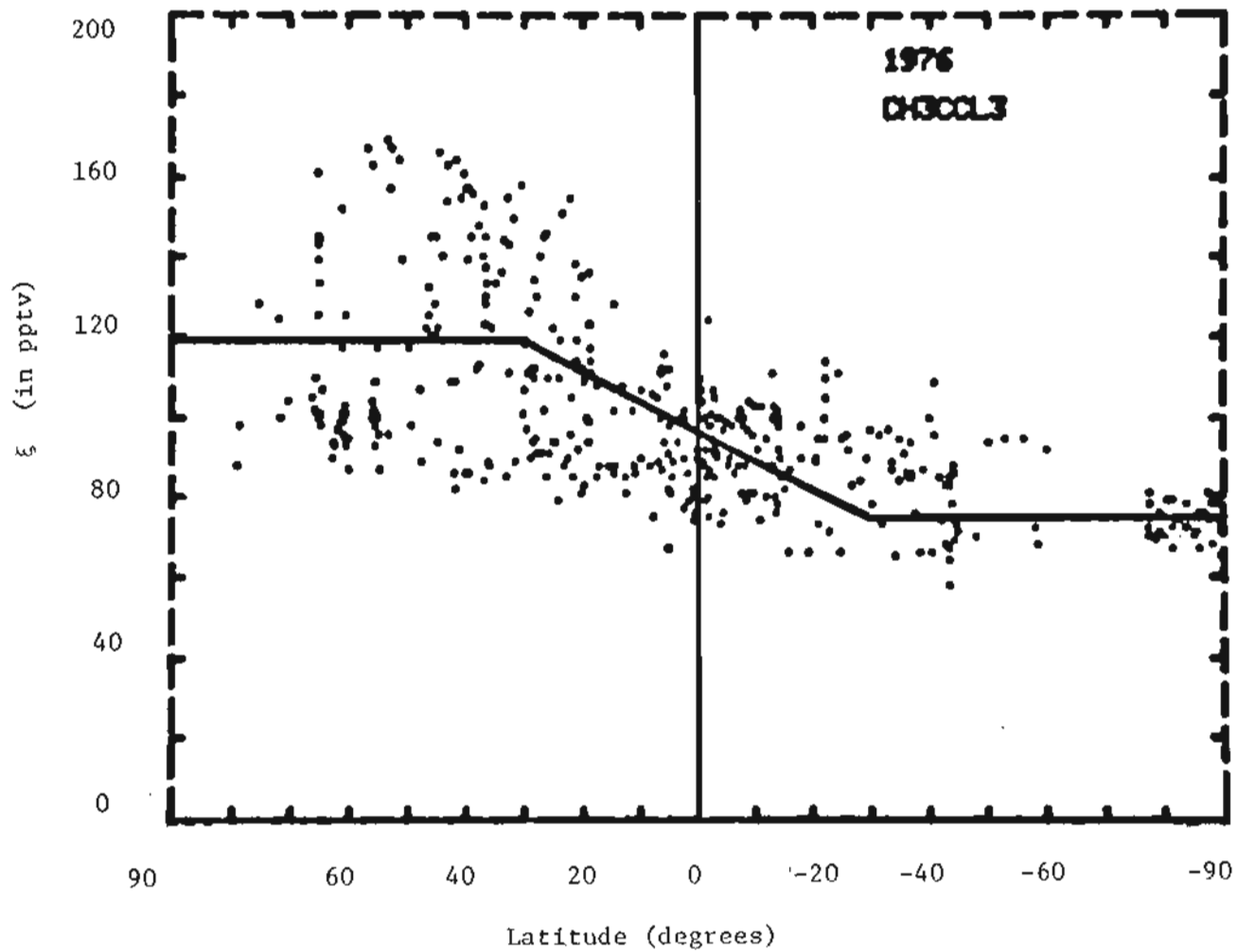


Figure (8.1): Simplified model for the latitudinal distribution of trace gases. (Points represent CH_3CCl_3 measurements)

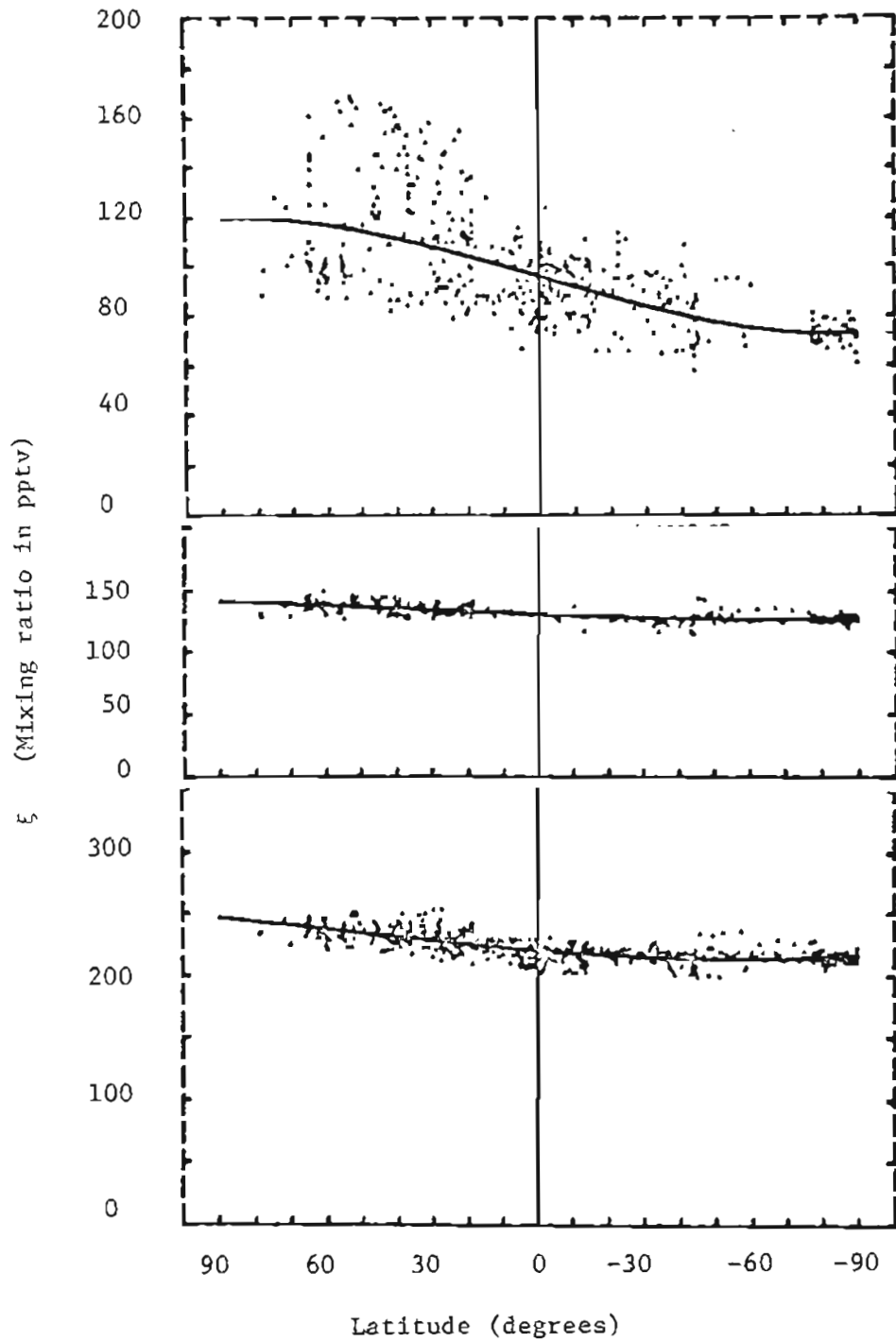


Figure (8.2): Global measurements of CH_3CCl_3 , F-11 and F-12 for 1976

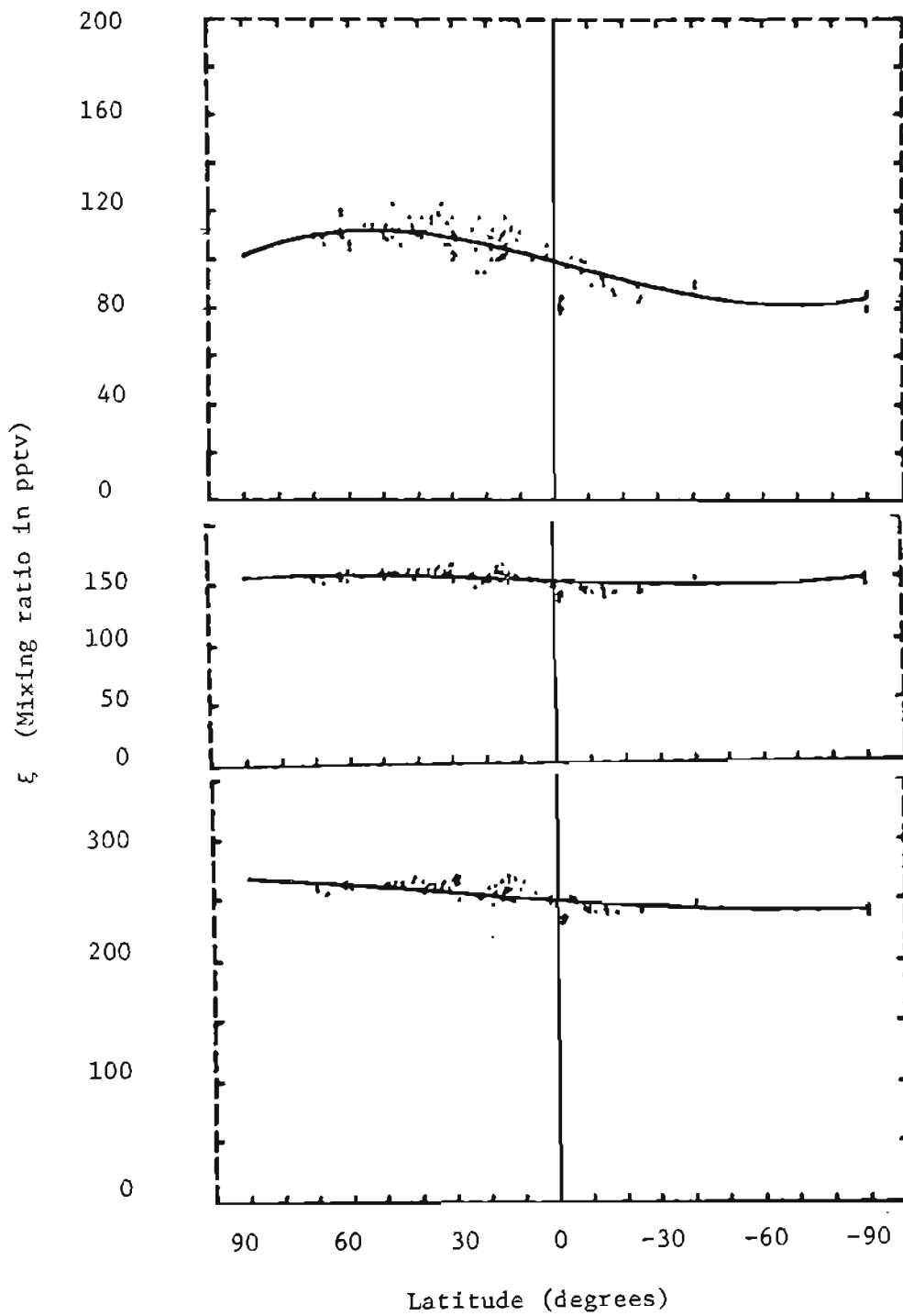


Figure (8.3): Global measurements of CH_3CCl_3 , F-11 and F-12 for 1977

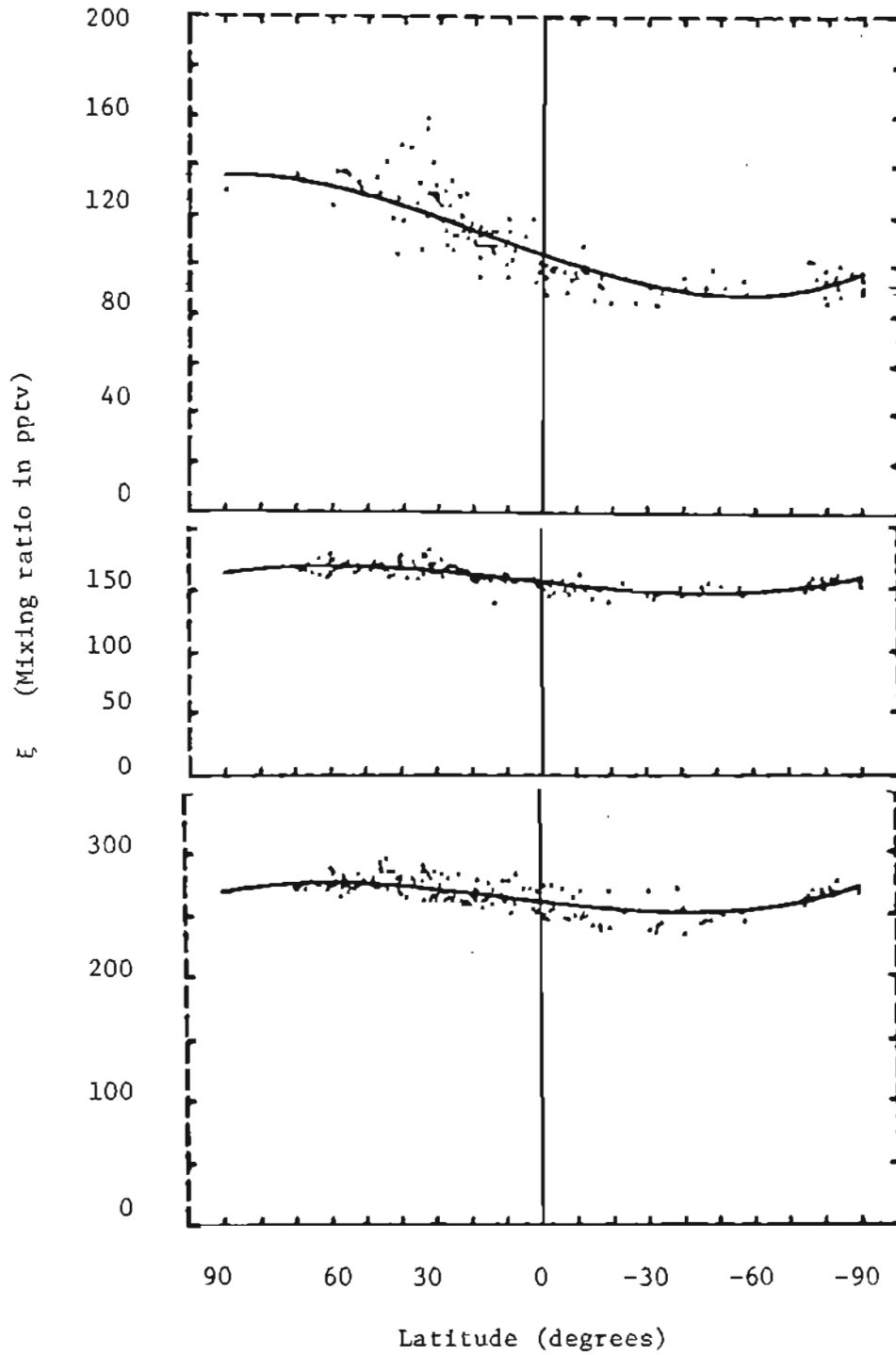


Figure (8.4): Global measurements of CH_3CCl_3 , F-11 and F-12 for 1978

CHAPTER 9. SOURCE FUNCTIONS: SMOOTHING AND SPECTRAL ANALYSIS

(a) General Ideas

The source strength of most anthropogenic trace gases is specified by a time series of numbers giving the total estimated release within each year. For trace gases that have natural sources, estimates of release are made in an analogous manner. The species conservation equation, in principle, treats the concentration and the source functions as continuous functions of time, though many types of spatial averages are often used. It is, therefore, necessary to transform the discrete yearly emissions data into a continuous function. There are several ways of accomplishing this, but systematic errors may be introduced by the method chosen. Suppose that $f(t)$ is the true continuous source function describing the emissions (in mass per unit time). Though $f(t)$ is unknown, it can be approximated from the knowledge of the yearly emissions data $\tilde{S}(t)$, where $\tilde{S}(t)$ is given by:

$$\tilde{S}(t) = \int_t^{t+1} f(t') dt' \quad (9.1)$$

Often $\tilde{S}(t)$ is approximated by an exponential as in the case of CH_3CCl_3 , F-11, F-12 and F-22. In other words, the discrete data $\tilde{S}(t_i)$ (emissions over the entire year t_i) is fitted (by least squares methods) to a function ae^{bt} . $f(t)$ is not equal to ae^{bt} but can be approximated

by $f(t) \approx S(t) = a'e^{bt}$. The transformation $a \rightarrow a'$ reflects the smoothing transformation where the absolute rate (dS/dt) of the increasing source is smaller at the beginning of each year than at the end (even though actual emissions data $\tilde{S}(t)$ does not resolve the emissions behaviour within the span of a year). In general, the transformation of any function on which $S(t')$ lies, to an approximate version of $f(t)$, defines the method by which time is treated in the species conservation equation.

When the lifetime of the trace gas τ is $\gg 1$ yr, the exact behaviour of $f(t)$ within a year does not have much effect on the lifetimes calculated by using the mass conservation equation. It is, however, important that the total emissions between times 0 and T satisfy

$$\int_0^T S(t') dt' \approx \sum_{i=1}^N \tilde{S}(t_i) \quad (9.2)$$

where $t_1 = 0$, $t_N = T$, and $S(t')$ is the approximated version of $f(t')$.

The purposes of this chapter are (1) to formulate one method for obtaining $S(t)$ from discrete emissions data $\tilde{S}(t)$. This method draws particular attention to the constraint (9.2) on small and large time scales. (2) As found in Chapters 4 and 5, a source function $S(t)$ may have complicated "spectral" properties (non-exponential sources). These are discussed here in more detail, including methods of solving

the mass conservation equation when cyclic terms are present, and obtaining smoothed versions from $\tilde{S}(t)$ for these more complicated source functions.

(b) Smoothing of Source Functions Described by Simple Exponentials

The main idea is very simple. The true source function $f(t)$ is approximated by a smooth source function which has the same shape as the function on which $\tilde{S}(t)$ lies. In the case when $\tilde{S}(t)$ lies on a simple exponential function, it is simply assumed that $f(t) \simeq a'e^{b't}$

$$\tilde{S}(t) = \int_t^{t+\delta} a'e^{b't} dt = ae^{bt} \quad (9.3)$$

or $\frac{a'}{b'} (e^{b'\delta} - 1) e^{b't} = ae^{bt} \quad (9.4)$

Thus $b \longrightarrow b' = b \quad (9.5a)$

$$a \longrightarrow a' = \frac{ba}{(e^{b\delta} - 1)} \quad (9.5b)$$

where (9.5a) and (9.5b) are to be considered as transformations of "a" and "b" necessary to convert the discrete $\tilde{S}(t)$ to a smoothed $S(t)$ for use in the mass conservation equations. Therefore

$$f(t) \simeq \frac{ab}{(e^{b\delta} - 1)} e^{bt} = S(t) \quad (9.6)$$

a and b are the same as those necessary to find the exponential function on which the discrete $\tilde{S}(t)$ lies. If time is assumed to be given in years, δ is the time in years over which the discrete source emissions are reported. Thus, $\delta = 1$ is applicable to all emissions data which are reported in terms of yearly emissions.

The simpler, often used method (for $\delta = 1$) is to take the function on which $\tilde{S}(t_i)$ lie, let's call it $\tilde{S}(t)$, and approximate $f(t)$ by:

$$f(t) \quad \tilde{S}(t) = S(t - \frac{1}{2}) \quad (9.7)$$

so that if $\tilde{S}(t) = ae^{bt}$; $S(t) = ae^{-\frac{1}{2}b} e^{bt}$ which is the same as transforming $a \rightarrow a'$ where

$$a' = ae^{-b/2} \quad (9.8)$$

In this method the annual rate of emissions implied by $\tilde{S}(t_i)$ is adjusted to hold at the middle of the year. This general idea can be further refined if desired.

Equations (9.8) and (9.6) are approximately equal if b is small ($a' = a/1 + \frac{1}{2}b$). For more complicated source functions, the methods of eqn. (9.7) and (9.3) may yield different results.

The use of eqn. (9.3) can easily be extended to the time scale $\delta = T$ to impose the constraint (9.2).

It is always a good idea to check whether the constraint (9.2) is satisfied by whatever smooth function one has chosen for the source

($S(t)$). If not, a different source function must be chosen to avoid introducing unnecessary systematic biases in the results.

(c) Complex Source Functions

Let us suppose now that the source function has some steady form, but superimposed on this are cyclic fluctuations. To express a simple example of such behaviour, one may write the source function $\tilde{S}(t)$ as:

$$\tilde{S}(t) \sim S_o(t) [1 + \alpha \cos (\omega t + \phi)] \quad (9.9)$$

and $\tilde{S}_o(t) \sim S_o(t) = ae^{bt}$

where the symbol \sim is used to indicate that the discrete source data lie on the function on the right hand side of \sim .

$$\tilde{\Delta} = \frac{\tilde{S}(t) - \tilde{S}_o(t)}{\tilde{S}_o(t)} \sim \alpha \cos (\omega t + \phi) \quad (9.10)$$

$\tilde{\Delta}$ shows that the deviation of the "true" source function, from a simple steady source function $\tilde{S}_o(t)$, is a cyclic function given by $\alpha \cos (\omega t + \phi)$.

Examples of such behaviour were considered for the case of CH_3CCl_3 in Chapters 4 and 5.

The discrete yearly release data $\tilde{S}(t)$ are used to find the parameters a , b , α , ω , and ϕ , and determine the function $ae^{bt}[1 + \alpha \cos (\omega t + \phi)]$ on which $\tilde{S}(t)$ lies. How should a , b , α , ω , and ϕ be transformed to get the correct source function $S(t)$ such that

$$\int_t^{t+\delta} a' e^{bt} [1 + \alpha' \cos(\omega t + \phi')] dt$$

$$= a e^{bt} [1 + \alpha \cos(\omega t + \phi)] \quad ? \quad (9.11)$$

Note that ω is not altered. Eqn. (9.11) can be divided into two pieces so that the solution of the previous section applies to the first piece

so

$$a' = \frac{ab}{(e^{b\delta} - 1)} \quad \text{and} \quad b' = b$$

This leaves:

$$\int_t^{t+\delta} a' e^{bt} \alpha' \cos(\omega t + \phi') dt$$

$$= a e^{bt} \alpha \cos(\omega t + \phi) \quad (9.12)$$

After some tedious algebra (sketched in Appendix I), one finds that

$$\alpha' = \frac{(b^2 + \omega^2)(e^{b\delta} - 1)}{b\omega [A^2 + B^2]^{1/2}} \alpha \quad (9.13)$$

$$\phi' = \text{Tan}^{-1} \left\{ \frac{A \cos \phi + B \sin \phi}{B \cos \phi - A \sin \phi} \right\} \quad (9.14)$$

$$A = e^{b\delta} \cos \omega\delta - \frac{b}{\omega} \sin \omega\delta - 1$$

$$B = e^{b\delta} \sin \omega\delta + \frac{b}{\omega} \cos \omega\delta - \frac{b}{\omega} \quad (9.15)$$

The transformation of $\phi \longrightarrow \phi'$ can be substantial. The ambiguity in the angle in eqn. (9.15) is resolved by considering the signs of the numerator and the denominator of the term inside the parentheses { } since they are proportional to the $\sin \phi'$ and $\cos \phi'$ respectively. Alternatively ϕ' is determined as the angle which satisfies:

$$\sin \phi' = \frac{1}{\sqrt{A^2 + B^2}} (A \cos \phi + B \sin \phi)$$

$$\cos \phi' = \frac{1}{\sqrt{A^2 + B^2}} (B \cos \phi - A \sin \phi)$$

Again one may use $a \rightarrow a'$, as in Eqn. (9.8), and so $\phi \rightarrow \phi' = \phi - \omega/2$. This corresponds to (9.7), and here α is not modified. The results of this section are different from those based on (9.7), however, in the calculations of the particular case of CH_3CCl_3 (Chapters 4 and 5), the results were not significantly altered by using (9.7).

(d) Complex Source Functions: Fourier Analysis

The true source function can have more complex behaviour than discussed in section (9.c) as, for example, in the case of CO (Rust et al., 1979). Most cyclic features of the source term can be described by a Fourier spectrum, thus Δ defined by eqn. (9.10) can be generalized to:

$$\Delta = c + \sum_{n=0}^{\infty} \alpha_n \cos (\omega_n + \phi_n)$$

The c term can be absorbed into the S_0 term and rewriting Δ as $[1 + c]^{-1} \sum_n \alpha_n \cos(\omega_n t + \phi_n)$, so it will not be treated further. In case the $S_0(t)$ is as before, i.e., $ae^{bt} = \tilde{S}_0(t)$, then

$$\tilde{S}(t) \sim \tilde{S}_0(t) \left[1 + \sum_{n=0}^{\infty} \alpha_n \cos(\omega_n t + \phi_n) \right]$$

The generalization of eqns (9.13) and (9.14) can be expressed as:

$$\alpha_n \longrightarrow \alpha'_n = \frac{(b^2 + \omega_n^2)(e^{b\delta} - 1)}{b\omega_n [A_n^2 + B_n^2]^{1/2}} \quad (9.16)$$

$$\phi_n \longrightarrow \phi'_n \text{ where } \phi'_n \text{ satisfies:} \quad (9.17)$$

$$\sin \phi'_n = \frac{1}{\sqrt{A_n^2 + B_n^2}} (A_n \cos \phi_n + B_n \sin \phi_n)$$

$$\cos \phi'_n = \frac{1}{\sqrt{A_n^2 + B_n^2}} (B_n \cos \phi_n - A_n \sin \phi_n)$$

$$A_n = e^{b\delta} \cos \omega_n \delta - \frac{b}{\omega_n} \sin \omega_n \delta - 1$$

$$B_n = e^{b\delta} \sin \omega_n \delta + \frac{b}{\omega_n} \cos \omega_n \delta - \frac{b}{\omega_n}$$

so that

$$S(t) = a'e^{bt} \left[1 + \sum_n \alpha'_n \cos(\omega_n t + \phi'_n) \right] \quad (9.18)$$

One of the good features of such source functions is that they allow exact solutions of the species conservation equation averaged over any

spatial scale. For the global conservation equations, $d\xi/dt = S(t) - \eta\xi$, with the source given by eqn. (9.18), the solution can be derived as follows:

The primes on a' , α'_n and ϕ'_n are dropped for notational convenience.

Eqn. (9.2) becomes:

$$\begin{aligned} \xi(t) &= \xi_0 e^{-\eta t} + e^{-\eta t} \int_0^t a e^{bt'} [1 + \sum_n \alpha_n \cos(\omega_n t' + \phi_n)] e^{\eta t'} dt' \\ &= T_1 + T_2 \end{aligned} \quad (9.19)$$

The first term is simply the usual one:

$$\xi_0 e^{-\eta t} + \frac{a}{b + \eta} [e^{bt} - e^{-\eta t}] = T_1 \quad (9.20)$$

The second term is T_2

$$T_2 = e^{-\eta t} \int_0^t a e^{bt'} \sum_n \alpha_n \cos(\omega_n t' + \phi_n) e^{\eta t'} dt'$$

or

$$T_2 = e^{-\eta t} a \sum_n \alpha_n \operatorname{Re} \int_0^t e^{(b + \eta)t'} e^{i(\omega_n t' + \phi_n)} dt' \quad (9.21)$$

where $\operatorname{Re}[f(z)] =$ real part of the complex function $f(z) = f_0(z) + i f_1(z)$

$$T_2 = a \operatorname{Re} \sum_n \frac{\alpha_n e^{i\phi_n}}{(b + \eta) + i\omega_n} [e^{(b + i\omega_n)t} - e^{-\eta t}] \quad (9.22)$$

If
$$\operatorname{Re} \frac{\alpha_n e^{i\phi_n}}{(b+\eta) + i\omega_n} \ll \frac{a}{b+\eta} e^{(b+\eta)t} \quad (9.23)$$

then
$$T_2 \approx a \operatorname{Re} \sum_n \frac{\alpha_n e^{i\phi_n}}{(b+\eta) + i\omega_n} e^{bt} e^{i\omega_n t} \quad (9.24)$$

or
$$\begin{aligned} T_2 &\approx a e^{bt} \sum_n \frac{\alpha_n}{(b+\eta)^2 + \omega_n^2} \operatorname{Re} \left\{ [(b+\eta) + i\omega_n] e^{i(\omega_n t + \phi_n)} \right\} \\ &= a e^{bt} \sum_n \frac{\alpha_n \omega_n}{(b+\eta)^2 + \omega_n^2} [\sin(\omega_n t + \phi_n) \\ &\quad + \frac{b+\eta}{\omega_n} \cos(\omega_n t + \phi_n)] \end{aligned} \quad (9.25)$$

and

$$\xi(t) \approx T_1 \text{ (eqn. 9.20)} + T_2 \text{ (eqn. 9.25)} \quad (9.26)$$

For the special case there there is only one term (as discussed in Section 9.c)

$$\begin{aligned} \xi \approx \frac{a}{b+\eta} e^{bt} \left\{ 1 + \frac{\alpha \omega (b+\eta)}{(b+\eta)^2 + \omega^2} [\sin(\omega t + \phi) \right. \\ \left. + \frac{b+\eta}{\omega} \cos(\omega t + \phi)] \right\} \end{aligned} \quad (9.27)$$

Eqn. (9.27) was used in Chapters 4 and 5, and applied to CH_3CCl_3 .

For fluctuations that are very rapid so that $\omega_n \gg (b+\eta)$ in eqn. (9.26), then such components are damped out as long as α_n is not very large. So fluctuations with periods much less than the lifetime (actually period $T \ll 2\pi/(b+\eta)$) are not significant in modifying the global concentrations as long as their amplitudes are not excessive. This statement is independent of the practical limitations of finding cycles in the discrete data $\tilde{S}(t)$. In other words, if there were real cycles of high frequency ω , their effects would be very small as long as their am-

plitudes are not large (eqn. 9.26).

For the practical case of analyzing source data which are given only in terms of total emissions over a period δ , cycles with periods $T \leq \delta$ are not resolved. Therefore, the only frequencies that appear in yearly (or δ) emissions data are $\omega < 2\pi/\delta$ (or $\leq \sim 6/\text{yr}$).

Rapid cycles below the time resolution δ can still give apparent slow cycles (of much lower ω) in the yearly emissions data. The rapid cycles can, therefore, be a mechanism by which slow cycles appear in the discrete data $\tilde{S}(t)$. In such a case the amplitude of the fast cycles is large so as to produce slow cycles of non-vanishing magnitude. Figure (9.1) illustrates a hypothetical case ($b = 0$).

This is by no means the only mechanism, or even the most likely one, to produce the slow cycles in the yearly emissions data. The only point here is that if fast cycles of high amplitude exist for the sources of long-lived species, then they can be approximated by slower cycles of low amplitude. When slow cycles exist, their amplitude can be used to determine whether it is probable that they are created by faster cycles. If the slow cycles are have appreciable amplitudes, then it requires a very large amplitude for the fast cycles if they are to generate the slow cycles. The physical situation at hand has to be analyzed to decide if it is possible to have such large amplitude fast cycles.

When the lifetime of the trace gas in question is short, the behaviour of the true source function $f(t)$ can make a big difference in assessing the global budget, and yearly release estimates can become virtually useless.

Most of the preceding statements apply only to globally averaged concentrations, whereas in environments near the sources a variety of fluctuations are observed over periods of days to months. It is difficult to separate the effects of changing source terms from meteorologically controlled transport of air containing high concentrations of the trace gas in question.

Although only globally averaged mass conservation equation has been considered in detail here, the results are valid for smaller spatial averagings. The use of the globally averaged equation should only be taken as an example rather than as the domain of applicability of the results presented here. For example, the solutions for hemispherically averaged conservation equation follow easily from the discussion in Chapter 10.

(e) Conclusions

The main calculations in this chapter are designed to approximate the discrete yearly averaged source data by a continuous function that can be used in any form of the global species conservation equation.

The general idea, expressed by the equation $\int_t^{t+\delta} S(t') dt' = \tilde{S}(t)$, where $S(t')$ is the smoothed source function and $\tilde{S}(t)$ the discrete emissions data, was applied to several special cases. These cases cover a wide range of possible source functions. For most practical cases the time over which the source emissions are reported is a year, thus $\delta =$

1. Even if a source function is not covered by the cases studied, the same procedure can be applied to obtain $S(t)$ from the discrete values $\tilde{S}(t)$.

It was also shown that the smoothing transformations derived for a simple fluctuating source function is easily generalizable to the Fourier spectrum of the source function. Furthermore, the spatially averaged mass conservation equation can still be solved exactly regardless of the complicated nature of the source spectrum as long as one can write the source function in terms of a Fourier series. When the mass conservation equation is averaged over smaller spatial domains, the methods discussed here can be easily generalized to a system of differential equations (in place of (9.1)) by the techniques discussed in Chapter 10.

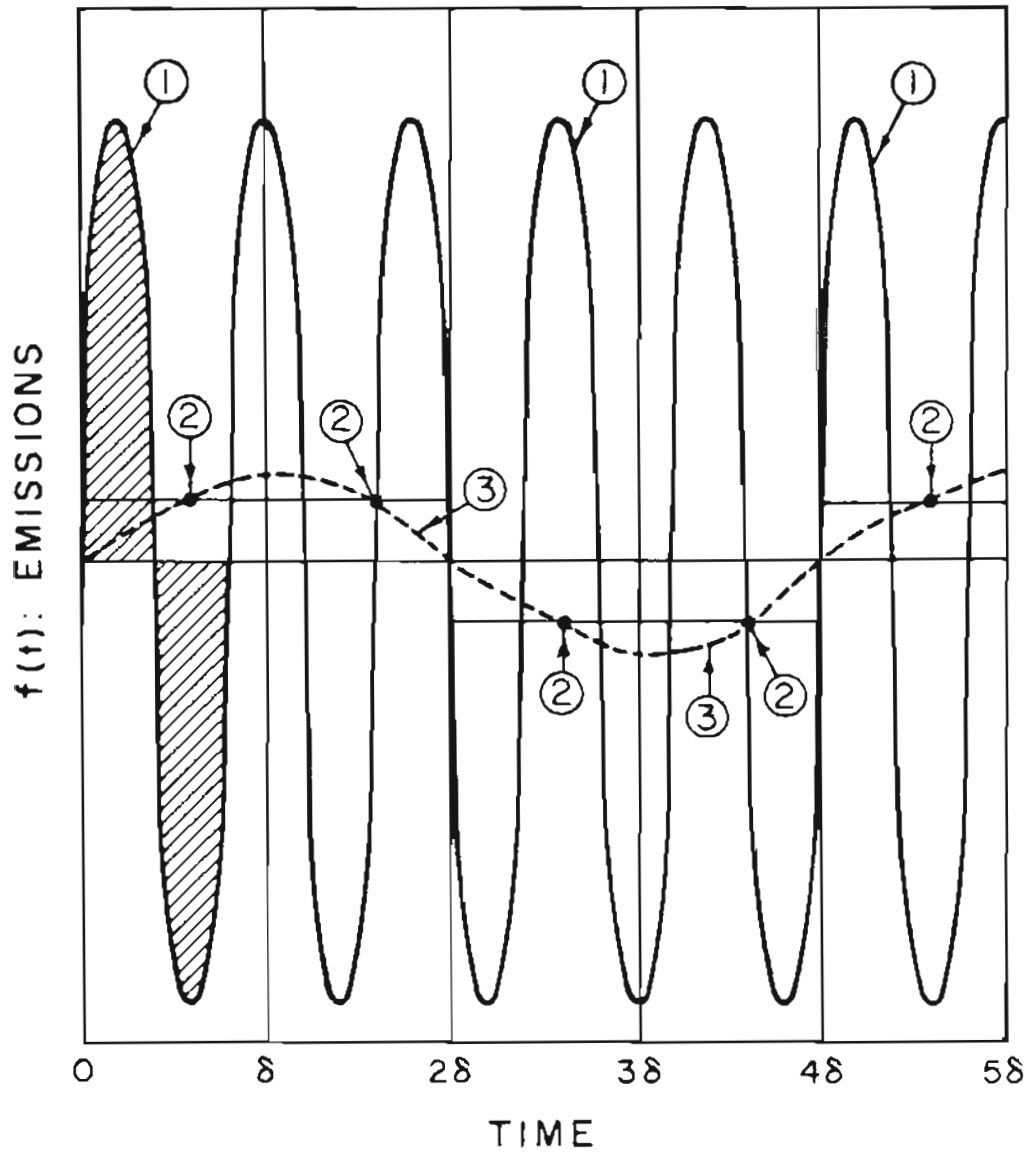


Figure (9.1): The appearance of cycles in source functions:

- (1) Hypothetical true source function $\omega = \frac{5}{2} \frac{\pi}{\delta} > \frac{2\pi}{\delta}$.
- (2) Integrated value of $f(t)$: $\int_t^{t+\delta} f(t') dt'$ making up $\tilde{S}(t)$
- (3) Smoothed $S(t)$ through the points of $\tilde{S}(t)$

$$\omega = \frac{\pi}{\delta} < \frac{2\pi}{\delta} ; \text{ with small amplitude.}$$

CHAPTER 10: GLOBAL BOX MODELS:
FORMULATION AND SOLUTIONS.

(a) General Ideas

The changes in the global environment caused by increasing anthropogenic emissions into the atmosphere are controlled by the motions of the atmosphere and the chemistry in the atmosphere. Various aspects of these general ideas have been discussed in the main chapters of this work.

A powerful tool in the theoretical analysis of the dispersal and fate of atmospheric trace gases is the species conservation (or mass conservation) equation. It is based on a balance between the distribution and magnitude of the sources, the dispersal of the trace gases (transport), and the sinks of these gases. The purpose of this chapter is not to discuss the theory in detail, but to formulate simplified equations that can be applied to a large number of trace gases. The applicability of a particular version of the mass conservation equation to a given trace gas depends on more detailed knowledge of the behaviour of the trace gas. Here, a simple catalog is developed which gives additional details for the theoretical models used in the main text of this work. The graphical catalog of section (i) is a quick reference for the type of theories described here.

(b) Many Box Theory

The many box theory is a discrete version of the continuous mass conservation equation:

$$(1/n) \frac{\partial}{\partial t} C = S - L - \frac{1}{n} \underline{\nabla} \cdot C \underline{v} \quad (10.1)$$

C is the number density of the trace gas, n the local number density of air and \underline{v} the mean velocity vector. S and L represent the sources and sinks (losses). When losses are by first order processes $L = \eta C$, $\eta = \sum_k \eta_k$ where η_k are the sink strengths of the various loss processes indexed by k . Equation (10.1) is simplified by various averaging procedures and other assumptions, finally leading to K-theory versions which may incorporate motions in 1, 2 or 3 dimensions (depending on which coordinate variables are allowed to vary continuously). The many box theory simply forms discrete averages over any number of divisions of the atmosphere.

Suppose the atmosphere (troposphere and the stratosphere) is divided into N boxes, indexed by i . Losses are assumed to be of the first order, and the transport term has to be specified by a time $\bar{\tau}_{ij}$ representing transport between boxes i and j . The mass conservation equation can be written as:

$$\frac{d}{dt} \underline{C} = \underline{S} - \underline{\eta} \wedge \underline{C} - \underline{\bar{\tau}} \cdot \underline{C} \quad (10.2)$$

$$(\underline{\eta} \wedge \underline{C})_j = \eta_j C_j \quad (10.3)$$

\underline{C} is a column vector $[C_1 \dots C_N]^T$ (\underline{x}^T is the transpose of a vector \underline{x}), where C_i is the number of molecules of a given trace gas in box i . \underline{S} is the column vector $[S_1 \dots S_N]^T$ where S_i is the source strength (molecules emitted per unit time) in box i and \underline{n} is the column vector $[n_1 \dots n_N]^T$. $\overleftrightarrow{\Omega}$ is a matrix ($N \times N$) which describes the transport of molecules of the trace gas into and out of box i ($\sum_{j=1}^N \Omega_{ij} C_j$). To simplify the discussion, $\overleftrightarrow{\Omega}$ is defined as follows:

$$\overleftrightarrow{\Omega} \cdot \underline{C} = \underline{n} \wedge \underline{C} + \overleftrightarrow{\Omega}' \cdot \underline{C} \quad (10.4)$$

so that eqn. (10.2) becomes:

$$\frac{d}{dt} \underline{C} = \underline{S} - \overleftrightarrow{\Omega} \cdot \underline{C} \quad (10.5)$$

Equation (10.2) can be solved as:

$$\underline{C} = \exp [-\overleftrightarrow{\Omega} t] \underline{C}_0 + \exp [-\overleftrightarrow{\Omega} t] \cdot \int_0^t \exp [\overleftrightarrow{\Omega} t'] \cdot \underline{S}(t') dt' \quad (10.6)$$

The arrows \leftrightarrow will be dropped from here on, but it is understood that Ω is a matrix.

$$\exp [\Omega t] \equiv \sum_{n=0}^{\infty} \frac{\Omega^n t^n}{n!} \quad (10.7)$$

A new matrix, P , has to be defined to obtain a useable version of eqn. (10.6). P is defined by the relationship:

$$P \Omega P^{-1} = \Lambda \quad (10.8)$$

$$\Lambda = \begin{bmatrix} \lambda_1 & & 0 \\ & \cdot & \\ 0 & & \lambda_N \end{bmatrix} \quad (10.9)$$

where λ_k ($k = 1, \dots, N$) are the eigenvalues of Ω . It is assumed that the Jordan Canonical form of Ω is given by eqn. (10.9). Some λ_k may appear more than once and some λ_n may even be zero, but the roots of the polynomials $\det[\Omega - \lambda I] = 0$ are simple. (Roots being simple means that there are no solutions of the minimal polynomial of $(\Omega - \lambda I)$ of the type $(\lambda - X)^n = 0$ with $n > 1$.) With eqns. (10.8) and (10.9), eqn. (10.6) can be written as:

$$\underline{C} = (P^{-1} e^{-\Lambda t} P) \underline{C}_0 + P^{-1} e^{-\Lambda t} \int_0^t e^{\Lambda t'} P \underline{S} dt' \quad (10.10)$$

Note that eqns. (10.7) and (10.8) imply that:

$$P e^{-\Omega t} P^{-1} = e^{-\Lambda t} = \begin{bmatrix} e^{-\lambda_1 t} & & 0 \\ & \cdot & \\ 0 & & e^{-\lambda_N t} \end{bmatrix}$$

Eqn. (10.10) is the general solution. It gives the total number of molecules of a trace gas in each box. If necessary, the C_i can be divided by V_i (volume of box i) to get the mean density of the trace gas in box i ; and C_i can be divided N_i (number of molecules of air in box i) to get ξ_i , the mean mixing ratio of the trace gas in box i .

If \underline{S} is constant in time, the solution of (10.10) is:

$$\underline{C} = (P^{-1} e^{-\Lambda t} P) \underline{C}_0 + P^{-1} (I - e^{-\Lambda t}) \Lambda^{-1} P \underline{S} \quad (10.11a)$$

If \underline{S} is $\underline{S}_0 e^{bt}$

$$\underline{C} = (P^{-1} e^{-\Lambda t} P) \underline{C}_0 + P^{-1} [e^{bIt} - e^{-\Lambda t}] (\Lambda + bI)^{-1} P \underline{S}_0 \quad (10.11b)$$

I is the $N \times N$ identity matrix. After a long time the asymptotic limits of (10.11a) and (10.11b) are:

$$\underline{C}_\infty = \Omega^{-1} \underline{S} \quad (10.12)$$

$$\underline{C}_\infty = P^{-1} (\Lambda + bI)^{-1} P \underline{S}_0 e^{bt} \quad (10.13)$$

In eqn. (10.13) the concentration in every box rises at the same exponential rate; thus the ratio of the burdens in any two boxes becomes constant.

(c) Simple Global Model

The simplest of all spatially averaged forms of the mass conservation equation is the complete global average. This makes $N = 1$ and the spatial integration of eqn. (10.1) is carried out over the whole troposphere and the stratosphere. Eqn. (10.10) becomes

$$\xi = \xi_0 e^{-\eta t} + e^{-\eta t} \int_0^t S(t') e^{\eta t'} dt' \quad (10.14)$$

$$\xi = \frac{C}{N_\infty}$$

N_∞ is the total number of molecules in the troposphere and the stratosphere; $\eta = 1/\tau$ where τ is the global lifetime of the trace gas.

(d) Two-Box Theories

There are two kinds of two-box theories: (i) One box is the entire troposphere and the other one is the entire stratosphere. (ii) one box is the northern hemisphere troposphere and the stratosphere and the second box is the southern hemisphere troposphere and the stratosphere.

(i) Troposphere - stratosphere

$$\frac{d}{dt} \xi_T = \tilde{S}_T - \eta \xi_T - \eta_T \frac{N_S}{N_T} [\xi_T - \xi_U] \quad (10.15a)$$

$$\frac{d}{dt} \xi_U = \tilde{S}_U - \eta \xi_U + \eta_T [\xi_T - \xi_U] \quad (10.15b)$$

$\tau = 1/\eta$ is the tropospheric lifetime of the trace gas; $\bar{\tau} = 1/\bar{\eta}$ is the stratospheric lifetime; N_S and N_T are the number of molecules of air in the troposphere and the stratosphere. ξ_T and ξ_U are the mean mixing ratios of the trace gas in the troposphere and the stratosphere (upper atmosphere) respectively. Often there are no sources in the stratosphere, so that $S_n = 0$.

$$\Omega = \begin{bmatrix} (\eta + \eta_T \frac{N_S}{N_T}) & -\eta_T \frac{N_S}{N_T} \\ -\eta_T & (\bar{\eta} + \eta_T) \end{bmatrix} \quad (10.16)$$

$\eta_T = 1/\tau_T$ where τ_T is the stratospheric-tropospheric transport time.

It is easy to show that:

$$\lambda_1 = \frac{1}{2} (d + a) + \frac{1}{2} [(a - d)^2 + 4bc]^{\frac{1}{2}} \quad (10.17a)$$

$$\lambda_2 = \frac{1}{2} (d + a) - \frac{1}{2} [(a - d)^2 + 4bc]^{\frac{1}{2}} \quad (10.17b)$$

$$a = \eta + \eta_T \frac{N_S}{N_T}, \quad b = \eta_T \frac{N_S}{N_T}, \quad d = (\bar{\eta} + \eta_T), \quad c = \eta_T \quad (10.17c)$$

$$P = \begin{bmatrix} c/(a - \lambda_2) & 1 \\ c/(a - \lambda_2) & 1 \end{bmatrix} \quad (10.18)$$

$$P^{-1} = \frac{(a - \lambda_1)(a - \lambda_2)}{c(\lambda_1 - \lambda_2)} \begin{bmatrix} 1 & 1 \\ -c/(a - \lambda_2) & c/(a - \lambda_1) \end{bmatrix} \quad (10.19)$$

$$\begin{aligned} \begin{bmatrix} \xi_T \\ \xi_U \end{bmatrix} &= P^{-1} \begin{bmatrix} e^{-\lambda_1 t} & 0 \\ 0 & e^{-\lambda_2 t} \end{bmatrix} P \begin{bmatrix} \xi_{T0} \\ \xi_{U0} \end{bmatrix} + \\ &P^{-1} \begin{bmatrix} e^{-\lambda_1 t} & 0 \\ 0 & e^{-\lambda_2 t} \end{bmatrix} \int_0^t \begin{bmatrix} e^{\lambda_1 t'} & 0 \\ 0 & e^{\lambda_2 t'} \end{bmatrix} P \begin{bmatrix} \tilde{S}_T(t') \\ \tilde{S}_n(t') \end{bmatrix} dt' \end{aligned} \quad (10.20)$$

(ii) Northern - southern hemispheres.

$$\frac{d}{dt} \xi_n = \tilde{S}_n - \eta_n \xi_n - \eta_T [\xi_n - \xi_s] \quad (10.21a)$$

$$\frac{d}{dt} \xi_s = \tilde{S}_s - \eta_s \xi_s + \eta_T [\xi_n - \xi_s] \quad (10.21b)$$

ξ_n , ξ_s are the northern and southern hemisphere mean mixing ratios. η_n and η_s are the northern and southern hemisphere mean lifetimes (including the stratosphere). $\tau_T = 1/\eta_T$ is the interhemispheric transport time.

$$\Omega = \begin{bmatrix} (\eta_n + \eta_T) & -\eta_T \\ -\eta_T & (\eta_s + \eta_T) \end{bmatrix} \quad (10.22)$$

$$\lambda_1 = \frac{1}{2} (a + d) + \frac{1}{2} [(d - a)^2 + b^2]^{\frac{1}{2}} \quad (10.23a)$$

$$\lambda_2 = \frac{1}{2} (a + d) - \frac{1}{2} [(d - a)^2 + b^2]^{\frac{1}{2}} \quad (10.23b)$$

$$a = \eta_n + \eta_T, \quad b = \eta_T, \quad d = (\eta_s + \eta_T) \quad (10.24)$$

P and P^{-1} are the same as eqns. (10.18) and (10.19) with a , b , d as in eqn. (10.24) and $b = c$. The solution of ξ_n , ξ_s is given by eqn. (10.20).

(e) Three-Box Theory

There is only one, never before used, theory in this category. The three boxes are the northern hemisphere troposphere, southern hem-

isphere troposphere and the entire stratosphere. The mass conservation equation assumes the following form:

$$\frac{d\xi_n}{dt} = S_n - \eta_n \xi_n - \bar{\eta}_T (\xi_n - \xi_s) - \bar{\eta}_s \frac{N_s}{N_T} (\xi_n - \xi_u) \quad (10.25a)$$

$$\frac{d\xi_s}{dt} = S_s - \eta_s \xi_s + \bar{\eta}_T (\xi_n - \xi_s) - \bar{\eta}_s \frac{N_s}{N_T} (\xi_s - \xi_u) \quad (10.25b)$$

$$\frac{d\xi_u}{dt} = S_u - \eta_u \xi_u + \frac{1}{2} \bar{\eta}_s (\xi_n + \xi_s) - \bar{\eta}_s \xi_u \quad (10.25c)$$

ξ_n is the northern troposphere mixing ratio, ξ_s the southern troposphere mixing ratio, ξ_u the stratospheric mean mixing ratio. η_s and η_n are the southern and northern hemisphere tropospheric lifetimes and η_u is the mean stratospheric lifetime. $\bar{\eta}_T$ is the interhemispheric transport time and $\bar{\eta}_s$ is the stratospheric-tropospheric exchange time (time for the exchange of the whole stratosphere with the troposphere).

$$\Omega = \begin{bmatrix} (\eta_n + \bar{\eta}_T + \bar{\eta}_s \frac{N_s}{N_T}) & -\bar{\eta}_T & -\bar{\eta}_s \frac{N_s}{N_T} \\ -\bar{\eta}_T & (\eta_s + \bar{\eta}_T + \bar{\eta}_s \frac{N_s}{N_T}) & -\bar{\eta}_s \frac{N_s}{N_T} \\ -\frac{1}{2} \bar{\eta}_s & -\frac{1}{2} \bar{\eta}_s & (\eta_u + \bar{\eta}_s) \end{bmatrix} \quad (10.26)$$

The eigenvalue equation for Ω gives a cubic polynomial which may be solved by the available mathematical techniques (see for example Mastow

et al., 1963, p. 159). The solutions for ξ_n , ξ_s and ξ_u are described by the appropriate restriction of eqn. (10.9) to this case. The matrix P can also be deduced in a manner analogous to the case of the previous section, and the four-box theories considered in the next section.

(f) Four-Box Theories

There are many ways to divide the atmosphere into four pieces. Two methods stand out as the physically more appropriate divisions.

(i) Latitudinal theory.

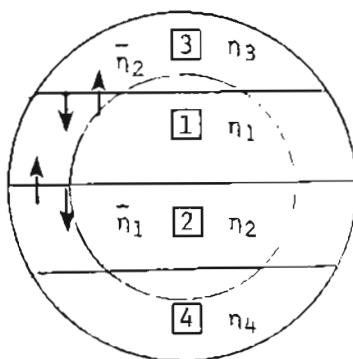
The first method is to consider the atmosphere from ground level to the top of the stratosphere and take all four boxes to separate the atmosphere latitudinally. The first division is along the equator, then each hemisphere is divided once again at about $\pi/6$ radians. To an extent this is an appropriate division along the main latitudinal barriers to transport from north to south (or south to north). It is also a division in which the number of molecules of air in the atmosphere are approximately equally divided among the four boxes. The resulting theory is:

$$\frac{d}{dt} \xi_1 = S_1 - \eta_1 \xi_1 - \bar{\eta}_1 (\xi_1 - \xi_2) - \bar{\eta}_2 (\xi_1 - \xi_3)$$

$$\frac{d}{dt} \xi_2 = S_2 - \eta_2 \xi_2 + \bar{\eta}_1 (\xi_1 - \xi_2) - \bar{\eta}_2 (\xi_2 - \xi_4)$$

$$\begin{aligned}\frac{d}{dt} \xi_3 &= S_3 - \eta_3 \xi_3 + \bar{\eta}_2 (\xi_1 - \xi_3) \\ \frac{d}{dt} \xi_4 &= S_4 - \eta_4 \xi_4 + \bar{\eta}_2 (\xi_2 - \xi_4)\end{aligned}\quad (10.27)$$

The picture given below illustrates the divisions and the numbering:



The explanations of the symbols ξ_k , η_k ($k = 1 - 4$), $\bar{\eta}_1$, $\bar{\eta}_2$ and S_k are obvious from the figure and the discussion in Chapter 5.

$$\Omega = \begin{bmatrix} (\eta_1 + \bar{\eta}_1 + \bar{\eta}_2) & -\bar{\eta}_1 & -\bar{\eta}_2 & 0 \\ -\eta_1 & (\eta_2 + \bar{\eta}_1 + \bar{\eta}_2) & 0 & -\bar{\eta}_2 \\ -\eta_2 & 0 & (\eta_3 + \bar{\eta}_2) & 0 \\ 0 & -\bar{\eta}_2 & 0 & (\eta_4 + \bar{\eta}_2) \end{bmatrix}\quad (10.28)$$

The eigenvalue equation for Ω can again be solved by standard mathematical techniques (see Mastow et al., (1963) p. 160-161). P and P^{-1} are given as follows:

$$P = \begin{bmatrix} A(\lambda_1) & B(\lambda_1) & D(\lambda_1) & 1 \\ A(\lambda_2) & B(\lambda_2) & D(\lambda_2) & 1 \\ A(\lambda_3) & B(\lambda_3) & D(\lambda_3) & 1 \\ A(\lambda_4) & B(\lambda_4) & D(\lambda_4) & 1 \end{bmatrix} \quad (10.29)$$

$$A(\lambda_k) = [(g - \lambda_k)(f - \lambda_k) - c^2]/bc \quad (10.30a)$$

$$B(\lambda_k) = (g - \lambda_k)/c \quad (10.30b)$$

$$D(\lambda_k) = [(g - \lambda_k)(f - \lambda_k) - c^2]/b(d - \lambda_k) \quad (10.30c)$$

$$k = 1, \dots, 4$$

$$a = \Omega_{11}, \quad b = \bar{\eta}_1, \quad c = \bar{\eta}_2, \quad d = \eta_3 + \bar{\eta}_2, \quad f = \Omega_{22} = (\eta_2 + \bar{\eta}_1 + \bar{\eta}_2), \quad g = \Omega_{44} = \eta_4 + \bar{\eta}_2$$

P^{-1} can be deduced from the standard technique, namely:

$$P^{-1} = \frac{P^+}{\det P} \quad (10.31)$$

where P^+ is the adjoint of P (any standard text may be consulted for evaluating eqn. (10.31); for example, Smiley, 1965).

The algebra of such a theory is considerably simpler when $\eta_1 = \eta_2$ and $\eta_2 = \eta_4$. This means that the sink strengths (or lifetimes) are symmetrical in latitude, so that the total lifetime of the trace gas is the same in the northern and southern hemispheres. The details of this theory are given in Chapter 5 and its section in Appendix I. This is a nice approximation and gives elegant symmetric equations, but it is likely that the approximation is not completely appropriate for those

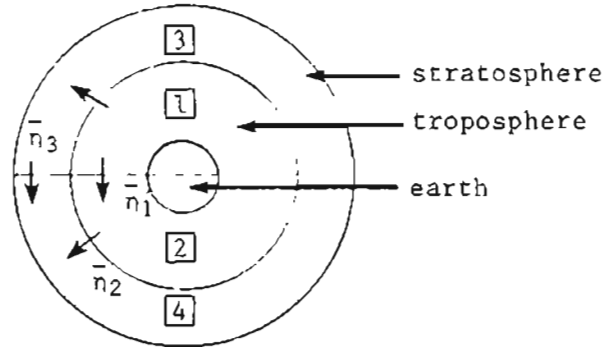
trace gases which have dominant tropospheric sinks with respect to HO interaction. Current evidence suggests that there is a lot more (factor of two) CO in the northern hemisphere than in the southern hemisphere. This is due to both natural land processes and anthropogenic emissions. In addition, other gases -- terpenes and isoprene, etc. -- are probably more abundant in the northern hemisphere boundary layer. These gases are believed to control (especially CO due to its high concentrations) the tropospheric HO densities, because they are the major sink of HO. So, it is probable that HO densities are significantly higher in the southern hemisphere, thus making $\tau_1 > \tau_2$ and $\tau_3 > \tau_4$ (of course $\tau_3 > \tau_1$ and $\tau_4 > \tau_2$ because of reduced HO densities at high latitudes). It is, therefore, recommended that in such conditions η_k should all be assumed as different from each other. I would like to add that this consideration was left out of the theory in Chapter 5 since the main problem in that chapter was to show that the form and "depth" of the changing CH_3CCl_3 gradient were dependent primarily on the fluctuating source. The conclusions of the assessment would not be changed by assuming shorter southern hemisphere lifetimes.

(ii) Troposphere-stratosphere theory:

Another useful four-box theory is to divide the atmosphere into the northern and southern tropospheres and the northern and southern stratospheres. The equations are:

$$\begin{aligned}
 \frac{d\xi_1}{dt} &= S_1 - n_1\xi_1 - \bar{n}_1(\xi_1 - \xi_2) - \bar{n}_2 \frac{N_S}{N_T} (\xi_1 - \xi_3) \\
 \frac{d\xi_2}{dt} &= S_2 - n_2\xi_2 + \bar{n}_1(\xi_1 - \xi_2) - \bar{n}_2 \frac{N_S}{N_T} (\xi_2 - \xi_4) \\
 \frac{d\xi_3}{dt} &= -n_3\xi_3 - \bar{n}_2(\xi_3 - \xi_1) - \bar{n}_3(\xi_3 - \xi_4) \\
 \frac{d\xi_4}{dt} &= -n_4\xi_4 - \bar{n}_2(\xi_4 - \xi_2) + \bar{n}_3(\xi_3 - \xi_4)
 \end{aligned}
 \tag{10.32}$$

The division of the atmosphere is illustrated in the figure below:



$$\Omega = \begin{bmatrix}
 (n_1 + \bar{n}_1 + \frac{N_S}{N_T} \bar{n}_2) & -\bar{n}_1 & -\bar{n}_2 \frac{N_S}{N_T} & 0 \\
 -\bar{n}_1 & (n_2 + \bar{n}_1 + \bar{n}_2 \frac{N_S}{N_T}) & 0 & -\bar{n}_2 \frac{N_S}{N_T} \\
 -\bar{n}_2 & 0 & (n_3 + \bar{n}_2 + \bar{n}_3) & -\bar{n}_3 \\
 0 & -\bar{n}_2 & -\bar{n}_3 & (n_4 + \bar{n}_2 + \bar{n}_3)
 \end{bmatrix}
 \tag{10.33}$$

When $\bar{n}_3 \rightarrow 0$ the matrix P is the same as eqns. (10.29) and (10.30), but

where a, b, c, d, f and g are defined as follows:

$$\begin{aligned}
 a &= (\eta_1 + \bar{\eta}_1 + \frac{N_S}{N_T} \bar{\eta}_2); \quad b = \bar{\eta}_1; \quad c = \bar{\eta}_2 \frac{N_S}{N_T} \\
 d &= (\eta_3 + \bar{\eta}_2), \quad f = (\eta_2 + \bar{\eta}_1 + \bar{\eta}_2 \frac{N_S}{N_T}) \\
 g &= (\eta_4 + \bar{\eta}_2)
 \end{aligned} \tag{10.34}$$

$\eta_3 \rightarrow 0$ is a reasonable approximation (see Reiter, 1975). If $\eta_3 \neq 0$, then P can be evaluated from eqn. (10.8).

(g) Five-Box Theory

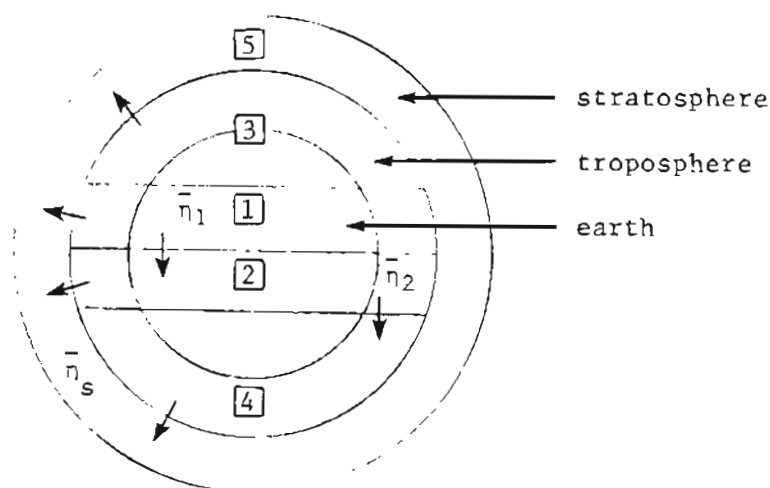
Though five-box theories are not used, they can be formulated. An appropriate five-box theory is one with four boxes in the troposphere divided along latitudes just like the four-box theory of the preceding section (f.1). The fifth box is the entire stratosphere. This allows for good latitudinal resolution and still separates the stratosphere and the troposphere. The equations become:

$$\begin{aligned}
 \dot{\xi}_1 &= S_1 - \eta_1 \xi_1 - \bar{\eta}_1 (\xi_1 - \xi_2) - \bar{\eta}_2 (\xi_1 - \xi_3) \\
 &\quad - \bar{\eta}_S \frac{N_S}{N_T} (\xi_1 - \xi_5) \\
 \dot{\xi}_2 &= S_2 - \eta_2 \xi_2 + \bar{\eta}_1 (\xi_1 - \xi_2) - \bar{\eta}_2 (\xi_2 - \xi_4) \\
 &\quad - \bar{\eta}_S \frac{N_S}{N_T} (\xi_2 - \xi_5) \\
 \dot{\xi}_3 &= S_3 - \eta_3 \xi_3 + \bar{\eta}_2 (\xi_1 - \xi_3) - \bar{\eta}_S \frac{N_S}{N_T} (\xi_3 - \xi_5)
 \end{aligned} \tag{10.35}$$

$$\dot{\xi}_4 = S_4 - n_4 \xi_4 + \bar{n}_2 (\xi_2 - \xi_4) - \bar{n}_S \frac{N_S}{N_T} (\xi_4 - \xi_5)$$

$$\dot{\xi}_5 = -n_5 \xi_5 + \bar{n}_S \frac{1}{4} (\xi_1 + \xi_2 + \xi_3 + \xi_4) - \bar{n}_S \xi_5$$

\bar{n}_S is the time during which the entire stratosphere is exchanged with the troposphere (not with each smaller box, $\bar{n}_S \sim 0.5 - 0.6/\text{yr}$, Reiter, 1975). The divisions of the atmosphere are described by the figure below:



The appropriate matrices P and P^{-1} may be constructed by the same methods as used before. The eigenvalue equation for Ω may no longer be algebraically solvable. This is due to the well-known theorem of Abel and Galois. For certain assumptions regarding the symmetries of lifetimes in the northern and southern hemispheres, it may be possible to solve the eigenvalue equation. The more pragmatic reader will certainly not be dismayed by the insolvability of fifth, or higher, order pol-

ynomials since approximation techniques are available and well known.

(h) Six-, Seven-, and Eight-Box Theories

The group of theories with six, seven, and eight boxes are also possible for the same type of problem discussed in the preceding sections. Within the context of the present chapter an appropriate six-box theory is one which is the same as the five-box theory discussed in the last section, except that the stratosphere is also divided into the northern and southern pieces. Seven-box theories are not convenient in this context, and would not contribute anything more than the six- and eight-box theories. Therefore, the possible seven-box theories will not be discussed further. An appropriate eight-box theory is one with four tropospheric boxes and attached to each tropospheric box is its own adjacent stratospheric box. For the type of value such box theories have, it is unlikely that any more than eight boxes would ever be necessary.

The equations for the six-box theory are:

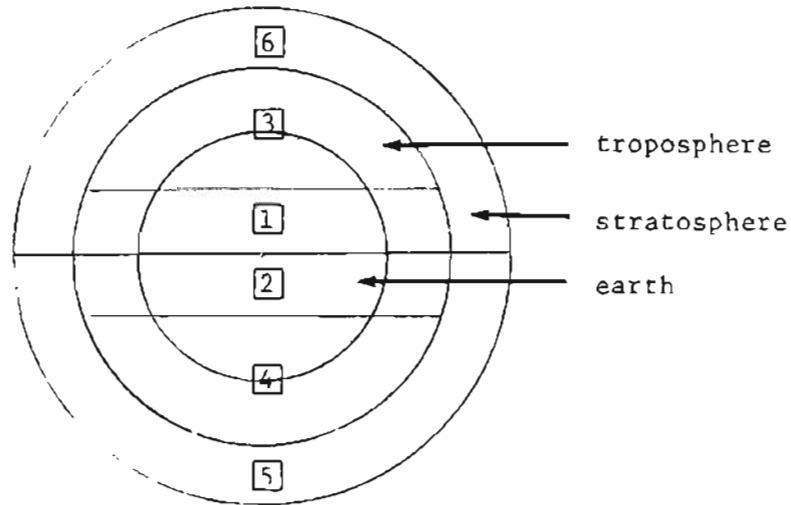
(10.36)

$$\begin{aligned}\dot{\xi}_1 &= S_1 - \eta_1 \xi_1 - \bar{\eta}_1 (\xi_1 - \xi_2) - \bar{\eta}_2 (\xi_1 - \xi_3) - \bar{\eta}_S \frac{N_S}{N_T} (\xi_1 - \xi_6) \\ \dot{\xi}_2 &= S_2 - \eta_2 \xi_2 + \bar{\eta}_1 (\xi_1 - \xi_2) - \bar{\eta}_2 (\xi_2 - \xi_4) - \bar{\eta}_S \frac{N_S}{N_T} (\xi_2 - \xi_5) \\ \dot{\xi}_3 &= S_3 - \eta_3 \xi_3 + \bar{\eta}_2 (\xi_1 - \xi_3) - \bar{\eta}_S \frac{N_S}{N_T} (\xi_3 - \xi_6) \\ \dot{\xi}_4 &= S_4 - \eta_4 \xi_4 + \bar{\eta}_2 (\xi_2 - \xi_4) - \bar{\eta}_S \frac{N_S}{N_T} (\xi_4 - \xi_5)\end{aligned}$$

$$\dot{\xi}_5 = -\eta_5 \xi_5 + \frac{1}{2} \bar{\eta}_5 (\xi_2 + \xi_4) - \bar{\eta}_5 \xi_5 - \bar{\eta}_4 (\xi_5 - \xi_6)$$

$$\dot{\xi}_6 = -\eta_6 \xi_6 + \frac{1}{2} \bar{\eta}_5 (\xi_1 + \xi_3) - \bar{\eta}_5 \xi_6 + \bar{\eta}_4 (\xi_5 - \xi_6)$$

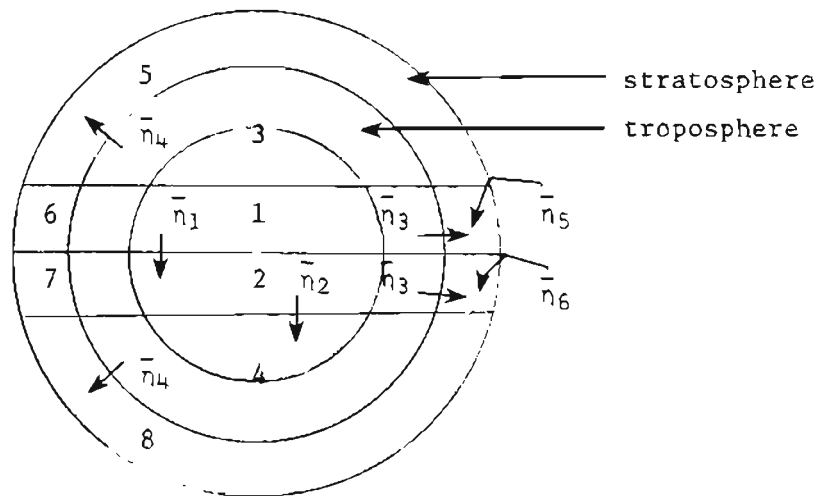
The figure below illustrates the divisions of the atmosphere:



The eight-box theory is described by the following equations:

$$\begin{aligned} \dot{C}_1 &= S_1 - \eta_1 C_1 - \bar{\eta}_1 (C_1 - C_2) - \bar{\eta}_2 (C_1 - C_3) - \bar{\eta}_3 \frac{N_6}{N_1} C_1 + \bar{\eta}_3 C_6 \\ \dot{C}_2 &= S_2 - \eta_2 C_2 + \bar{\eta}_1 (C_1 - C_2) - \bar{\eta}_2 (C_2 - C_4) - \bar{\eta}_3 \frac{N_6}{N_1} C_2 + \bar{\eta}_3 C_7 \\ \dot{C}_3 &= S_3 - \eta_3 C_3 + \bar{\eta}_2 (C_1 - C_3) - \bar{\eta}_4 \frac{N_5}{N_3} C_3 + \bar{\eta}_4 C_5 \\ \dot{C}_4 &= S_4 - \eta_4 C_4 + \bar{\eta}_2 (C_2 - C_4) - \bar{\eta}_4 \frac{N_5}{N_3} C_4 + \bar{\eta}_4 C_8 \\ \dot{C}_5 &= -\eta_5 C_5 + \bar{\eta}_4 \frac{N_5}{N_3} C_3 - \bar{\eta}_4 C_5 - \bar{\eta}_5 \left(\frac{N_6}{N_5} C_5 - C_6 \right) \\ \dot{C}_6 &= -\eta_6 C_6 + \bar{\eta}_3 \frac{N_6}{N_1} C_1 - \bar{\eta}_3 C_6 + \bar{\eta}_5 \frac{N_6}{N_5} C_5 - \bar{\eta}_5 C_6 - \bar{\eta}_6 (C_6 - C_7) \\ \dot{C}_7 &= -\eta_7 C_7 + \bar{\eta}_3 \frac{N_6}{N_1} C_2 - \bar{\eta}_3 C_7 + \bar{\eta}_6 (C_6 - C_7) \\ \dot{C}_8 &= -\eta_8 C_8 + \bar{\eta}_4 \frac{N_5}{N_3} C_4 - \bar{\eta}_4 C_3 - \bar{\eta}_5 \left(\frac{N_6}{N_5} C_8 - C_6 \right) \end{aligned} \quad (10.37)$$

To demonstrate the equations more clearly the eight-box theory is formulated in terms of the total burdens C_k ($k = 1, \dots, 8$) instead of the mixing ratio ξ . It is easy to convert $C_k \rightarrow \xi_k$ ($C_k = \xi_k N_k$ where N_k are the number of molecules of air in the k -th box. N_k were derived in the last chapter). The following figure illustrates the regions:



\bar{n}_3 here is the reciprocal of the time it takes for the contents of box 6 to be exchanged with box 1 and \bar{n}_5 is the reciprocal of the time it takes for the contents of box 6 to be exchanged with box 5. In terms of number of molecules of air in each box it is assumed that the two hemispheres are symmetric. In all the theories discussed, it is assumed that S_k , the source term, is the emissions in the k -th box in molecules per unit time, divided by the number of molecules of air in the k th box. This holds for all theories expressed in terms of the mixing ratios. For the 8-box theory given above the source is not divided by N_k .

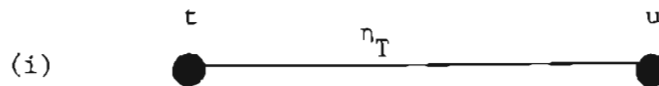
(i) Graphical Summary

Graph theory can be used as a descriptive tool to catalog the various theories discussed in this chapter. A vertex is a box and an edge (line) joining two vertices represents exchange between the joined boxes. The designations t or u mean the boxes are entirely composed of the troposphere or the stratosphere respectively; whereas $t + u$ means that the box contains both tropospheric and stratospheric air. The subscripts n and s refer to northern and southern hemispheres.

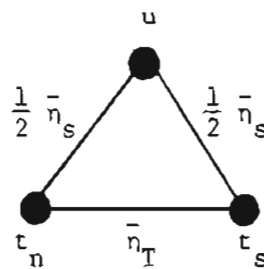
$t + u$



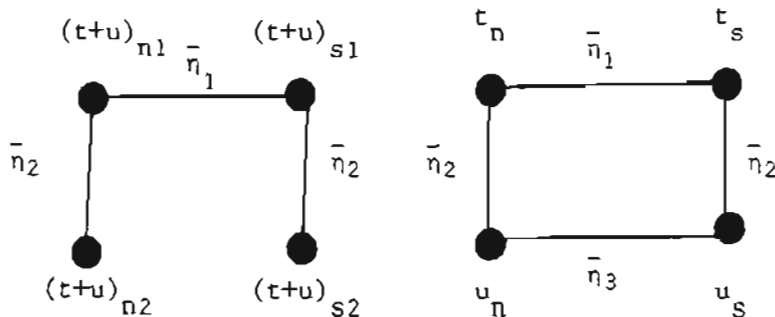
(sec. c)



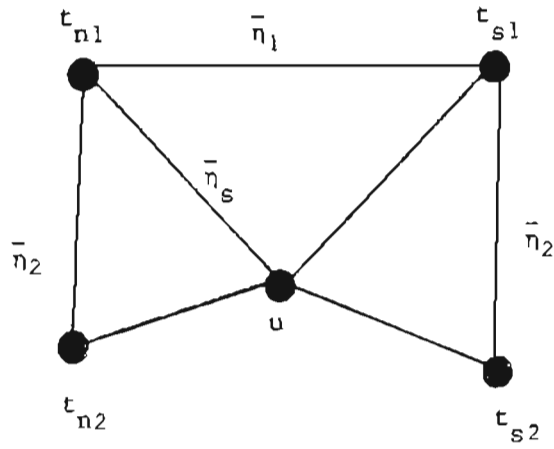
(sec. d)



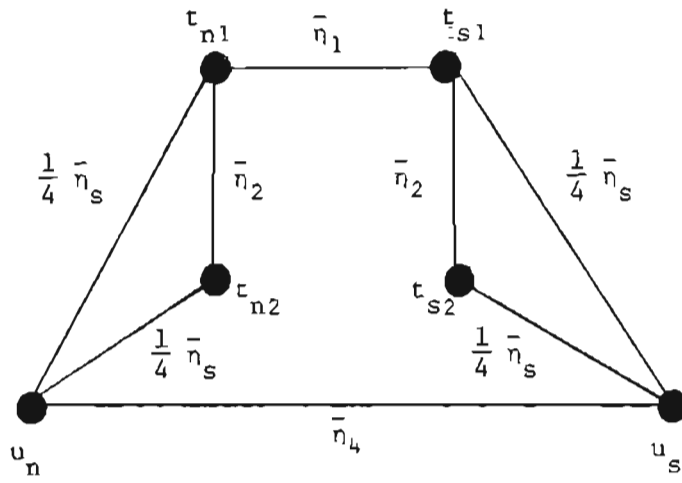
(sec. e)



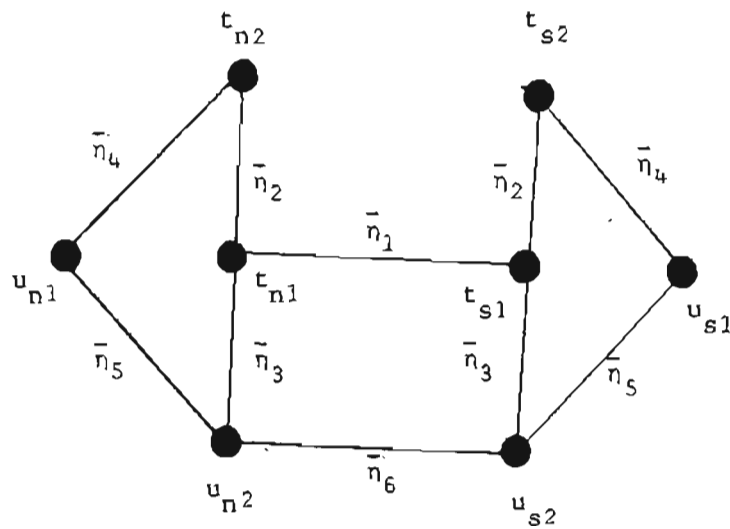
(sec. f)



(sec. g)



(sec. h)



(sec. h)

The nine theories represented above have been discussed in this chapter.

(j) Conclusions

In this chapter various theories were constructed to analyze the distribution and lifetimes of relatively inert trace gases in the atmosphere. The atmosphere was divided into discrete units of varying sizes. Specifically, theories with one to eight boxes were considered.

The final solutions of the equations have not been considered here because the behaviour of the source function in time is different for different trace gases. It is a rather simple matter to evaluate the ξ_k or C_k for any theory discussed here when the source function is known. Many of the possible source functions were discussed in Chapter 4. With the aid of the results of Chapter 4 eqn. (10.9) can be easily evaluated.

It is also possible to include the oceans into such theories as discussed here. This can become necessary for the theoretical evaluation of highly soluble trace gases. The methods outlined here are generalizable to the inclusion of oceanic boxes with some additional effort.

In many cases of interest such theories are powerful tools in explaining the behaviour of trace gases.

CHAPTER 11. CONCLUSIONS

(a) Review

The purposes of this chapter are to review and discuss the main results of this dissertation, as well as to address some broader environmental issues. The first aim is designed to present a compact version of this work, which will better serve those readers who know the techniques used in the calculations or are interested only in a review of the results.

In general the lifetime is an important variable characterizing a trace gas. The lifetime, along with the mechanisms by which a trace gas is destroyed, are the main variables which control the environmental effects of the trace gas. Longer-lived trace gases have the undesirable property of accumulating rapidly if they are due to recent anthropogenic activity, thus making them potentially harmful in the future. Chapters 2 and 3 were devoted to calculations of lifetimes of several trace gases.

There are two independent ways of calculating lifetimes of trace gases when the loss processes are of the first order, i.e., the loss of the trace gas dC/dt is proportional to the concentration C ($dC/dt = -\eta C$). This is assumed to be the case for the trace gases considered in this work. The first method considers the balance between the amounts of the gas emitted per unit time and the measured ambient concentrations. This procedure essentially contains three ingredients: the

source strength, the lifetimes and the ambient concentrations (specified by S , τ and C). Knowing any two of these variables, the third can be deduced. Usually the lifetime is regarded as the unknown and chosen to bring the known source strength in agreement with measured ambient concentrations. Generally there is no one lifetime which prevails over the whole atmosphere or at all times, and the single number, τ , is a weighted mean of various lifetimes in the different regions of the atmosphere. In Chapter 2 this budget procedure was applied to three important trace gases: CFCl_3 (F-11), CCl_2F_2 (F-12) and CH_3CCl_3 . The source strength was taken to be given by estimates of F-11 and F-12 by McCarthy et al. (1977) and updated by reports from Alexander Grant and Co. (1979). The measured concentrations were those obtained by R. A. Rasmussen (personal communication) over five years at two high latitude sites -- the U.S. Pacific northwest ($\sim 45^\circ\text{N}$) and the south pole (-90°S). The results of the analysis suggest that a lifetime for F-11 or F-12 of less than 20 years is extremely unlikely. $\tau_{\text{F-11}}$ was estimated to be ~ 50 yrs and $\tau_{\text{F-12}}$ was estimated to be > 70 yrs. These long lifetimes are expected on the basis of the stratospheric sinks for these compounds, thus implying that the data of Rasmussen show an absence of any significant tropospheric sinks for these compounds. This conclusion is in agreement with most other analyses using other data. There are, however, grave difficulties in pinning down the lifetimes of F-11 and F-12 based on the available data. The lifetime of methylchloroform (CH_3CCl_3) using the same techniques is more exact. Again Rasmussen's (personal

communication) measurements over the past five years were used and the source was assumed to be that given by Neely and Plonka (1978) and updated by Neely and Farber (1979). It appears that a total lifetime of 8.5 years is most appropriate. It is possible that the lifetime of CH_3CCl_3 is as low as 6 years or as high as 11 years, but these limits are unlikely. The lifetime of CH_3CCl_3 is most probably between 8 and 10 years. It is also likely that there is a significant difference between the lifetime of CH_3CCl_3 in the northern and southern hemispheres due to the probable uneven distribution of HO radicals in the two hemispheres. HO radicals are the main tropospheric sink for CH_3CCl_3 . The behaviour of CH_3CCl_3 is discussed in several later chapters. All three trace gases, F-11, F-12 and CH_3CCl_3 , are, because of their relatively long lifetimes and high, increasing ambient concentrations, a threat to the stratospheric ozone layer and the enhancement of the atmospheric greenhouse effect.

The second method of calculating lifetimes does not depend on either the source strengths or the ambient concentrations. It starts with delineating the actual sink mechanisms. Next, the global strengths of these sinks are estimated as they affect particular trace gases. For example, when the main sink of a trace gas is reaction with HO radicals, the lifetime of a trace gas is often estimated by $\tau \sim \{K[\overline{\text{HO}}]\}^{-1}$ (K is the rate constant of the reaction of the trace gas with HO radicals at the average global tropospheric temperature, and $[\overline{\text{HO}}]$ is

the average density of hydroxyl radicals in the troposphere). Obviously, the two methods of calculating lifetimes must agree, otherwise there is something wrong with our understanding of the sink mechanisms (e.g., HO densities), source strength of the trace gas, ambient concentrations, rate constants of reactions or other sink strengths. In Chapter 3, trace gases (particularly those containing hydrogen atoms), which have a significantly fast reaction rate with atmospheric hydroxyl radicals, were considered. Furthermore, the mechanisms and atmospheric gases which control the atmospheric HO radical densities were also considered. These theoretically expected densities were reviewed in the light of the currently available measured densities of HO radicals. It appears that there are large uncertainties in the estimation of globally yearly averaged HO densities. The final conclusion was that the global ground level average HO densities should be between $5 - 10 \times 10^5$ molecules/cm³. These estimates were based on forcing the lifetimes of CH₃CCl₃, deduced by the two methods discussed above, to agree. The current data on reaction rates indicate that CH₄ has a longer lifetime than CH₃CCl₃, thus giving $\tau_{\text{CH}_4} \sim 14$ yrs. This lifetime is significantly longer than most budget estimates (see, for example, Seinfeld, 1977) which range from 2 yrs. to 6 yrs. The current understanding of the CH₄ budget is, therefore, questionable. It appears that the true global emissions of CH₄ should be lower than previously estimated. The longer CH₄ lifetime also has an effect on the global CO budget since CH₄ even-

tually yields CO after its reaction with HO. If the CH₄ lifetime is long, then less CO is produced by this mechanism than previously thought. There are other hydrocarbons emitted in large quantities to the atmosphere that can also produce CO in the atmosphere (such as isoprene). These were also mentioned.

Other findings of Chapter 3 showed that the lifetimes of F-21 and F-22 should be about 3 and 23 yrs respectively. The lifetimes of CH₃CF₂Cl and CHFClCF₃ were found to be about 25 and 10 yrs respectively. These chlorine-containing compounds are propellents, and may come into greater use as F-11 and F-12 are removed from this application. Their long lifetimes indicate the need for a more careful study of these compounds.

The physical bases for two equations commonly used for estimating lifetimes by this second method were discussed in considerable detail. A new simple equation was recommended. The new equation differs most significantly from the usual equations when the rate constant is strongly temperature-dependent. The new equation takes into account the rarefaction of the atmosphere with height, and the temperature lapse rate with height. It also involves the commonly observed latitudinal profile of trace gases. Generally, it seems that the greatest uncertainty in calculating lifetimes is the highly variable (and unknown) HO density distribution with respect to season, latitude, longitude, and height and in particular the effective (time) averaged magnitude of hydroxyl radicals in the troposphere.

There is also a significant question regarding other sinks of

CH_3CCl_3 . When budget methods are used to estimate the global lifetime, it does not separate the various mechanisms by which CH_3CCl_3 is removed from the atmosphere, but gives a composite number. There are at least two other possible sinks, namely the heterogeneous destruction of CH_3CCl_3 on sandy surfaces or in dust storms and the stratospheric sink. These two sinks should be subtracted from the total lifetime before arriving at the lifetime due to HO reactions. Such a consideration requires a lowering of the mean HO levels to make the global lifetime of CH_3CCl_3 deduced by budget methods agree with that resulting from HO reaction. In order to prevent the theoretically deduced global HO densities from becoming too small, these other two sinks have to be regarded as weak (compared to HO reaction) on the global scale.

The emissions of trace gases over the years past are controlled by many factors and not subject to any generally acceptable theoretical function describing the time-release history. If there is one common function which appears to be most generally applicable, it is the exponential; so that the source is written as $S = ae^{bt}$ where (a) and (b) are constants and S the emissions at time t (measured from some suitable point). There are reasons why such a form should hold but the idea that the emissions function can have residual structure was introduced in Chapter 4. If S (true) are the best estimates of the yearly emissions of a trace gas, then the residual structure is defined by $\Delta = S$ (true) - ae^{bt} (where a and b are determined by least squares methods applied

to $\ln S$ (true). Δ would be zero if the source was really exponential. Moreover, if $|\Delta|$ is small compared to S , then the residual function Δ really doesn't have any observable effect on global concentrations of the trace gas. For CH_3CCl_3 it turned out that Δ was not only quite large, but also had an interesting structure -- it was cyclic, describable by a cosine function with a period of about 7 years. A kind of Fourier analysis of the function Δ was carried out, revealing some lesser cycles as well. The effects of the cyclic variations of the source were studied in Chapter 4, and a general theory was constructed. It is no surprise that a time-varying source will produce time-varying ambient global concentrations, but it was found that the amplitude of the variations of ambient global concentrations is damped and in fact the magnitudes of the rises and declines of the ambient concentrations depend in a complex way on the lifetime of the trace gas, the frequency and amplitude of the source cycle and other variables. These effects are discussed in detail in Chapter 5.

The situation, which led to the consideration of the effects of such complex source behaviour as described above, was the apparent failure of the idea of taking $S = ae^{bt}$, in describing the observed increase of CH_3CCl_3 in the atmosphere based on five years of self-consistent measurements. The observed rate of increase was found to be faster than the rate of increase of methylchloroform emissions over the last 5-6 yrs, but the observed rate was significantly slower than the average rate of increase of CH_3CCl_3 emissions over the last 20 years. When

the cyclic terms were added to the exponential source function, the observed rate of increase of CH_3CCl_3 over the last five years, and the theoretically expected rate of increase coincided. Statistical calculations were also carried out, which supported the general idea that addition of Δ was necessary in order to explain the observed growth of CH_3CCl_3 in the atmosphere. This success in explaining the growth rate of CH_3CCl_3 was satisfying in its own right, but it also lent support to the consistency of the measurements carried out over several years.

Consideration of the measured ratio of northern hemisphere to southern hemisphere concentrations of CH_3CCl_3 , called R_0 , revealed more structure. The ratio was large in early 1975 and declined significantly until early 1978 and began to rise again since then. I tried several possible explanations, but the only one which was successful was the inclusion of the Δ cycle in the emissions history. This work is reported in Chapter 5. The most sophisticated theories considered in Chapter 5 developed subtle delays and balances but based on the best source data available, all the effects conspired to make the theory coincide with observations. A series of statistical tests were performed which supported the contention that there was, indeed, a true trend in the gradient R_0 not only for CH_3CCl_3 but also for F-11. Thus, it appears likely that the gradient R_0 , of CH_3CCl_3 (and also F-11) was larger in earlier times (particularly 1975) and has since declined. This resolves some of the experimental variance between earlier measurements

of other groups and current measurements. Furthermore, the analysis indicates that the measured gradient at any time is subject to complex influences of the long-term behaviour of the emissions history.

In Chapter 5, a simple criterion was also developed to decide if a trace gas has southern hemisphere sources. The idea was based on the measured north-south gradient (ratio) R . Since the variable R is a (dimensionless) ratio of measured concentrations, it is not very susceptible to absolute accuracy of the measurements, and thus becomes more appropriate for drawing conclusions. The method developed implied that $\text{CH} = \text{CH}$ (acetylene), C_2H_6 , C_2H_4 , CO , COS , CH_3Cl and CH_4 all have significant sources in the southern hemisphere. This analysis is most easily applicable to relatively short-lived trace gases ($\tau < \sim 2$ yrs).

In Chapter 6, various possible scenarios for the future emission of CH_3CCl_3 were considered, leading to the conclusion that CH_3CCl_3 concentrations in the atmosphere can become 2-4 times as high as the current levels. This would make CH_3CCl_3 more prominent in endangering the ozone layer.

In Chapter 7, CHClF_2 (F-22) was studied in the light of recent global measurements made by Rasmussen. The global average of ~ 47 pptv was deduced. This turned out to be significantly higher than could be accounted for by the emissions history given by McCarthy et al. (1977) and Alexander Grant & Co. (1979). In order to explain the apparent excess of F-22 several possibilities were studied. A natural source of

12-20 million kg per year would be sufficient to explain the difference. The extra source need not be natural, but due to some other industrial emissions which end up as the relatively stable F-22 in the atmosphere (Rasmussen has detected F-22 in plumes of aluminum plants). Another possibility is the conversion of F-12 to F-22. It turned out that a slow conversion ($\tau_{\text{F-12}} \sim 100$ yrs or more) would be sufficient to account for the excess, so that there will be little effect on the atmospheric concentration of F-12. The more mundane possibilities are that the measurements are biased towards the high side or that the release estimates are too low. The production data indicate that more than enough F-22 has been produced to account for the global burden based on Rasmussen's measurements, but the release estimates show that a sizeable portion of the produced F-22 is unreleased. Current kinetics data imply a longer lifetime for F-22 in the troposphere than CH_3CCl_3 (by more than a factor of 2). Thus, F-22 can also contribute to the stratospheric chlorine budget, especially if it is being emitted in increasing quantities. F-22 will probably become more and more prominent in future considerations of the effects of anthropogenic activity on our environment.

Chapter 4, 8 and 10 are not reviewed here. The interested reader may read these chapters or the last sections of these chapters which contain the main conclusions.

(b) Environmental Action

"In the middle of the gentlemen's cabin burned a solar lamp, swung from the ceiling . . .

"Here and there, true to their place, but not their function, swung other lamps, barren planets, which had either gone out from exhaustion, or been extinguished by such occupants of berths as the light annoyed, or who wanted to sleep, not see." (Herman Melville - The Confidence Man, 1857).

The work I have reported in this dissertation is directed towards putting a logical framework around some observed effects of anthropogenic activity on our environment, and to establish certain properties (such as lifetimes) of atmospheric trace gases. It is a tiny part of the development of theory to understand the presence of man-made and natural gases in the atmosphere. The nature of the work is such that it lends itself neither to forecasts of doom, nor to hope for the future environment. What is apparent is that there are now relatively large quantities of trace gases in the atmosphere, some of which are completely man-made while others are being increased due to human activities. The 18th-22nd most abundant gases in our present atmosphere are entirely man-made except for one (CCl_3F , CCl_2F_2 , CH_3CCl_3 , and CCl_4). Not only will these gases not go away in the future, but there is every indication that their concentrations will continue to rise. Human activities have also added significant amounts to existing gases such as CO_2 , CO , CH_4 , CH_3Cl , SO_2 . Anthropogenic contribution to chlorine in the stratosphere is now estimated to exceed the natural.

It is necessary to think about the extent to which it is possible to protect the environment as we understand it today. In this regard it is not possible to offer much hope. The very real socio-political problems will take precedence over uncertain influences of human activities on our future global environment. As the population rises, and political awareness grows in the so-called third world countries, many environmental efforts will fail while others become stopgap measures quickly offset by the growth of needs and population. Aside from this problem, there is an inherent weakness in the science itself. It is not possible to predict with satisfactory accuracy how the changes in the environment will affect our future world and the overall ecology of this planet earth. This weakness is exploited to no end by those who stand to lose from particular precautionary environmental action. The ozone debate is a simple example of this much wider issue. It is likely that the release of the fluorocarbons 11 and 12 will continue because of the impasse that now exists. If nothing happens in the future, the environmentalists of today will be ridiculed, and the issue will be cited to undermine their credibility on whatever new environmental issues that may be present at the time. If the proof comes by the depletion of the ozone layer causing widespread human misery, what solace will there be in saying "we told you so"? Besides, those responsible will accuse their predecessors and assure the public that it can never happen in their time. There is an absence of scientific cer-

tainty in all predictions of the future deterioration of the global environment, leaving the environmentalist little choice but to use his heart and conscience as much as he uses his science.

There is also the question whether there will be an acceptable future for which the environment can be saved. It is very difficult to draw a single image from history which would offer hope. If the world does end up forming a society ruled by egalitarian principles and social justice, at peace with itself and its environment and having given up by choice the power to kill, plunder and torture each other, it would not have happened because of man's past but in spite of it. There are many conceivable futures in which the problem of global environmental pollution can become the least of our worries. Obviously a more specific discussion of this subject will lead me too far from the topic of this chapter, so this seems to be a reasonable place to end this dissertation.

REFERENCES

- Alexander Grant & Co., 1978 World Production and Sales of Fluorocarbons FC-11, FC-12 and FC-22, Reports to the Manufacturing Chemists Association, (1979).
- Atkinson, R., K.R.Darnall, A.C.Lloyd, A.M.Winer and J.N.Pitts Jr., Kinetics and Mechanisms of the Reaction of Hydroxyl Radicals with Organic Compounds in the Gas Phase, Advances in Photochemistry, 11, 375-488 (1979).
- Ausloos, P., R.E.Rebbert and L.C.Glasgow, Photodecomposition of Chloromethanes Adsorbed on Silica Surfaces, J.Res. NBS, 82, 1 (1977).
- Barry, R.G., and R.J.Chorley, Atmosphere, Weather and Climate (Methuen & Co., London, 1978).
- Bolin, B., E.T.Degens, S.Kempe and P.Ketner (Editors), The Global Carbon Cycle (John Wiley, N.Y., 1979).
- Boughner, R.E., The Effect of Increased Carbon Dioxide Concentrations on Stratospheric Ozone, J. Geophys. Res. 83, 1326-1332 (1978).
- Brase, Charles and Corrine Brase, Understandable Statistics: Concepts and Methods (D.C.Heath & Co., Mass., 1978).
- Campbell, M.J., J.C.Sheppard and B.F.Au, Measurement of Hydroxyl Concentration in Boundary Layer Air by Monitoring CO Oxidation, Geophys. Res. Lett., 6, 175-178 (1979).
- Chameides, W.L. and J.C.G.Walker, Ozone: The Possible Effects of Tropospheric-Stratospheric Feedback, Science, 190, 1294-1295 (1975)
- Chang, Jenq Sian and F.Kaufman, Kinetics of the Reaction of Hydroxyl Radicals with some Halocarbons: CHFCl_2 , CHF_2Cl , CH_3CCl_3 , C_2HCl_3 and C_2Cl_4 , J. Chem. Phys., 66, 4989-4994 (1977a).
- Chang, Jenq Sian and F.Kaufman, Upper Limits of the Rate Constants for the Reactions of CFCl_3 (F-11), CF_2Cl_2 (F-12) and N_2O with OH. Estimates of Corresponding Lower Limits to their Tropospheric Lifetimes., Geophys. Res. Lett., 4, 192-194 (1977b).
- Chang, J.S. and J.E.Penner, Analysis of Global Budgets of Halocarbons, Atmospheric Environment, 12, 1867-1873 (1978).

- Climatic Impact Assessment Program, The Natural Stratosphere of 1974: CIAP Monograph No.1 (Dept of Transportation, Washington D.C., 1975).
- Crutzen, P.J., Ozone Production in an Oxygen-Hydrogen-Nitrogen Oxide Atmosphere, J. Geophys. Res., 76, 7311-7327 (1971).
- Crutzen, P.J. and J. Fishman, Average Concentrations of OH in the Troposphere, and the Budgets of CH₄, CO, H₂ and CH₃CCl₃, Geophys. Res. Lett., 4, 321-324 (1977).
- Crutzen, P.J., I.S.A. Isaksen and J.R. McAfee, The Impact of the Chlorocarbon Industry on the Ozone Layer, J. Geophys. Res., 83, 345-363 (1978).
- Cunnold, D., F. Alyea and R. Prinn, A Methodology for Determining the Atmospheric Lifetimes of Fluorocarbons, J. Geophys. Res., 83, 5493-5500 (1978).
- Czeplak, G. and C. Junge, Studies of Interhemispheric Exchange in the Troposphere by a Diffusion Model, Turbulent Diffusion in Environmental Pollution (F.N. Frenkiel and R.E. Munn, editors), (Academic Press, N.Y., 1974).
- Davis, D.D., G. Machado, B. Conaway, Y. Oh and R. Watson, A Temperature Dependent Kinetics Study of the Reaction of OH with CH₃Cl, CH₂Cl₂, CHCl₃ and CH₃Br, J. Chem. Phys., 65, 1268-1274 (1976).
- Davis, D.D., W. Heaps and T. McGee, Direct Measurements of Natural Tropospheric Levels of OH via an Aircraft Borne Tunable Dye Laser, Geophys. Res. Lett., 3, 331-333 (1976).
- DeMore, W.B. (Chairman, NASA Panel), Chemical Kinetic and Photochemical Data for Use in Stratospheric Modelling: Evaluation No. 2, (Jet Propulsion Laboratory: Cal Tech, Pasadena, Calif., 1979).
- Edwards, A.L., An Introduction to Linear Regression and Correlation, (W.H. Freeman & Co., San Francisco, 1976).
- Fink, H.J. and O. Klais, Global Distribution of Fluorocarbons, Ber. Bunsenges Phys. Chem., 82, 1147-1150 (1978).
- Giddings, J.C., Chemistry, Man and Environmental Change: An Integrated Approach (Canfield Press, San Francisco, 1973).
- Glasgow, L.C., J.P. Jesson and R.B. Ward, Urban-Nonurban Relationships of Halocarbons..., Atmospheric Environment, 12, 962 (1978).

- Graedel, T.E. and D.L.Allara, Tropospheric Halocarbons: Estimates of Atmospheric Chemical Production, Atmospheric Environment 10, 385-388 (1976).
- Graedel, T.E., Chemical Compounds in the Atmosphere (Academic Press, N.Y., 1978).
- Gribbin, J. (editor), Climatic Change (Cambridge Univ Press, London, 1978).
- Groves, K.S., S.R.Mattingly and A.F.Tuck, Increased Atmospheric Carbon Dioxide and Stratospheric Ozone, Nature, 273, 711-715, (1978).
- Groves, K.S. and A.F.Tuck, Simultaneous Effects of CO₂ and Chlorofluoromethanes on Stratospheric Ozone, Nature, 280, 127-129 (1979).
- Gutowsky, H.S. (Panel Chairman), Halocarbons: Effects on Stratospheric Ozone (National Academy of Sciences, Wash. D.C., 1976).
- Heiklen, J., Atmospheric Chemistry (Academic Press, N.Y., 1976).
- Hollander, M. and D.A.Wolfe, Nonparametric Statistical Methods, (J.Wiley & Sons, N.Y., 1973).
- Houghton, J.T. The Physics of Atmospheres (Cambridge Univ Press, London, 1977).
- Hov, Ø. and I.S.A.Isaksen, Hydroxyl and Peroxy Radicals in Polluted Tropospheric Air, Geophys. Res. Lett., 6, 219-222 (1979).
- Hudson, R.D. (editor), Chlorofluoromethanes in the Stratosphere (NASA Publ. 1010, Wash D.C., 1977).
- Jeong, K-M and F.Kaufman, Rates of the Reaction of 1,1,1-Trichloroethane (Methyl Chloroform) and 1,1,2-Trichloroethane with OH, Geophys. Res. Lett., 6, 757-759 (1979).
- Johnston, H.S., Global Ozone Balance in the Natural Stratosphere, Rev. Geophys. & Space Phys., 13, 637-649 (1975).
- Kerr, R.A., Global Pollution: Is Arctic Haze Actually Industrial Smog? Science, 205, 290-293 (1979).
- Kurylo, M.J., P.C.Anderson and O.Klais, A Flash Photolysis Resonance Fluorescence Investigation of the Reaction OH + CH₃CCl₃ → H₂O + CH₂CCl₃, Geophys. Res. Lett., 6, 760-762 (1979).

- Levy II, H., Photochemistry of the Troposphere, Advances in Photochem., 9, 369-524 (1974).
- Lovelock, J.E., Methyl Chloroform in the Troposphere as an Indicator of OH Radical Abundance, Nature, 267, 32 (1977).
- Makide, Y. and F.S.Rowland, Tropospheric Concentrations of Methylchloroform, CH_3CCl_3 , in January 1978, and Estimates of its Atmospheric Residence Time. Paper presented before the Division of Environmental Chemistry, American Chemical Society; Honolulu, Hawaii; April 1-6 (1979).
- Mann, H.B., Nonparametric Tests Against Trend, Econometrica, 13, 245-259 (1945).
- Mastow, G.D., J.H.Sampson and J-P.Meyer, Fundamental Structures of Algebra (McGraw-Hill, N.Y., 1963).
- Mayer, E.W., F.S.Rowland and Y. Makide, Interhemispheric Gradients of Atmospheric Methane Between the Northern and Southern Hemispheres, 1978. Paper presented before the Division of Environmental Chemistry; American Chemical Society; Honolulu, Hawaii April 1-6 (1979).
- McCarthy, R.L., F.A.Bower and J.P.Jesson, The Fluorocarbon-Ozone Theory-I: Production and Release- World Production and Release of CCl_3F and CCl_2F_2 (Fuorocarbons 11 and 12) Through 1975, Atmospheric Environment, 11, 491-497 (1977).
- McConnell, J.C. and H.I.Schiff, Methyl Chloroform: Impact on Stratospheric Ozone, Science, 199, 174 (1978).
- Meadows, D.H., D.L.Meadows, J.Randers and W.W.Behrens III, The Limits of Growth (Universe Books, N.Y., 1973).
- Molina, M.J. and F.S.Rowland, Stratospheric Sink for Chlorofluoromethanes: Chlorine Atom-Catalysed Destruction of Ozone, Nature, 249, 810-812 (1974).
- Neely, W.B. and J.H.Plonka, Estimation of Time Averaged Hydroxyl Radical Concentration in the Troposphere, Env. Sci. & Tech., 12, 317-321 (1978).
- Neely, W.B. and H. Farber, 1977 and 1978 emissions estimates for methylchloroform, personal communication (1979).

- Neiburger, M., J.G.Edinger and W.D.Bonner, Understanding Our Atmospheric Environment (W.H.Freeman & Co., San Francisco, 1973).
- Newell, R.E., D.G.Vincent and J.W.Kidson, Interhemispheric Mass Exchange from Meteorological and Trace Substance Observations, Tellus, 21, 641-647 (1969).
- Penner, J.E., M.B.McElroy and S.C.Wofsy, Sources and Sinks for Atmospheric H₂: A Current Analysis with Projections for the Influence of Anthropogenic Activity, Planetary & Space Sci., 25, 521-540, (1977).
- Perner, D., D.H.Ehhalt, H.W.Pätz, U.Platt, E.P.Röth and A. Volz, OH Radicals in the Lower Troposphere, Geophys. Res. Lett., 3, 466-468 (1976).
- Pierotti, D., L.E.Rasmussen and R.A.Rasmussen, The Sahara as a Possible Sink for Trace Gases, Geophys. Res. Lett., 5, 1001-1004 (1978).
- Ramanathan, V., Greenhouse Effect Due to Chlorofluorocarbons: Climatic Implications, Science, 190, 50-52 (1975).
- Rasmussen, R.A., Interlaboratory Comparisons of Fluorocarbon Measurements, Atmospheric Environment, 12, 2505-2508 (1978).
- Reiter, E.R., Stratospheric-Tropospheric Exchange Processes, Rev. Geophys. & Space Sci., 13, 459-474 (1975).
- Robinson, E., Hydrocarbons in the Atmosphere, Pageoph, 116, 372-384 (1978).
- Rowland, F.S. and M.J.Molina, Estimated Future Atmospheric Concentrations of CCl₃F (Fluorocarbon-11) for Various Hypothetical Tropospheric Removal Rates, J. Phys. Chem., 80, 2049-2055 (1976).
- Rust, B.W., R.M.Rotty and G.Marland, Inferences Drawn from Atmospheric CO₂ Data, J. Geophys. Res., 84, 3115-3122 (1979).
- Seiler, W. and C.Junge, Carbon Monoxide in the Atmosphere, J. Geophys. Res., 75, 2217 (1970).
- Seinfeld, J.H., Air Pollution: Physical and Chemical Fundamentals, (McGraw-Hill, N.Y., 1975).

- Singh, H.B., Atmospheric Halocarbons: Evidence in Favor of Reduced Hydroxyl Radical Concentrations in the Troposphere, Geophys. Res. Lett., 4, (1977a).
- Singh, H.B., Preliminary Estimation of Average Tropospheric HO Concentrations in the Northern and Southern Hemispheres, Geophys. Res. Lett., 4, 453-456 (1977b).
- Singh, H.B., L.J.Salas, H.Shigeishi and E.Scribner, Global Distribution of Selected Halocarbons, Hydrocarbons, SF₆ and N₂O. Phase II Interim Report to the U.S.Environmental Protection Agency (1978).
- Singh, H.B., L.J.Salas, H.Shigeishi and E.Scribner, Atmospheric Halocarbons, Hydrocarbons and Sulfur Hexafluoride: Global Distributions, Sources and Sinks, Science, 203, 899-903 (1979).
- Smiley, M.F., Algebra of Matrices (Allyn & Bacon, Boston, 1965).
- Stewart, R.W. and M.I.Hoffert, A Chemical Model of the Troposphere and Stratosphere, J. Atm. Sci., 32, 195-210 (1975)
- Stoiber, R.E., D.C.Leggett, T.F.Jenkins, R.P.Murmann and W.I.Rose, Organic Compounds in Volcanic Gas from Santiaguito Volcano, Guatemala, Geol. Soc. Amer. Bull., 82, 2299-2302 (1971).
- Thompson, B., Hazardous Gases and Vapors: Infrared Spectra and Physical Constants (Beckman Instruments Inc. Tech. Report No.595, Fullerton, Ca, 1974).
- Verniani, F., The Total Mass of the Earth's Atmosphere, J. Geophys. Res., 71, 385-391 (1961).
- Walker, J.C.G., Evolution of the Atmosphere (Macmillan Publishers, N.Y., 1977).
- Wang, W.C., Y.L.Yung, A.A.Lacis, T.Mo and J.E.Hansen, Greenhouse Effects Due to Man-Made Perturbations of Trace Gases, Science 194, 685-690 (1976).
- Warneck, P., OH Production Rates in the Troposphere, Planetary & Space Sci., 23, 1507-1518 (1975).
- Warneck, P., The Role of Chemical Reactions in the Cycle of Atmospheric Trace Gases, Especially CH₄. Proc. Symp. on Microbial Production and Utilization of Gases (H₂, CH₄, CO), Göttingen 1975 (E.Goltze KG, Göttingen, 1976).

- Watson, R.T., G.Machado, B.Conaway, S.Wagner and D.D.Davis, A Temperature Dependent Kinetics Study of the Reaction of OH with CH_2ClF , CHCl_2F , CHClF_2 , CH_3CCl_3 , $\text{CH}_3\text{CF}_2\text{Cl}$ and $\text{CF}_2\text{ClCFCl}_2$, J. Phys. Chem, 81, 256-262³(1977).
- Yung, Y.L., J.P.Pinto, R.T.Watson and S.P.Sander, Atmospheric Bromine and Ozone Perturbations in the Lower Stratosphere. Contribution No. 3215 of the Division of Geological and Planetary Sciences, California Institute of Technology; Pasadena Calif, (Preprint) (1979).
- Zimmerman, P.R., Determination of Emission Rates of Hydrocarbons from Indigenous Species of Vegetation in the Tampa/St.Petersburg, Florida Area. Final Report Submitted the the U.S.Environmental Protection Agency from the Air Pollution Research Section of the College of Engineering, Washington State University, Pullman, Wash. (1979).

APPENDIX I:

DETAILS OF CALCULATIONS

Chapter 2.

1. MEASUREMENTS OF CFC1_3 , CCl_2F_2 , CH_3CCl_3 , CCl_4 AND N_2O

	Pacific Northwest Concentration pptv	Antarctica Concentration pptv	Ratio N/S
January 1975			
F-11	125	90	1.39
CCl_4	130	120	1.08
CH_3CCl_3	90	54	1.67
January 1976			
F-12	228	195	1.17
F-11	138	113 (109)*	1.22
CCl_4	133	121	1.10
CH_3CCl_3	98	57	1.72
January 1977			
F-12	251	216	1.16
F-11	154	127 (128)*	1.21
CCl_4	144	128	1.13
CH_3CCl_3	107	70	1.53
N_2O	330 ppbv	330 ppbv	1.00
January 1978			
F-12	280	244	1.15
F-11	166	145 (149)*	1.14
CCl_4	154	123	1.25
CH_3CCl_3	117	85	1.38
N_2O	332 ppbv	331 ppbv	1.00
January 1979			
F-12	300	260	1.15
F-11	173	154	1.12
CCl_4	140	135	1.04
CH_3CCl_3	135	95	1.42
N_2O	332 ppbv	332 ppbv	1.00

*Tasmania Data

2. α and ζ from eqns. (2.6) and (2.7):

ζ	0.15	0.20	0.25	0.5	1.0
α	0.844	0.853	0.862	0.91	1.00

3. Lifetimes, eqn. (2.4)

(a) CH_3CCl_3 , global average theory

ξ_T (pptv)	$\ln \xi_T$	t
72	4.277	0 1/1975
77.5	4,350	1 1/1976
88.5	4.483	2 1/1977
101	4.615	3 1/1978
115	4.745	4 1/1979

$$\xi_T = 70.37e^{0.1201t}$$

$$\xi_* = 308 \text{ pptv}$$

(b)	time	release (millions of lbs)
	1/1975-1/1976	804
	1/1976-1/1977	914
	1/1977-1/1978	980
	1/1978-1/1979	1100

$$S_* = 3801 \times 10^6 \text{ lbs} = 73 \text{ pptv} \quad (10^6 \text{ lbs} = 0.0192 \text{ pptv})$$

Choosing ζ and using the eqns. (2.1) - (2.7), the results of

Table (2.1) follow.

(c) F-11 global average theory.

$$\xi_T = 110.95 e^{0.1053t}$$

$$\text{For } \xi_T = ae^{bt} \quad \xi_* = \alpha \int_0^T ae^{bt} dt = \frac{\alpha a}{b} (e^{bT} - 1)$$

Source: $341 \times 10^6 \text{ kg/yr} = 19.3 \text{ pptv/yr.}$

$N = 10.641 \times 10^{43} \text{ molecules (see Chapter 8)}$

$10^6 \text{ kg} = 0.04118 \text{ pptv.}$

Taking $\zeta = 0.2$ gives $\tau = 56$ and assuming $\xi_{1*} = 0.9\xi_*$ gives $\tau = 32 \text{ yrs.}$
(i.e., measurements are too high by 10%).

(d) F-12 global average theory.

$$\xi_T = 212.53 \times e^{0.0957t}$$

Source: $413 \times 10^6 \text{ kg/yr} = 19.3 \text{ pptv/yr}$

$10^6 \text{ kg} = 0.0468 \text{ pptv}$

$S_* = 58 \text{ pptv (3 yrs.)}$

Take $S'_* = 1.1 S_*$, $\xi'_* = 0.9\xi_*$, $\Delta\xi' = 0.9\Delta\xi$, $\zeta = 0.25 \Rightarrow \tau > 70 \text{ yrs.}$

4. Simulation method (eqn. 2.8)

$S = 765.5 e^{0.1047t}$ in millions of lbs per yr.

Cumulative release for the year is $\int_t^{t+1} S dt'$,

$$\xi = \xi_0 e^{-\eta t} + \frac{14.7}{0.1047 + \eta} (e^{0.1047t} - e^{-\eta t}) \text{ (in pptv)}$$

time	ξ^1 (pptv)	$\xi(\tau)$ (pptv) for specified τ				
		τ (yrs) = 6	8	9	10	12
1/1975	64.3	64	63.5	63.0	62.5	62.5
1/1976	69.2	68.5	70.6	71.1	71.3	72.4
1/1977	79.0	73.8	78.5	79.9	80.9	83.1
1/1978	90.2	80.1	87.3	89.6	91.4	94.8
1/1979	102.7	87.4	97.0	100.3	102.9	107.6

Figure (2.1) is based on this table.

ξ^1 based on measured concentrations, $\zeta = 0.25$.

Calculations, assuming that the measured values (ξ^1) are too high by 10%:

time	ξ^1 (pptv)	$\tau = 6$	8
1/1975	57.9	58	56
1/1976	62.3	63.4	64
1/1977	71.1	69.5	72.7
1/1978	81.2	76.5	82.1
1/1979	92.4	84.3	92.5

5. Hemispherically averaged theory:

(a) CH_3CCl_3 , eqns. (2.15) and (2.16)

time	ξ_{nT}	$\ln \xi_{nT}$	ξ_{sT}	$\ln \xi_{sT}$
1/1975	85.4	4.447	58.6	4.071
1/1976	92.8	4.530	62.2	4.130
1/1977	102.3	4.628	74.7	4.310
1/1978	112.9	4.727	89.1	4.490
1/1979	129.9	4.867	100.1	4.606

$$\xi_{nT} = 84.1 e^{0.1037t} ; \quad \xi_{sT} = 56.6 e^{0.143t}$$

The subscript T refers to tropospheric values. To get ξ_n and ξ , multiply by α , which is taken to be 0.862 in this study corresponding to $\zeta = 0.25$. This gives the results of Table (2.2).

(b) CH_3CCl_3 simulation method

ξ_{no} and ξ_{so} are corrected for latitudinal variation and smaller stratospheric concentrations ($\zeta = 0.25$). In all cases $S_{\text{n}} = 29.4 e^{0.1047t}$ (pptv/yr)

(i) $\tau_{\text{T}} = 1.2$ yrs, $\tau_{\text{n}} = 12$ yrs, $\tau_{\text{s}} = 6$ yrs, ($\tau = 8.5$ yrs)

$\xi_{\text{no}} = 72$ pptv, $\xi_{\text{so}} = 46.5$ pptv (based on measurements)

$$\xi_{\text{n}} = 3.6 e^{-1.792t} - 6.79 e^{0.123t} + 75.254 e^{0.1047t}$$

$$\xi_{\text{s}} = -4.604 e^{-1.792t} - 6.583 e^{0.123t} + 57.733 e^{0.1047t}$$

Predicted values of ξ_{n} and ξ_{s} :

time	ξ_{n}	ξ_{s}
1/1975	72	46.5
1/1976	78.2	57.5
1/1977	87.6	65.9
1/1978	98.3	74.5
1/1979	110.2	83.7

(ii) $\tau_{\text{T}} = 1.2$ yrs, $\tau_{\text{n}} = 16$ yrs, $\tau_{\text{s}} = 8$ yrs, ($\tau = 11$ yrs)

$\xi_{\text{on}} = 72$ pptv, $\xi_{\text{os}} = 46.5$ pptv

$$\xi_{\text{n}} = 3.87 e^{-1.761t} - 16.43 e^{-0.0933t} + 84.63 e^{0.1047t}$$

$$\xi_{\text{s}} = -4 e^{-1.761t} - 15.87 e^{-0.0933t} + 66.4 e^{0.1047t}$$

Predicted values of ξ_n and ξ_s

time	ξ_n	ξ_s
1/1975	72	46.5
1/1976	79.7	58.6
1/1977	90.8	68.6
1/1978	103.5	78.9
1/1979	117.3	90.0

(iii) $\tau = 1.2$ yrs, $\tau_n = 8$ yrs, $\tau_s = 4$ yrs ($\tau \approx 5$ yrs),

$$\xi_{on} = 72 \text{ pptv}, \xi_{os} = 46.5 \text{ pptv}.$$

$$\xi_n = 3.19 e^{-1.856t} + 7.381 e^{-0.185t} + 61.647 e^{0.1047t}$$

$$\xi_s = -3.42 e^{-1.856t} + 6.92 e^{-0.185t} + 43.14 e^{0.1047t}$$

Predicted values of ξ_n and ξ_s

time	ξ_n	ξ_s
1/1975	72	46.5
1/1976	75.1	53.1
1/1977	81.2	57.9
1/1978	88.6	63.0
1/1979	101.1	68.9

Figure (2.2) is based on the three tables in this section.

(c) Simulation method for F-11

$$S_n = 28 \text{ pptv/yr}, \xi_{on} = 103 \text{ pptv}, \xi_{on} = 81 \text{ pptv},$$

$$\tau_T = 1.3 \text{ yrs}, A_o = 184 \text{ pptv}, B_o = 22 \text{ pptv} \text{ and } \zeta = 0.2$$

Time			$\tau = 10 \text{ yrs}$		20 yrs	
	ξ_n	ξ_s	ξ_n	ξ_s	ξ_n	ξ_s
1/1975	102.8	80.6	103	81	103	81
1/1976	115.1	97.3	105.6	87.3	110.4	91.9
1/1977	128.4	111.3	109.3	92.1	118.8	101.0
1/1978	139.6	127.4	113.0	95.9	127.0	109.4
1/1979	145.5	133.4	116.4	99.2	134.9	117.3

Time	$\tau = 30 \text{ yrs}$		50 yrs		∞	
	ξ_n	ξ_s	ξ_n	ξ_s	ξ_n	ξ_s
1/1975	103	81	103	81	103	81
1/1976	112.1	93.4	113.4	94.6	115.5	96.5
1/1977	122.2	104.2	124.9	106.8	129.2	110.8
1/1978	132.1	114.3	136.4	118.4	143.1	124.9
1/1979	141.9	124.0	147.7	129.8	157.1	138.9

Based on measured values with $\zeta = 0.2$.

Apparently $\tau = 30\text{-}50$ years is in agreement with the data.

If it is assumed that the true source is 20% bigger than that assumed earlier, then the following results:

($S = 33.6 \text{ pptv/yr} = 408 \text{ million kg/yr}$)

Predicted concentrations:

Time	$\tau = 10$ yrs		$\tau = 20$ yrs	
	ξ_n	ξ_s	ξ_n	ξ_s
1/1975	103	81	103	81
1/1976	109.6	88.8	114.6	93.2
1/1977	116.1	95.5	125.8	104.6
1/1978	122.0	101.4	136.6	115.4
1/1979	127.3	106.8	146.8	125.7

Figure (2.3) is based on the two tables given in this section, 5 c.)

Chapter 3.(1) Calculations of τ_{HO}

The numbers in the tables are values of τ_{HO} (yrs) for selected values of τ_h (yrs), τ_s (yrs), and τ (yrs)

$\tau_s = 30$ yrs								
	τ_h	10	20	30	50	70	100	∞
τ								
6	30	12.0	10.0	8.8	8.4	8.1	7.5	
7	105	16.7	13.1	11.2	10.5	10.0	9.1	
8	--	24.0	17.1	14.0	12.9	12.2	10.9	
9	--	36.0	22.5	17.3	15.7	14.8	12.9	
10	--	60.0	30.0	21.4	19.1	17.6	15.0	
11	--		41.3	26.6	23.1	21.0	17.4	
12	--		60.0	33.3	28.0	25.0	20.0	

$\tau_s = 40$ yrs								
	τ_h	10	20	30	50	70	100	∞
τ								
6	24	10.9	9.2	8.2	7.9	7.6	7.1	
7	56	14.7	11.8	10.2	9.7	9.3	8.5	
8	--	20.0	15.0	12.5	11.7	11.1	10.0	
9	--	27.7	18.9	15.1	13.9	13.0	11.6	
10	--	40.0	24.0	18.2	16.5	15.4	13.3	
11	--	--	--	21.8	19.4	17.9	15.2	
12	--	--	--	26.1	22.7	20.7	17.1	

$\tau_s = 50$ yrs

	τ_h 10	20	30	50	70	100	∞
τ							
6	21.4	10.3	8.8	7.9	7.5	7.3	6.8
7	--	13.7	11.1	9.7	9.2	8.9	8.1
8	--	18.2	13.9	11.8	11.0	10.5	9.5
9	--	24	17.2	14.1	13.0	12.3	11.0
10	--	--	21.3	16.7	15.2	14.3	12.5
11	--	--	26.3	19.6	17.6	16.4	14.1
12	--	--	33.0	23.1	20.4	18.8	15.8

(2) Calculations of $\overline{[HO]}$

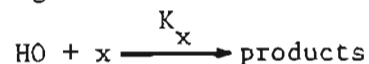
The numbers in the tables are values of $[HO]$ in molecules per cm^3 for selected values of τ_h , τ_s and τ

$\tau_s = 30$ yrs

	τ_h 10	20	30	50	70	100	∞
τ							
6	0.9	2.2	2.7	3.1	3.2	3.3	3.6
7	0.2	1.61	2.1	2.4	2.6	2.7	3.0
8	--	1.11	1.6	1.9	2.1	2.2	2.5
9	--	--	1.2	1.6	1.7	1.8	2.1
10	--	--	--	1.3	1.4	1.5	1.8
11	--	--	--	1.0	1.2	1.3	1.6
12	--	--	--	--	--	--	1.4

$\tau_s = 40 \text{ yrs}$						
τ_h	20	30	50	70	100	∞
τ						
6	2.5	2.9	3.3	3.4	3.6	3.8
7	1.8	2.3	2.7	2.8	2.9	3.2
8	1.4	1.8	2.2	2.3	2.4	2.7
9	1.0	1.4	1.8	2.0	2.1	2.3
10	--	1.1	1.5	1.6	1.8	2.0
11	--	--	1.2	1.4	1.5	1.8
12	--	--	--	1.2	1.3	1.6
 $\tau_s = 50 \text{ yrs}$						
τ_h	20	30	50	70	100	∞
τ						
6	2.6	3.1	3.4	3.6	3.7	4.0
7	2.0	2.4	2.8	2.9	3.0	3.3
8	1.5	2.0	2.3	2.5	2.6	2.9
9	1.1	1.6	1.9	2.1	2.2	2.5
10	--	1.3	1.6	1.8	1.9	2.2
11	--	--	1.4	1.5	1.7	1.9
12	--	--	1.2	1.3	1.4	1.7

(3) Relative strengths of HO sinks.



The strength of species x as a sink for HO is given by:

$$\sigma_x = K_x [\text{x}]$$

under steady state conditions. Let R be defined as:

$$R = \frac{K_x [\text{x}]}{K_{\text{CO}} [\text{CO}]}$$

where R gives the approximate strength of the sink of HO by reactions with species x relative to CO. The bigger R is, the more important species x is in determining HO densities. The table given below reviews the strengths of some atmospheric gases.

Boundary Layer Calculations:

Species x	$K_x \frac{\text{cm}^3}{\text{molec-sec}}$	$[\text{x}] (\text{ppb})$	R_x
CO	$\sim 1.4 \times 10^{-13}$	~ 120	1
CH ₄	$\sim 6.3 \times 10^{-15}$	~ 1400	0.5
NO ₂	$4-6 \times 10^{-12}$	~ 1	0.3
HNO ₃	8.5×10^{-14}	~ 10	0.05
H ₂	5.8×10^{-15}	~ 500	0.17
CH ₃ Cl	4.2×10^{-14}	~ 0.6	0.001
NH ₃	1.5×10^{-13}	~ 6	0.05
C ₅ H ₈	$5-6 \times 10^{-11}$	~ 0.5	1.5-2

The ratios R_x cannot be simply extrapolated to global scales. The concentrations assumed in the column $[\text{x}]$ are ambient levels reported in

the references (Giddings, 1973; Heicklen, 1976; and Walker, 1977). The rate constants are from DeMore et al. (1979), Atkinson et al. (1978) and Graedel (1978).

This table is constructed as a heuristic aid and should not be taken as a statement of the global HO sink.

(4) Equations for $\langle \tau \rangle$

One refinement of eqn. (3.16) is to divide the troposphere into three pieces by latitude: (1) $-\pi/2 \leq \phi \leq -\pi/6$; (2) $-\pi/6 \leq \phi \leq \pi/6$; and (3) $\pi/6 \leq \phi \leq \pi/2$. Assume that the regions (1) and (3) have the same atmospheric characteristics (same density, scale height, tropopause height, etc.). Regions (1) and (3) are specified by: z_{T1} , H_1 , ρ_{o1} , T_{o1} and ℓ_2 . Region (2) is specified by z_{T2} , H_2 , ρ_{o2} , T_{o2} and ℓ_2 . In this case eqn. (3.6) becomes:

$$\langle \tau \rangle = \frac{H_2 (1 - e^{-z_{T2}/H_2}) + \frac{\rho_{o1}}{\rho_{o2}} H_1 (1 - e^{-z_{T1}/H_1})}{(K_{o2}/\Gamma_2) (1 - e^{-\Gamma_2 z_{T2}}) [\overline{HO}]_{o2} + \frac{\rho_{o1}}{\rho_{o2}} (K_{o1}/\Gamma_1) (1 - e^{-\Gamma_1 z_{T1}}) [\overline{HO}]_{o1}}$$

where

$$\Gamma_i = \frac{1}{H_i} + \frac{1}{h_i} + \beta_i \quad i = 1, 2$$

$$\beta_i = \frac{E \ell_i}{T_{oi}^2} \quad i = 1, 2$$

It is assumed that z_T is the average tropopause height in the regions from $-\pi/2 \leq \phi \leq -\pi/6$ and $\pi/6 \leq \phi \leq \pi/2$. The tropopause height between $-\pi/6 < \phi < \pi/6$ is fairly constant (at about 16 km) (Reiter, 1975).

$\overline{[HO]}_{o_2}$ and $\overline{[HO]}_{o_1}$ are the mean hydroxyl radical concentrations in regions (2) and (1) respectively. $\overline{[HO]}_{o_2}$ is much smaller than $\overline{[HO]}_{o_1}$ ($\overline{[HO]}_{o_2} / \overline{[HO]}_{o_1} \sim 0.2 - 0.5$), thus making the lower half of the troposphere between $\phi \leq |\pi/6|$ the region where most of the destruction of trace gases, with HO sinks, takes place.

The lifetime within smaller regions of the troposphere can be written as:

$$\langle \tau \rangle_v = \frac{\int_v \rho \xi dv}{\int_v k[HO] \rho \xi dv}$$

where v is the appropriate volume in the troposphere.

Chapter 4.1. Analysis of the global CH_2CCl_3 emissions:(a) Table 1: Source analysis for CH_2CCl_3

Year	Time	$\ln S^{(1)(2)}$	$\Delta_1(t)^{(3)}$	$\alpha \cos(\omega t + \phi)^{(4)}$	$\Delta_2(t)$
1963	0	4.718	-0.157	-0.152	-0.005
1964	1	4.828	-0.178	-0.207	+0.029
1965	2	5.081	-0.100	-0.092	-0.008
1966	3	5.481	+0.147	+0.100	+0.047
1967	4	5.663	+0.176	+0.208	-0.032
1968	5	5.768	+0.128	+0.147	-0.019
1969	6	5.790	-0.003	-0.035	-0.032
1970	7	5.832	-0.114	-0.188	+0.074
1971	8	5.908	-0.191	-0.187	-0.004
1972	9	6.230	-0.022	-0.033	+0.011
1973	10	6.620	+0.215	+0.148	+0.067
1974	11	6.685	+0.127	+0.208	-0.081
1975	12	6.690	-0.021	+0.096	-0.117
1976	13	6.821	-0.043	-0.093	+0.050
1977	14	6.888	-0.129	-0.207	+0.078
1978	15	7.003	-0.167	-0.150	-0.017

1. S = discrete source in millions of lbs/yr.
2. $\ln S = \ln a + bt$; least squares values for $\ln a$, b are 4.85 and 0.153/yr respectively.
3. $\Delta_1 = \ln S - \alpha_0 - (\ln a + bt)$; $\alpha_0 = 0.025$
4. $\alpha = 0.21$, $\omega = 0.94$ rad/yr, $\phi = 2.38$ rad. (see table 2).
5. $\Delta_2 = \Delta_1 - \alpha \cos(\omega t + \phi)$.

(b) Determination of ω and ϕ in Δ_1 .

Table (2)

t	$\cos^{-1} \left[\frac{\Delta_1}{\alpha} \right]$	
0	2.42	$\alpha = 0.21$
1	3.70	Least squares values of ω and ϕ are
2	4.22	$\omega = 0.94$ rad/yr, $\phi = 2.38$ rad
3	5.21	
4	5.71	
5	7.20	
6	7.87	
7	8.43	
8	9.00	
9	10.89	
10	12.57	
11	13.49	
12	14.24	
13	14.34	
14	14.80	
15	16.36	

(c) $\Delta_2(t)$ for CH_3CCl_3 (1972-1977)

Table (3)

t	Yr	Δ_2^1	$\Delta_2 = -0.01 + 0.11 \cos(1.57t + 5.1)$	$\Delta_3 = \Delta_2^1 - \Delta_2$
0	1972	+0.011	+0.032	-0.021
1	1973	+0.092	+0.092	0.000
2	1974	-0.072	-0.051	-0.021
3	1975	-0.117	-0.112	-0.005
4	1976	+0.051	+0.031	+0.020
5	1977	+0.086	+0.092	-0.006

$$\langle |\Delta_2^1| \rangle = 0.072 \quad \langle |\Delta_3^1| \rangle = 0.012$$

$\Delta_2(t)$ is defined by:

$$\frac{\tilde{S}}{ae^{bt}} - 1 - \alpha \cos(\omega t + \phi) = \Delta_2(t)$$

$$\tilde{a} = ae^{\alpha_0} \quad (\text{see table 1})$$

The Δ_2 defined as above compensates for the error in making the approximation $\exp[\alpha \cos(\omega t + \phi)] = 1 + \alpha \cos(\omega t + \phi)$

Comments on tables (1) and (2)

$$\frac{1}{N+1} \sum_{i=0}^N \Delta_1(t_i) = 0.12 = \bar{\Delta}_1$$

$$\frac{1}{N+1} \sum_{i=0}^N \Delta_2(t_i) = 0.04 = \bar{\Delta}_2$$

These are the average deviations of the emissions data from $\ln S = \ln a + bt$ and $\ln S = \ln a + bt + \alpha_0 + \alpha \cos(\omega t + \phi)$, respectively. If the

theoretical expression for the source is $S_1 = ae^{bt}$, then the relative error between this function and the emissions data is

$$\begin{aligned}\frac{\delta S_1}{S_1} &\equiv \frac{S_1 - S}{S_1} = (1 - e^{\Delta_1}) \\ &\approx - [\Delta_1(t) + \frac{1}{2} \Delta_1^2(t)] \\ &\approx - \Delta_1(t)\end{aligned}$$

This holds since the source data are $S = ae^{bt} e^{\Delta_1}$; by the definition of Δ_1 . Similarly, if the theoretical source expression is $S = ae^{bt} e^{\alpha_0 + \alpha \cos(\omega t + \phi)}$ then $S = S_2 e^{\Delta_2}$ so that the error is

$$\frac{\delta S_2}{S_2} = \frac{S_2 - S}{S_2} = (1 - e^{\Delta_2}) \approx -\Delta_2$$

or

$$\left| \frac{\delta S_1}{S_1} \right| \approx |\Delta_1| \quad \left| \frac{\delta S_2}{S_2} \right| \approx |\Delta_2|$$

2. Comparison of time series data for CH_3CCl_3 with the prediction of steady and fluctuating source theories.

(a) Source term given by $S = ae^{bt}$

$$\xi_0 \approx 9 \text{ ppt} \quad , \quad \frac{a'}{b+\eta} = 10.401 \text{ pptv}$$

$$T_0 = \left(\xi_0 - \frac{a'}{b+\eta} \right) e^{-\eta t} \approx -1.4 e^{-\eta t}$$

$$\xi = T_0 + \frac{a'}{b+\eta} e^{bt} \quad (\text{Table 4})$$

Table (4): Concentrations predicted by simple source theory and observations:

$$\tau = 12.8 \text{ yrs}$$

Year	ξ Predicted	ξ Meas.	$\delta\xi/\xi$	Time (yrs)
1/75	65 pptv	72	-0.094	12
1/76	76	77½	-0.018	13
1/77	88	88½	+0.003	14
1/78	103	101	+0.026	15
1/79	120	115	+0.048	16

Mean deviation ≈ 0.04 (≈ 0.024 for the last four yrs)

(b) Source term with Δ_1

$$S = a' e^{bt} [1 + \alpha' \cos(\omega t + \phi')]$$

$$\xi = \left[\xi_0 - \frac{a'}{b+\eta} - \frac{\omega \alpha' a'}{\omega^2 + (b+\eta)^2} f_0(\phi') \right] e^{-\eta t} +$$

$$\left[\frac{\omega \alpha' a'}{\omega^2 + (b+\eta)^2} f_0(\phi' + \omega t) + \frac{a'}{b+\eta} \right] e^{bt}$$

$$= a_0 e^{-\eta t} + a_1 e^{bt}$$

for $\tau = 11.8$ yrs: $a_0 = -1.9$ pptv,

$$a_1 = [10.43 + 0.546 f_0(\phi' + \omega t)]$$

Table (5): Concentrations predicted by fluctuating source theory with Δ_1 included.

Yr.	ξ Predicted	ξ Meas.	$\delta\xi/\xi$	Time (yrs)
1/75	67.4 pptv	72	0.064	12
1/76	79.6	77 $\frac{1}{2}$	0.027	13
1/77	90.1	88 $\frac{1}{2}$	0.018	14
1/78	100.1	101	0.009	15
1/79	113.6	115	0.012	16

Mean deviation ≈ 0.026 (≈ 0.016 for the last four yrs).

(c) Source term with Δ_1 and Δ_2

$$S = a^{-1} e^{bt} [1 + \alpha' \cos(\omega t + \phi') + \Delta_2 H(t-T)]$$

$$\Delta_2 = \alpha_* + \tilde{\alpha}_* \cos(\omega_* t + \phi_*) \quad (\text{from 1972-1977})$$

$$\xi = \hat{\xi} + \frac{A\alpha_*}{b+\eta} (e^{bt} - e^{-\eta t}) + \frac{\omega_* A \tilde{\alpha}_*}{\omega_*^2 + (b+\eta)^2} \left\{ e^{bt} f_o(\omega_* t + \phi_*) \right.$$

$$\left. - e^{-\eta t} f_o(\phi_*) \right\} H(t-T) = \hat{\xi} + T_2$$

$$H(t-T) = \begin{cases} 0 & t < T \\ 1 & t \geq T \end{cases} ; \quad A = a e^{bT} \quad (T = 9 \text{ yrs})$$

$\hat{\xi}$ = predicted concentrations when only Δ_1 is taken into account.

$$T_2 = +0.52, -1.29, -0.57, +1.42, +1.30 \quad \text{pptv}$$

$$t = 1/75, 1/76, 1/77, 1/78, 1/79 \quad \text{yr}$$

Table (6): Concentrations predicted by fluctuating source theory with Δ_1 and Δ_2 included

Yr.	ξ Predicted	ξ Meas.	$\delta\xi/\xi$	Time (yrs)
1/75	67.9 pptv	72	0.057	12
1/76	78.3	77 $\frac{1}{2}$	0.010	13
1/77	89.5	88 $\frac{1}{2}$	0.011	14
1/78	101.5	101	0.005	15
1/79	114.9	115	0.001	16

Mean deviation = 0.016 (= 0.007 for the last four years)

(d) Corrections of a , ω , ω_* , ϕ , ϕ_* : discrete to continuous source approximations (CH_3CCl_3):

$$S = ae^{bt} [1 + \Delta_1 + \Delta_2]$$

$$= S_0 [1 + \Delta_1 + \Delta_2].$$

Table (4):

$S_0 (\Delta_1, \Delta_2 = 0)$	S (with Δ_1)		S (with Δ_1 and Δ_2)	
$a = 127.7$	$a=131.0$	$a'=121.2$	$\tilde{\alpha}_* = 0.11$	$\tilde{\alpha}'_* = 0.12$
$a' = 118.2$	$\alpha=0.21$	$\alpha'=0.22$	$\phi_* = 5.2$	$\phi'_* = 4.3$
	$\phi=2.38$	$\phi'=1.91$		

Units: $[a]$ = millions of lbs; $[\alpha] = [\tilde{\alpha}_*]$ = dimensionless

$[\phi] = [\phi_*]$ = radians

3. Comment on Lifetimes.

The lifetimes that fit the global averages are higher than the true lifetimes of CH_3CCl_3 . The reason is that the source is divided by the total number of molecules in the total atmosphere, but the decline of the mixing ratio of CH_3CCl_3 in the stratosphere is not taken into account. These complications were avoided so that the observed mixing ratios could be used with a minimum of additional assumptions. It is assumed that the time varying stratospheric content is proportional to the tropospheric content as can be expected after a long time of almost exponential release, then the true average mixing ratio is smaller than that assumed here, but its rate of increase is the same as that which the observed time series gives (~ 0.12 – 0.13 per yr). For this reason, the increase of the concentration is the appropriate variable to compare. Since the true global mixing ratio is smaller than that adopted here, the true lifetimes are also smaller than those obtained here. In Chapter 8 these questions are discussed in greater detail.

If the true measured global mixing ratios are reduced by the same fraction every year to take the lower mixing ratio of the stratosphere into account (Chapter 8), the slope predicted by the simple source theory will remain the same ($0.153/\text{yr}$) as already discussed, though the lifetime in the global equation will go down. The fractional deviations of the observed and predicted concentrations will also remain the

same. If the source fluctuations are introduced, the magnitude of the fluctuations will increase due to a smaller lifetime. Since the fluctuating theory predicts maximum concentrations in 1/75-1/76 and minimum around 1/79, the maximum will be a little higher than before and the minimum a little lower. Therefore, the slope predicted by the fluctuating source theory (with the Δ_1 cycle) will become a little smaller if the lifetimes are shortened. This will bring it even closer to the slope of the time series measurements than found in this chapter.

Summary: If the lifetimes are reduced, as they should be to bring them closer to the true lifetimes, then the slope of the measured values and that predicted by the simple source theory will remain the same, but that for the fluctuating source theory will be in even better agreement with observations than before.

4. Statistical analysis for the slope of CH_3CCl_3 time series data:

(a) Tests of Slope

$$D_i = \ln \xi_i - \beta_o t_i$$

	$\beta_o = 0.15$	$\beta_o = 0.14$	$\beta_o = 0.13$
t	D_i	D_i	D_i
1	4.13	4.14	4.15
2	4.05	4.07	4.09
3	4.03	4.06	4.09
4	4.02	4.06	4.10
5	3.99	4.04	4.09

(i, j)	$\beta_0 = 0.15/\text{yr.}$ $\delta(D_j - D_i)$	$\beta_0 = 0.14/\text{yr.}$ $\delta(D_j - D_i)$	$\beta_0 = 0.13/\text{yr.}$ $\delta(D_j - D_i)$
(1, 2)	-	-	-
(1, 3)	-	-	-
(1, 4)	-	-	-
(1, 5)	-	-	-
(2, 3)	-	-	0
(2, 4)	-	-	+
(2, 5)	-	-	0
(3, 4)	-	0	+
(3, 5)	-	-	0
(4, 5)	-	-	-
$C = \sum_{i < j}^n \delta(D_j - D_i) =$	-10	-9	-3

$$\left. \begin{array}{l} H_0: \beta_0 = 0.15/\text{yr.} \\ H_1: \beta_0 < 0.15/\text{yr.} \end{array} \right\} \text{reject at 0.008 level.}$$

$$\left. \begin{array}{l} H_0: \beta_0 = 0.14/\text{yr.} \\ H_1: \beta_0 < 0.14/\text{yr.} \end{array} \right\} \text{reject at 0.04 level.}$$

(b) Confidence intervals and estimates of slope based on the Theil test.

$$N = \binom{n}{2};$$

Procedure: 1. evaluate the N sample slopes

$$S_{ij} = (Y_j - Y_i)/(t_j - t_i); i < j$$

2. Order the S_{ij} :
 $S^{(1)} \leq \dots \leq S^{(N)}$

3. $\hat{\beta}$ = estimate of slope

$\hat{\beta}$ = median $\{S_{ij}\}$:

$\hat{\beta} = S^{(k+1)}$ if N is odd and $N = 2k + 1$

$\hat{\beta} = \frac{1}{2} [S^{(k)} + S^{(k+1)}]$ if N = even and $N = 2k$.

t_i	1	2	3	4	5
Y_i	4.277	4.350	4.483	4.615	4.745

$\{S_{ij}\} = \{0.073, 0.103, 0.113, 0.117, 0.133, 0.133, 0.117, 0.132,$
 $0.131, 0.130\}$

$0.073 < 0.103 < 0.113 < 0.117 \leq 0.117 < 0.130 < 0.131 < 0.132$
 $< 0.133 \leq 0.133$

$\hat{\beta} = 0.124/\text{yr.}$

91.6% confidence interval.

Procedure: $(1 - \alpha)$ specifies the confidence coefficient with the Kendall k-statistic.

$C_\alpha = K(\frac{\alpha}{2}, n) - 2$ so that

$P_0 \{-C_\alpha < C < C_\alpha\} = (1 - \alpha).$

Define:

$$M_1 = \frac{1}{2} (N - C_\alpha)$$

$$M_2 = \frac{1}{2} (N + C_\alpha)$$

The $(1 - \alpha)$ confidence interval (β_L, β_U) is: $\beta_L = S^{(M_1)}$,
 $\beta_U = S^{(M_2 + 1)}$ where $S^{(j)}$ are the ordered values of S_{ij} obtained for
 the estimate of slope.

We choose $\alpha = 0.084$ which gives $C_\alpha = 6$, so that $M_1 = 2$, $M_2 = 8$,
 thus

$$\beta_L = 0.103/\text{yr} \text{ and } \beta_U = 0.133/\text{yr}.$$

$$P_\beta \{ \beta_L < \beta < \beta_U \} = 0.916$$

5. Fluctuations in the source strengths of CFCl_3 (F-11), CF_2Cl_2 (F-12)
 and CHClF_2 (F-22).

Δ_1 is computed and plotted for F-11, F-12, and F-22 from the re-
 lease estimated by McCarthy et al. (1977).

Time	Year	F-11 (CFCl ₃)		F-12 (CCl ₂ F ₂)		F-22 (CHClF ₂)	
		ln R	ln R-(a+bt)	ln R	ln R-(a+bt)	ln R	ln R-(a+bt)
0	1949	1.31	-0.690	3.19	0.068	-2.30	
1	1950	1.69	-0.472	3.30	0.057	-2.30	
2	1951	2.01	-0.312	3.41	0.046	-1.61	
3	1952	2.38	-0.106	3.45	-0.035	-1.20	
4	1953	2.69	0.042	3.57	-0.036	-0.92	
5	1954	2.91	0.100	3.70	-0.027	-0.51	
6	1955	3.12	0.148	3.82	-0.028	-0.22	
7	1956	3.34	0.206	3.97	0.001	0.18	-0.040
8	1957	3.46	0.164	4.10	0.01	0.10	-0.328
9	1958	3.40	-0.058	4.14	-0.071	0.34	-0.296
10	1959	3.42	-0.200	4.25	-0.082	0.99	0.146
11	1960	3.69	-0.092	4.43	-0.023	1.19	0.138
12	1961	3.94	-0.004	4.55	-0.024	1.28	0.020
13	1962	4.17	0.064	4.69	-0.005	1.53	0.062
14	1963	4.37	0.102	4.86	0.044	1.72	0.044
15	1964	4.54	0.110	5.01	0.073	1.92	0.036
16	1965	4.68	0.088	5.14	0.082	2.09	-0.002
17	1966	4.78	0.026	5.26	0.081	2.28	-0.020
18	1967	4.93	0.014	5.40	0.100	2.51	0.002
19	1968	5.06	-0.018	5.49	0.069	2.79	0.074
20	1969	5.21	-0.030	5.61	0.068	3.01	0.086
21	1970	5.34	-0.062	5.69	0.027	3.14	0.008
22	1971	5.45	-0.114	5.76	-0.024	3.27	-0.070
23	1972	5.57	-0.156	5.86	-0.045	3.43	-0.278
24	1973	5.71	-0.178	5.95	-0.076	3.58	-0.176
25	1974	5.83	-0.220	6.05	-0.097	3.73	-0.234
26	1975	5.83		6.02		3.85	-0.322
27	1976	5.85		6.06			

28	1977	5.79	6.02	
29	1978	5.73	5.85	
a		2.0	2.88	0.22
b		0.162/yr	0.121/yr	0.208
mean deviation		0.12	0.05	0.12

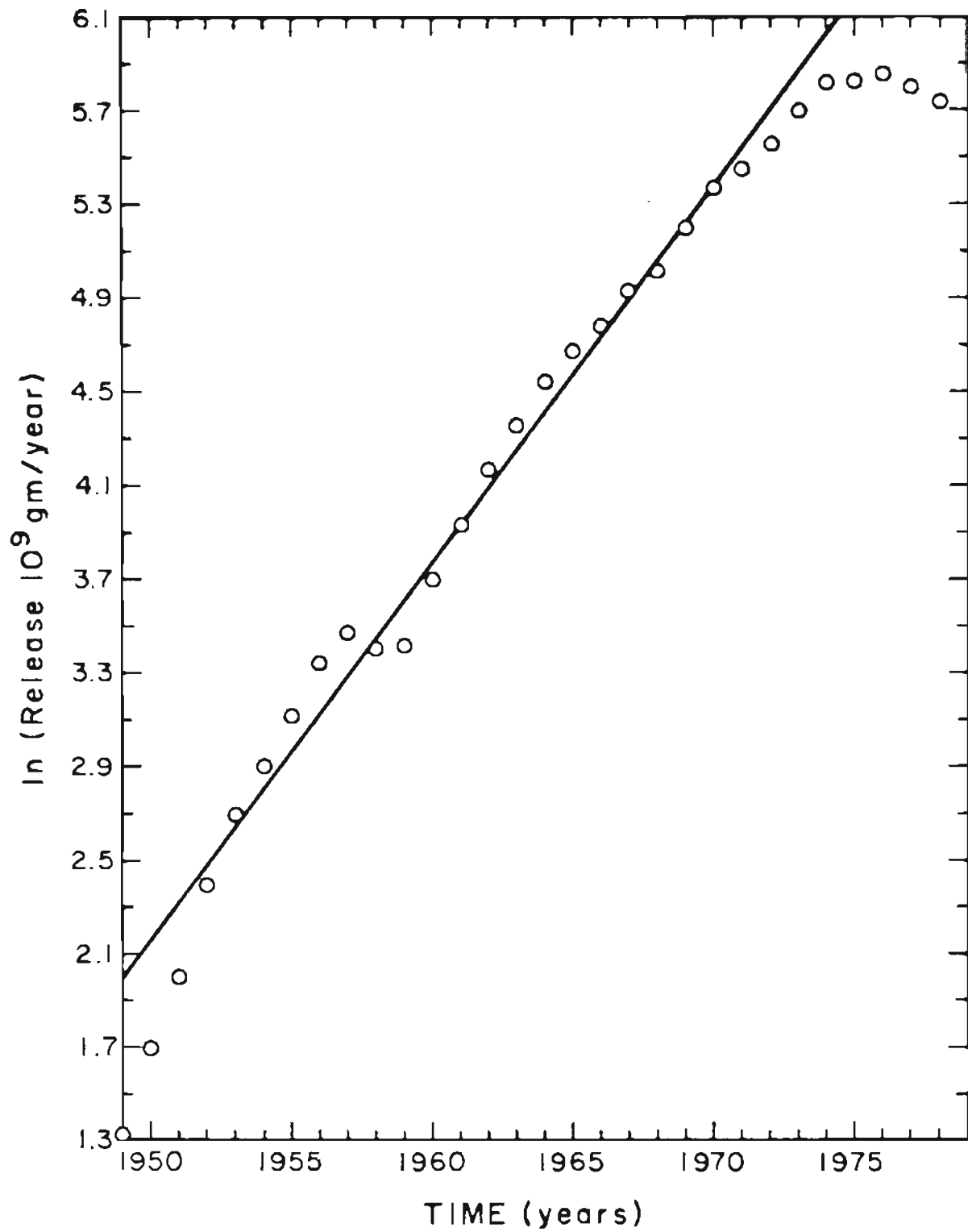


Figure (A4.1): Global emissions of CCl_3F (F-11) from 1949-1978.

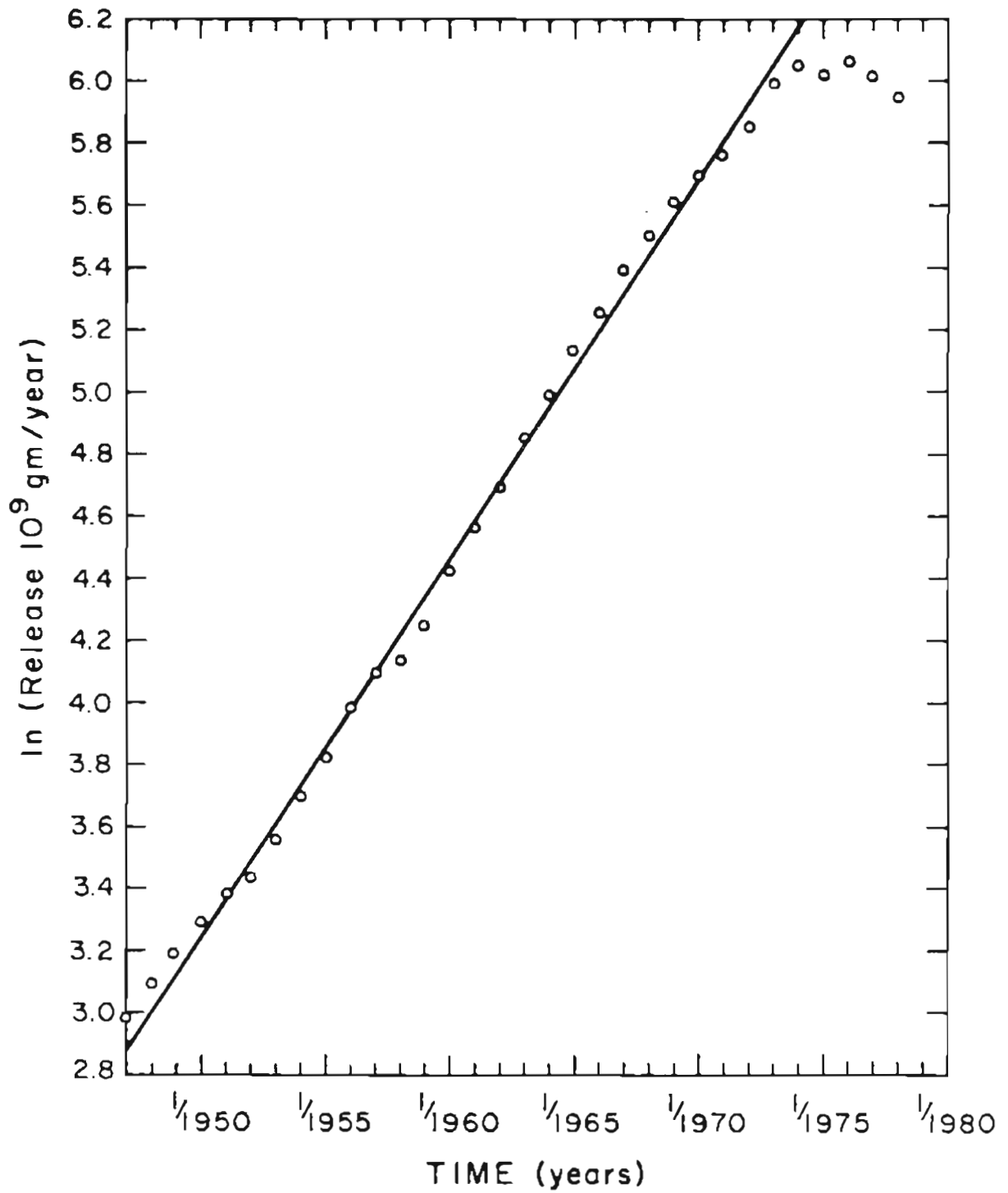


Figure (A4.2): Global emissions of CCl₂F₂ (F-12) from 1947-1978.

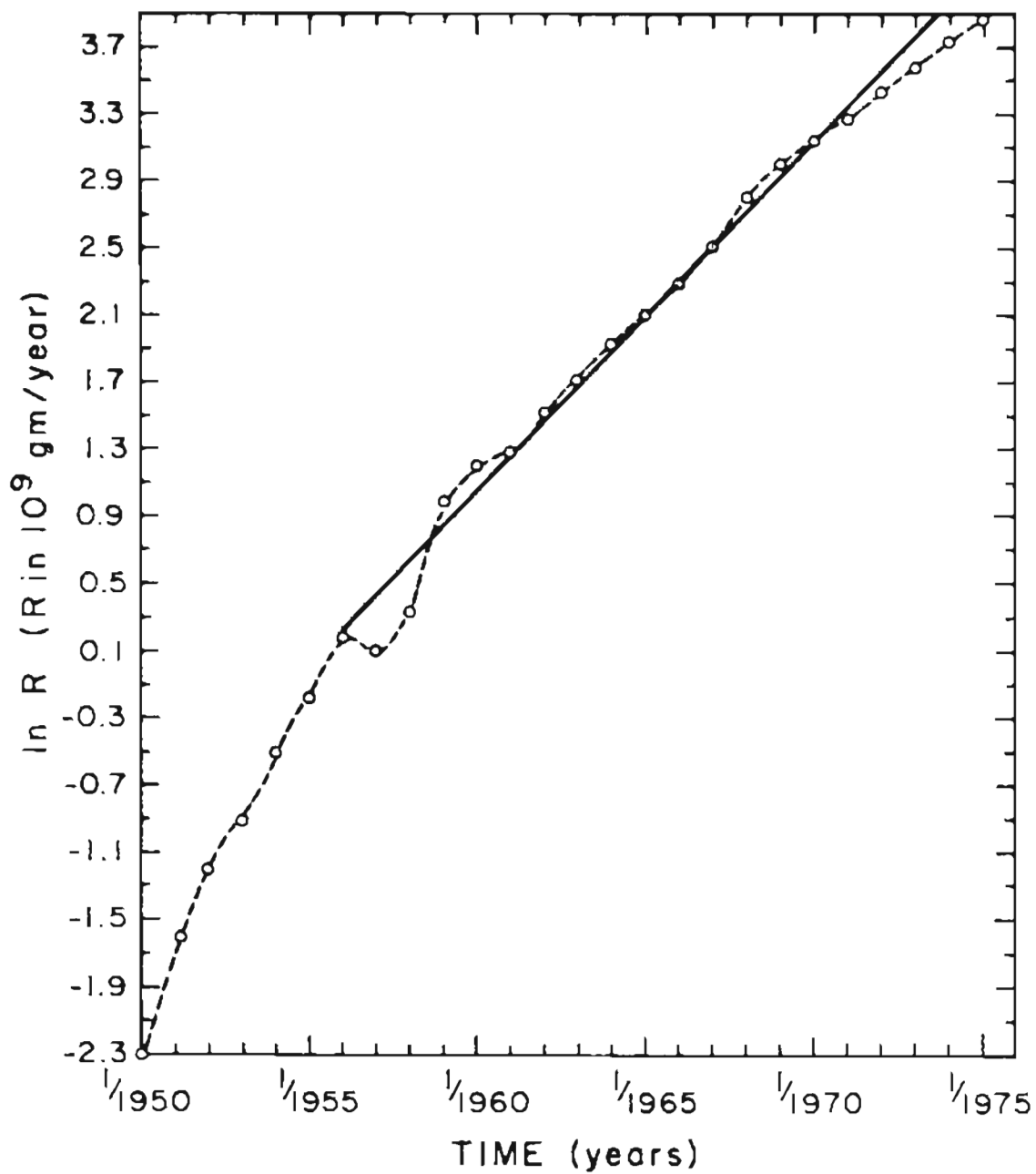


Figure (A4.3): Global emissions of CHClF₂ (F-22) from 1950-1976.

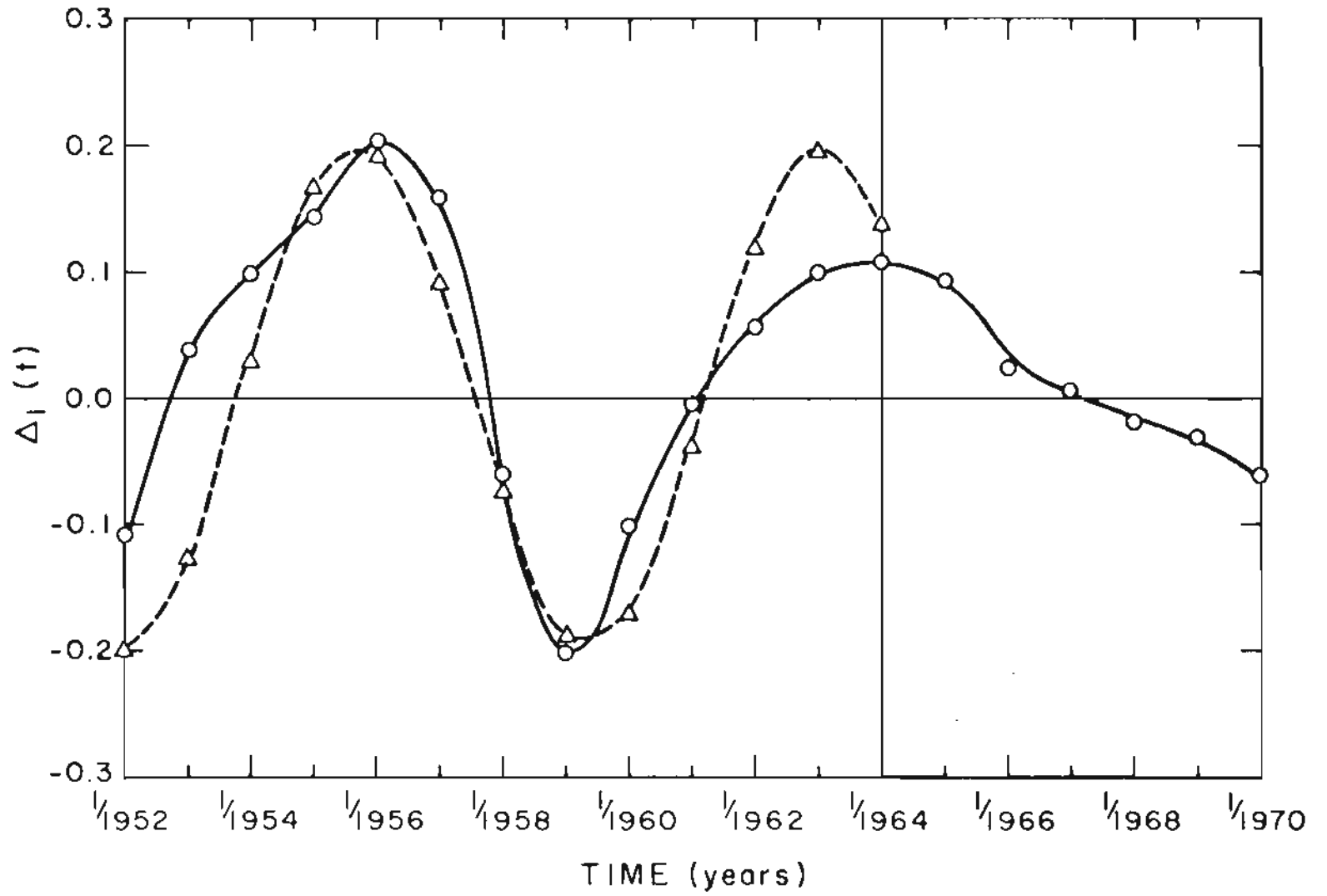


Figure (A4.4): Δ_1 function for the global emissions of CCl_3F (F-11).

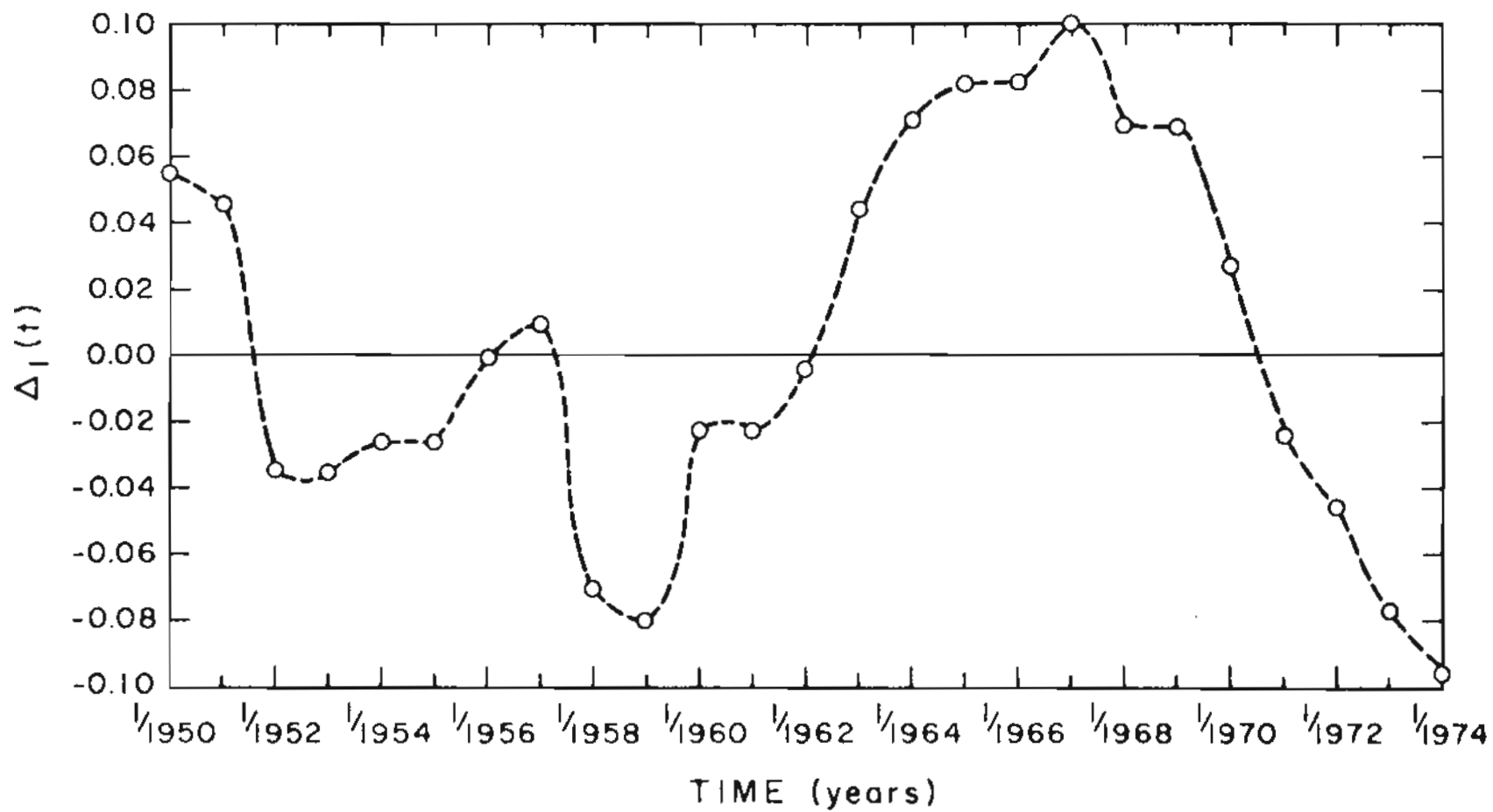


Figure (A4.5): Δ_1 function for the global emissions of CCl_2F_2 (F-12).

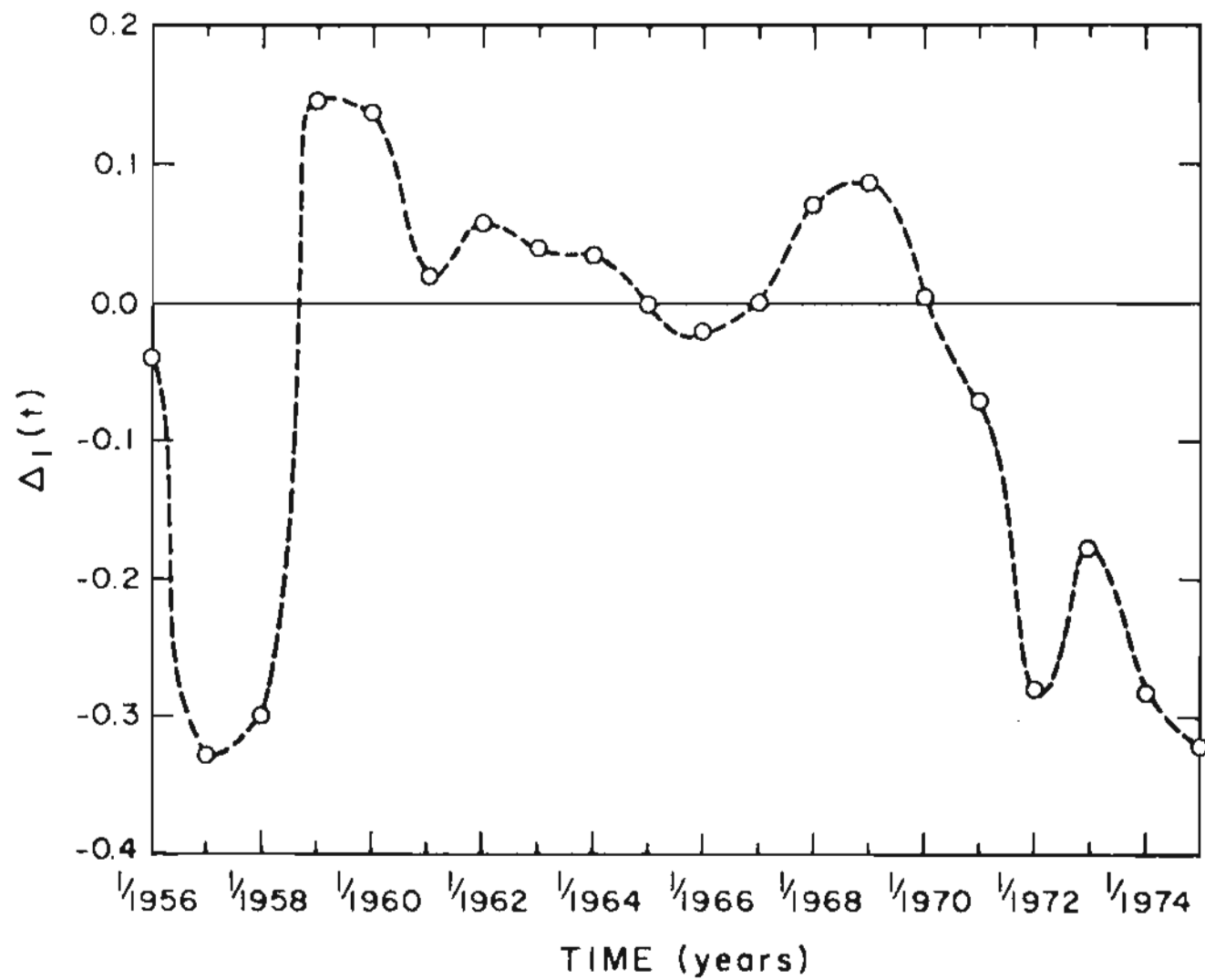


Figure (A4.6): Δ_1 function for the global emissions of CHClF_2 (F-22).

Chapter 5:

1. Statistical tests for trends of the gradient R_0 .

(a) Theil test

$$\delta (D_j - D_i)$$

(i, j)	CCl ₄	CCl ₃ F	CCl ₂ F ₂
(1, 2)	+1	-1	-1
(1, 3)	+1	-1	-1
(1, 4)	+1	-1	-1
(1, 5)	-1	-1	-1
(2, 3)	+1	-1	-1
(2, 4)	+1	-1	0
(2, 5)	-1	-1	
(3, 4)	+1	-1	
(3, 5)	-1	-1	
(4, 5)	-1	-1	
$C = \sum_{i < j} (D_j - D_i) =$	+2	-10	-5

$H_0: \beta_0 = 0$ accept for CCl₄, CCl₂F₂
 reject for CCl₃F

(b) t-test - trend and parallelism

Definition of symbols (see Edwards, 1976).

1. Variables R_0 , T (time).
2. Least squares slope: b_1

$$b_1 = \frac{\sum (R_o - \bar{R}_o) (T - \bar{T})}{\sum (T - \bar{T})^2}$$

where $\sum a$ is used to indicate $\sum_{i=1}^N a_i$ and \bar{a} is the mean of a_i .

$$3. (R_o - R_o')^2 = \sum (R_o - \bar{R}_o)^2 - \frac{\sum (R_o - \bar{R}_o) (T - \bar{T})^2}{\sum (T - \bar{T})^2}$$

$$4. S_{R,T}^2 = \frac{\sum (R_o - R_o')^2}{N - 2} = \text{residual variance}$$

where N is the number of observations

and $N-2$ are the degrees of freedom.

$$5. S_b = \left(\frac{S_{R,T}^2}{\sum x^2} \right)^{1/2} = \text{standard error of the regression coefficient where } x_i = (T_i - \bar{T}).$$

$$6. t = \frac{b - \beta}{S_b} \text{ to test the hypothesis } H_0: b = \beta \text{ versus}$$

alternatives $H_1: b > \beta$ or $b < \beta$, as the case may be.

H_0 is rejected if the calculated value of t is outside the critical values of t from the t -distribution for $N - 2$ degrees of freedom. Thus, the critical values of t for $N = 5$ are $t \geq 3.182$, $t \leq -3.182$. In this analysis the level of significance for rejecting the null hypothesis was fixed at $\alpha = 0.025$.

(i) CH_3CCl_3 $H_0: \beta = 0$, $H_1: \beta < 0$

$$b_* = -0.084$$

$$S_{R,T}^2 = 0.0063$$

$$S_b = 0.0251$$

$$df = 3$$

$$t = \frac{-0.084}{0.0251} = -3.35$$

Reject H_0

(ii) CCl_3F (F-11) $H_0: \beta = 0$, $H_1: \beta < 0$

$$b_1 = -0.062$$

$$S_{R,T}^2 = 0.0023$$

$$S_b = 0.0151$$

$$df = 3$$

$$t = -4.1$$

Reject H_0

(iii) CCl_4 $H_0: \beta = 0$, $H_1: \beta \neq 0$ $\alpha = 0.05$

$$b_1 = +0.007$$

$$S_{R,T}^2 = 0.0086$$

$$S_b = 0.0294$$

$$df = 3$$

$$t = 0.24$$

Accept H_0 .

(c) Test of parallelism for $\ln\xi_n$ and $\ln\xi_s$ as functions of time:

1. Common residual variance

$$S^2(\ln\xi_n | \ln\xi_s) = \frac{\Sigma y_1^2 - \frac{(\Sigma xy_1)^2}{\Sigma x_1^2} + \Sigma y_2^2 - \frac{(\Sigma xy_2)^2}{\Sigma x_2^2}}{N_1 + N_2 - 4}$$

$$y_1 = (\ln\xi_n - \overline{\ln\xi_n}), \quad y_2 = (\ln\xi_s - \overline{\ln\xi_s})$$

$$x_1 = x = x_2 = (T - \bar{T})$$

$$df = N_1 + N_2 - 4$$

2. Standard error of the difference between the two regression coefficients.

$$S_{b_n - b_s} = \left[S^2(\ln\xi_n | \ln\xi_s) \left(\frac{1}{\Sigma x_1^2} + \frac{1}{\Sigma x_2^2} \right) \right]^{\frac{1}{2}}$$

$$3. \quad t = \frac{(b_n - b_s) - (\beta_n - \beta_s)}{S_{b_n - b_s}}$$

The test of parallelism is $H_0: \beta_n - \beta_s = 0$ versus the alternative $\beta_n - \beta_s < 0$.

For CH_3CCl_3 ; $\alpha = 0.01$

$$b_n = 0.099; \quad b_s = 0.153 \quad (\text{per year})$$

$$b_n - b_s = -0.054$$

$$S^2(\ln\xi_n | \ln\xi_s) = 0.00125$$

$$S_{b_n - b_s} = 0.0158$$

$$df = 6$$

$$t = - 3.42$$

Reject H_0 . (critical $t = - 3.143$).

(d) Confidence interval for CH_3CCl_3 gradient.

$$b_{*L} = b_* - S_b t$$

$$b_{*u} = b_* + S_b t$$

For the 90% confidence interval $t = 2.353$ ($df = 3$)

$$b_{*L} = - 0.154$$

$$b_{*u} = - 0.025$$

2. Theoretical investigations of R_0 as a function of time.

(a) Use of eqn. (5.5):

$$\omega = 0.94, \alpha = 0.22, \phi' = 1.91$$

$$\sigma = 0.053$$

time	$t_* = 2 \text{ yrs } (\tilde{R}_0 = 1.56)$		$t_* = 2.5 \text{ yrs } (\tilde{R}_0 = 1.53)$	
	R_0 / \tilde{R}_0	R_0	R_0 / \tilde{R}_0	R_0
1/1975	1.093	1.71	1.102	1.69
1/1976	1.056	1.65	1.083	1.66
1/1977	0.979	1.53	0.999	1.53
1/1978	0.922	1.44	0.922	1.41
1/1979	0.926	1.44	0.908	1.39

(b) Two-box theory.

$$\tau = 11 \text{ yrs}, \omega = 0.9/\text{yr.}, \phi' = 1.94$$

τ_*	a_0	a_1	b_0	b_1	\bar{R}
1.7	0.062	0.036	0.046	-0.014	1.415
1.5	0.061	0.035	0.048	-0.013	1.366

time	$\tau_* = 1.7$		$\tau_* = 1.5$	
	R	R_0	R	R_0
1/1975	1.49	1.72	1.434	1.63
1/1976	1.47	1.69	1.411	1.60
1/1977	1.41	1.59	1.357	1.51
1/1978	1.35	1.50	1.309	1.44
1/1979	1.34	1.49	1.301	1.44

ω was taken as 0.9 rad/yr instead of 0.94 rad/yr to get a slightly better agreement between the source data and the source function during the past few years.

(c) Four-box theory.

Details of figures (5.4) and (5.5)

Fig. (5.4): Δ_1 cycle only

$$\eta = 0.12/\text{yr}; \bar{\eta} = 0.08/\text{yr}; \eta_T = 1.14/\text{yr}$$

(mean lifetime $\langle \tau \rangle = 10$ yrs).

η_0	a_0	a_1	b_0	b_1	\bar{R}_0
5	0.067	0.048	0.036	-0.023	1.524 (curve 1)
4	0.068	0.05	0.035	-0.025	1.57 (curve 2)
3.5	0.069	0.051	0.034	-0.025	1.604 (curve 3)

R_0			
time	Curve 1	Curve 2	Curve 3
1/1975	1.64	1.70	1.74
1/1976	1.57	1.62	1.66
1/1977	1.47	1.51	1.60
1/1978	1.41	1.44	1.47
1/1979	1.44	1.48	1.51

Fig. (5.5): Δ_1 and Δ_2 cycles

Figure (5.5) is based on the same assumptions as Figure (5.4) except that the Δ_2 cycle is added. The coefficients a_2 , a_3 , b_2 , and b_3 are based on $\omega_* = 1.57$, $\phi_* = 4.3$, $\tilde{\alpha}_* = 0.12$ as found in the previous chapter. The time t in the sine and cosine of $\omega_*t + \phi_*$ is 0 in 1975. The effects of this cycle are computed for the years from 1976 - 1979.

$\eta = 0.12/\text{yr}$; $\bar{\eta} = 0.08/\text{yr}$; $\eta_T = 1.14/\text{yr}$.

η_0	a_2	a_3	b_2	b_3	
5	0.028	0.015	0.005	-0.011	curve 1
4	0.028	0.017	0.005	-0.01	curve 2

time	R_o	
	Curve 1	Curve 2
1/1975	1.64	1.70
1/1976	1.59	1.65
1/1977	1.514	1.56
1/1978	1.39	1.42
1/1979	1.39	1.43

(d) Further details of the theory and calculation procedures:

The matrix P:

$$P \text{ satisfies } P^{-1}P = \Lambda = \begin{bmatrix} \lambda_1 & 0 & 0 & 0 \\ 0 & \lambda_2 & 0 & 0 \\ 0 & 0 & \lambda_3 & 0 \\ 0 & 0 & 0 & \lambda_4 \end{bmatrix}$$

$$j = 1, 2, 3, 4$$

$$P_{j1} = [(a - \lambda_j)(d - \lambda_j) - c^2]/bc \quad (1)$$

$$P_{j2} = (d - \lambda_j)/c \quad (2)$$

$$P_{j3} = [(a - \lambda_j)(d - \lambda_j) - c^2][b(d - \lambda_j)]^{-1} \quad (3)$$

$$\Rightarrow P_{13} = P_{23} = -1$$

$$P_{33} = P_{43} = +1 \quad \text{follows}$$

from the eigenvalue equation of M

$$P_{j4} = 1 \text{ for all } j. \quad (4)$$

$$a = (\eta + \eta_T + \eta_o) \quad (5)$$

$$b = \eta_T \quad (6)$$

$$c = \eta_o \quad (7)$$

$$d = (\bar{n} + \eta_0) \quad (8)$$

$$P_{32} = -1 + \frac{1}{2}(\bar{n} - \eta)/\eta_0 \approx -1 \quad (9)$$

$$P_{42} = 1 + \frac{1}{2}(\bar{n} - \eta)/\eta_0 \approx +1 \quad (10)$$

$$P_{31} = \frac{1}{\eta_0 \eta_T} \left[\frac{1}{2} (\eta - \bar{n}) + \eta_T \right] \left[-\eta_0 - \frac{1}{2}(\eta - \bar{n}) \right] \approx -1 \quad (11)$$

$$P_{41} \approx 1 \quad (12)$$

$$P_{12} = -P_{11} \quad \text{follows from the eigenvalue}$$

$$P_{22} = -P_{21} \quad \text{equation}$$

The equations for the eigenvalues are:

$$\lambda_1 = \frac{1}{2} (\eta + 2\eta_T + 2\eta_0 + \bar{n}) + \frac{1}{2} [(\eta + 2\eta_T - \bar{n})^2 + 4\eta_0^2]^{\frac{1}{2}}$$

$$\lambda_2 = \frac{1}{2} (\eta + 2\eta_T + \eta_0 + \bar{n}) - \frac{1}{2} [(\eta + 2\eta_T - \bar{n})^2 + 4\eta_0^2]^{\frac{1}{2}}$$

$$\left. \begin{aligned} \lambda_3 &\approx \frac{1}{2} (\eta + \bar{n}) + 2\eta_0 \\ \lambda_4 &\approx \frac{1}{2} (\eta + \bar{n}) \end{aligned} \right\} \quad \text{for } 4\eta_0^2 \gg (\eta - \bar{n})^2$$

If $4\eta_0^2$ is not much bigger than $(\eta - \bar{n})^2$

$$\lambda_3 = \frac{1}{2} (\eta + 2\eta_0 + \bar{n}) + \frac{1}{2} [(\eta - \bar{n})^2 + 4\eta_0^2]^{\frac{1}{2}}$$

$$\lambda_4 = \frac{1}{2} (\eta + 2\eta_0 + \bar{n}) - \frac{1}{2} [(\eta - \bar{n})^2 + 4\eta_0^2]^{\frac{1}{2}}$$

Therefore P is:

$$P \approx \begin{bmatrix} p & -p & -1 & 1 \\ q & q & -1 & 1 \\ -1 & -1 & 1 & 1 \\ 1 & 1 & 1 & 1 \end{bmatrix} \quad (13)$$

$$p = - (d - \lambda_1) / c \quad (14)$$

$$q = (d - \lambda_2) / c \quad (15)$$

$$P^{-1} = \frac{1}{-||P||} \begin{bmatrix} \cdot & \cdot & \cdot & \cdot \\ \cdot & \cdot & \cdot & \cdot \\ -4q & -4p & 2(p+q) & 2(p+q) \\ 4q & 4p & 2(p+q) & 2(p+q) \end{bmatrix} \quad (16)$$

$||P||$ is the determinant of P and $||P|| = -8(p+q)$

Let the source vector be:

$$\underline{S} = \begin{bmatrix} S_1 \\ S_2 \\ S_3 \\ 0 \end{bmatrix}, \quad S_2 \gg S_2, S_1 \quad (17)$$

$$\begin{aligned}
\xi_3 = \frac{1}{||P||} \left\{ -4qe^{-\lambda_1 t} \int_0^t S_{*1} e^{\lambda_1 t'} dt' \right. \\
- 4pe^{-\lambda_2 t} \int_0^t S_{*2} e^{\lambda_2 t'} dt' \\
+ 2(p+q) e^{-\lambda_3 t} \int_0^t S_{*1} e^{\lambda_2 t'} dt' \\
\left. + 2(p+q) e^{-\lambda_4 t} \int_0^t S_{*4} e^{\lambda_4 t'} dt' \right\} \quad (18)
\end{aligned}$$

ξ_4 = same as ξ_3 except that the signs of the first two terms are positive instead of negative.

$$S_{*1} = pS_1 - pS_2 - S_3 \quad (19)$$

$$S_{*2} = -qS_1 + qS_2 - S_3 \quad (20)$$

$$S_{*3} = -S_1 - S_2 + S_3 \quad (21)$$

$$S_{*4} = S_1 + S_2 + S_3 \quad (22)$$

The gradient R_0 is:

$$R_0 = \frac{\xi_3}{\xi_4} \quad (23)$$

$||P||$ cancels and the integrals $e^{-\lambda_j t} \int_0^t S_{*j} e^{\lambda_j t'} dt'$ can be solved by

the techniques discussed in Chapters 9 and 10.

$$S_1 = \epsilon_1 a e^{bt}, \quad S_2 = \epsilon_2 a e^{bt}, \quad S_3 = (1 - \epsilon_1 - \epsilon_2) a e^{bt} \quad [\Delta_1 + \Delta_2]$$

$$\bar{R}_0 \approx \bar{R}_0 \left[\frac{1 + a_0 \sin A + a_1 \cos A + a_2 \sin B + a_3 \cos B}{1 + b_0 \sin A + b_1 \cos A + b_2 \sin B + b_3 \cos B} \right] \quad (24)$$

$$A = \omega t + \phi \quad (\Delta_1 \text{ cycle})$$

$$B = \omega_* t + \phi_* \quad (\Delta_2 \text{ cycle})$$

$$\bar{R}_0 = \frac{\alpha_0 + \alpha_1 + \alpha_2 + \alpha_3}{-\alpha_0 - \alpha_1 + \alpha_2 + \alpha_3} \quad (25)$$

$$\alpha_0 = \frac{-4q}{(b + \lambda_1)} [p(\epsilon_1 - \epsilon_2) - (1 - \epsilon_1 - \epsilon_2)] \quad (26)$$

$$\alpha_1 = \frac{-4p}{(b + \lambda_2)} [-q(\epsilon_1 - \epsilon_2) - (1 - \epsilon_1 - \epsilon_2)] \quad (27)$$

$$\alpha_2 = \frac{2(p + q)}{(b + \lambda_3)} [1 - 2(\epsilon_1 + \epsilon_2)] \quad (28)$$

$$\alpha_3 = \frac{2(p + q)}{(b + \lambda_3)} \quad (29)$$

If $\Delta_1 = \alpha \cos(\omega t + \phi)$

$$a_0 = \left[\sum_{k=0}^3 \alpha_k \right]^{-1} \alpha \omega \left[\frac{4q}{\omega^2 + (b + \lambda_1)^2} + \frac{4p}{\omega^2 + (b + \lambda_2)^2} \right. \\ \left. + 2(p + q) \left(\frac{1}{\omega^2 + (b + \lambda_3)^2} + \frac{1}{\omega^2 + (b + \lambda_4)^2} \right) \right] \quad (30)$$

$$b_0 = (-\alpha_0 - \alpha_1 + \alpha_2 + \alpha_3)^{-1} \alpha \omega \left[\frac{-4q}{\omega^2 + (b+\lambda_1)^2} - \frac{4p}{\omega^2 + (b+\lambda_2)^2} + 2(p+q) \left(\frac{1}{\omega^2 + (b+\lambda_3)^2} + \frac{1}{\omega^2 + (b+\lambda_4)^2} \right) \right] \quad (31)$$

a_0 and b_0 are rewritten as:

$$a_0 = (\alpha_0 + \alpha_1 + \alpha_2 + \alpha_3)^{-1} \alpha \omega [w + x + y + z] \quad (32)$$

$$b_0 = (-\alpha_0 + \alpha_1 + \alpha_2 + \alpha_3)^{-1} \alpha \omega [-w - x + y + z] \quad (33)$$

Then

$$a_1 = (\alpha_0 + \alpha_1 + \alpha_2 + \alpha_3)^{-1} \alpha [(b+\lambda_1)w + (b+\lambda_2)x + (b+\lambda_3)y + (b+\lambda_4)z] \quad (34)$$

$$b_1 = (-\alpha_0 - \alpha_1 + \alpha_2 + \alpha_3)^{-1} \alpha [-(b+\lambda_1)w - (b+\lambda_2)x + (b+\lambda_3)y + (b+\lambda_4)z] \quad (35)$$

If there is a Δ_2 cycle: $\Delta_2 = \alpha_* \cos(\omega_* t + \phi_*)$

a_2 and a_3 are the same as a_0 and a_1 respectively, except ω is replaced by ω_* and α by α_* . Similarly b_2 and b_3 are the same as b_0 and b_1 except $\omega \rightarrow \omega_*$ $\alpha \rightarrow \alpha_*$.

(e) Summary of Additional Calculations.

(i) Selected values of \bar{R}_0 for various conditions.

η	0.1	0.09	0.09	0.1	0.12	0.1	0.1	0.1
$\bar{\eta}$	0.07	0.07	0.07	0.07	0.1	0.08	0.08	0.08
η_T	0.8	1.14	1.00	0.8	1.14	0.7	0.8	1.14
ϵ_1	0.3	0	0	0.2	0.1	0.1	0.1	0.1
ϵ_2	0	0	0	0	0.1	0.1	0.1	0.1
η_0	1.7	8	8	3	4	6	6	6
Calculated \bar{R}_0	1.89	1.55	1.61	1.93	1.59	1.66	1.61	1.47

(ii) Δ_1 cycle with $\omega = 0.9$ radians/yr.

Since the source function in later years is somewhat better represented by a shorter ω , figure (A5.1) illustrates the results of the four-box theory for $\omega = 0.9$. Curves (1) and (2) in figure (A5.1) are based on the same assumptions as figure (5.4) except $\omega \rightarrow 0.9/\text{yr}$. In curve (1) $\eta = 0.12/\text{yr}$, $\eta_0 = 4/\text{yr}$, $\bar{\eta} = 0.08/\text{yr}$ and $\eta_T = 1.14/\text{yr}$. Curve (2) is based on the same assumptions as curve (1) except that η_0 is taken to be 5/yr. For curve (2), $a_0 = 0.072$, $a_1 = 0.054$, $b_0 = 0.039$ and $b_1 = 0.025$.

(iii) Additional data on the changing CH_3CCl_3 gradient.

Some independent data on the changing CH_3CCl_3 gradient are also available, and support the contentions of Chapter 5. These data were obtained by the Washington State University (Pullman, Washington) group and are indicated on figure (A5.1) by squares (\square). These were taken at times slightly different from those of Rasmussen's data after 1/1977. Otherwise the figure is exactly the same as figure

(iv) Rasmussen's data for F-11, F-12, CH_3CCl_3 , CCl_4 , and N_2O from 1975 - 1979, for various trace gases are taken from the Concorde air sampling program, and for C_2 - hydrocarbons from MCA, NSF, and NASA supported projects.

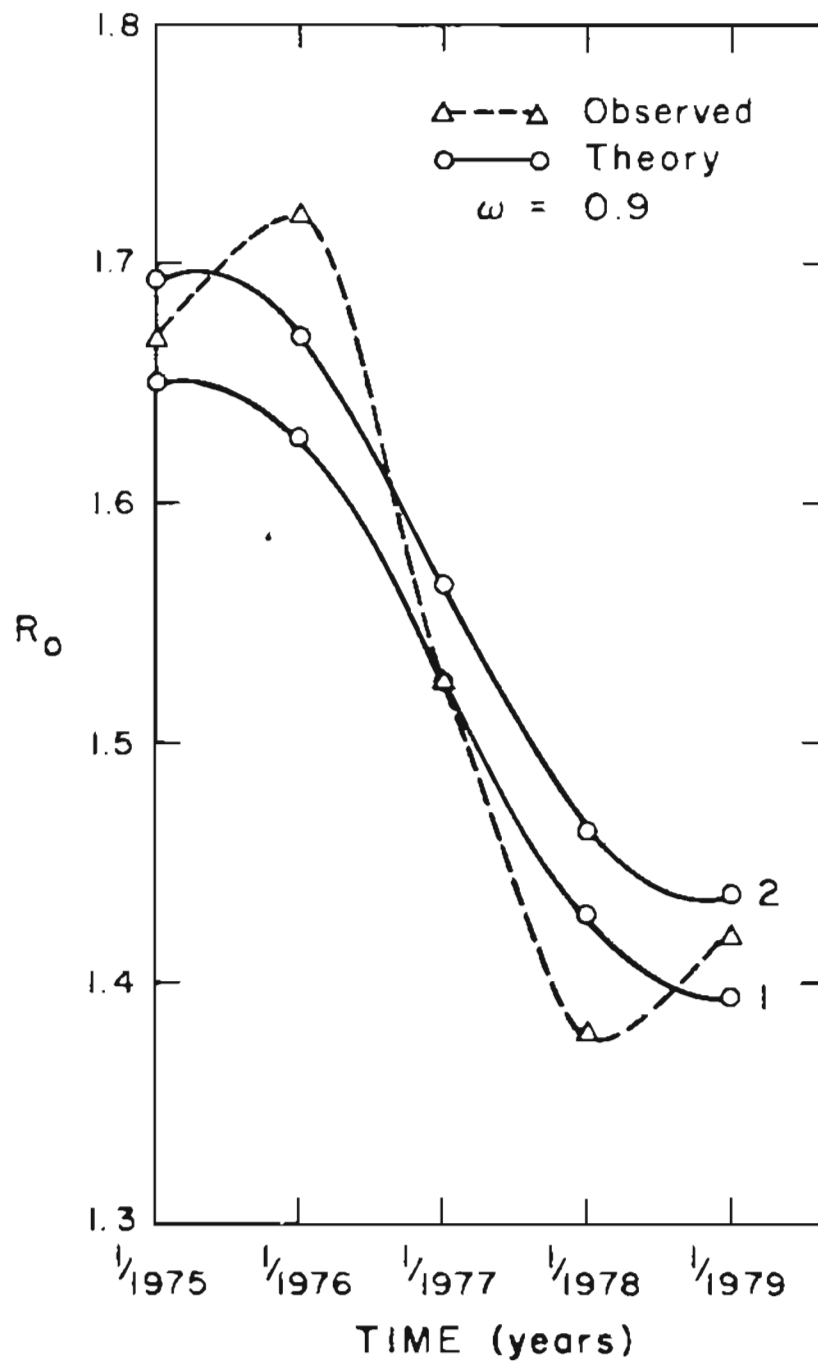


Figure (A5.1): Observed CH_3CCl_3 gradient and the four box theory. (Same as figure 5.4, except $\omega = 0.9$)

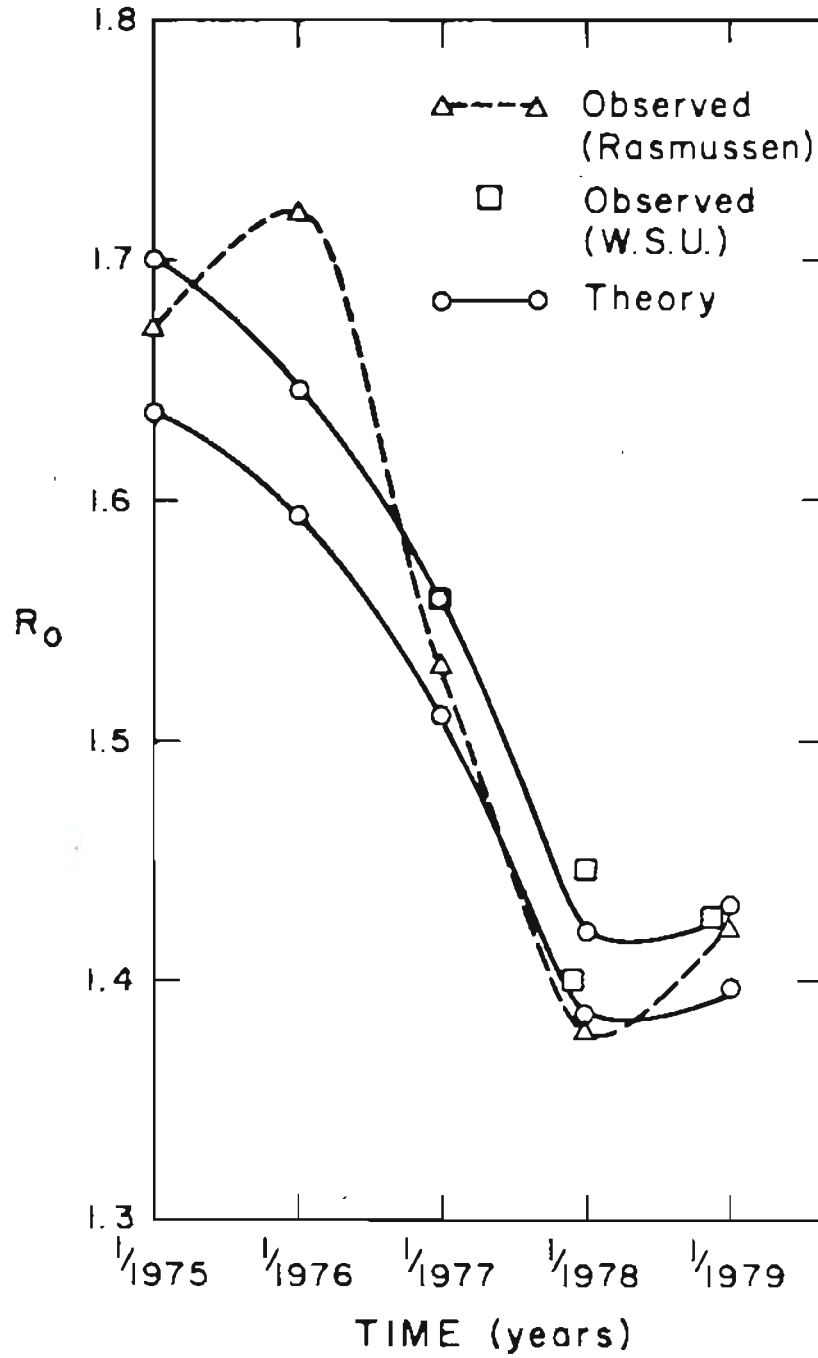


Figure (A5.2): Observed CH_3CCl_3 gradient and the four box theory with the Δ_2 cycle (same as figure 5.5 with additional observations).

Chapter 6.

Calculations of expected CH_3CCl_3 concentrations:

(i) $\tau_T = 1.2$ yrs, $\tau_n = 12$ yrs, $\tau_s = 6$ yrs. Calculations of ξ_n , ξ_s (northern, southern hemispheres) using eqns. (9.10) and (9.11)

$$\lambda_1 = 1.792, \quad \lambda_2 = 0.124$$

$$\xi_n = -e^{-1.792t} - 77.1 e^{-0.124t} + 190.1$$

$$\xi_s = e^{-1.792t} - 73.3 e^{-0.124t} + 158.4$$

$$S_n = 42.2 \text{ pptv/yr} \approx 1.1 \times 10^9 \text{ lbs/yr.}$$

$$S_s = 0$$

pptv				
t	ξ_n	ξ_s	ξ_{nT}	ξ_{sT}
0	112	86	130	100
1	121.8	93.8	141.3	108.8
2	129.9	101.2	150.7	117.4
3	137.0	107.9	158.9	125.1
4	143.1	113.8	166.1	132.0
5	148.6	119.0	172.4	138.0
10	167.8	137.2	194.7	159.2
15	178.1	147.0	206.6	170.5
20	183.6	152.3	213.0	176.6
∞	190.1	158.4	220	184

$$(ii) S_n = 42.2 \text{ pptv/yr. } e^{0.08t}; S_s = 0$$

Other variables are the same as before.

$$\xi_n = -\frac{1}{2} e^{-1.792t} - 7e^{-0.124t} + 119.4e^{0.08t}$$

$$\xi_s = \frac{1}{2} e^{-1.792t} - 6.6e^{-0.124t} + 92.2e^{0.08t}$$

t	pptv			
	ξ_n	ξ_s	ξ_{nT}	ξ_{sT}
0	112	86	130	100
1	123.1	94.1	142.8	109.2
2	134.7	103.0	156.2	119.5
3	147.0	112.7	170.5	130.7
4	160.2	123.0	185.8	142.6
5	174.4	134.0	202.3	155.5
10	263.7	203.3	305.9	235.8
15	395.3	305.1	458.6	353.9
20	590.8	456.1	685.4	529.1

(iii) Calculations using longer and shorter lifetimes were carried out in the same way as those shown above. These are plotted in Figures (9.2) and (9.2).

Chapter 7:

(a) Release of F-22

			in $10^6 \frac{\text{gm}}{\text{yr}}$	in pptv $\frac{\text{trop.}}{\text{yr}}$
1/1950 - 1/1960:	$S_{T_1} = a_1 e^{b_1 t}$	$b_1 = 0.320$	$a_1 = 0.12$	0.0096
1/1960 - 1/1968:	$S_{T_2} = a_2 e^{b_2 t}$	$b_2 = 0.187$	$a_2 = 2.92$	0.234
1/1968 - 5/1979:	$S_{T_3} = a_3 e^{b_3 t}$	$b_3 = 0.158$	$a_3 = 15.05$	1.206

Cumulative release:

The cumulative releases based on the values of a_i and b_i shown above were calculated. The values of a_i have been adjusted according to the results of Chapter 9. These calculations of cumulative releases were made to make sure that the functions adopted for $S(t)$ reproduce the total amount of F-22 emitted.

$$S_c(t_i, t_j) = \int_{t_i}^{t_j} S(t) dt$$

time	$S_c (\times 10^{-9} \text{ Kg})$	$S_M (\times 10^{-9} \text{ Kg})$
1/1950 - 1/1960	8.82	8.9
1/1960 - 1/1968	54.1	54.1
1/1968 - 1/1976	242.0	241.5

S_c = Cumulative release based on a_i, b_i given above. S_M = sum of yearly releases, during the periods shown at the left hand side, as estimated by McCarthy et al. (1977)

(b) Solution of conservation equation (7.11)

$$\bar{\xi}_u = \frac{\eta_T}{\lambda_1 - \lambda_2} (\Omega_2 - \Omega_1)$$

$$\bar{\xi}_T = \frac{1}{\lambda_1 - \lambda_2} [(a - \lambda_2) \Omega_1 + (\lambda_1 - a) \Omega_2]$$

$$a = \eta + \eta_T \frac{N_S}{N_T}$$

$$\Omega_i = e^{-\lambda_i t} \int_0^t S e^{\lambda_i t'} dt' \quad i = 1, 2$$

$$\begin{aligned} \Omega_i &= \frac{a_1}{b_1 + \lambda_i} \left[e^{b_1 t_1} e^{\lambda_i (t_1 - t)} - e^{-\lambda_i t} \right] \\ &+ \frac{a_2}{b_2 + \lambda_i} \left[e^{b_2 (t_2 - t_1)} e^{\lambda_i (t_2 - t)} - e^{-\lambda_i (t - t_1)} \right] \\ &+ \frac{a_3}{b_3 + \lambda_i} \left[e^{b_3 (t - t_2)} - e^{\lambda_i (t_2 - t)} \right] \end{aligned}$$

$$t_1 = 10 \text{ yrs (1/1960)} \quad t = 0 \text{ at 1/1950}$$

$$t_2 = 18 \quad (1/1968)$$

$$t_3 = 29.4 \quad (5/1979)$$

$$\Omega_1 \approx \frac{a_3}{b_3 + \lambda_1} e^{b_3 (t - t_2)}$$

$$\lambda_{\begin{pmatrix} 1 \\ 2 \end{pmatrix}} = \frac{1}{2} (d + a) (\pm) \frac{1}{2} [(d - a)^2 + 4bc]^{1/2}$$

$$a = \eta + \eta_T \frac{N_S}{N_T}, \quad b = \eta_T \frac{N_S}{N_T}$$

$$c = \eta_T, \quad d = \bar{\eta} + \eta_T$$

$$\bar{\xi} = (\bar{\xi}_u N_S + \bar{\xi}_T N_T) / N_\infty$$

Table (I) shows the numerical values of λ_1 , λ_2 , Ω_1 , Ω_2 , $\bar{\xi}_u$, $\bar{\xi}_T$ and $\bar{\xi}$ for various values of η and $\bar{\eta}$.

Table (I)

$\bar{\tau}$	τ	λ_1	λ_2	Ω_1	Ω_2	$\bar{\xi}_u$	$\bar{\xi}_T$	$\bar{\xi}$
5	7	0.900	0.153	6.904	22.810	12.35	20.3	18.8
5	9	0.895	0.126	6.937	25.485	14.0	22.7	21.1
5	12	0.891	0.102	6.963	27.740	15.2	24.8	23.1
5	15	0.889	0.088	6.977	29.238	16.1	26.2	24.4
5	20	0.887	0.073	6.990	31.024	17.1	27.9	25.9
5	25	0.8855	0.0645	7.000	32.128	17.8	28.9	26.9
5	30	0.8847	0.0586	7.006	32.940	18.2	29.7	27.6
5	∞	0.8806	0.029	7.033	37.659	20.9	34.0	31.6
7	7	0.852	0.143	7.232	24.090	13.8	21.0	19.7
7	10	0.846	0.107	7.276	27.238	15.7	23.9	22.4
7	15	0.840	0.079	7.319	30.284	17.5	26.7	25.0
7	20	0.838	0.065	7.334	32.128	18.6	28.4	26.6
7	30	0.835	0.051	7.356	34.043	19.7	30.2	28.3
7	∞	0.831	0.022	7.386	38.962	22.6	34.7	32.5
10	7	0.818	0.135	7.484	24.728	14.6	21.2	20.0
10	10	0.810	0.100	7.546	27.940	16.7	24.2	22.8
10	15	0.804	0.072	7.593	31.026	18.6	27.0	25.5
10	20	0.801	0.0585	7.617	32.940	19.8	28.8	27.1
10	30	0.799	0.0445	7.633	35.043	21.1	30.8	29.0
10	∞	0.794	0.0163	7.673	40.646	24.6	35.8	33.8

Table (I) continued:

$\bar{\tau}$	τ	λ_1	λ_2	Ω_1	Ω_2	ξ_u	ξ_T	ξ
15	7	0.792	0.1275	7.689	25.400	15.5	21.5	20.4
15	10	0.783	0.0935	7.763	28.631	17.6	24.5	23.2
15	15	0.777	0.0665	7.813	31.878	19.6	27.5	26.0
15	20	0.774	0.053	7.838	34.053	21.1	29.4	27.9
15	30	0.771	0.039	7.863	35.931	22.2	31.2	29.5
15	∞	0.766	0.0112	7.906	41.139	25.5	35.9	34.0
20	7	0.779	0.124	7.796	25.600	15.8	21.5	20.5
20	10	0.770	0.090	7.871	29.200	18.2	24.8	23.6
20	15	0.763	0.0634	7.931	32.130	20.1	27.5	26.2
20	20	0.760	0.0499	7.957	34.209	21.4	29.4	27.9
20	30	0.757	0.0362	7.983	36.400	22.9	31.4	29.8
20	∞	0.751	0.0085	8.036	41.718	26.3	36.2	34.4
∞	7	0.741	0.112	8.125	26.755	17.2	22.0	21.1
∞	10	0.731	0.079	8.217	30.284	19.6	25.2	24.2
∞	20	0.720	0.040	8.320	35.767	23.4	30.1	28.9
∞	30	0.716	0.027	8.358	38.022	25.0	32.2	30.9
∞	∞	0.710	0.000	8.416	43.640	28.8	37.2	35.7

(c) Natural Sources:

Table (II) contains the values of the natural source strength, S_* , as a function of $\bar{\tau}$ and τ ; based on equation (7.18). $\bar{\xi}_T(\eta, \bar{\eta})$ in Eqn. (7.18) is taken from Table (I).

Table (II)

$\bar{\tau}$	τ	S_* (pptv trop/yr)	S_* (10^9 gr/yr)	$\bar{\tau}$	τ	S_* (pptv trop/yr)	S_* (10^9 gr/yr)
5	7	4.646	58	15	7	3.930	49
	12	2.544	32		10	2.506	32
	20	1.563	20		20	1.084	14
	30	1.119	14		30	0.712	9
	∞	0.411	5		∞	0.138	1.8
7	7	4.324	53	20	7	3.853	48
	10	2.855	36		10	2.471	31
	20	1.371	17		20	1.031	13
	30	0.961	12		30	0.656	8
	∞	0.297	4		∞	0.104	1.3
10	7	4.122	51	∞	7	3.520	44
	10	2.668	33		10	2.139	27
	20	1.223	15		20	0.818	10
	30	0.820	11		30	0.473	6
	∞	0.199	2.5				

(d) Conversion of F-12

F-12 Source function:

$$(1947) 0 \leq t < 27 \text{ yrs (1974): } S_1 = 0.786e^{0.121t} = a_1 e^{b_1 t}$$

$$(1974) 27 \leq t < 32.4 \text{ yrs (5/1979): } S_2 = 19.5 = a_2$$

S in ppt v/yr in the whole atmosphere.

Solution of Eqn. (7.22):

$$\begin{aligned} \bar{\xi}_*(t_*) &= \tilde{\eta}_c \frac{a_1}{b_1 + \eta_0} \left[\frac{1}{b_1 + \tilde{\eta}} \left(e^{(b_1 + \tilde{\eta})t_1} - 1 \right) - \frac{1}{(\tilde{\eta} - \eta_0)} \right. \\ &\quad \left. \left(e^{-(\eta_0 - \tilde{\eta})t_1} - 1 \right) \right] e^{-\tilde{\eta}t_*} + \tilde{\eta}_c \frac{a_1}{b_1 + \eta_0} \left[e^{(b_1 + \eta_0)t_1} - 1 \right] \frac{1}{(\tilde{\eta} - \eta_0)} \\ &\quad \left[e^{-\eta_0 t_*} - e^{-(\eta_0 - \tilde{\eta})t_1} e^{-\tilde{\eta}t_*} \right] + \tilde{\eta}_c \frac{a_2}{\eta_0} \left[\frac{1}{\tilde{\eta}} \left(1 - e^{\tilde{\eta}t_1} e^{-\tilde{\eta}t_*} \right) \right. \\ &\quad \left. - \frac{e^{\eta_0 t_1}}{\tilde{\eta} - \eta_0} \left(e^{-\eta_0 t_*} - e^{-(\eta_0 - \tilde{\eta})t_1} e^{-\tilde{\eta}t_*} \right) \right] \end{aligned}$$

$\eta_0 = \tilde{\eta}_c + \tilde{\eta}_r$, $\tilde{\eta}$ = global lifetime of F-22, η_0 = global lifetime of F-12, $t_1 = 27$ yrs, $t_* = 32.4$ yrs.

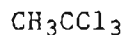
Table (III) contains the results of numerical calculations based on the solution of eqn. (7.22) shown above:

Table (III)

$\tilde{\tau}$	$\tilde{\tau}$	$\bar{\xi}_*(t_*)$ pptv
80	10	14.2
	20	18.6
	30	21.2
100	10	11.5
	20	14.7
	30	16.2
	∞	19.1
133	10	8.8
	20	11.2
	30	12.4
	∞	15.1
200	10	6.0
	20	7.7
	30	8.5
	∞	11.0

Chapter 8:

Global and Hemispherical Averages.

1. Polynomials (ϕ in radians)

	α_0	α_1	α_2	α_3
1976	95.97	-24.12	0.135	3.83
1977	99.59	-20.76	-2.64	6.21
1978	104.50	-27.46	4.77	6.17

2. Model Atmosphere.

Assumptions: Model atmosphere (Houghton, 1977). (1) For the region between 0°-30°, the values of p and T at 10° are assumed to hold. Similarly for the region between 30°-60°, the values of p and T at 40° are used; and for 60°-90°, the values at 70°. (2) Northern and southern hemispheres are assumed symmetrical. (3) At each of these latitudes a seasonal average is first formed. ($\langle p_h \rangle$)

		$\langle p_h \rangle^*$			
(a)	$\int \cos\phi d\phi$	h = 8 km	16 km	50 km	100 km
0-30°	0.5	377.6	110.1	0.812	0.3×10^{-3}
30°-60°	0.37	361.8	105.2	0.770	0.264×10^{-3}
60°-90°	0.13	336.9	98.5	0.724	0.238×10^{-3}
	$\bar{p}_h =$	366.5	106.8	0.785	0.279×10^{-3}

* All pressures are in mb.

$$\bar{p}_h = \int_0^{\pi/2} \langle p_h \rangle \cos\phi d\phi$$

(b) Mass and Number of Molecules.

	Mass x 10 ⁻²¹ gm	N _o x 10 ⁻⁴³
0-8 km	3.210	6.673
8-16	1.354	2.815
16-50	0.555	1.153
0-50	5.119	10.641

(c) Density Scale Height for 8-16 km.

N₂ = number of molecules in the region between 8-16 km. (H₁ = 8 km, H₂ = 16 km)

$$\begin{aligned}
 N_2 &= 2\pi \int_{-\pi/2}^{\pi/2} \int_{R+z_o+H_1=R'}^{R+z_o+H_2} \bar{\rho}(R') e^{-(r-R')/H} r^2 \cos\phi dr d\phi \\
 &= 2\pi R'^2 \bar{\rho}(R') \int_{-\pi/2}^{\pi/2} \int_0^{H_2-H_1} e^{-z/H} dz \cos\phi d\phi \\
 &= 4\pi R'^2 \bar{\rho}(R') H [1 - e^{-(H_2-H_1)/H}] \\
 &= \frac{1}{g_o} [\bar{p}_1 S_1 - \bar{p}_2 S_2] \tag{1}
 \end{aligned}$$

$$\rho(R') = \left\langle \frac{p(R')}{T(R')} \right\rangle = \text{seasonal average of density}$$

$$\bar{\rho}(R') = \int_0^{\pi/2} \rho(R') \cos\phi d\phi$$

From the same model atmosphere

$$\bar{\rho}(R') = 1.085 \times 10^{19} \text{ molecules/cm}^3$$

Putting in the numbers, eqn. (1) implies:

$$H(1 - e^{-8/H}) = 5.078$$

or $H \approx 8$ km. This scale height is also consistent with

$$H = 8[\ln(\bar{\rho}_{H_1}/\bar{\rho}_{H_2})]^{-1} \text{ derived from the same model atmosphere.}$$

Figures 8.2, 8.3, and 8.4 polynomials

$$\xi = a_0 + a_1\phi + a_2\phi^2 + a_3\phi^3$$

		a_0	a_1	a_2	a_3
1976	CH ₃ CCl ₃	96.0	0.421	4.10×10^{-5}	-2.03×10^{-5}
	F-11	130.8	0.102	4.31×10^{-4}	-3.26×10^{-6}
	F-12	221.0	0.223	1.28×10^{-3}	-7.49×10^{-6}
1977	CH ₃ CCl ₃	99.6	0.362	-8.04×10^{-5}	-3.30×10^{-5}
	F-11	149.1	0.145	3.30×10^{-5}	-1.38×10^{-5}
	F-12	249.0	0.200	5.94×10^{-4}	7.46×10^{-6}
1978	CH ₃ CCl ₃	104.5	0.479	-1.45×10^{-3}	-3.28×10^{-5}
	F-11	155.9	0.304	6.21×10^{-4}	-3.37×10^{-5}
	F-12	261.6	0.343	1.14×10^{-3}	-4.40×10^{-5}

Note that ϕ is in degrees. For integration a_1 should be converted to the appropriate units in radians.

Chapter 9:

Transformations for smoothing fluctuating source terms:

$$\int_t^{t+\delta} a' \alpha' e^{bt} \cos(\omega t + \phi') dt = a \alpha e^{bt} \cos(\omega t + \phi) \quad (9.1)$$

$$x = \omega t + \phi', \quad dx = \omega dt$$

$$t = (x - \phi')/\omega \quad \omega > 0$$

$$\begin{aligned} \int_t^{t+\delta} e^{bt} \cos(\omega t + \phi') dt &= \int_{\delta t + \phi'}^{\omega t + \phi' + \omega \delta} e^{-b\phi'/\omega} e^{b/\omega x} \cos x \frac{dx}{\omega} \\ &= \frac{1}{\omega} e^{-b/\omega \phi'} \left[\frac{e^{b/\omega x} (\sin x + \frac{b}{\omega} \cos x)}{1 + b^2/\omega^2} \right]_{\omega t + \phi'}^{\omega t + \phi' + \omega \delta} \end{aligned} \quad (9.2)$$

Using the trigonometric identities for $\cos(x + \omega)$ and $\sin(x + \omega)$ eqn.

(4.2) reduces to:

$$\frac{\omega}{b^2 + \omega^2} e^{bt} \left\{ A \sin x + B \cos x \right\} = \int_t^{t+\delta} e^{bt} \cos(\omega t + \phi') dt \quad (9.3)$$

where

$$A = e^{b\delta} \cos \omega \delta - \frac{b}{\omega} \sin \omega \delta - 1 \quad (9.4)$$

$$B = e^{b\delta} \sin \omega\delta + \frac{b}{\omega} \cos \omega\delta - \frac{b}{\omega} \quad (9.5)$$

Eqn. (4.1) becomes:

$$\frac{a'\alpha'\omega}{b^2+\omega^2} [A \sin x + B \cos x] = a \alpha \cos (\omega t + \phi) \quad (9.6)$$

$$\text{Let } \lambda = \frac{a'\alpha'\omega}{(b^2+\omega^2)a\alpha} \quad (9.7)$$

so that eqn. (4.6) can be written as:

$$\begin{aligned} \lambda [A \cos \phi' - B \sin \phi'] \sin \omega t + \lambda [A \sin \phi' + B \cos \phi'] \cos \omega t \\ = \cos \omega t \cos \phi - \sin \omega t \sin \phi \end{aligned} \quad (9.8)$$

or

$$\lambda [A \cos \phi' - B \sin \phi'] = -\sin \phi \quad (9.9)$$

$$\lambda [A \sin \phi' + B \cos \phi'] = \cos \phi \quad (9.10)$$

$$\begin{bmatrix} \cos \phi \\ \sin \phi \end{bmatrix} = \lambda \begin{bmatrix} A & B \\ B & -A \end{bmatrix} \begin{bmatrix} \sin \phi' \\ \cos \phi' \end{bmatrix} \quad (9.11)$$

$$\sin \phi' = \frac{1}{\lambda [A^2+B^2]} (A \cos \phi + B \sin \phi) \quad (9.12a)$$

$$\cos \phi' = \frac{1}{\lambda [A^2+B^2]} (B \cos \phi - A \sin \phi) \quad (9.12b)$$

$$\sin^2 \phi' + \cos^2 \phi' = 1 = \frac{1}{\lambda^2 [A^2+B^2]^2} [A^2+B^2] \quad (9.13)$$

$$\lambda = \frac{1}{\sqrt{A^2+B^2}} = \frac{a' \alpha' \omega}{a \alpha (b^2+\omega^2)} \quad (9.14)$$

$$\frac{1}{[A+B]^{1/2}} = \frac{b \alpha' \omega}{(e^{b\delta}-1) \alpha (b^2+\omega^2)} \quad (9.15)$$

$$\alpha' = \frac{(b^2+\omega^2) (e^{b\delta}-1)}{b\omega[A^2+B^2]^{1/2}} \alpha \quad (9.16)$$

from eqn. (4.12a):

$$\phi' = \text{Tan}^{-1} \left\{ \frac{A \cos \phi + B \sin \phi}{B \cos \phi - A \sin \phi} \right\} \quad (9.17)$$

For $\delta = 1$.

$$\alpha' = \frac{(b^2+\omega^2) (e^b-1)}{b\omega[A^2+B^2]^{1/2}} \alpha \quad (9.18)$$

$$A = e^b \cos \omega - \frac{b}{\omega} \sin \omega - 1 \quad (9.19)$$

$$B = e^b \sin \omega + \frac{b}{\omega} \cos \omega - \frac{b}{\omega} \quad (9.20)$$

APPENDIX II: SUMMARY OF COMMONLY USED MATHEMATICAL SYMBOLS

Chapter 2.

Symbol	Description
τ	Global lifetime of a trace gas.
τ_x	Global lifetime of trace gas x.
ξ	Global mixing ratio.
ξ_T	Global mixing ratio in the troposphere - total number of molecules of the trace gas/ N_T
ξ_u	Global mixing ratio in the stratosphere.
N_T	Number of molecules of air in the troposphere.
N_S	Number of molecules of air in the stratosphere.
$N_\infty = N_S + N_T$	Total number of molecules of air in the atmosphere.
$\zeta = \xi_u / \xi_s$	Ratio of stratospheric-tropospheric mixing ratios.
S_T	Total global source strength of a trace gas = number of molecules of the trace gas released/ N_T .
$\eta = 1/\tau$	Reciprocal of lifetime.
ξ_n	Total mixing ratio of a trace gas in the northern hemisphere (includes both stratosphere and troposphere).
ξ_s	Total mixing ratio of a trace gas in the southern hemisphere.
X_x	Indicates $\int_0^T x(t)dt$, where x is S, S_n , ξ_n , ξ_s , etc.
S_n	Number of molecules of a trace gas released/number of molecules of air in one hemisphere -- $S_n = 2S / (N_T + N_S)$
τ_T	Interhemispheric transport time

Symbol	Description
$\eta_T = 1/\tau_T$	Reciprocal of the transport time.
$\underline{\xi}$	Vector: $\begin{pmatrix} \xi_n \\ \xi_s \end{pmatrix}$
\underline{S}	Vector: $\begin{pmatrix} S_n \\ S_s \end{pmatrix}$
Ω	A matrix, described in the text. It represents the sink strengths and interhemispheric transport.
τ_n, τ_s	Mean lifetimes of a trace gas in the northern (n) and southern (s) hemispheres.
Chapter 3.	
C	Concentration in molecules per unit volume.
$\overline{[HO]}$	Globally, yearly averaged hydroxyl radical density in the troposphere
$\overline{[HO]}_0$	Globally, yearly averaged hydroxyl radical density at ground level.
ρ	Density of air
$\langle \tau \rangle, \bar{\tau}, \bar{\bar{\tau}}$	Various types of globally averaged lifetimes.
ϕ	Latitude in radians with $-\pi/2$ as the south pole and $+\pi/2$ as the north pole.
λ	Longitude (0 - 2π).
z	Height above ground level.
t	Time
z_T	Mean tropopause height above ground level.

Symbol	Description
$K = Ae^{-E/T}$	Rate constant for the reaction of a trace gas with hydroxyl radicals.
T_o	Mean global ground level temperature.
ℓ	Mean temperature lapse rate in the troposphere.
h	Density scale height of hydroxyl radicals in the troposphere.
H	Density scale height of air in the troposphere.
$\beta = \frac{E\ell}{T_o^2} + \frac{1}{h}$	(see K above for E)
$\Gamma = \beta + \frac{1}{H}$	(see β and H above)
$\delta, \delta', \delta''$	The ratios of lifetimes predicted by various theories.
$n(x)$	Density of atmospheric gas x.
η_x	x = h, o, or s - reciprocal of global lifetimes of a trace gas due to various sink mechanisms.
η, τ, S, ξ	These symbols have the same meanings as in Chapter 2.

Chapter 4.

$f(t)$	True continuous source term in emissions per unit time.
δ	A (small) increment of time.
ω	Frequency in radians per year.
Δ	Relative deviation of one source function from another.

Symbol	Description
α	Amplitude of a sine function.
ϕ	Phase in a sine function. The context is the guide for distinguishing this ϕ from latitude.
η, τ, ξ, S	These symbols have the same meanings as in Chapter 2. S has several variations but it is always a source term.
Chapter 5	
$f_0(x)$	$= \sin x + \frac{b+\eta}{\omega} \cos x$. The b is the exponential rate of increase of the source, $S = ae^{bt}$.
R_T	Total release $= \int_0^t S(t') dt'$.
F	Dimensionless ratio: $\frac{\xi(t)}{R_T(t)}$
$\Delta_1(t)$	The first difference or relative difference between the true source function and a theoretical model source function.
$\Delta_2(t)$	When a theoretical model is assumed for Δ_1 , Δ_2 represents the difference between the true source function and the theoretical model of the source including Δ_1 .
H_0, H_1	Null hypothesis and alternative
$K(\alpha, n)$	Kendall's K - statistic
α	Statistical level of significance. Other uses of α in this chapter have to be distinguished from the context.
β	Slope of a line.

Symbol	Description
η, τ, S, ξ	These symbols have the same meanings as in Chapter 2. Some variations of these symbols also occur, the exact meanings of which are explained in the text.
α, ω, ϕ	Same as in Chapter 4.
 Chapter 6.	
R, R_0	These are called "gradients" in this work and elsewhere. The term gradient is simply chosen for convenience and intuitive meaning. It is possible that this term may be confused with $(\xi_n - \xi_s)$ or $\nabla \chi$. It shouldn't be. R is the ratio of the total number of molecules of a trace gas in the northern hemisphere to the total number of molecules of the same trace gas in the southern hemisphere. R_0 is simply the ratio of the concentration of a trace gas at $\phi \geq \pi/4$ radians to the concentration of the same trace gas at $\phi \leq -\pi/4$.
δ_R	$= R_0(\max) - R_0(\min)$ where the max and min are with respect to time.
$\lambda_1, \lambda_2, \lambda_3, \lambda_4$	Eigenvalues of a matrix.
$\tau_0, \eta_0 = 1/\tau_0$	τ_0 : transport time within a hemisphere.
$\eta, \tau, s_n, \xi_h,$ $\tau_T, \underline{\xi}, \underline{S}$	Same as in Chapter 2.
$\alpha, \omega, \phi, \Delta_1, \Delta_2$	Same as in Chapter 5. α is used for more than one variable in this chapter.
*	Subscript $*$ in this chapter does <u>not</u> have the same meaning as in Chapter 2.

Symbol	Description
Chapter 7	
$\langle f \rangle_{\rho}$	Density (of air) weighted stratospheric average of a function $f(z)$.
M	A matrix: same as Ω in Chapter 2.
λ_1, λ_2	Eigenvalues of M .
$\tau_T (=1/\eta_T)$	Stratospheric-tropospheric transport time. This is <u>not</u> the same use of τ_T as in all other chapters.
$\xi, \underline{\xi}, \underline{S}, \eta, \tau, \tau_T, S, N_S, N_T$	Same as in Chapter 2.
*	Subscript * does <u>not</u> have the same meaning as in Chapter 2.
Chapter 8	
$f(\phi, t)$	A function (antisymmetric) of latitude and time describing the distribution of a trace gas.
a	Constant mixing ratio of a trace gas beyond some southern latitude $\phi < -\phi_0$.
b	Constant mixing ratio of a trace gas above some northern latitude $\phi > \phi_0$.
$z_T(\phi)$	Tropopause height (time averaged) as a function of latitude.
r	Spatial radial coordinate - "height" measured from the center of the earth.
h_u	Average density scale height of air in the stratosphere.
p	Atmospheric pressure.
g	Acceleration of gravity.
z	Radial coordinate, measured from the surface of the earth.

Symbol	Description
m	Mass (of air).
μ	Molecular weight.
H_1 and H_2	Fixed heights above ground level.
H	Density scale height of air in the troposphere.
R	Radius of the earth.
$\xi, N_T, N_S, \tau, \zeta$	These symbols and their variations have the same general meaning as in Chapter 2.
C, ρ	These symbols and variations have the same general meaning as in Chapter 3.
R, R_0	Same as in Chapter 6. Conflict of symbols is resolved by context.
f, a, b	Same as in Chapter 8.

Other common symbols are also used in this chapter, usually with the same meaning as in other chapters.

Chapter 9.

a_0	Constant source function: emissions/unit time
$\underline{\xi}, \xi_n, \xi_s, \tau_T,$ $\tau_s, S_n, \underline{S}$	Same as in Chapter 2.
λ_1, λ_2	Same as in Chapter 7.

Symbol	Description
Chapter 10.	
<u>C</u>	Column vector of n dimensions representing concentrations in molecules per unit volume.
<u>S</u>	Column vector of n dimensions: source strength.
Ω	n x n matrix composed of transport times and lifetimes.
P	An n x n transformation matrix which takes Ω to its Jordan canonical form.
λ_i	i = 1, . . . , n, eigenvalues of Ω .
Λ	Diagonal matrix of eigenvalues $\Lambda_{ij} = \delta_{ij} \lambda_j$ (no sum).
det X	Determinant of matrix X.
η_i	Reciprocal of lifetime in region specified by index i.
$\bar{\eta}_i$	Transport time from one compartment to another.

VITA

M. Aslam Khan Khalil was born in Jhansi, U.P., India, on 7th January, 1950, the son of Shameem and Ahsan Khalil. He grew up in Abbotabad, Pakistan, and in 1960 moved with his family to Chittagong, now in Bangladesh. He and his family moved to Minneapolis, Minn., in 1963. In 1966 he was graduated from Alexander Ramsey Sr. High School in St. Paul, Minn., and entered the Institute of Technology of the University of Minnesota at Minneapolis. In 1970 he received a Bachelor of Physics degree from I.T. (Univ. of Minn.) and a B.A. in Mathematics and Psychology from the College of Liberal Arts (Univ. of Minn.). In the same year he entered the graduate school of Virginia Polytechnic Institute and State University of Blacksburg, Virginia. In 1972 he received an M.S. degree in Physics from VPI. In 1971 he joined the graduate school of the University of Texas at Austin and worked with Prof. E.C.G.Sudarshan on the relativistic quantum mechanics and field theory of particles with spin. He received a Ph.D. in physics from the University of Texas in 1976. Aslam Khalil is the author of several articles resulting from his research at the Center for Particle Theory of the Univ. of Texas and the continuation of this work in Canada and Oregon. These articles have been published in international journals including the Physical Review D (USA), Il Nuovo Cimento (Italy), Journal of Mathematical Physics (USA), Journal of Physics A (England), Progress of Theoretical Physics (Japan), and the Encyclopedia of Physics (John Wiley, USA). In 1973 Aslam Khalil married Giti Ara Eshraghi from Tehran, Iran. After spending the 1976-77 academic year in Toronto, Ontario, and Winnipeg, Manitoba, Aslam Khalil joined the Department of Environmental Science at the Oregon Graduate Center in September 1977. In June 1978 he joined Prof. R.A.Rasmussen and his research group and is currently working with Prof. Rasmussen. In January 1979 he was granted an M.S. in Environmental Science.

Permanent Address: 17 Diefenbaker St., St.John's, Newfoundland,
A1A 2M2, Canada.

This dissertation was typed by Ms. Edie Taylor.